NGU Report no. 2001.042

Abstracts – GEODE field workshop 8-12th July 2001 on ilmenite deposits in the Rogaland anorthosite province, S. Norway

NGU
Norges geologiske undersøkelse
Geological Survey of Norway

REPORT

Report no.: 2001.042	ISSN 0800-3416	Grading: Open

Title:
Abstracts – GEODE field workshop 8-12th July 2001 on ilmenite deposits in the Rogaland anorthosite province, S. Norway.

Authors: Korneliussen, A. (ed.)	Client: GEODE / ESF /NGU
County:	Commune:
Map-sheet name (M=1:250.000) Stavanger and Mandal	Map-sheet no. and -name (M=1:50.000)
Deposit name and grid-reference:	Number of pages: 147 Price (NOK): 167 Map enclosures:

Fieldwork carried out:	Date of report: 12 June 2001	Project no.: 2865.01	Person responsible: Nigel Cook

Summary:

This report is a compilation of 48 abstracts submitted to the GEODE field workshop on *Ilmenite Deposits in the Rogaland Anorthosite Province, South Norway* 8-12th July 2001 at Lundheim Folkehøgskole at Moi, Rogaland, Norway.

The workshop is organised by the working group for the project *Ilmenite deposits in the Rogaland Anorthosite province* (http://www.ngu.no/prosjekter/Geode/index.htm), a subproject under the ESF's GEODE-project "The Fennoscandian Shield Precambrian Province".

Keywords:	Mineral resources	Titanium
Ilmenite	Anorthosite	Norway
Abstracts	GEODE	

CONTENTS

Page

Workshop participants

Updated 25th June 2001.

Name	Institution	Address	Email
Andersen, Tom	Universitetet i Oslo	Laboratorium for isotopgeologi, Geologisk museum, Sars gt. 1, 0562 Oslo, Norway	tom.andersen@toyen.uio.no
Årebäck, Hans	Göteborg University/Boliden Mineral	Guldgatan 7, S-93632 Boliden, Sweden	hans.areback@boliden.se
Belevtsev, Aleksandr	Institute of Geochemistry, Mineralogy and Ore Formation, NAS	03680 Palladin Pr., 34 Kyiv-142, Kyiv, Ukraine	shurbel@torba.com
Berge, Kari	Titania A/S	Titania, N-4380 Hauge i Dalane, Norway	kari.berge@nli-usa.com
Bingen, Bernard	Geological Survey of Norway	N-7491 Trondheim, Norway	bernard.bingen@ngu.no
Bjørlykke, Arne	Geological Survey of Norway	N-7491 Trondheim, Norway	Arne.Bjorlykke@ngu.no

Bobrov, Alexander	Ukr. Sat. Geol., Research Institute, NAS	Avtozavodskaia st. 78, UA-04114, Kyiv, Ukraine	ukrdgri@geologiya.com.ua
Bogdanova, Svetlana	Dept. of Geology, Lund University	Sölvegatan 13, S-223 62 Lund, Sweden	svetlana.bogdanova@geol.lu.se
Bolle, Olivier	University of Liège	Bd. du Rectorat - Bât. B20; B-4000 Liège, Belgium	bolle@lucid.ups-tlse.fr
Brown, Laurie	Univ. Massachusetts	Dept. Geosciences, Univ. Massachussetts, Amherst, MA 01003, USA	lbrown@geo.umass.edu
Cawthorn, Grant	University of the Witwatersrand	School of Geosciences, University of the Witwatersrand, Private Bag 3, Wits 205, South Africa	065RGC@cosmos.wits.ac.za
Charlier, Bernard	University of Liège	Rosmel 116, 4651 Battice, Belgium	bernard.charlier@student.ulg.ac.be
Chernet, Tegist	Geological Survey of Finland	FIN-02151 Espoo, Finland	Tegist.Chernet@gsf.fi
Demaiffe, Daniel	Univ. Bruxelles	Depart Geology, CP 160/02 50, Av. Roosevelt, 1050 Bruxelles, Belgium	ddemaif@ulb.ac.be
Dickson, Amanda	Grant Institute of Geology and Geophysics, University of Edinburgh	4 Waverley Park, Edinburgh, UK	a.l.dickson@sms.ed.ac.uk
Didenko, Petro	Center of Environmental Radiogeochemistry	03680 Palladin Pr., 34a, Kyiv-142, Kyiv, Ukraine	center@radgeo.freenet.kiev.ua
Diot, Hervé	La Rochelle University	Pôle Sciences & Technologie, Earth Sciences Department Av Michel CREPEAU, F17042 La Rochelle Cedex 1, France	hdiot@univ-lr.fr
Duchesne, Jean-Clair	University of Liège	Bat. B20, B 4000 Sart Tilman, Belgium	jc.duchesne@ulg.ac.be
Esipchuk, Konstantin	Instiute of Geochemistry, Mineralogy and Ore Formation	03680 Palladin Pr. 34 Kyiv-142, Kyiv, Ukraine	skobvm@i.com.ua
Femenias, Olivier	Univ. Bruxelles	Depart Geology, CP 160/02 50, Av. Roosevelt, 1050 Bruxelles, Belgium	
Fershtater, German	Institute of Geology and Geochemistry	Pochtovy per., 7, Ekaterinburg, 620151, Russia	gerfer@online.ural.ru
Force, Eric	Rio Tinto and Univ. Arizona	Box 617, Mt. Lemmon AZ 85619, USA	ejforce@aol.com
Gauthier, Michel	Département des Sciences de la Terre	Université du Québec á Montréal, cp 8888, succ. 'Centre-Ville', Montréal, Canada H3C 3P8, Canada	gauthier.michel@uqam.ca
Gautneb, Håvard	Geological Survey of Norway	N-7491 Trondheim, Norway	Havard.Gautneb@ngu.no
Gursky, Dmitry	Ukr. Sat. Geol. Research Institute	Avtozavodskaia st. 78, UA-04114, Kyiv, Ukraine	ukrdgri@geologiya.com.ua
Hagen, Ragnar	Titania A/S	N-4380 Hauge i Dalane, Norway	ragnar.hagen@nli-usa.com
Hannah, Judith	AIRIE Program, Colorado State University	Department of Earth, Fort Collins, CO 80523-1482, USA	
Hellström, Fredrik	Göteborg University, Department of Earth Sciences, Geology	Box 460, S-40530 Göteborg, Sweden	fredrik@gvc.gu.se

Holloker, Kurt	Union College	Union College, Schenectady, N.Y., USA	
Hunt, Amelia	Grant Institute of Geology and Geophysics, University of Edinburgh	42 Craigmillar Park, Edinburgh, EH16 5PS, UK	a.g.hunt@sms.ed.ac.uk
Kärkkäinen, Niilo	Geological Survey of Finland	Betonimiehenkuja 4, FIN-02151 Espoo, Finland	niilo.karkkainen@gsf.fi
Korneliussen, Are	Geological Survey of Norway	N-7491 Trondheim, Norway	are.korneliussen@ngu.no
Kryvdik, Stepan	Instiute of Geochemistry, Mineralogy and Ore Formation	03680 Palladin Pr., 34 Kyiv-142, Kyiv, Ukraine	igmof@mail.kar.net
Kullerud, Kåre	Department of Geology, University of Tromsø	Dramsveien 201, N-9037 Tromsø	kaarek@ibg.uit.no
Latypov, Rais	University of Oulu	Institute of Geosciences, P.O. Box 3000, FIN - 90014, University of Oulu, Finland	Rais.Latypov@oulu.fi
Lindsley, Donald H.	Department of Geosciences	State University of New York at Stony Brook, Stony Brook, NY 11794-2100, USA	donald.lindsley@sunysb.edu
Maijer, K	Utrecht University	Muntstraat 30, NL-3961 AL Wijk bij Duurstede, Netherland	
Marker, Mogens	Geological Survey of Norway	N-7491 Trondheim, Norway	Mogens.Marker@ngu.no
McEnroe, Suzanne	Geological Survey of Norway	N-7491 Trondheim, Norway	Suzanne.McEnroe@ngu.no
McLimans, Roger	DuPont	104 Jackson Laboratory, DuPont Chambers Works, Deepwater, NJ08023, USA	Roger.K.McLimans@usa.dupont.com
Meyer, Gurli	Geological Survey of Norway	N-7491 Trondheim, Norway	Gurli.Meyer@ngu.no
Mitrokhin, Alexander	Geological faculty of Kyiv University	Vasilkovskaya st., 94, Kyiv, Ukraine	mitr@mail.univ.kiev.ua
Morisset, Caroline-Emmanuelle	Université de Liège/Université du Québéc á Montréal	rue Longienne, 1, 4000 Liège, Belgium	caromorisset@hotmail.com
Nechaev, Sergey	Ukr. St. Geol. Research Institute	Avtozavodskaia st. 78, Ua-04114 Kyiv, Ukraine	hydro@ukrnet.net
Perreault, Serge	Ministére des Ressources Naturelles du Québec Géologie Québec	456, avenue Arnaud, local 1.04, Sept-Îles (Québec), Canada G4R 3B1, Canada	serge.perreault@mrn.gouv.qc.ca
Ponomarenko, Oleksandr	Institute of Geochemistry, Mineralogy and Ore Formation, NAS	03680 Palladin Pr., 34 Kyiv-142, Kyiv, Ukraine	pan@cki.ipri.kiev.ua
Raaness, Agnes M.	NTNU	Dr. Sands v. 13, 7052 Trondheim, Norway	raaness@pvv.ntnu.no
Robins, Brian	University of Bergen, Department og Geology	Allégt. 41, N-5007 Bergen, Norway	brian.robins@geol.uib.no
Robinson, Peter	Geological Survey of Norway	N-7491 Trondheim, Norway	Peter.Robinson@ngu.no
Schiellerup, Henrik	Geological Survey of Norway	N-7491, Trondheim, Norway	henrik.schiellerup@geo.ntnu.no

Schumacher, John C.	University of Bristol	Dept. of Earth Sciences, Wills Memorial Building, Queen's Road, Bristol BS8 1RJ, UK	j.c.schumacher@bristol.ac.uk
Shnyukov, Sergey E.	Kiev University	Mineralogical, Geochemical and Analytical Research Centre, Department of Geology, Kiev National Taras Shevchenko University, 90 Vasylkivska, Kiev, 03022, Ukraine	shnyukov@mail.univ.kiev.ua
Shumlyanskyy, Leonid	Kyiv University	P.O.Box 291, Kyiv 01001, Ukraine	lshum@mail.univ.kiev.ua
Skjerlie, Kjell-Petter	Department of Geology, University of Tromsø	Dramsveien 201, N-9037 Tromsø	Kjell@ibg.uit.no
Skobelev, Vladamir	Institute of Geochemistry, Mineralogy and Ore Formation, NAS	03680 Palladin Pr., 34 Kyiv-142, Kyiv, Ukraine	skobvm@i.com.ua
Stanaway, Kerry J.	Rio Tinto Iron and Titanium	770 Sherbrooke St Quest #1800, Montreal Quebec H3A 1G1, Canada	kerry.stanaway@rtit.com
Stein, Holly	AIRIE Program, Colorado State University	Department of Earth Resources, Colorado State University Fort Collins, CO 80523-1482 USA	hstein@cnr.colostate.edu
Stepanov, Vladimir	Institute of Geology Karelian Research Centre	Pushkinskaya St., 11, Petrozavodsk, Karelia, 185610, Russia	vladimir.stepanov@krc.karelia.ru
Stepanyuk, Leonid M.	Institute of Geochemistry, Mineralogy and Ore Formation, NAS	03680 Palladin Pr., 34 Kyiv-142, Kyiv, Ukraine	skobvm@i.com.ua
Sukhanov, Mikhail		Institute of Geology of Ore Deposits, Petrography, Mineralogy and Geochemistry of Russian Academy of Sciences, Moscow 109017, Staromonetny 35, Russia	anorth@igem.ru
Tegner, Christian	Geological Survey of Norway	N-7491 Trondheim, Norway	Christian.tegner@ngu.no
Terry, Michael P.	Old Dominion University	Old Dominion University, Norfolk, VA, USA	
Vander Auwera, Jacqueline	Universite de Liege	Geology (B20) - Sart Tilman, 4000 Liége, Belgium	jvdauwera@ulg.ac.be
Vrålstad, Tore	Norsk Hydro ASA, Hydro Agri, Operational support	0240 Oslo, Norway	Tore.Vralstad@hydro.com
Wilson, J. Richard	Department of Earth Sciences	University of Aarhus, 8000 Århus C, Denmark	jrw@geo.aau.dk
Wiszniewska, Janina	Polish Geologial Institute	4, Rakowiecka str., 00-975 Warszawa, Poland	jwis@pgi.waw.pl
Zagnitko, Vasyl	Instiute of Geochemistry, Mineralogy and Ore Formation, NAS	03680 Palladin Pr., 34 Kyiv-142, Kyiv, Ukraine	igmof@mail.kar.net

Andersen T, Griffin WL, Pearson NJ & Andresen A:

Sveconorwegian rejuvenation of the lower crust in South Norway

Tom Andersen[1], William L. Griffin[2], Norman J. Pearson[2] & Arild Andresen[3]
[1] Laboratorium for isotopgeologi (MGM-lab), Geologisk museum, Sars gate 1, N-0562 Oslo, Norway. [2] GEMOC, Department of Earth and Planetary Sciences, Macquarie University, Sydney NSW 2109, Australia. [3] Institutt for geologi, Postboks 1047 Blindern, N-0316 Oslo, Norway

Recent Re-Os isotope data on the c. 0.93 Ga Rogaland Igneous Complex (RIC) suggest an origin by partial melting of a mafic, lower crustal protolith, without a contribution of mantle-derived Sveconorwegian material (Schiellerup et al. 2000). Without challenging this conclusion, it should be noted that there is ample evidence of mafic magmatism in south Norway during the Sveconorwegian period (e.g. Munz and Morvik 1991, Haas et al. 2000), which suggests that rejuvenation of the lower continental crust by underplating of mantle-derived magmas could have taken place. The emplacement of the anorthosites and assoicated rocks of the RIC corresponds in time to a widespread event of posttectonic, A-type granitic magmatism in SW Scandinavia, which gives an opportunity to map the distribution of deep crustal components across this part of the Baltic Shield (Andersen and Knudsen 2000). Sr, Nd and Pb isotope data on late Sveconorwegian granites suggest that they define mixing trends between crustal components and a component with a juvenile isotopic signature (Andersen et al. 2001a). As pointed out by Andersen (1997) and Schiellerup et al. (2000), the presence of an endmember with a positive epsilon Nd does not necessarily indicate that mantle-derived magmas were injected into the crust at the time of deep crustal melting; in fact, such a component may reside in mafic rocks within the deep crust for several hundered million years without totally loosing its depleted mantle Nd isotopic signature.

The hafnium isotope composition of zircon in an ingeous rock is a powerful tracer of interaction between the mantle and the lower crust in the past. New laser ablation ICP-MS hafnium isotope data on zircons in Proterozoic granitoids from south Norway allows a better characterization of crustal protoliths in south Norway than has previously been possible, and also provide a definitive test on the presence or absence of Sveconorwegian, mantle-derived material in the deep crust of the southwestern part of the Baltic Shield.

In terms of Hf isotope systematics, two distinct, pre-Sveconorwegian crustal components can be recognized in south Norway:

i: A Paleoproterozoic component, characterized by depleted mantle Hf isotope model ages (t_{HfM}) > 1.80 Ga. This component resides in the granitoids of the 1.65-1.83 Ga Trans-scandinavian Igneous Belt (TIB). U-Pb ages and Hf isotope data on detrital zircons from clastic metasediments indicate that equivalent rocks were present in the source region(s) of Proterozoic sediments in the Telemark and Bamble sectors (Haas et al. 1999), and Sr, Nd and Pb data on late Sveconorwegian granites suggest that a similar component can be traced in the deep crust from the area east of the Oslo Rift, across south Norway to the area west of the Mandal-Ustaoset shear zone (Andersen et al. 2001a). In late Sveconorwegian time, the Paleoproterozoic crustal component is characterized by a very distinct hafnium isotope composition, with $^{176}Hf/^{177}Hf \leq 0.2819$ (Fig. 1).

ii: A Mesoproterozoic component with t_{HfM} in the range *1.6-1.7 Ga*, residing in 1.52-1.60 (-1.66 ?) Ga calcalkaline, metaigneous rocks. These rocks are the products of subduction-related magmatism along the SW margin of the Baltic Shield, and can be traced from SW Sweden, across the Oslo Rift and as far as the southwesternmost part of the Bamble Sector (Andersen et al. 2001b). Both juvenile, mantle-derived material and material with a crustal

prehistory were involved in the petrogenesis of these rocks, whose Hf isotope composition in late Sveconorwegian time spans a narrow range at $^{176}Hf/^{177}Hf \approx 0.28215$ (Fig. 1).

A juvenile, depleted-mantle component, was involved in the formation of the Mesoproterozoic calcalkaline rocks, and may later have contributed to the lower crust in one or more underplating event(s). The Hf isotopic composition of a depleted mantle reservoir in Sveconorwegian time can be given by $^{176}Hf/^{177}Hf > 0.28245$ (Fig. 1).

Figure 1 shows accumulated probability distribution curves of initial $^{176}Hf/^{177}Hf$ ratios of suites of single zircons separated from Sveconorwegian granitoids. All three groups shown give broad distribution curves, which suggest that the zircons crystallized from inhomogeneous magmas, comprising components from several distinct sources. Whereas the low-$^{176}Hf/^{177}Hf$ parts of the ranges observed suggest the involvement of a Paleoprotorozoic crustal component, a significant proportion of the zircons separated from the granitoids show more radiogenic $^{176}Hf/^{177}Hf$ than the Mesoprotoerozoic crustal component. This indicates the involvement of Sveconorwegian, mantle derived material in the petrogenesis of these rocks.

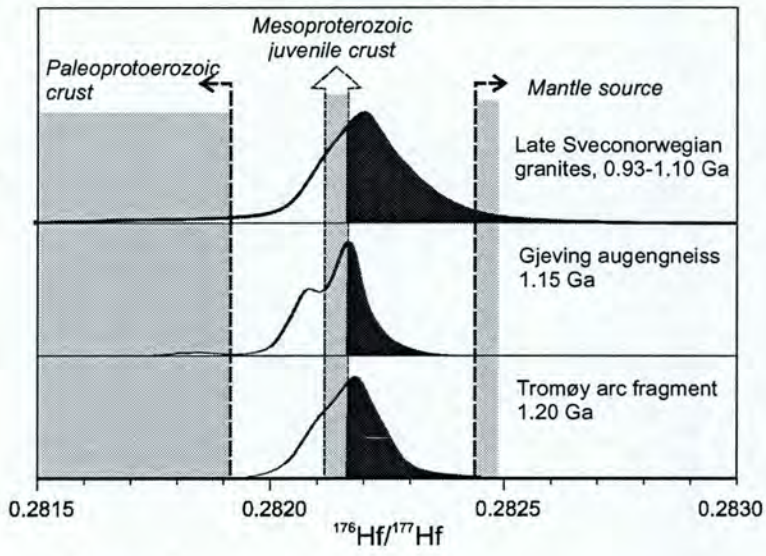

Figure 1

Acumulated probability plots of time-corrected $^{176}Hf/^{177}Hf$ of zircons from Sveconorwegian granitoids from south Norway, compared to regional hafnium components. The black parts of the distribution curves represent zircons which cannot have crystallized from a magma formed only from the regional, crustal protoliths, and which therefore require the presence of a Sveconorwegian, mantle-derived component in the lower crust.

The Tromøy complex is a fragment of a Sveconorwegian oceanic island arc system, accreted onto the Baltic Shield prior to granulite-facies metamorphism at c. 1.10 Ga (Knudsen and Andersen 1999). The mantle-derived component in these rocks was introduced in the island-arc setting, and does not give evidence of underplating of the continental crust. On the other hand, both the 1.15 Ga augengneiss and the 0.93-1.10 Ga granites were emplaced within the continent, and the presence of a significant component of mantle-derived hafnium in their zircons is a clear indication that the granitic magmas did not form by simple remelting of a Mesoprotoerozoic, deep crustal protolith. Input of mantle-derived material to the lower crust during the Sveconorwegian period is thus necessary to account for the initial Hf isotope characteristics of these rocks.

References

Andersen, T. 1997: Radiogenic isotope systematics of the Herefoss granite, South Norway: an indicator of Sveconorwegian (Grenvillian) crustal evolution in the Baltic Shield. Chem. Geol., 135, 139-158.

Andersen, T. and Knudsen, T.-L. 2000: Crustal contaminants in the Permian Oslo Rift, South Norway: Constraints from Precambrian geochemistry. Lithos, 53, 247-264.

Andersen, T., Andresen, A. and Sylvester, A.G. 2001a. Nature and distribution of deep crustal reservoirs in the southwestern part of the Baltic Shield: Evidence from Nd, Sr and Pb isotope data on late Sveconorwegian granites. Journal of the Geological Society, London, in press.

Andersen, T., Griffin, W.L., Jackson, S.E. and Knudsen, T.-L. 2001b. Timing of mid-Proterozoic calcalkaline magmatism across the Oslo Rift: Implications for the evolution of the southwestern margin of the Baltic Shield. Geonytt 2001, 1, 25.
Haas, G.J.L.M. de, Andersen, T. and Nijland, T.J. 2000. Mid-Proterozoic evolution of the South Norwegian lithosphere. Geonytt 2000, 1, 56.
Haas, G.J.L.M. de, Andersen, T. and Vestin, J. 1999. Application of detrital zircon geochronology to assembly of a Proterozoic terrain – an example from the Baltic Shield. Journal of Geology, 107, 569-586.
Knudsen, T.L. and Andersen, T., 1999. Petrology and geochemistry of the Tromøy calc-alkaline gneiss complex, South Norway, an alleged example of Proterozoic depleted lower continental crust. *Journal of Petrology*, 40, 909-933.
Munz, I.A. and Morvik, R. 1991. Metagabbros in the Modum complex, southern Norway: an important heat source for Sveconorwegian metamorphism. Precambrian Research 52, 97-113. Corrigendum: Precambrian Research 53, 305.
Schiellerup, H., Lambert, D.D., Prestvik, T., Robins, B., McBride, J.S. and Larsen, R.B. 2000. Re-Os isotopic evidence for a lower crustal origin of massive-type anorthosites. Nature 405, 781-784.

Belevtsev AR, Belevtsev RY, Golub EN, Spivak SD & Yakovlev BG:

The Korosten Gabbro-Anorthosite Complex, Ukrainian Shield: physical and chemical conditions of genesis

Belevtsev A.R., Belevtsev R.Ya., Golub E.N., Spivak S.D. & Yakovlev B.G.

1. The large Korosten pluton (about 100 km in diameter) is precisely isolated in the Northwest part of the Ukrainian shield (USh), due to availability of the peculiar complex of magmatic rocks – granite-rapakivi, gabbro-norite and anorthosite, which formation 1800-1750 Ma ago finished the Ush consolidation as a stable segment of the Precambrian continental terrestrial crust, though the thermal and tectonic activity of the Korosten pluton had been proceeded up to 1300 Ma.

Basic rocks – gabbro-norite, anorthosite, gabbro, pyroxenites occupy 25-30 % square of Korosten pluton and compose the two large massifs: Volodar-Volyn' massif in the Southwest part of the pluton, Chepovichy massif – in the centre of the pluton, and small Fedorov massif in the Southeast part of the pluton. Rocks of the pluton practically are not affected by plastic deformations and dynamic-thermal metamorphism.

In magmatic basic rocks the lamination and oriented textures of magmatic flow are marked. The deep structure of the pluton, after geophysical data, is determined by presence of subhorizontal rather low-thick (1-2 km) bodies of basic rocks in granitic crust.

2. Petrographical and petrochemical indications of rocks

These is characteristic mineral paragenesis of basic rocks: plagioclase + augite + inverted pigeonite + olivine + ilmenite + hornblende + apatite, less often biotite, orthoclase, quartz, cummingtonite, magnetite. An essential indications of basic rocks (gabbro-norite and anorthosite) are their high iron content (*F = 60-70 %) and titanium content. Typical mafic minerals of basic rocks are ferruginous inverted pigeonite, augite and olivine. Augite is depleted by aluminium oxide (0,4- 0,7 %). On the AFM diagram the basic rocks situate mostly in the area of ferruginous tholeiite, and granites – ferruginous granite, being drawed up on the line similar to the trend of differentiation of the Bushweld type tholeiitic magma. On

the petrochemical diagrams monzonites fill the gap between composition of gabbroides and granites of the pluton.

3. PT-conditions of gabbroides formation

Temperature. The difference between liquidus and solidus temperature of basic magma is considerable by low iron content and practically disappears at ferruginous magma. Temperature of solidus (cotectic) crystallization of medium ferruginous gabbroides in waterless conditions is 1170-1150°C, and at ferruginous gabbroides (F = 60-75) about 1100-1050°C. The presence of water reduces T of basic magma crystallization, for example, by P_{H2O} = 100 МПа it decrease at 100-150°C. Availability of the ferruginous inverted pigeonite in gabbroides corresponds to the temperature of pyroxene equilibrium not less than 850-900°C. The temperature of two-pyroxene equilibrium in gabbro-norite by geothermometers is 850-900°C, seldom being lowered to 800°C (in monzonites). The temperature of plagioclase-amphibole equilibrium in gabbroides is 600-800°C.

Pressure of water. Some indirect data, such as plagioclase/mafic minerals relation in gabbro-norite, the presence of differentiations of basic magma – labradorites and ultramafites, and also porphyry plagioclase segregations testify to dryness of tholeiitic magma – initial magma of basic rocks of the Korosten pluton. At the same time gabbroides frequently contain the high-temperature brown hornblende as porphyroblast, and as inclusions in pyroxene and plagioclase. The most probable, the pressure of water by gabbroides crystallization was small (less than 50 MPa), and T of crystallization of ferruginous tholeiitic magma was about 1000-1100°C. The temperature of autometamorphism and two-pyroxene equilibrium is 800-900°, and plagioclase-hornblende equilibrium – 600-800°C.

General pressure of equilibrium crystallization of the Korosten pluton rocks was minor (no more than 100 MPa). To it testify the low aluminium content in augite (0,4 - 0,7 %), the presence of andalusite in aluminiferous rocks, and also fayalite and quartz association in basic rocks, monzonites and granites. General pressure by olivine-hypersthene geobarometer in rocks of the Korosten pluton is 200±50 MPa. This pressure corresponds to depth of 5-10 km. The formation of basic rocks occurred in rather reduction conditions, to what the presence of fayalite, essential ilmenite prevalence above magnetite and low content of hematite component in ilmenite (no more than 3-5%) testify. Pure ilmenite without hematite impurity predominates, that corresponds to the oxygen magnetite-wustite buffer or even to wustite area, that testifies to a significant role in fluid, equilibrium with basic magma, reduction gases – hydrogen, methane etc.

4. Kinetics of magmatism

The initial stages of the pluton petrogenesis, connected to early intrusions of basic rocks, total heating and melting of acid rocks of the ancient continental crust, are not reflected by isotope dating of the pluton rocks, which mainly fixes the last phases of magmatic process and postmagmatic recrystallization. For cooling down a such large pluton as Korosten on 200°C it is necessary not less than 5-10 Ma. Real duration of the pluton cooling down from 800-900°C to 500-600°C – 30-50 Ma. The duration of progressive heating and period of maximum temperatures isn't known. Probable period of the pluton formation is from 2000 to 1750 Ma, i.e. about 250 Ma.

5. Petrogenetic model of the Korosten pluton

Pluton was generated on place of "hotspot" in mantle, through which the basic magma, heat and fluids moved into continental crust. The form of the pluton is funnel-shaped – as an inverted cone.

In the pluton structure there are two main components – granite matrix and subhorizontal bodies of basic rocks from 1-2 to 5-6 km in thickness. These bodies are traced in the whole pluton section and make up to 30 % of its volume. The subhorizontal bodies of basic rocks represented a system of magmatic chambers, here the composition of tholeiitic magma was naturally changed as a result of magmatic differentiation – upwards the iron content in magma increases and basicity decreases both on the whole pluton section, and within the limits of each intrusive body.

The dynamics of basic magma was rather active in the period of its rising from mantle, and magmatic flowing in magma differentiation.

6. Prospecting of the ore mineralization

Prospecting of the ore mineralization of the pluton are mainly connected to the tholeiitic magma differentiation in subhorizontal intrusions. Primary tholeiitic magma, generated in mantle, have the high iron content (F = 20-40), and it, being lifted in terrestrial crust, is differentiated in magmatic chambers. Differentiated and laminated large subhorizontal intrusive bodies of tholeiitic magma may contain the platinum, chromium, titanium, nickel, cobalt and copper deposits. The magnitude of such ore deposits depends on size of intrusions, which on Korosten pluton are quite considerable. One of the most perspective area for detail searches can be southwest margin of the Korosten pluton, located at 5-10 km from the boundary of the Volodar-Volyn' gabbroides massif. There is on geophysical data a large anomaly of gravity, which connected to the large gabbroides massif. It's rather probable, that this massif contains a laminated magnesium ore-bearing complex.

* Note: $F = FeO+Fe_2O_3/MgO+FeO+Fe_2O_3$

Bingen B, Austrheim H & Whitehouse M:

Ilmenite–zircon relationships in meta-anorthosites. Example from the Bergen Arc (Caledonides of W Norway) and implications for zircon geochronology

Bernard Bingen [1], Håkon Austrheim [2], Martin Whitehouse [3]
[1] Geological Survey of Norway, 7491 Trondheim, Norway. [2] Mineralogisk Geologisk Museum, University of Oslo, 0562 Oslo, Norway. [3] Swedish Museum of Natural History, SE-104 05 Stockholm, Sweden

The Proterozoic Lindås Nappe is situated in the Caledonides of W Norway and mainly made of a Proterozoic anorthosite–charnockite complex. It was affected by penetrative Sveconorwegian granulite-facies metamorphism, followed by a fluid-driven eclogite- and amphibolite-facies Caledonian overprint. This overprint is spatially restricted along fractures and shear zones (Austrheim & Griffin, 1985; Cohen et al., 1988; Jamtveit et al., 1990; Boundy et al., 1992; Boundy et al., 1996; Austrheim et al., 1997; Bingen et al., 2001b). In this study, formation of metamorphic zircon was investigated in mafic lithologies. Petrographic observations with optical microscopy, backscattered electron imaging and cathodoluminescence imaging were realized in thin section of whole-rocks and polished mount of zircon separates. SIMS analyses (Cameca IMS1270) were realized on zircon for age determination and estimation of trace element concentrations (Th and REEs).

In mafic granulites and amphibolites, a luminescent anhedral zircon overgrowth surrounds a magmatic zoned core. The overgrowth gives an average age of 924 +/- 58 Ma with a Th/U = 0.52 and the magmatic core gives an age of 952 +/- 32 Ma with a Th/U = 1.27. The REE pattern of zircon in a two-pyroxene granulite displays a Ce positive anomaly and enrichment in HREE. The REE pattern of the luminescent overgrowth is parallel to the one of the magmatic core, but is characterized by distinctly lower concentrations. In the granulites, a continuous rim of zircon or a discontinuous corona of ca. 10 µm rounded to flat zircon crystals is commonly observed in thin section at the outer margin of ilmenite grains. Baddeleyite (ZrO2) and srilankite (Ti2ZrO6) blebs are reported around ilmenite included in feldspar or pyroxene. Baddeleyite is interpreted as an exsolution product from magmatic ilmenite. Srilankite was probably formed as a reaction product between ilmenite and baddeleyite during granulite-facies metamorphism in silica deficient subsystems. The zircon corona around ilmenite and the luminescent zircon overgrowth were also formed as a reaction product during granulite-facies metamorphism, where silica was available at grain boundaries. Textures suggest that magmatic ilmenite was a main source of Zr to form metamorphic zircon (Bingen et al., 2001a).

In massive amphibolites, relic ilmenite grains are surrounded by a corona of titanite and a discontinuous corona of micro-zircons. Amphibolite-facies overprint is not associated with any significant growth or dissolution of zircon.

An unsheared eclogite displays a zircon population with an euhedral oscillatory-zoned overgrowth showing well-terminated edges and tips. The overgrowth yields an age of 424 +/- 5 Ma (weighted average of 31 analyses). It is characterized by a Th/U ratio lower than 0.13, a Ce positive anomaly and an enrichment in HREE. The REE pattern of the overgrowth is not significantly different from the one of the Proterozoic core, although some of the analyses of the overgrowth are specifically poor in all trace elements. In thin section, a corona of micro-zircon grains is observed at some distance around rutile, and locally these micro-zircons show a prismatic overgrowth. The specific low-Th zircon growth event is related to eclogite-facies forming reactions, involving breakdown of a two-pyroxene + garnet + plagioclase + ilmenite assemblage to form a garnet + omphacite + rutile assemblage in the presence of a fluid. The low Th content of this zircon probably stems from the coeval precipitation of clinozoisite. This oscillatory zoned zircon records fluid infiltration and coeval Caledonian eclogitization in the crust.

References

Austrheim, H., Erambert, M., and Engvik, A.K. (1997) Processing of crust in the root of the Caledonian continental collision zone: the role of eclogitization. Tectonophysics, 273, 129–153.

Austrheim, H., and Griffin, W.L. (1985) Shear deformation and eclogite formation within granulite-facies anorthosites of the Bergen Arcs, western Norway. Chemical Geology, 50, 267–281.

Bingen, B., Austrheim, H., and Whitehouse, M. (2001a) Ilmenite as a source for zirconium during high-grade metamorphism? Textural evidence from the Caledonides of W. Norway and implications for zircon geochronology. Journal of Petrology, 42, 355–375.

Bingen, B., Davis, W.J., and Austrheim, H. (2001b) Zircon U-Pb geochronology in the Bergen Arc eclogites and their Proterozoic protoliths, and implications for the pre-Scandian evolution of the Caledonides in western Norway. Geological Society of America Bulletin, 113, 640–649.

Boundy, T.M., Essene, E.J., Hall, C.M., Austrheim, H., and Halliday, A.N. (1996) Rapid exhumation of lower crust during continent-continent collision and late extension: evidence from 40Ar/39Ar incremental heating of hornblendes and muscovites, Caledonian orogen, western Norway. Geological Society of America Bulletin, 108, 1425–1437.

Boundy, T.M., Fountain, D.M., and Austrheim, H. (1992) Structural development and petrofabrics of eclogite facies shear zones in the granulite facies complex, Bergen Arcs, W Norway: implications for deep crustal deformational processes. Journal of Metamorphic Geology, 10, 127–146.

Cohen, A.S., O'Nions, R.K., Siegenthaler, R., and Griffin, W.L. (1988) Chronology of the pressure-temperature history recorded by a granulite terrain. Contributions to Mineralogy and Petrology, 98, 303–311.

Jamtveit, B., Bucher-Nurminen, K., and Austrheim, H. (1990) Fluid controlled eclogitization of granulites in deep crustal shear zones, Bergen arcs, Western Norway. Contributions to Mineralogy and Petrology, 104, 184–193.

Bingen B & Stein H:

Re-Os dating of the Ørsdalen W–Mo district in Rogaland, S Norway, and its relationship to Sveconorwegian high-grade metamorphism

Bernard Bingen [1] & Holly Stein [1,2]
[1] Geological Survey of Norway, Leiv Eirikssons vei 39, 7491 Trondheim, Norway (bernard.bingen@ngu.no)
[2] AIRIE Program, Department of Earth Resources, Colorado State University, Fort Collins, CO 80523-1482 USA (hstein@cnr.colostate.edu)

In the Rogaland–Vest Agder sector of the Sveconorwegian orogen (S Norway), a granulite-facies metamorphic domain is exposed around the 931 ± 3 Ma Rogaland anorthosite complex (Duchesne et al., 1985; Schärer et al., 1996). This domain is characterized by a succession of three main isograds with increasing grade towards the west: the orthopyroxene isograd in leucocratic rocks, the osumilite isograd in paragneiss, and the pigeonite isograd in leucocratic rocks (Tobi et al., 1985). The osumilite- and pigeonite-isograds are indicative of very high-temperature and dry conditions. Osumilite-bearing assemblages provide P–T estimates of 5.5 kbar–800-850°C (Holland et al., 1996). There is little doubt that osumilite-bearing assemblages developed as a result of granulite-facies contact metamorphism related to the intrusion of the anorthosite complex (M2 metamorphism), as the osumilite isograd is parallel to the external contact of the plutonic complex. Available petrological data and geochronological data on monazite in the region nevertheless point to high-grade metamorphism, possibly in granulite-facies conditions, before the intrusion of the anorthosite complex (M1 metamorphism) (Tobi et al., 1985; Bingen & van Breemen, 1998). In this work, we use the Re-Os chronometer applied to molybdenite hosted in small metamorphic deposits, to further explore the geochronology of polyphase metamorphism in Rogaland.

Reliable and precise ages for molybdenite crystallization can be obtained by the Re–Os method using improved analytical methods (Markey et al., 1998). The Re–Os chronometer applied to molybdenite has been shown to maintain its systematics through high-grade metamorphism (Stein et al., 1998; Raith and Stein, 2000). The method is thus suitable for obtaining primary ages of molybdenite deposition, regardless of metamorphic overprinting. Among the small molybdenite-bearing deposits in Rogaland, the Ørsdalen district was mined for wolframite, scheelite, and molybdenite between 1904 and 1921. It is located between the orthopyroxene and osumilite isograds. It occurs in a granitic to granodioritic gneiss unit that commonly contains metamorphic garnet and/or orthopyroxene. The mineralized zone is restricted to two ca. 50 m thick layers. The layers show amphibolite lenses and contain thin (<1 m) glassy quartz + feldspar leucocratic veins, both elongate parallel to the gneiss foliation (Heier, 1955; 1956; Urban, 1971; 1974; Olerud, 1980). The mineralization is closely associated with the quartz-rich veins.

Samples were collected at the Mjåvassknuten (MJ samples, also called Strossekrater) and Stopulen (ST samples, also called Sandness) prospects, situated along the two mineralized layers. Sample NO00-MJ1 is taken from irregular, coarse-grained, glassy quartz + plagioclase + orthoclase leucocratic masses that are associated with a fine-grained and dark-coloured granulite, rich in brown-red biotite. Both the leucocratic masses and the host contain disseminated dark red garnet and orthopyroxene (up to 1 cm orthopyroxene crystals in the leucocratic masses). Molybdenite occurs as clots and patches larger than 1 cm that are made of fine- to coarse-grained crystals. It is dominantly hosted in the leucocratic masses and associated with scheelite. Molybdenite, biotite and Fe-Ti oxide minerals are commonly surrounded by a fine-grained symplectite of garnet + quartz. Samples NO00-MJ2 and -ST1 are from concordant, clear, glassy quartz-rich veins in biotite gneiss. The molybdenite is concentrated along vein margins as mm to cm-sized blebs to stringers.

The Re-Os data for the three molybdenite samples are presented in Table 1 and Figure 1, and their model ages all overlap at the 2-sigma level of uncertainty. The data set includes a replicate run and model age for MJ2. Their weighted mean model age is 971.4 ± 3.6 Ma. Together, the four age determinations provide a 2-sigma Model 3 isochron age (Ludwig, 1999) of 973.3 ± 8.2 Ma with the expected zero initial ^{187}Os of -0.10 ± 0.88. Inclusion of the zero point, implicit in Re–Os model ages for molybdenite and in the plotting of molybdenite data in ^{187}Re-^{187}Os space, provides a Model 3 age of 972.9 ± 3.8 Ma.

Table 1: Re-Os data and ages for the Mjåvassknuten and Stopulen W-Mo prospects, Ørsdalen district (Rogaland), Southern Norway

AIRIE Run[1]	Sample No.	Re, ppm[2,3]	^{187}Re, ppm[2,3]	^{187}Os, ppb[2,3]	Age, Ma[4,5]
Mjåvassknuten					
CT-301	NW00-MJ1	9.846 (6)	6.188 (4)	100.9 (2)	970 ± 3
CT-308	NW00-MJ2	12.834 (9)	8.066 (6)	131.96 (7)	974 ± 3
CT-313	NW00-MJ2	12.242 (8)	7.694 (5)	125.63 (7)	972 ± 3
Stopulen					
CT-323	NW00-ST1	1.1131 (8)	0.6996 (5)	11.385 (6)	969 ± 3

[1] All analyses are by Carius tube dissolution (CT), and were made over a period of three months.
[2] Re and ^{187}Os uncertainties are absolute at 2□ for last digit indicated; percent error in Re and ^{187}Os concentrations are 0.066 to 0.070% and 0.05 to 0.15%, respectively.
[3] Blank corrections for molybdenites are insignificant; molybdenite laboratory blanks are Re = 17-18 pg, and Os = 6-8 pg with a variable $^{187}Os/^{188}Os$ ranging from 0.5 to 8.3.
[4] Uncertainties include error in (1) ^{185}Re and ^{190}Os spike calibrations, 0.05% and 0.15%, respectively, (2) magnification with spiking, (3) mass spectrometric measurement of isotopic ratios, and (4) the ^{187}Re decay constant (0.31%).
[5] Ages are calculated by $^{187}Os = {}^{187}Re\ (e^{\square t} - 1)$ where □ = ^{187}Re decay constant and t = age; ^{187}Re decay constant used is 1.666×10^{-11} yr^{-1} with an uncertainty of 0.31% (Smoliar et al., 1996).

The agreement of four Re-Os ages using three different samples is a clear verification of a robust Re-Os chronometer in molybdenite, and points to an event of deposition of molybdenite at about 973-971 Ma. This age is younger than any possible deposition age or magmatic crystallization age for the amphibolite lenses associated with the deposit. A presumably Mesoproterozoic stratiform volcanogenic origin for the deposit, as proposed by Urban (1971; 1974) is thus not supported by the new data. The field and petrographic relations in sample MJ1 (and other similar samples collected at this locality) indicate that the

leucocratic molybdenite-, garnet- and orthopyroxene-bearing quartz + feldspar masses represent veins and pods of partial melt or segregated veins formed during an event of granulite-facies metamorphism. By direct inference, we propose that the molybdenite age of 973–971 Ma is directly related to the formation of the leucocratic veins and pods. This event is related to the granulite-facies metamorphic and deformation event that produced coarse-grained metamorphic assemblages, resulted in a strong foliation in the country rocks and aligned the veins within this foliation. The occurrence of garnet + quartz symplectite around molybdenite shows that the deposit was affected by an event of static high-grade metamorphism after deposition (M2 metamorphism). The Re–Os systematics in molybdenite were not affected by this event.

Figure 1

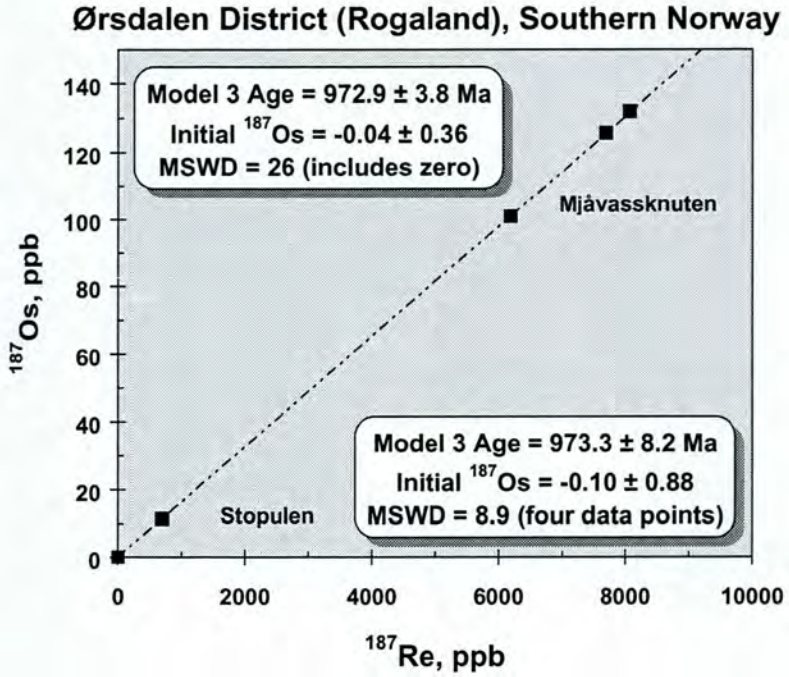

The age of 973–971 Ma for molybdenite deposition lies within the range of Sveconorwegian metamorphism in the orogen. In the easternmost sector of the orogen in SW Sweden, called the Eastern Segment, a high-pressure granulite facies domain with local occurrence of eclogite-facies rocks is described (Möller, 1998). The timing of high-grade metamorphism including eclogite-facies overprint is well constrained between 980 and 960 Ma (Johansson et al., 2001). This metamorphism probably resulted from thrusting of the allochthonous terranes onto the foreland of the orogen. In the westernmost sector of the orogen, in Rogaland, single-grain monazite U–Pb ages define a range between 1024 and 970 Ma for M1 regional metamorphism and between 930 and 925 Ma for M2 contact metamorphism (Bingen and van Breemen, 1998). The occurrence of negatively discordant monazite grains at 970 Ma in some biotite-bearing gneiss samples suggests that the age of 970 Ma is geologically significant and corresponds to crystallization of metamorphic monazite. The new data on the Ørsdalen district point to the formation of mineralized quartz + feldspar granulite-facies veins at 973–971 Ma, and thus give independent evidence that M1 regional metamorphism reached granulite-facies conditions at 973–971 Ma. Available data suggest a protracted nature for M1 metamorphism between ca. 1025 and 970 Ma. They also point to the superposition of two granulite-facies metamorphic events in Rogaland (M1 and M2 events), and that osumilite-bearing mineral associations formed during the second of the two events. Superposition of two granulite-facies events may provide a mechanism to dehydrate a gneiss basement sufficiently for the

development and preservation of osumilite-bearing assemblages, and may be an explanation for the rarity of osumilite-bearing assemblages in granulite-facies terrains.

Acknowledgements
This work was supported by the Geological Survey of Norway and by a Fulbright Senior Research Fellowship to HJS in 2000. The Re-Os analyses were made by Mr. Richard Markey at AIRIE, Colorado State University.

References

Bingen, B., and van Breemen, O. (1998) U–Pb monazite ages in amphibolite- to granulite-facies orthogneisses reflect hydrous mineral breakdown reactions: Sveconorwegian Province of SW Norway. Contributions to Mineralogy and Petrology, 132, 336–353.

Duchesne, J.-C., Maquil, R., and Demaiffe, D. (1985) The Rogaland anorthosites: facts and speculations. In A.C. Tobi, and J.L. Touret, Eds. The deep Proterozoic crust in the north Atlantic provinces, NATO-ASI C158, p. 449–476. Reidel, Dordrecht.

Heier, K. (1955) The Ørsdalen tungsten deposit. Norsk Geologisk Tidsskrift, 35, 69–85.

Heier, K. (1956) The geology of the Ørsdalen district. Rogaland, S. Norway. Norsk Geologisk Tidsskrift, 36, 167–211.

Holland, T.J., Babu, E.V., and Waters, D.J. (1996) Phase relations of osumilite and dehydration melting in pelitic rocks: a simple thermodynamic model for the KFMASH system. Contributions to Mineralogy and Petrology, 124, 383–394.

Johansson, L., Möller, C., and Söderlund, U. (2001) Geochronology of eclogite facies metamorphism in the Sveconorwegian Province of SW Sweden. Precambrian Research, 106, 261–275.

Ludwig, K.R. (1999) User's manual for Isoplot/Ex version 2.02, a geochronological toolkit for Microsoft Excel. Berkeley Geochronology Center Special Pubication, Berkeley, USA.

Markey, R.J., Stein, H.J., and Morgan, J.W. (1998) Highly precise Re–Os dating for molybdenite using alkali fusion and NTIMS. Talanta, 45

Möller, C. (1998) Decompressed eclogites in the Sveconorwegian (-Grenvillian) orogen of SW Sweden: petrology and tectonic implications. Journal of Metamorphic Geology, 16, 641–656.

Olerud, S. (1980) Geologiske og geokjemiske undersøkelser rundt Ørsdalen W–Mo forekomst. Norges geologiske undersøkelse, Trondheim.

Raith, J.G., and Stein, H.J. (2000) Re–Os dating and sulfur isotope composition of molybdenite from tungsten deposits in western Namaqualand, South Africa: Implications for ore genesis and the timing of metamorphism. Mineralium Deposita, 35, 741–753.

Schärer, U., Wilmart, E., and Duchesne, J.-C. (1996) The short duration and anorogenic character of anorthosite magmatism: U–Pb dating of the Rogaland complex, Norway. Earth and Planetary Science Letters, 139, 335–350.

Smoliar, M.I., Walker, R.J., and Morgan, J.W. (1996) Re-Os isotope constraints on the age of Group IIA, IIIA, IVA, and IVB iron meteorites: Science, 271, 1099–1102.

Stein, H.J., Sundblad, K., Markey, R.J., Morgan, J.W., and Motuza, G. (1998) Re-Os ages for Archean molybdenite and pyrite, Kuittila-Kivisuo, Finland and Proterozoic molybdenite, Kabeliai, Lithuania: testing the chronometer in a metamorphic and metasomatic setting. Mineralium Deposita, 33, 329–345.

Tobi, A.C., Hermans, G.A., Maijer, C., and Jansen, J.B.H. (1985) Metamorphic zoning in the high-grade Proterozoic of Rogaland-Vest Agder, SW Norway. In A.C. Tobi, and J.L. Touret, Eds. The deep Proterozoic crust in the north Atlantic provinces, NATO-ASI C158, p. 477–497. Reidel, Dordrecht.

Urban, H. (1971) Zur Kenntnis der schichtgebundenen Wolfram–Molybdän-Vererzung im Örsdalen (Rogaland), Norwegen. Mineralium Deposita, 6, 177–195.

Urban, H. (1974) Zur Kenntnis der präkambrischen, schichtgebundenen Molybdänitvorkommen in Südnorwegen. Geologische Rundschau, 63, 180–190.

Bolle O, Diot H, Lambert JM, Launeau P & Duchesne JC:

Emplacement mechanism of the Tellnes ilmenite deposit (Rogaland, Norway) revealed by a combined magnetic and petrofabric study

Olivier Bolle[1], Hervé Diot[2], Jean-Marc Lambert[1], Patrick Launeau[3], Jean-Clair Duchesne[1]
[1]Université de Liège, Bd. du Rectorat, Bât. B20, B-4000 Sart Tilman, Belgium (obolle@ulg.ac.be)
[2]Université de La Rochelle, Av. M. Crépeau, F-17042 La Rochelle Cedex 01, France
[3]Université de Nantes, 2 rue de la Houssinière, BP 92208, F-44322 Nantes, France

The Tellnes ilmenite deposit (TID) (Sokndal district, Rogaland, Norway) is the second most important ilmenite orebody that is in production in the world today (it represented 5% of the world's TiO_2 production in 1999). This world-class Fe-Ti mineralization consists of an ilmenite norite lens-shaped body (> 400 m x 2700 m), outcroping in the central part of the Åna-Sira anorthosite, one of the main geological units of the Late-Proterozoic Rogaland igneous complex. The TID has an obvious intrusive character, and a time gap of more than 10 Myr separates its emplacement (at 920 ± 3 Ma) from the Åna-Sira anorthosite crystallization (at 932 ± 3 Ma) (U-Pb zircon ages; Schärer *et al.*, 1996). The TID has not suffered regional tectonic reworking and metamorphism, in sharp contrast to many North American occurrences of Fe-Ti deposits associated with anorthosites (Duchesne, 1999). It thus provides a special opportunity to study genetic and structural primary relationships between anorthosites and ilmenite deposits.

To picture the poorly constrained internal structure of the TID, anisotropy of low-field magnetic susceptibility (AMS) (see Borradaile and Henry, 1997 for a recent review) was measured on samples from 49 sites, mainly located in the open-pit dug for the TID working. In agreement with previous petrographical studies (e.g. Gierth and Krause, 1973), the microscopical description of these samples reveals an extremely complex magnetic mineralogy. However, simple considerations based on the variation of the bulk magnetic susceptibility (3.1 to 84.3 mSI in the ore) and determinations of coercivity spectra suggest that magnetic mineralogy in most samples is dominated by large (usually some tens to several hundreds of □m large) grains of magnetite. Measurements of anisotropy of partial anhysteretic remanence (pAARM) (Jackson *et al.*, 1988) in representative ore samples further indicate that AMS is carried mainly by these coarse-grained magnetites: pAARM determined after magnetization in a 0-20 mT window, and assumed to be related to the large magnetite grains, is strikingly coaxial with AMS. The magnetic study was complemented by an image analysis (IA) investigation (based on the intercept method of Launeau and Robin, 1996), performed on about twenty samples. IA demonstrates that the AMS principal axes are parallel to the corresponding shape principal axes of the opaque subfabric (ilmenite ± magnetite ± sulfides), with an angular departure of usually less than 10°. Since the opaque subfabric mimics the petrofabric of the ore, mainly defined by a common shape-preferred orientation of silicate prismatic crystals (plagioclase + orthopyroxene), these results imply that AMS in the TID can be equated with the petrofabric.

The pattern of the magnetic foliations evidenced in the TID depicts the 3D shape of the orebody, i.e. a SE plunging elongated trough whose NE and SW flanks dip SW and NE, respectively, which presents some apophyses, and that ends to the SE in a dyke-like unit. The pattern of the magnetic lineations is relatively homogenous, with a calculated average value at N159° SSE 18°, an orientation strikingly similar to that of the magnetic foliation best axis

(N156° SSE 16°). This N155°-160° SSE 15°-20° axis is interpreted as the average direction of the magma flow during emplacement of the TID in the form of a noritic crystal mush (see also Wilmart *et al.*, 1989). A horsetail splay-shaped network of noritic dykes, connected to the dyke-like SE tip of the TID, probably represents the feeding-zone of the orebody. Hence, a SE to NW lateral spreading of the crystal mush along the average N155°-160° SSE 15°-20° direction can be inferred. The shape of the TID outcrop substantiates that injection of the crystal mush from the SE feeding-zone was favoured by the opening of a dextral weakness-zone in the Åna-Sira anorthosite. A previous activation of this weakness-zone, at 931 ± 5 Ma (Schärer *et al.*, 1996), would have allowed the emplacement of a several-km-long jotunitic dyke (the Tellnes main dyke; Wilmart *et al.*, 1989) to which the TID is associated in a same geological unit.

Borradaile, G.J., Henry, B., 1997. *Earth-Sci. Rev.* **42**, 49-93.
Duchesne, J.C., 1999. *Mineral. Depos.* **34**, 182-198.
Gierth, E., Krause, H., 1973. *Norsk Geol. Tidsskr.* **53**, 359-402.
Jackson, M., Gruber, W., Marvin, J., Banerjee, S.K., 1988. *Geophys. Res. Lett.* **15**, 440-443.
Launeau, P., Robin, P.Y.F., 1996. *Tectonophys.* **267**, 91-119.
Schärer, U., Wilmart, E., Duchesne, J.C., 1996. *Earth Planet. Sci. Lett.* **139**, 335-350.
Wilmart, E., Demaiffe, D., Duchesne, J.C., 1989. *Econ. Geol.* **84**, 1047-1056.

Brown L, McEnroe S & Smethurst M.:

Tectonic setting of the Egersund-Ogna anorthosite, Rogaland, Norway, and the position of Fennoscandia in the Late Proterozoic

Laurie Brown[1], Suzanne McEnroe[2], Mark Smethurst[2]
[1] Dept. Geosciences, Univ. Mass., Amherst MA 01003 USA; [2] Norwegian Geol. Surv., N-7491 Trondheim, Norway (lbrown@geo.umass.edu)

A detailed magnetic study has been undertaken on the Egersund-Ogna anorthosite body of the Rogaland Igneous Complex, southeastern Norway. The anorthosite, with published U-Pb ages of 930 Ma, is part of a larger complex of massif-type anorthosites and the Bjerkreim-Sokndal layered intrusion. Thirteen paleomagnetic sites were collected in the body, representing various parts of the body. Average susceptibilities range from 0.03 to 2.24 x 10-3 SI and NRM intensities range from 0.004 to 1.54 A/m. Corresponding Q values range from 3 to 148 with a mean value of 36, indicating remanent-controlled magnetic anomalies. Remanent directions from all samples are characterized by steep negative inclinations with southwest to northeast variable declinations. Thermal demagnetization reveals square shouldered demagnetization curves, with little or no loss of intensity until 550 or 575° C. Alternating field demagnetization produces a wide range of demagnetization behaviors with mean destructive fields varying from less than 5 mT to greater than 80 mT. There is little evidence of overprinting or secondary components, and all information points to a remanence gained during initial cooling of the anorthosite. Mean directional data for the 13 sites are I = -81.7° and D = 326.8°, a95 = 6.0. Assuming this mean direction represents normal polarity, paleolatitude for southern Fennoscandia at this time is 70°S. The magnetic pole calculated for Egersund-Ogna is at -44° latitude and 198° longitude, in good agreement with earlier poles determined from other Rogaland Igneous Complex rocks. This work supports reconstructions

that place Baltica in high (southern) latitude at approximately 900 Ma. Apparent polar wander paths for Baltica at this time are ambiguous with both clockwise or counter-clockwise loops proposed. These data confirm the presence of mid-latitude poles in the late Proterozoic, but at this point are unable to discern between suggested scenarios.

Cawthorn G:

Genesis of magmatic oxide deposits - a view from the Bushveld Complex

Grant Cawthorn
University of the Witwatersrand, School of Geosciences, University of the Witwatersrand, Private Bag 3, Wits 205, South Africa 065RGC@cosmos.wits.ac.za

The Bushveld Complex has over half the world's chromium and vanadium deposits, contained in numerous oxide-rich layers and, in the case of vanadiferous magnetite, discordant pipes. Their genesis is still enigmatic. Models will be reviewed, highlighting where unresolved problems and contradictory evidence still exist.

Chromitite Layering

Many models exist to explain the origin of chromitite layers, and all explain certain aspects of their geology. However, what is frequently lacking is a quantitative assessment of the envisaged processes, specifically a mass-balance evaluation. Chromitites contain about 45% Cr_2O_3 or 300,000 ppm Cr. Mafic magmas may contain between 100 and 1,000 ppm Cr. Hence, even if every atom of Cr could be extracted from a magma, between 300 and 3,000 units of magma would be needed to make one unit of chromitite. For example, allowing for the density of chromitite being 1.5 times that of a magma, a one metre-thick layer of chromitite would need between 300 and 3,000 metres of magma. However, the supposition that some process could remove every ion of Cr from the magma is obviously invalid, and so very much greater thicknesses of magma need to be involved. It should be recalled also that most layers of chromitite can be traced for many 10s if not 100 km in the east and west Bushveld (and may extend for 300 km if the principle of connectivity of the two limbs is accepted). Processes that can operate on such huge volumes of magma need to be evaluated.

The most widely accepted model for chromitite formation is that of magma mixing. In its earliest form Irvine (1975) suggested that contamination of magma could lower the solubility limit of Cr in a magma and so induce chromite separation (Fig. 1a). This model was superceded (Irvine, 1977) by a variation (Fig. 1b), in which mixing of differentiated magma (C) and primitive magma (A) caused the mixed magma (M) to lie in the chromite stability field. Excess chromite is formed until the magma returns to the cotectic whereupon chromite (0.2%) is joined by other silicate minerals (99.8%). The effect on the Cr budget of the magma as this process occurs can be seen in Fig. 2. The degree of supersaturation of the magma with respect to chromite increases as the difference in MgO content of the mixing magmas also increases. It is for this reason that it has been claimed that near the base of large layered intrusions chromitite layers are not developed, because the resident magma is not very different from the added, primitive magma. However, even for magmas that are very different, the extent of supersaturation may not exceed 100 ppm Cr. If this figure represents the extractable Cr as chromite prior to silicate saturation, a 1 m thick chromitite layer would require the processing of 4,500 metres of magma.

There is a second aspect that also needs to be considered, namely the small-scale field relations. A few chromitite layers have gradational contacts, but most have very sharp contacts (Fig. 3). The mixing process would have to be instantaneous in order to produce such a sharp contact. The mixing of such huge thicknesses of magma over such large horizontal distances so effectively seems extremely difficult to envisage.

The mineral compositions can also give a clue as to the plausibility of this process. In the case of the Bushveld Complex, the parent magma contains 13% MgO and crystallizes orthopyroxene with an mg# of 90. Magmas crystallizing plagioclase in the Upper Critical Zone contain about 7% MgO and crystallize orthopyroxene mg# 82. Mixing of these two magmas ought to produce a mixed magma producing orthopyroxene with mg# about 86. Magmas addition ought to be recognized by reversals in mineral composition. Inspection of the mg# below and above the economically most important, and thickest layer - Lower Group (LG)6 chromitite layer, shows that the composition actually shows a forward jump in mg# not a reversal (Fig. 4).

The extent of crystal settling versus bottom growth in layered complexes remains unresolved. If bottom growth is the mechanism by which layers form, it becomes necessary for Cr to diffuse to the base of the magma column to sustain chromite growth. Diffusion of such huge quantities of Cr as would be needed to produce a 1 m thick layer of chromitite, during which time no other cumulus crystals may form, seems implausible. If crystal settling has taken place, then Stokes Law, with or without the complexities of non-Newtonian behaviour, needs to be applied. Although chromite has a high density, its small grain size relative to silicate grains, makes is unlikely to sink more rapidly than mafic minerals. Hence, the question in producing a chromitite layer reverts to why are there no other silicate minerals growing and sinking while the chromite is accumulating? With reference to Fig. 1, the olivine to chromite ratio at the cotectic is about 99.8 to 0.2. To make a 1 m-thick chromitite layer from a magma on the cotectic would require that 500 m of olivine crystals would have to remain suspended. Hence, the crystal settling model still requires a process that will drive the liquid into the chromite stability field.

An alternative model was originally proposed by Osborn (1980) and has been elaborated upon by Lipin (1993). In this model a pressure increase occurs in the magma chamber. The process can be seen in terms of two phase diagrams of the same system but at different pressures. The stability field of chromite increases with pressure relative to pyroxene and plagioclase (Fig. 5). There is no change in the magma composition, which may lie at the three-phase cotectic, at low pressure, but an increase in pressure causes the magma to lie in the chromite field. Demonstration of pressure changes in magma chambers is hard to prove. However, the fountaining of basic lava, followed by draining of lava lakes over a period of days in active volcanoes demonstrates that pressure can fluctuate at least under volcanoes. The physical mechanism operative within a large magma chamber is harder to postulate. However, if magma is added to the chamber, the sides must expand or the roof be raised. In the latter case, the pressure at the base of the chamber must increase. Alternatively, if the extra load of added magma causes the floor to collapse (Carr et al., 1994), the magma at the base would be subjected to an increase in pressure. If magma at the base is subjected to this increase in pressure chromite saturation could occur. Whether a sufficient column of magma could be affected remains speculative, again emphasising the mass balance problem. However, the effect of pressure can be transmitted everywhere instantaneously within the chamber, and so crystal-sharp boundaries to layers could be envisaged.

It has also been suggested that new magma is added carrying a suspension of chromite crystals, which produce a layer (Eales, 2000). This model begs the question, what process in the deeper magma chamber or source area permitted the formation of such a huge volume of crystals of chromite?

To attempt to reduce the volume problem discussed above, it has also been proposed that the chromite accumulates preferentially near to a feeder and that thickness decreases away from the feeder. It implies that more evolved rock types ought to be present further away from the feeder. However, in the case of the Bushveld chromitite layers no regular change in thickness has been recorded. (Sudden changes in thickness of chromitite layers across features such as the Steelpoort lineament may reflect changes in the volume of magma flowing away on either side of this postulated feeder, but does not support the concept of increased thickness close to feeders.)

As a final salutary note, the initial $^{87}Sr/^{86}Sr$ of one chromitite layer has recently been reported (Schoenberg et al., 1999). Their results are shown in Fig. 6. The high ratio observed in the chromitite layer itself compared to its footwall suggests that massive degrees of crustal contamination has occurred, in line with the original model of Irvine (1975). However, what is more remarkable is that the hanging wall rocks have a ratio that does not show evidence of this contamination. The implication is that the chromitite formed from a large volume of contaminated magma, but that the overlying pyroxenite formed from a magma that did not show this contamination effect.

Magnetitites

While most occurrences of magnetitites are as layers in the Upper Zone of the Bushveld Complex, pipes or almost pure magnetite up to 300 m in diameter and narrow dykes, are also recorded from both the Upper and Main Zones. The layers show a progressive decrease in their V content upward (Fig. 7). Similar models to those for chromitite formation have also been applied to the generation of magnetitite layers. Some of the models may be questioned on similar grounds to those listed above. Other processes and other problems are summarised below.

One unique model that has been applied to magnetitite layers is that of liquid immiscibility. Although immiscible silicate and iron-rich liquids are known to occur and have been demonstrated experimentally, the applicability is questionable. If a dense iron-rich liquid did form it ought to sink into the underlying plagioclase crystal much, and not form a regular planar base (Fig. 8). Further if this dense liquid did accumulate into a planar body, it would not be possible for plagioclase crystals to sink into it to form a gradational upper contact (Fig. 8). Finally, the composition of such immiscible liquids has been shown by Philpotts (1983) to contain only 30% FeO (total). It is hardly of a magnetitite composition, and so still requires that a large proportion of silicate material has to be removed for it to form a pure magnetitite layer. Finally, the composition of the silicate magma at which immiscibility occurs is highly evolved, containing little MgO and CaO and so being incapable of forming the olivine and plagioclase compositions observed in association with magnetitite layers.

As with chromitite layers contacts at the base of magnetitite layers are extremely sharp (Fig. 8), although upper contacts are often gradational (Fig. 8). The efficacy of magma mixing to produce such abrupt contacts is questionable. The Upper Zone displays a remarkably constant and high initial Sr isotope ratio (Kruger et al., 1987). This magma is inferred to be the mixture from several partially crystallized magmas, all with different ratios that produced the lower zones. It is unlikely that a new magma, added to the chamber could have exactly the same ratio as this complexly mixed resident magma. Hence, the constancy of initial ratio throughout the entire Upper Zone argues against addition of significant volumes of distinct magma. Analyses of plagioclase in the footwall and hangingwall of several layers, shown in Fig. 9, suggest that they are related by differentiation and not addition of magma. Since these rocks are quite evolved (An_{55-60}) addition of undifferentiated magma ought to produce significant reversals, but are not observed. There is a fairly regular upward decrease in the V content of the magnetite (Fig. 7). Again if undifferentiated magma, with high V content, is

being added to the system reversals or irregular trends might be expected. Finally, it is possibly significant that the footwall to every magnetitite layer in the eastern limb is an anorthosite. Random addition of magma would not be expected to produce an anorthosite below the magnetitite layer.

Cr is highly compatible in magnetite and is a sensitive indicator of fractionation. Its abundance decreases extremely rapidly in vertical sections through magnetitite layers (Fig. 10), and also shows abrupt reversal even within layers. The rate of depletion is not consistent with crystal settling from a large volume of magma, which ought to produce either homogeneous layers are subdued depletion in Cr.

The succession of anorthosite underlying and frequently overlying magnetitite layers begs the question as to why no pyroxene is present. If plagioclase can form and sink, so should a pyroxene, hence its absence means that the magma has moved out of the stability field of pyroxene. Where mafic minerals are present in the succession, in one case olivine, it shows an abrupt reversal above magnetitite layers, whereas the coexisting plagioclase shows no such reversal (Fig. 11). However, above the magnetitite layer the olivine evolves very rapidly back to the composition it had below the reversal. Such rapid evolution of both the Cr in magnetitite layers and olivine above such layers, suggest that only a thin column of magma is involved. Removal of magnetitite causes a relative Mg/Fe increase in this magma, resulting in the olivine reversal, but magnetite crystallization would have no effect on the An content of the plagioclase. These features are explicable if pressure increases and bottom growth are the mechanism of formation of such layers (Cawthorn and McCarthy, 1980).

The discordant bodies of magnetitite cannot be attributed to pressure changes, and different processes must be involved. They cannot be attributed to immiscible liquids (Scoon and Mitchell, 1994) for the same reasons as discussed above. Iron-rich liquids only contain about 30% FeO (total) and so remaining silicate still has to be removed. Also the liquids are highly evolved and would not be able to produce magnetite with high V contents as are found in the ore body at Kennedy's Vale (Willemse, 1969).

Discordant silicate-rich pipes have been modeled as the result of infiltration of a magma that selectively replaces pre-existing non-liquidus minerals with liquidus minerals (Cawthorn et al., 2000). However, if this model is applied to the magnetitite pipes it implies the existence of new magma being added to the Complex, that had magnetite on the liquidus. Such suggestions would support the concept of addition of magma to make magnetitite layers, which was rejected on isotopic grounds.

Ilmenite

Magnetitite layers in the Bushveld contain minimal primary ilmenite, in contrast to anorthosite hosted deposits in which ilmenite is dominant even to the exclusion of magnetite. However, is this dichotomy universal? In South Africa, there is another intrusion - Rooiwater Complex - in which ilmenite-magnetite layers are found. At the base of the oxide layers magnetite is dominant, whereas towards the top ilmenite is very abundant. Hence, ilmenite ores are not unique to anorthosite complexes. These layers contain minimal apatite, and so are amenable to mining. Immediately above the top layer, concentrations of P_2O_5 can reach several percent. The non-association of oxide and apatite is a further argument for questioning the hypothesis that oxide layers form as immiscible liquids because iron-rich liquids have been shown to preferentially concentrate any P in the magma.

References

Carr, H., Groves, D.I. and Cawthorn, R.G. 1994. The importance of synmagmatic deformation in the formation of the Merensky Reef potholes in the Bushveld Complex. *Econ. Geol.*, **89**, 1398-1410.

Cawthorn, R.G. and McCarthy, T.S. (1980). Variations in Cr content of magnetite from the upper zone of the Bushveld Complex; evidence for heterogeneity and convection currents in magma chambers. Earth & Planetary Science Letters 46, 3, 335-343.

Cawthorn, R.G., Harris, C. and Kruger, F.J. (2000). Eales, H.V. in press. South African Journal of Geology.

Irvine, T.N. 1975. Crystallization sequences in the Muskox intrusion and other layered intrusions – II. Origin of chromitite layers and similar deposits of other magmatic ores. *Geochim. Cosmochim. Acta*, **39**, 991-1020.

Irvine, T.N. 1977. Origin of chromitite layers in the Muskox intrusion and other stratiform intrusions: a new interpretations. *Geology*, **5**, 273-277.

Lipin, B.R. 1993. Pressure increases, the formation of chromitite seams, and the development of the Ultramafic Series in the Stillwater Complex, Montana. *J. Petrology*, **34**, 955-976.

Murck, B.W. and Campbell, I.H. 1986. The effects of temperature, oxygen fugacity and melt composition on the behaviour of chromium in basic and ultrabasic melts. *Geochim. Cosmochim. Acta*, **50**, 1871-1887.

Osborn, E.F. 1980. On the cause of the reversal of the normal fractionation trend an addendum to the paper by E.N. Cameron, "Evolution of the lower critical zone, central sector, eastern Bushveld Complex, and its chromite deposits. *Econ. Geol.*, **75**, 872-875.

Schoenberg, R., Kruger, F.J., Nagler, T.F., Meisel, T. and Kramers, J.D. 1999. PGE enrichment in chromitite layers and the Merensky Reef of the western Bushveld Complex; a Re-Os and Rb-Sr isotope study. *Earth Planetary Science Letters* **172**, 49-64.

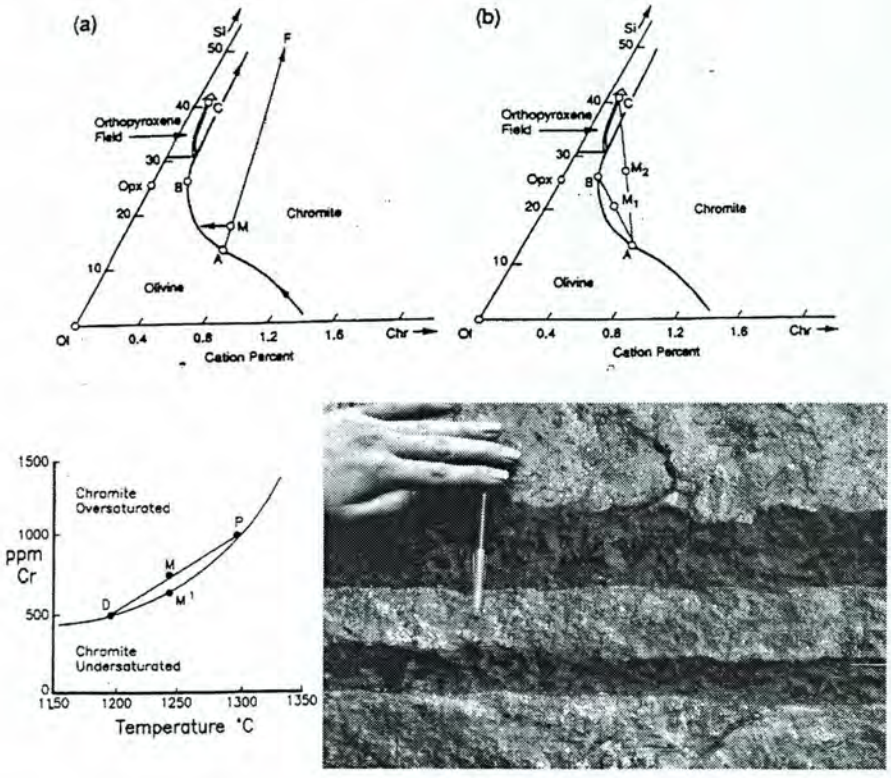

Fig. 1. Two interpretations of chromitite formation based on the phase diagram chromite - forsterite - SiO_2 (from Irvine, 1975 and 1977).

Fig. 2. Plot of Cr versus MgO content of magma (Murck and Campbell, 1986).

Fig. 3. Extremely sharp contacts of chromitite layer, Bushveld Complex.

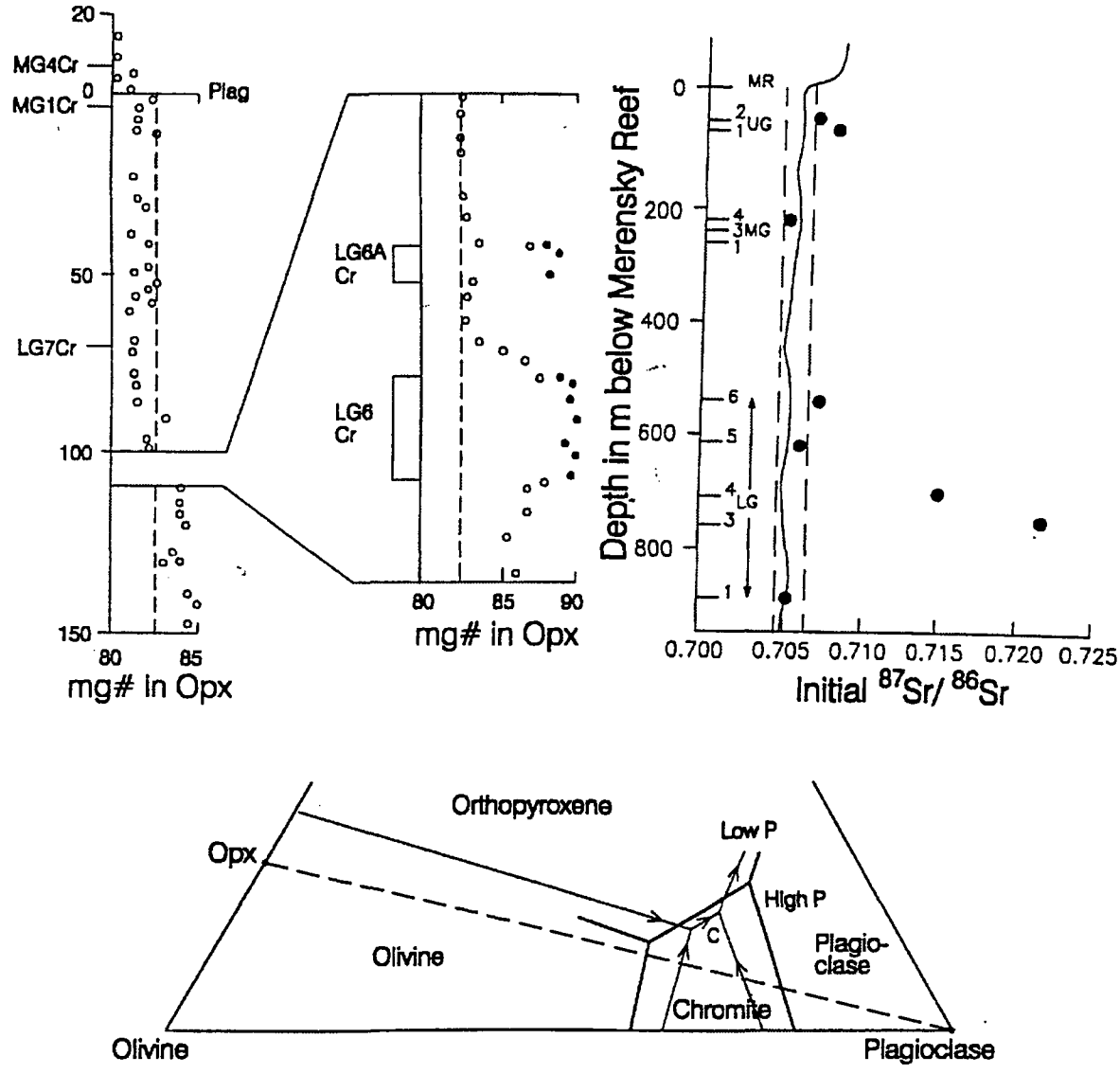

Fig. 4. Plot of mg# in orthopyroxene across the LG6 chromitite layer.

Fig. 5. Schematic phase relations in the natural system olivine-plagioclase-quartz at two different pressures.

Fig. 6. Plot of the initial $^{87}Sr/^{86}Sr$ in the several chromitite layers compared to the typical ratio throughout the Critcal Zone (from Schoenberg et al., 1999). The anomalously high value in the chromitite layer suggests a very large degree of contamination.

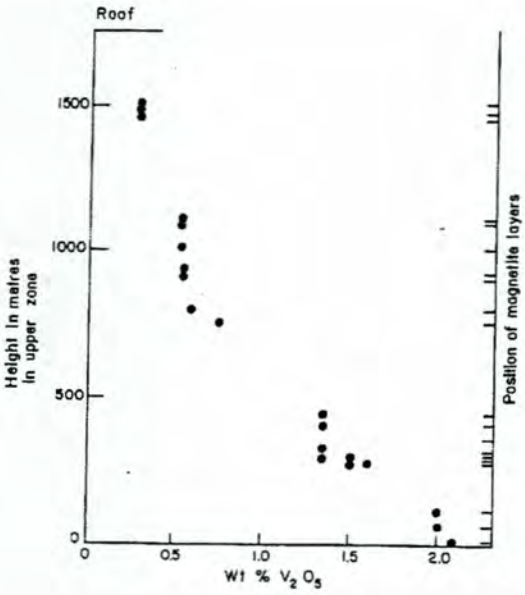

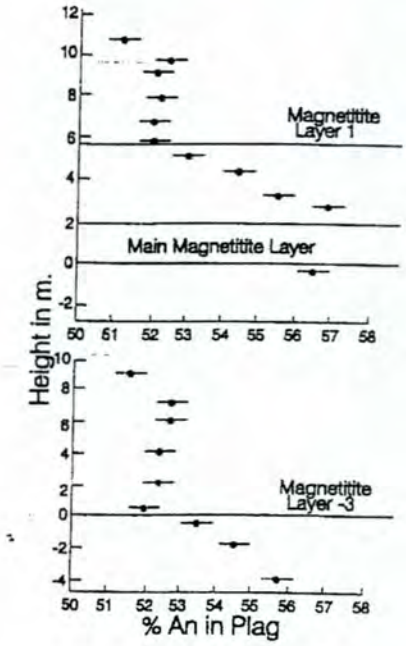

Fig. 7. Plot of V_2O_5 in magnetitite layers versus height in the Upper Zone, Bushveld Complex.

Fig. 8. Sharp lower and gradational upper contact of magnetitite layer, Bushveld Complex.

Fig. 9. Plot of An content in plagioclase across three magnetitite layers near the base of the Upper Zone

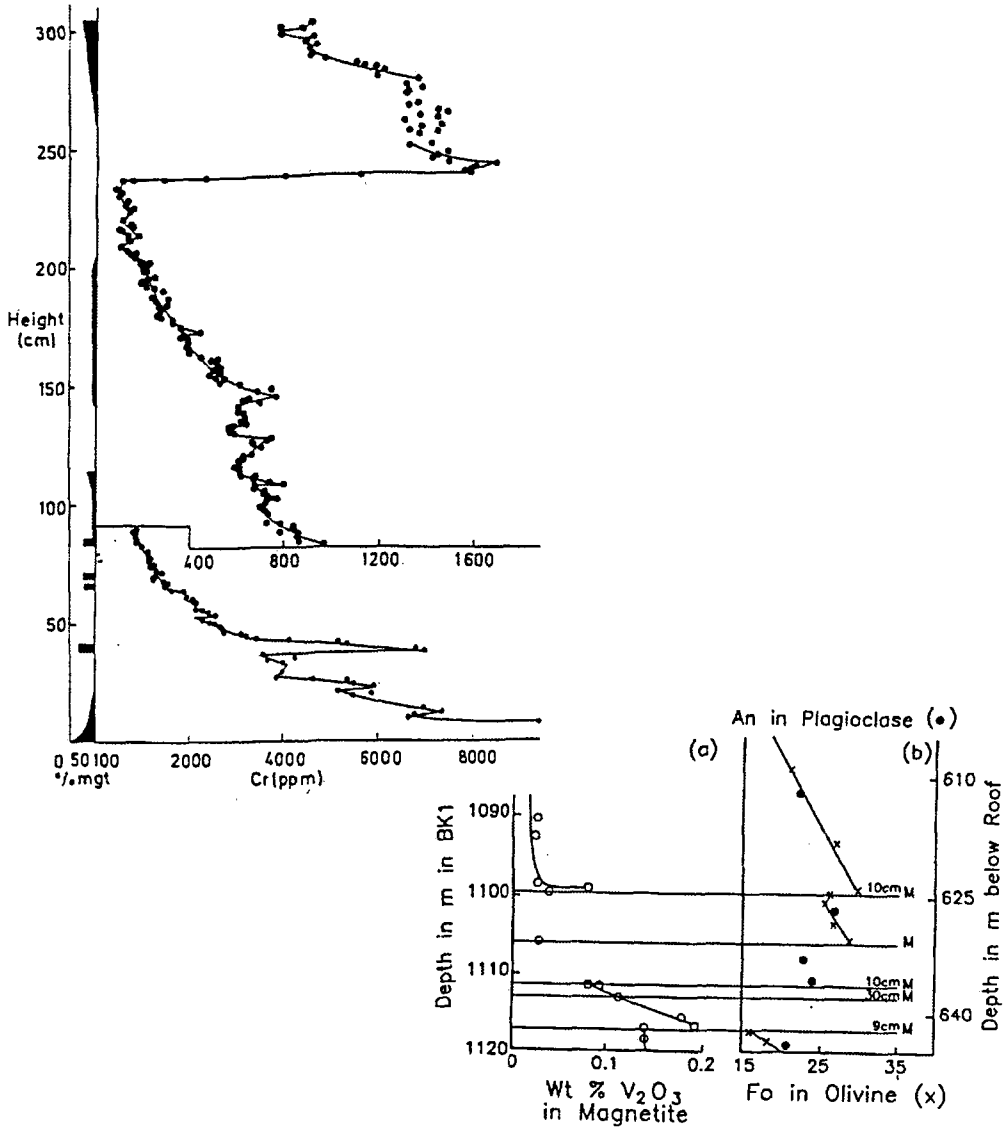

Fig. 10. Plot of Cr in magnetite separates from Main Magnetitite Layer versus height (Cawthorn and McCarthy, 1980).

Fig. 11. Plot of Fo in olivine and An in plagioclase through a short vertical interval that includes several magnetitite layers.

Charlier B & Duchesne JC:

Whole-rock geochemistry of the Bjerkreim-Sokndal layered series: bearing on crystallization processes of cumulus rocks

Bernard Charlier & Jean-Clair Duchesne
L.A. Géologie, Pétrologie et Géochimie, Université de Liège, Belgium

The crystallization processes of cumulate rocks from the Bjerkreim-Sokndal layered intrusion (Rogaland, southwest Norway) are investigated through a whole rock major and trace elements geochemical approach.

More than 100 whole-rock analyses of major elements from the layered series of the Bjerkreim lobe (MCU II to IV), mostly coming from the P. Michot's collection of rock analyses, have been plotted in Harker variation diagrams. They characteristically show well-defined linear trends for each element vs SiO_2. Some scattering is only observed in the K_2O and P_2O_5 diagrams, possibly due to variations in the amount of trapped interstitial liquid. Each linear trend corresponds to a distinct type of cumulate assemblage. Two types are particularly well represented: (1) phiC or leuconorite cumulate: plag (An48) + hemo-ilmenite + opx (± olivine ± magnetite) ; (2) phcimaC or gabbronorite cumulate: plag (An40) + opx + cpx + ilmenite + magnetite+ apatite.

The composition of the cumulates in each type oscillates between 2 poles: the first one is made up of plagioclase alone, and the second one is constituted by the sum of all mafic minerals. This implies that the relative proportion of the different mafic minerals (oxides, pyroxenes and apatite) remains constant during each specific stage of evolution, though cryptic layering is conspicuous (Wilson et al. 1996). The variation of the whole rock composition along the linear trend thus only results from variation in the relative abundance of the plagioclase in the rock. A purely gravity-controlled mechanism of accumulation is likely to modify the relative proportions of the mafics because of the large spread in density (from 5.2 for magnetite to 3.2 for apatite). A process of in-situ crystallization of all minerals together with oscillatory nucleation of plagioclase possibly better explains the geochemical observations.

Forty selected rocks were also analysed for trace elements. REE distributions clearly discriminate the two types of cumulates. Leuconorite cumulates show a large positive Eu anomaly (Eu/Eu*= 3 to 10), whereas norite cumulates have no Eu anomaly. This observation implies that the positive Eu anomaly of the plagioclase is exactly balanced by the negative anomalies of the mafics, and particularly by that of apatite the richest REE bearer. More data on the modal proportion and chemical composition of the minerals might help in solving this enigma.

For each type of cumulates, the linear trend is a locus for its average composition. This property permits to examine the relationships between cumulates at different stratigraphic positions, parental magma and liquid line of descent (LLD) defined by Duchesne & Wilmart (1997). The evolution from the jotunitic parental magma to an evolved jotunite can result from subtraction of an average leuconorite cumulate. A liquid fraction value of about 0.6 can be accurately estimated in the FeO_{tot}-SiO_2 where the LLD is particularly well defined. Then subtraction of a noritic cumulate from the evolved jotunite drives the liquid to more acidic compositions, but this does not seem to be sufficient to attain the LLD of the upper part of the massif. A third type of cumulates, the ultramafic cumulates of the "Transition Zone"

(Duchesne et al. 1987), have to play an important role at that stage together with contamination by roof material or other acidic melts.

References:

Duchesne, J.C., Denoiseux, B. & Hertogen, J. 1987: The norite-mangerite relationships in the Bjerkreim-Sokndal layered lopolith (SW Norway). *Lithos 20*, 1-17.

Duchesne, J.C. & Wilmart, E. 1997: Igneous charnockites and related rocks from the Bjerkreim-Sokndal layered intrusion (Southwest Norway): a jotunite (hypersthene monzodiorite)-derived A-type granitoid suite. *J. Petrol. 38*, 337-369.

Wilson, J.R., Robins, B., Nielsen, F., Duchesne, J.C. & Vander Auwera, J. 1996: The Bjerkreim-Sokndal layered intrusion, Southwest Norway. *In*: Cawthorn, R.G. (ed) *Layered Intrusions*. Elsevier, Amsterdam, 231-256.

Chernet T:

Effect of mineralogy and texture of sand and hard rock ilmenite in TiO_2 pigments production by the sulfate process, a case study on Australian ilmenite concentrate and Tellnes ilmenite concentrate, Norway

Tegist Chernet
Geological Survey of Finland, FIN-02151 Espoo, Finland
tegist.chernet@gsf.fi http://www.geocities.com/tegist_c

In producing TiO_2 pigments by the sulphate process the reactivity of the raw material with sulphuric acid is crucial. Two ilmenite concentrates, from sand (Australia) and hard rock (Tellnes, Norway) deposits were studied. For the former, the recovery of TiO_2 into the pigment was only moderate, whereas the latter showed a high recovery. This study shows that mineralogical and textural characteristics correlate with the observed recoveries.

In the sand ilmenite, alteration advances along grain boundaries and fractures resulting in the formation of poorly soluble phases that prevent the acid reaching the soluble ilmenite. Furthermore, the trace elements that tend to be concentrated during the alteration and the trace element signature of ilmenite from multiple source rocks affect the quality of the pigment.

Rare alteration in the hard rock ilmenite favours good solubility. Magmatic features i.e. exsolution and twinning have a positive effect on solubility. The dissolution of ilmenite and the extent of hematite exsolution was found to correlate. Hematite lamellae are partially dissolved as shown by oriented pits that promote percolation of the acid and result in a positive effect on the leaching of ilmenite. Structural discontinuities i.e. twinning and fracturing are favourable for the penetration of the leachates into the grains. The effect of a trace element on the quality of pigment is highly dependent on whether it is incorporated in the lattice of ilmenite or some insoluble phases.

A knowledge of Ti-bearing phases including their quantification and alteration can throw light on the raw material treatment enabling the metallurgist to deal with the problems in TiO_2 recovery. The distribution and the content of trace elements and deleterious minerals provide a useful guide to controlling both the quality of final product and the tailing. To conclude, careful mineralogical examination of any ilmenite concentrate is useful in evaluating its suitability for the process.

Didenko PI, Kryvdik SG & Zagnitko VM:

Ti, Mg, and O isotopic compositions in ilmenites from Ukrainian ore deposits as indicator of their crystallization conditions

[1]Didenko P.I., [2]Kryvdik S.G., [2]Zagnitko V.M.
[1]Center of Environmental Radiogeochemistry, NAS Ukraine, Kyiv, Ukraine
[2] Institute of Geochemistry, Mineralogy and Ore Formation, NAS Ukraine, Kyiv, Ukraine

A Cameca IMS-4f ion microprobe has been used for investigation of ilmenites from different rocks of the Ukrainian shield (gabbroids, alkaline pyroxenites, and carbonatites). Ilmenite crystallizes in a wide range of physico-chemical conditions, which usually results to isotope fractionation of such elements as O, C, S etc. Previous investigations had shown that the fractionation of Ti isotopes occurs also in space and some terrestrial minerals [1]. It is especially essential for space objects (-70 up to +273 ‰ for δ^{50}Ti). The terrestrial minerals in this respect are less investigated.

The appreciable fractionation of ^{49}Ti and ^{50}Ti isotopes was established in ilmenites from alkaline pyroxenites and carbonatites of the Chernigovka complex. The authors try to explain the reason for this fractionation proceeding from physico-chemical conditions of formation of these ilmenite-bearing rocks (temperature, fugacity of oxygen, alkalinity of rocks). In the example of two pairs of ilmenites from carbonatites and alkaline pyroxenites there was discovered an increasing tendency of contents of heavy (^{49}Ti and ^{50}Ti) isotopes in rocks, which were formed in more alkaline and oxydizing conditions (the second sample of each these pairs). It was supposed that this process occurs at some lower temperature. The primary temperature for crystallization of these rocks is accepted at about 1000 ^{0}C.

Hence, the processes of oxidation and increase of alkalinity of the environment, and, perhaps some decreasing of temperature, promote fractionation of Ti isotopes with increases in the heavy isotopes.

The Ti isotopic compositions were measured also in individual ilmenites from gabbroids of the Korosten pluton. In these samples δ^{49}Ti and δ^{50}Ti have rather insignificant values (0 and 1.5 ‰, accordingly). They are similar to ilmenites mentioned on these characteristics from carbonatites. The results of the microprobe analyses of these ilmenites from Korosten pluton have shown that they are also characterized by rather low contents of a hematite component (1.3-1.9 % Fe_2O_3). This testifies to the rather reduction conditions of their crystallization.

The Mg isotopic compositions were determined in ilmenites from basic and ultrabasic rocks of Korosten pluton and other complexes (Gorodnytza, Prutovka, and Varvarovka). The ultrabasic rocks of Gorodnytza intrusion are alkaline (jacupirangites and melteigites) and considered to be deep (mantle) formations (δ^{26}Mg=2 ‰). The Prutovka complex belongs to a differentiated intrusion, the basic and ultrabasic rocks (early differentiates) of which are nickel-bearing. This complex belongs to a Precambrian trap formation. Varvarovka complex is supposed to have had significant contamination from crustal granitoid material. Proceeding from these concepts, we explain determined distinctions in isotopic composition of Mg in ilmenites from these complexes. Thus the δ^{26}Mg in ilmenite from Prutovka complex is close to that in diabases, and δ^{26}Mg in ilmenites from Varvarovka complex is nearer to those in granites.

The data obtained allow assuming that the definite dependence of value of $\delta^{26}Mg$ from a degree of oxidability of iron (contents Fe_2O_3) in ilmenites is shown in Prutovka complex.

The tendency of increasing the O isotopes weight was established earlier in carbonates from carbonatites of the same complex [2]. It has been shown that to increasing of oxidability of iron in rock (and reduction of FeO in minerals) occurs appreciable increasing of values of $\delta^{18}O$ in carbonates from 5 up to 17.5 ‰. $\delta^{18}O$ in magnetite from these carbonatites (+2.3 up to +2.5 ‰) specify equilibrium isotope distribution between carbonates and oxides (magnetite, ilmenite) at rather high physico-chemical parameters. The isotope distribution of carbon between carbonates and graphite in the same rocks also specifies high temperature of crystallization equilibrium of these minerals.

Thus Ti, Mg, and O isotopic compositions in ilmenites depend from a type of rocks and its crystallization conditions (temperature, alkalinity, redox potential). Our investigations allow to make a conclusion that redox conditions probably are one of primary factors of magmatic process in the directed change of isotopic composition of ilmenite.

References

Zinner E. 1989. Isotopic measurements with the ion microprobe.- U.S.Geological bulletin 1890, p.145-162.

Kryvdik S.G., Zagnitko V.M., and Lugova I.P. 1997. Isotopic compositions of minerals from carbonatites of Chernigovka complex (Azov area) as indicator of crystallization conditions. Mineralogical Journal, Vol. 19, N6, p. 28-42.

Duchesne JC & Vander Auwere J:

Fe-Ti-V-P deposits in anorthosite complexes: the bearing of parental magma composition and crystallization conditions on the economic value

Jean-Clair Duchesne and Jacqueline Vander Auwere
L. A. Géologie, Pétrologie et Géochimie, University of Liège, Sart Tilman, Belgium.

Recent experimental data (Fram and Longhi, 1992; Longhi *et al.*, 1993; Vander Auwera and Longhi, 1994; Vander Auwera *et al.*, 1998; Longhi *et al.*, 1999) indicate that parental magmas of the AMC suite probably encompass a large continuum of compositions ranging from high-Al basalts to more ferroan and potassic compositions, represented by the primitive jotunites (hypersthene-bearing monzodiorites). Experimental phase equilibria show that both endmember magmas can account for the norite series which fractionates at 3-5 kb to silica-enriched liquids (Longhi *et al.*, 1999).

In Rogaland, comparison between phases experimentally obtained on a primitive jotunite (Vander Auwera and Longhi, 1994) and natural phases from the anorthosite massifs and from the Bjerkreim-Sokndal layered intrusion suggests that a liquid generally similar to this primitive jotunite was parental to both types of intrusions. Interestingly, in these two types of intrusions, Fe-Ti-V-P deposits have been recognized (Duchesne, 1999). In massive anorthosites, the ore-bodies occur as (deformed) dykes or pods ranging in composition from pure ilmenite (Jerneld) to ilmenite norite (Tellnes, Storgangen). Polybaric fractional crystallization and synemplacement deformation in rising anorthosite diapirs lead to relatively (poisonous) Mg- and Cr-rich ilmenite (± V-magnetite) deposits. Fractional crystallization in

layered magma chambers of jotunite magmas gives rise to voluminous " disseminated " mineralizations, containing low Mg and Cr ilmenite + Ti-magnetite ± REE-rich apatite, still of sub-economic value. Immiscibility is not the controlling mechanism, except maybe in some rare nelsonites (Hesnes).

Subsolidus re-equilibration leads to a thorough change in the oxide mineral composition towards an enrichment in end-member compositions (Duchesne, 1970). Reactions between the oxide minerals leave conspicuous microscopical evidence and regularly lower the hematite content and possibly the Cr content of ilmenite and the ilmenite and Al-spinel contents of the magnetite. Mg contents of ilmenite also seem to decrease, possibly through reactions with pyroxenes, but no reaction rims can be observed at the contact with pyroxene.

References

Duchesne, J.C. 1970. *Ann. Soc. Géol. Belg.* **93**, 527-544.
Duchesne, J.C., 1999. *Miner. Deposita*, **34**, 182-198.
Fram, M. and Longhi, J., 1992. *Amer. Min.*, **77**, 605-616.
Longhi, J., Fram, M., Vander Auwera, J., Monteith, J., 1993. *Amer. Min.*, **78**, 1016-1030.
Longhi, J., Vander Auwera, J., Fram, M. and Duchesne, J.C., 1999. *J. Petrol.*, **40**, 339-362.
Vander Auwera, J. and Longhi, J., 1994. *Contrib. Miner. Petrol.*, **118**, 60-78.
Vander Auwera, J., Longhi, J. and Duchesne, J.C., 1998. *J. Petrol.*, **39**, 439-468.

Esipchuk K:

Mineralogy, geochemistry and origin of the Korosten gabbro-anorthosite-rapakivi granite pluton (Ukraine)

Esipchuk, K.Yu.
Institute of Geochemistry, Mineralogy and Ore Formation, NAS Ukraine, Kyiv

The Korosten gabbro-anorthosite-rapakivi granite pluton is a multiple intrusion with a rather long period of formation (1800-1740 Ma). At least two different types of anorthosites (and gabbro) and several varieties of the granitoides can be distinguished [1, 3]. There are anorthosites older and younger than rapakivi granites. Older granitoids represented by dykes of spherulitic plagiogranite porphyries. The main granitoid intrusive phase is represented by hornblende-biotite and rapakivi granites which can be subdivided into several facies, distinguished from each other in terms of structure and composition. The more common among them are hornblende-biotite and biotite granites with typical rapakivi structure and biotite ovoid-free granites. In contacts of the granites with gabbro and anorthosites are developed monzonites, syenites and in places pyroxene-hornblende rapakivi with local fayalite. The next phase is represented by albitized fluorite- and topazbearing zinnwaldite granites. They form rather small stock-like bodies in the peripheral parts of the pluton and are also confined to the contact zone rapakivi granites with gabbro-anorthosites. One of the latest phases of the Korosten pluton are biotite granite-porphyries and syenite-porphyries, forming stocks and dykes within the exo- and endocontact areas of the rapakivi granites. Intrusion was completed by formation of dykes and veins of fine-grained biotite granites, orthophyries and quartz porphyries, aplites and pegmatites, diabases, gabbro-diabases and diabase porphyries.

Gabbro and anorthosites of the Korosten complex are characterized by slightly heightened F, B, Ba, Mo, Pb abundances. The concentration of the siderophile elements in them is rather low: Co – in 1,5-2 times lower in comparison with its mean concentration in basic rocks; Ni – in 4-15 times; Cr – in 4-8 times; Cu – in 1,5-12 times. Zn distribution in anorthosites and

gabbro is very irregular; Zn concentration in some samples is 1.2-1.6 times higher, but in another 1.5-2.5 times lower in comparison with its mean concentration in basic rocks; V concentration respectively 1.1-1.3 times higher and 1.1-2 times lower. As a rule more lower F, Rb and Zn concentrations are in anorthosites, but Sr – in gabbro. Light anorthosites of the first phase have very high B content: 10-90 ppm in comparison with 4 ppm in another basic rock of the Korosten complex: F, Ba, Mo and Pb concentrations in them are some higher then in later anorthosites. The basic rocks of the Korosten complex are characterized by lower Ni, Co, Cr, V concentration in comparison with continental and oceanic basalts. Rb, Ba, Sr, Zn and Pb concentrations in them are rather similar. K/Rb, Rb/Sr and Ba/Sr rations are the same as in continental basalts.

The rapakivi granites of the Korosten complex have the same chemical composition as granites this type from other regions, for example Baltic Shield [7,10]. They are generally metaluminous or slightly peraluminous, especially granites of the late phases. At the same time they have subalkaline composition.

The chemical composition of the different types of granitoids varies markedly. Rather low SiO_2 abundance one can see in quartz monzonites or syenites (to 63 wt. %) and melanocratic pyroxene-hornblende and hornblende-biotite rapakivi granites (to 70 wt. %). Granites of the main and late intrusive phases are characterized by high SiO_2 content (73-75 up to 77 %). They have also low abundances of CaO, MgO, Al_2O_3 , P_2O_5 as well a high Fe/Mg and K/Na rations. Relatively high Na_2O+K_2O contents (8-11 wt. %) show evident alkaline affinities, yet no peralkaline granites have been found in Korosten pluton. A generalized evolution trend from the earliest to the latest intrusive phases is marked by increasing SiO_2 and decreasing of TiO_2, Al_2O_3, FeO, MgO, CaO. The geochemical characteristics of the Korosten rapakivi granites are similar to the subalkaline A-type, interplate granites. V, Cr, Co and Ni contents are in 1.5-2 times lower than the average values for acid rocks. Typical is the increase of F, Rb, Sn, Pb, as well as decreasing Sr and Ba from granites of early to those of later phases.

The Rapakivi granites show light element enriched chondrite-normalised REE patterns with a distinct Eu minimum; this minimum is very pronounced in zinnwaldite granites. Chondrite-normalized REE patterns of the gabbro and anorthosites are more flat with distinct positive Eu anomaly.

The isotopic investigations [2,6] have shown the negative value of the ε_{Nd} in gabbro-anorthosites (-0.8) and rapakivi granites (-1.8). The initial ratio of the Sr isotopes is 0.703-0.706.

The Fe-Mg-silicates in these rocks are conspicuously rich in iron [4,9]. Amphibole is represented by ferrohastingsite, in places grunerite. There is a lack of distinction between the compositions of the hornblendes from different granite types, except that some of the later ones are richer in Rb content. Biotites correspond to siderophyllite with high Fe/(Fe+Mg). Si/Al and (Mg+Fe)/Al ratio become lower in biotites from younger granites, what indicates the decreasing of alkalinity in the process of pluton formation.

The titanomagnetites from anorthosites are very rich in V and have rather low Ti concentration. In granites they are characterized by very low V content, rather low Cr concentration but are very rich in Cu, Zn and especially Ge and Zr impurities.

Trace element contents of zircon within typical rapakivi granites are lower than within ovoid-free rapakivi granites: U 290-1700 ppm; Th 200-1200; Pb 70-800; Y 1750-6000; Yb 370-930 ppm respectively. Zircons from rapakivi granites and the related rocks have rather low Zr/Hf ratios in comparison with the orogenic granites.

All geological, mineralogical and geochemical data testify that the plutonic rocks have different magmatic sources. The magma for the gabbro and anorthosites were derived from the upper depleted mantle and lower crust. The magmas of the rapakivi granites were derived from the middle crust by 10-20 % partial melting dioritic source. Their fractionation and

contamination resulted in pyroxene-hornblende, biotite-hornblende, biotite and topaz-bearing zinnwaldite granites formation. The crystallization was mainly taking place under hypabyssal and near-surface conditions. Such a model is in accordance with geophysical data concerning the deep velocity structure of the pluton [8].

References

1.Amelin, Yu.V., Heaman, l.M., Verkhogliad, V.M. and Skobelev, V.M. 1994. Geochronological constraints on the emplacement history of an anorthosite-rapakivi granite suite: U-Pb zircon and baddeleyite study of the Korosten complex , Ukraine. Contrib. Mineralogy and Petrology, 116. – p. 411-419.

2. Dovbush, T.I., Skobelev, V.M. Some remarks on the origin of the Korosten anorthosite-rapakivi granite complex as based on isotope date. 2000. Heophysical journal, 4, 22. - p. 84-85.

3. Esipchuk, K.Ye., Sheremet, Ye.M., Zinchenko O.V. et.al. 1990. Petrology, geochemistry and metallogeny intrusive granitoids of the Ukrainian Shield (in Russian). Nauk. Dumka: Kyiv. – 236 p.

4. Esipchuk, K.Ye., Skobelev, V.M. 1998. Mineralogy of the Korosten rapakivi granites (Ukrainian Shield). Proceedings of the Institute of fundamental studies. Kyiv: Znanya. - p. 45-56.

5. Esipchuk, K.Ye., Sheremet, Ye. M. 1999. Trace elements in the rocks of the Korosten gabbro-anorthosite-rapakivi granite pluton. Preceedings of the Institute of fundamental studies. Kyiv. Znanya. - p. 66-75.

6. Esipchuk, K.Ye., Skobelev, V.M., Shcherbakov, I.B. et. al. 2000. Magmatism of the Ukrainian Shield. Mineralogical journal, 22, 5/6. – p. 82-94.

7. Haapala, I., Ramo T. 1990. Petrogenesis of the Proterozoic rapakivi granites of Finland. Geological Society of America. Special Paper, 246. – p. 275-286.

8. Ilchenko, T.V., Bukharev, V.P., Glevassky, E.B., 2000. Korosten pluton deep velocity structure and its geological implications. Geophysical journal, 4, 22. –p. 92

9. Lichak, I.L. 1983. Petrology of the Korosten pluton (in Russian). Nauk. Dumka. – 248 p.

10. Ramo, T.0. 1991. Petrogenesis of the Proterozoic rapakivi granites and related basic rocks of South Eastern Fennoscandia: Nd and Pb isotopic and general geochemical constraints. Geological Survey of Finland. Bull. 355. – 161 p.

Fershtater GB:

Subduction-related leucogabbro-anorthosite ilmenite-bearing series: an example of water-rich high-temperature anatexis, platinum belt of the Urals, Russia

G.B. Fershtater
Institute of Geology and Geochemistry, Pochtovy per., 7. Ekaterinburg, 620151, Russia.
gerfer@online.ural.ru

The platinum belt of the Urals is composed of zonal massifs belonging to Ural-Alaskan type of dunite-clinopyroxenite-gabbro rock series (420-430 Ma) with famous platinum and magnetite deposits related to dunites and clinopyroxenites – hornblendites respectively. The belt is assumed to be associated with a Late Ordovician-Silurian subduction zone dipping to the east. In the eastern part of the belt in some zonal massifs one can see a suite of hornblende leucogabbro, anorthosites and plagiogranites dikes and the leucogabbro-anorthosite-plagiogranite, the Chernoistochinsk massif which is described below.

The root zone of migmatized hornblende gabbro is exposed in the northern part of this massif (Fig. 1). The migmatization (partial melting) produces non-uniform rocks consisting of

leucocratic patches full of gabbro relics and hornblende piles. Direct field investigations show that segregation of these leucocratic portions form the hornblende leucogabbro representing the initial anatectic melt. The products of this melt crystallization form relatively homogeneous veins and small intrusive bodies in hornblende gabbros which are partly melted in places. Crystal fractionation of this leucogabbro melt gives rise to leucogabbro-anorthosite-plagiogranite rock series localized mainly as veins with gabbro xenoliths (Fig. 2). The hornblendite inclusions and schlieren represent the restitic phases. All the rocks have the same mineral composition which is as follows: hornblende+plagioclase+magnetite+ilmenite. Magnetite is a main opaque mineral in gabbro while ilmenite is predominant in anorthosites. Quartz appears in plagiogranites. The volume of these rocks is very small, not more than 3-5%. The amount of hornblende and An contents in plagioclase decrease from gabbro to granites from 50 to 3-5 % and from 45-50 to 25-30% correspondingly. The hornblende contents are the best visible index of partial melting and crystal fractionation degree, as is shown in Fig. 2. The compositional range of the rock series (Table 1) represents the products of partial melting reactions from protolith (1 - 3) to initial melt (4) and products of its fractional crystallization (5-8) to restitic phases (9,10). Partial melting produces the rocks impoverished in all elements which are concentrated in femic minerals, such as Mg, Fe, Ti, and in most rare elements with the exception of Sr, Ba and some others related to plagioclase. The magnitude of the positive Eu anomaly clearly increases in the range from gabbro to plagiogranite (Fig. 3). At the same time the ilmenite/magnetite ratio increases from 0.5 in gabbro to 10 in anorthosites.

The conditions of anatexis are shown in Fig. 4. It takes place in the field of hornblende stability, while the plagioclase with less anorthite contents than An_{60} has undergone the melting (shaded area at Fig. 4). Mass-balance calculations show that major- and trace-element compositions of leucogabbro correspond to approximately 60% degree of partial melting of hornblende gabbro. It is necessary to melt about 10% of hornblende and nearly-all the volume of plagioclase to produce the leucogabbro composition. A large body of experimental and geological works confirm well known data about the usual quartz-bearing composition of the anatectic melt resulting from partial melting of amphibolites. The mechanism discussed above can be realized when high temperature (may be because of small time interval between gabbro intrusion and anatectic events) is combined with high concentration of water coming from the subducted slab. It is believed that such quartz-absent anatexis was common at the early stages of Earth evolution and it can be the source of some autonomous anorthosites.

References

Fershtater G.B., Bea F., Borodina N.S. and Montero P. Anatexis of basites in paleosubduction zone and the origin of anorthosite-plagiogranite series of the Ural Platinum-bearing belt. Geochemistry International. 1998. V. 36, N 8. P. 684-697.

Rushmer T. Partial melting of two amphibolites: contrasting experimental results under fluid absent conditions // Contrib. Miner. Petrol. 1991. V.107. P. 41-59.

Yoder H.S. and Tilley C.E. Origin of basalt magmas: an experimental study of natural and synthetic rock systems. J. Petrol. 1962. V. 3, N 3

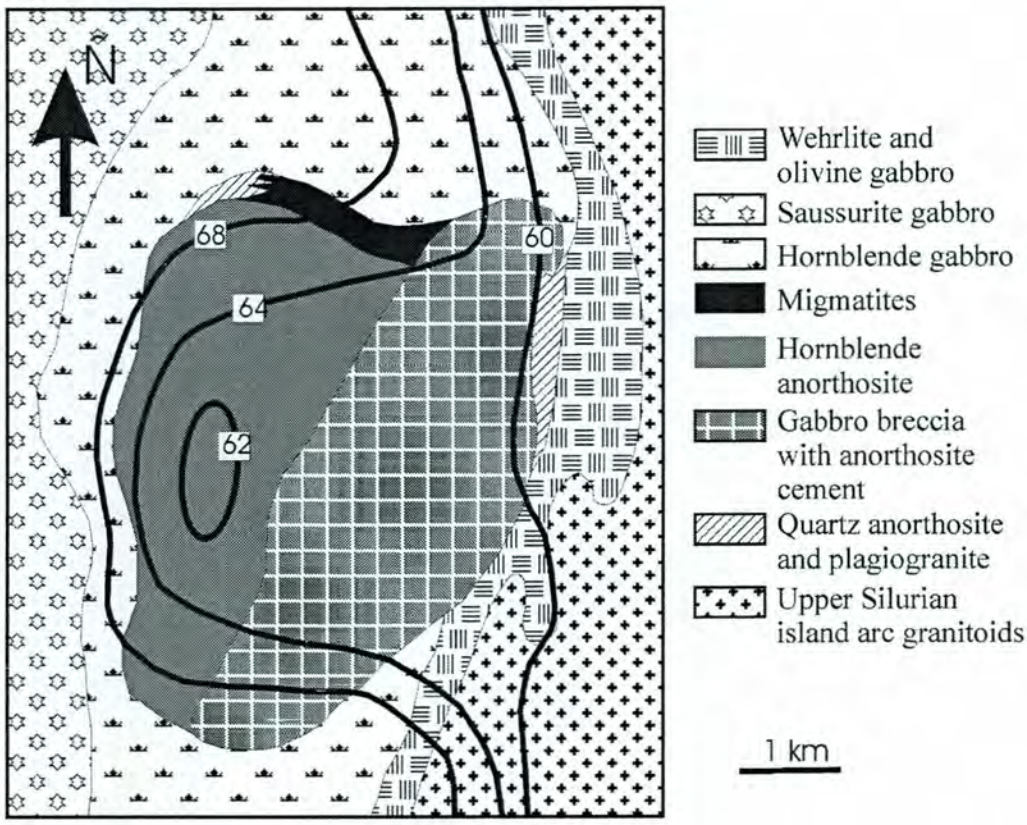

Fig. 1: Sketch-map of Chernoistochinsk massif.

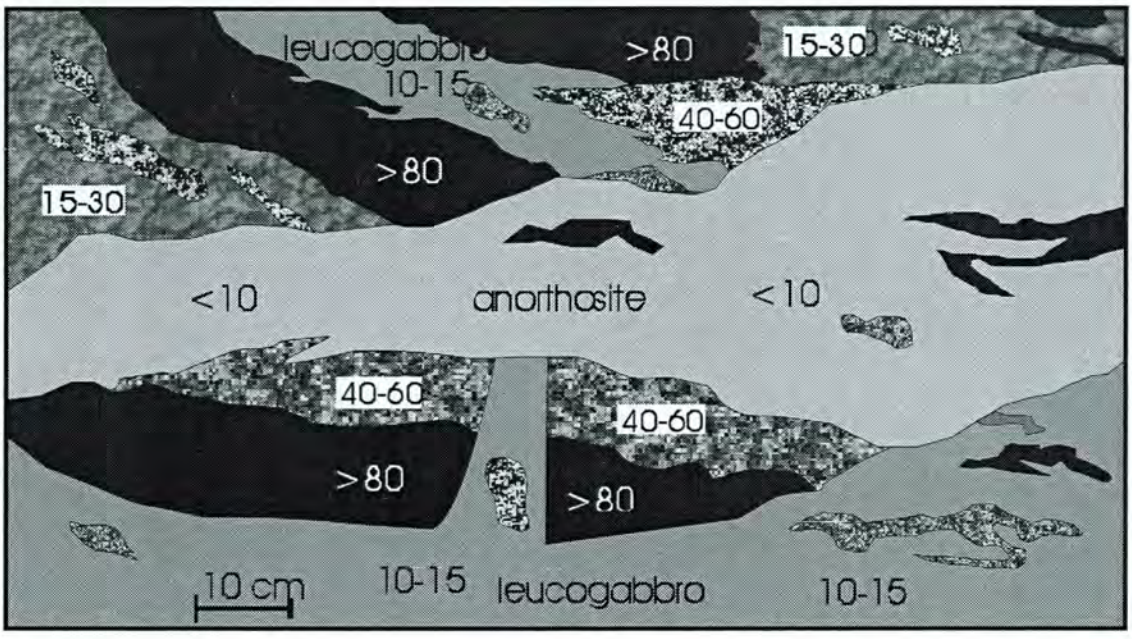

Fig 2: Small part of migmatite outcrop, migmatized gabbro with anorthosite vein (light) and hornblende restite (black). Numbers mark the hornblende contents.

Table 1: Major (w%) and trace (ppm) element composition of the rocks of Chernoistochinsk massif.

N	1	2	3	4	5	6	7	8	9	10	11	12	13
Sample	571	578	566	565	562	117	124	115	567	568	566	562	117
SiO_2	46,76	43,98	46,35	52,17	53,05	65,94	70,54	73,67	44,50	44,80	44,08	44,08	44,36
TiO_2	0,79	2,23	1,09	0,70	0,66	0,20	0,14	0,13	1,25	1,28	1,28	1,55	0,99
Al_2O_3	12,98	15,85	17,14	22,90	23,16	18,59	15,98	14,19	8,27	7,92	10,48	10,46	8,70
Fe_2O_3	6,18	7,41	4,87	4,00	2,91	0,99	0,90	0,56	8,65	8,36	5,61	5,67	5,99
FeO	6,46	8,61	7,67	2,15	3,88	1,53	1,76	2,04	10,41	11,13	11,61	10,75	12,57
MnO	0,24	0,26	0,21	0,10	0,09	0,03	0,03	0,03	0,39	0,39	0,30	0,48	0,42
MgO	8,03	4,99	5,11	2,10	1,85	0,70	0,52	0,28	10,75	10,80	11,08	11,31	11,73
CaO	11,96	10,06	11,72	8,37	8,26	6,08	5,44	4,28	11,09	11,19	11,38	11,05	11,12
Na_2O	3,08	2,69	3,10	6,16	4,97	4,78	3,73	3,78	1,39	1,39	1,52	1,24	1,22
K_2O	0,12	0,12	0,12	0,10	0,14	0,08	0,12	0,08	0,16	0,18	0,20	0,20	0,25
P_2O_5	0,07	0,28	0,22	0,28	0,26	0,08	0,03	0,04	0,24	0,09	0,02	0,06	nd.
Ппп	2,47	1,23	1,61	0,63	0,76	2,04	1,94	1,68	1,77	1,83	2,39	2,46	nd.
Li	2,44	2,20	1,83	2,07	2,37	0,00	0,00	0,00	2,18	1,31	13,52	0,00	1,74
Rb	0,63	0,35	0,00	0,00	0,00	0,13	0,11	0,04	0,38	2,00	1,91	0,09	0,31
Be	0,63	0,69	1,00	0,93	0,98	1,13	0,82	0,92	0,71	0,72	0,80	0,66	0,66
Sr	493	611	1366	1250	1515	725	768	763	166	94	128	139	93
Ba	64	71	110	119	126	88	114	103	48	66	128	65	56
Sc	67	62	9	10,3	9,6	8,6	5,4	4,6	50	57	58	65	64
V	362	475	145	179	155	66	52	26	326	406	468	451	500
Cr	72	1	3	2,2	9,2	2,6	1,7	82,9	729	704	34	69	22
Co	46	46	8	9,9	8,4	4,8	4,6	3,4	56	54	43	45	58
Ni	29	5	2	5,9	3,8	51,4	65,6	77,6	260	241	18	21	42
Cu	78,2	159,1	54,0	57	49	58	21	26	190	69	52	23	96
Zn	112,4	176,5	45,5	68,3	56,7	6,0	9,3	3,8	195	198	253	259	219
Ga	16,1	22,3	23,2	24,0	24,5	14,8	12,4	10,6	19	20	26	25	21
Y	21,8	25,2	6,3	9,0	7,7	1,5	1,3	0,8	42,6	47,7	38,3	48,1	36,2
Nb	1,51	4,18	0,95	1,20	1,36	0,21	0,23	0,21	5,40	3,26	4,23	2,59	4,33
Ta	0,11	0,28	0,07	0,08	0,09	0,28	0,36	0,26	0,69	0,19	0,05	0,00	1,71
Zr	20,06	17,12	6,11	6,21	7,09	1,56	0,69	0,30	42,5	38,1	57,5	40,6	27,0
Hf	0,70	0,71	0,27	0,27	0,23	0,14	0,07	0,04	1,56	1,58	2,40	1,68	1,26
Pb	3,18	7,90	3,46	4,29	4,01	0,00	0,23	0,00	4,14	4,14	10,04	4,26	10,55
U	0,02	0,03	0,00	0,00	0,04	0,00	0,00	0,00	0,06	0,10	0,49	0,00	0,03
Th	0,05	0,06	0,03	0,03	0,07	0,00	0,00	0,00	0,00	0,96	4,21	1,42	0,09
La	4,33	5,98	2,74	3,76	3,21	0,72	1,24	0,62	6,70	6,79	11,18	8,00	3,97
Ce	12,69	16,66	6,61	9,80	8,95	1,71	2,25	1,15	27,47	26,78	33,57	32,22	16,38
Pr	2,14	2,76	1,04	1,59	1,49	0,23	0,23	0,15	5,42	5,31	5,73	6,85	3,56
Nd	10,31	13,29	5,01	7,53	7,05	1,16	1,13	0,67	27,08	26,54	30,22	40,49	19,41
Sm	2,81	3,73	1,23	1,90	1,78	0,33	0,32	0,14	7,26	7,39	8,70	11,38	5,90
Eu	1,10	1,59	0,73	0,94	0,89	0,23	0,24	0,14	2,56	2,43	2,53	2,91	1,84
Gd	3,08	4,07	1,30	1,90	1,72	0,36	0,25	0,15	7,29	7,61	6,96	7,69	6,03
Tb	0,52	0,65	0,19	0,27	0,25	0,05	0,04	0,02	1,13	1,23	1,03	1,35	0,96
Dy	3,60	4,40	1,11	1,62	1,31	0,30	0,25	0,15	7,51	8,08	6,89	8,66	6,45
Ho	0,79	0,98	0,23	0,34	0,29	0,07	0,05	0,03	1,57	1,77	1,46	1,79	1,36
Er	2,14	2,62	0,62	0,88	0,79	0,16	0,10	0,08	4,34	4,78	3,76	4,81	3,63
Tm	0,33	0,39	0,09	0,13	0,11	0,02	0,01	0,01	0,64	0,72	0,54	0,69	0,53
Yb	2,19	2,49	0,53	0,79	0,67	0,15	0,13	0,08	4,06	4,81	3,45	4,21	3,44
Lu	0,31	0,35	0,08	0,11	0,09	0,02	0,02	0,01	0,56	0,66	0,49	0,60	0,49

1,2 - hornblende gabbro; 3 - partly melted gabbro; 4 - leucogabbro; 5 - anorthosite, 6 - quartz anorthosite, 7, 8 - plagiogranites; 9, 10 - hornblendites; 11-13 - hornblenbes from gabbro (11), anorthosite (12) and plagiogranite (13).

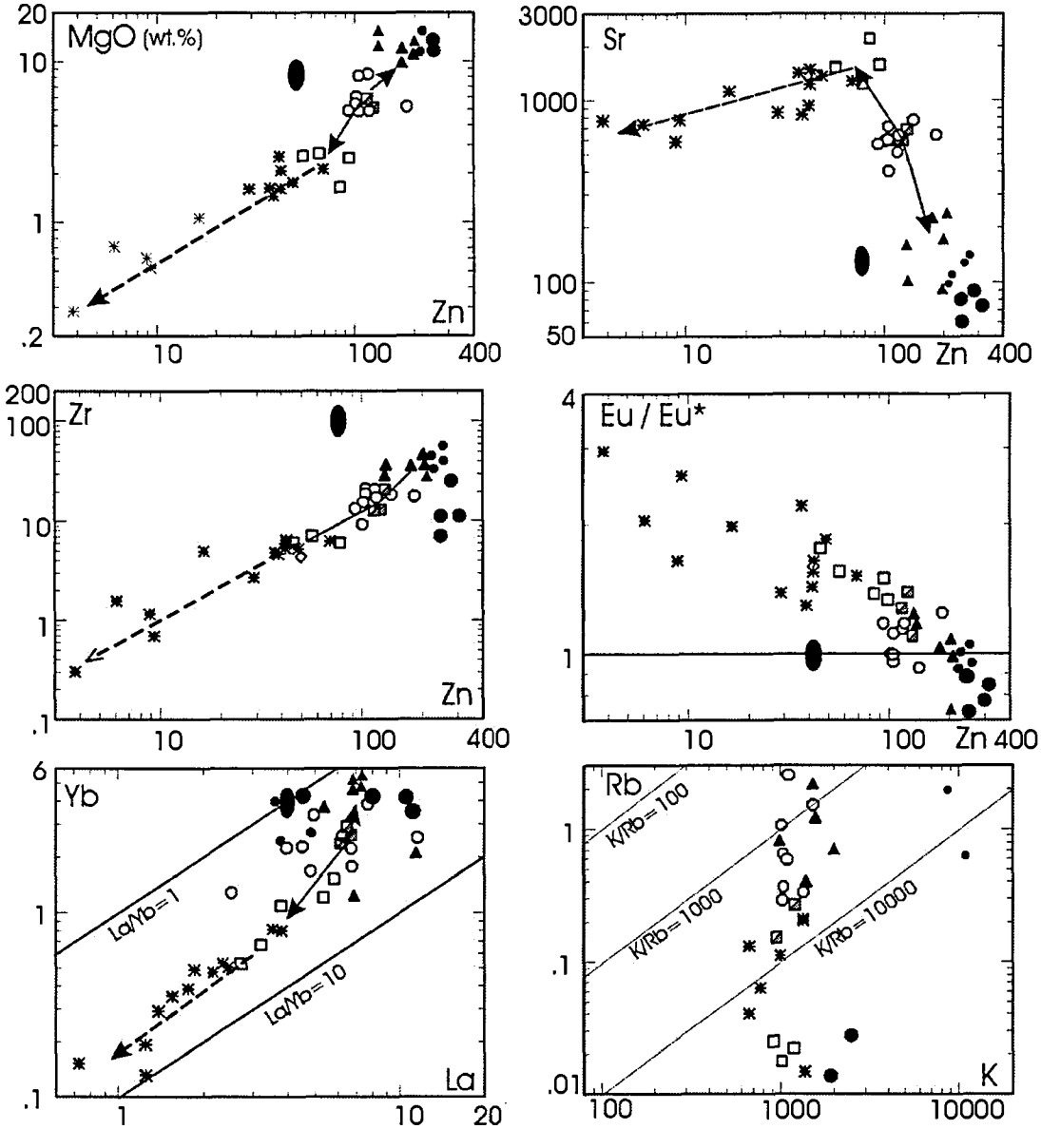

Fig. 3: Some diagrams showing the changes in chemical compositions during anatexis.

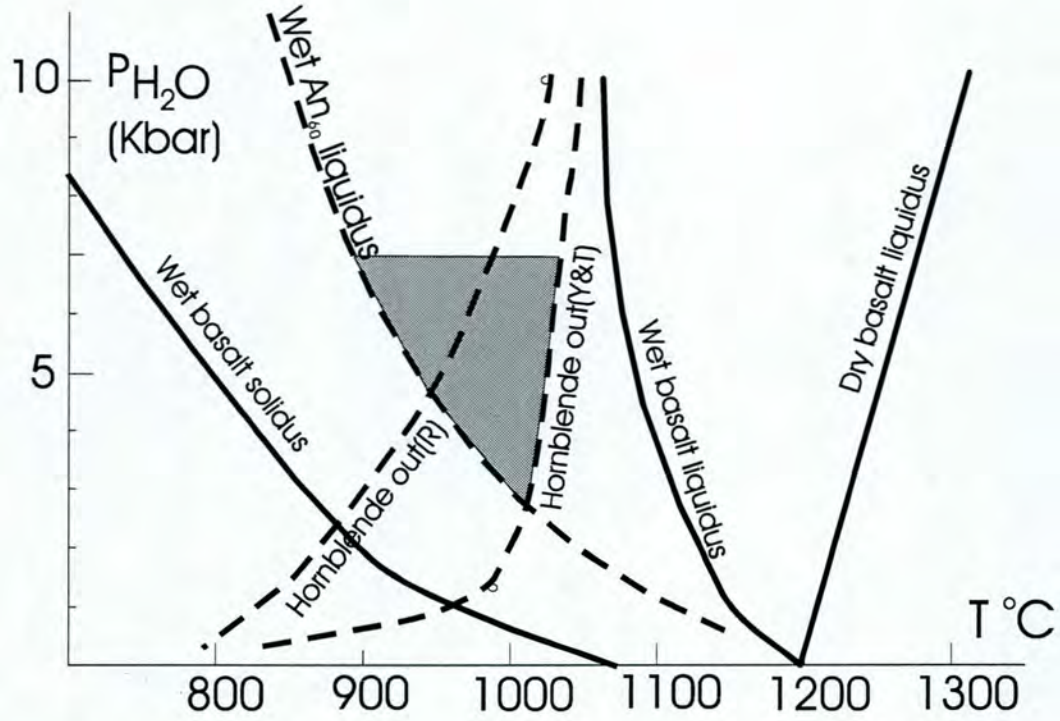

Fig. 4: P-T conditions of anatexis. Wet solidus and wet liquidus as well as An60 liquidus are represented by high-Al basalt (Yoder and Tilley, 1962) which is close in composition to hornblende gabbro of the Chernoistochinsk massif. Amphibole stability lines are after Yoder and Tilley (1962) and T.Rushmer (1991). Dashed area represents the assumed field of anatexis.

Fershtater GB & Kholodnov VV:

The Riphean layered intrusions of the Western Urals and related Ilmenite-Titanomagnetite deposits

G.B. Fershtater and V.V. Kholodnov
Institute of Geology and Geochemistry, Pochtovy per., 7. Ekaterinburg, 620151, Russia.
gerfer@online.ural.ru

The Riphean gabbro layered intrusions are localized inside the graben facies of sedimentary and volcanic rocks of the paleocontinental sector of the South Urals. Volcanic rocks overlie the gabbro intrusions and are represented mainly by tholeiitic basalts and by dikes and small intrusions of rhyolites. The intrusions are underlain avv by sedimentary carbonate rocks and contain xenoliths of both sediments and volcanics. Rb-Sr age of the volcanic rocks corresponds to 1346±41 ma, initial ratio $^{87}Sr/^{86}Sr$ is 0.7098±0.001(Krasnobaev and Semikhatov, 1986); the gabbros are a little younger. They show the age of 1300 ±42 and initial ratio $^{87}Sr/^{86}Sr$=0.7093±0.0067 (Gorozhanin, 1998).

Gabbro intrusions form 70 km long belt consisting of 4 isolated bodies dipping to the east. The angle of dip is about 60° (Fig.1). In two southern massifs (Matkal and Kopan) gabbros are represented by the two-pyroxene variety (gabbro-norites) and contain high-Ti titanomagnetite ore bodies up to 10-15 km lengthwise and 1-2 m in thickness which are parallel to the gabbro layering. These massive ores are surrounded by an aureole of

impregnation. The northern massifs (Medvedevka and Kusa) consist of hornblende gabbro and gabbro-amphibolites in the upper part and ilmenite gabbro-norites in the lower part (Table 1).

Table 1. Average chemical compositions of the gabbros

Massif	SiO_2	TiO_2	Al_2O_3	Fe_2O_3	FeO	MnO	MgO	CaO	Na_2O	K_2O	P_2O_5	LOI	Total
Matkal (3)	46,91	2,19	14,89	3,89	8,57	0,11	6,66	11,21	3,00	0,42	0.06	1.58	99.49
Kopan (29)	44,50	2,90	15,47	5,72	10,25	0,09	5,66	11,64	2,36	0,34	0.14	0.57	99.64
Medvedevka (11)	44,81	2,26	14,69	5,25	11,76	0.17	7,76	9,34	2,40	0,50	0.07	0.89	99.90
Kusa (21)	43,90	3,14	13,24	5,61	11,17	0,19	7,07	11,54	1,85	0,22	0.23	1.41	99.57
Kusa, ilmenite gabbro-norite (11)	42,20	6,07	13,11	5,01	13,29	0,24	6,13	9,49	2,14	0,33	0.16	1.87	100.04
Kusa, gabbro-amphibolite (19)	46,44	2,16	16,26	4,57	9,16	0,15	5,53	10,66	2,96	0,43	0.06	1.74	100.12

The ore bodies are concentrated here in the gabbro-amphibolites and consist of ilmenite or low-Ti titanomagnetite+ilmenite. Ilmenite ores mainly belong to impregnation type, while Ti-magnetite+ilmenite ores form both impregnation and massive types (Table 2).

Table 2. Average chemical compositions of the ores (wt.%)

Element	Ilmenite type		Titanomagnetite type	
	South group	North group	South group	North group
Fe	14-15	14-15	22-23	23-24
TiO_2	6-7	7	7	6-7
V_2O_5	0.12	0.12	0.25	0.25

The first ore type is situated mainly in the upper part of the massifs, the second type - in the central part. Most Ural geologists explain the clear differences in composition of gabbro and related ores between the southern and northern group of massifs by the metamorphic alteration taking place in the northern group.

Our data however, suggest that these differences are due to the P-T conditions of gabbro and ore formation. Rocks and ores of the southern group were formed at the depth of 4-6 km (P_{tot} = 1-2 kbars, P_{H2O}=0.5P_{tot}, T°C=900°-1100°, fluid was enriched in F) while in the northern group these parameters look as follows: depth of 20-25 km, P_{tot} = 8-4 kbars, P_{H2O}=0.7-0.9P_{tot}, T°C=850°-650°, fluid was enriched in Cl (Fig. 2, 3). Fluid enrichment in the northern group massifs is responsible for hornblende gabbro crystallization and their postmagmatic transformation into gabbro-amphibolites. Low temperature causes the separate crystallization of ilmenite and low-Ti titanomagnetite that leads to the specialization of the ore deposits.

The upper part of Kusa deposit were mined before 90-th. Proved reserves of both ore types in Matkal, Kopan and Medvedevka deposits, range up to 7 billion tons.

References

Alekseev A.A. and Alekseeva G.V. Kusa-Kopan intrusive complex (South Urals) as a fragment of a large layered pluton. Proceedings of RAS. 1992. V. 323, N 1. P. 133-136 (in Russian).

Buddington A.F. and Lindsley D.H. Iron-titanium oxide minerals and synthetic equivalents. J. Petrol. 1964. V. 5, N 2.

Fershtater G.B. An empirical plagioclase-hornblende barometer. Geochimia. 1990. N 3 (in Russian)

Gorozhanin V.M. Initial isotope composition of strontium in magmatic complexes of the South Urals. In book: Magmatism and Geodynamics (Ed. by V.A. Koroteev). 1998. Ekaterinburg. P. 98-108 (in Russian).

Krasnobaev A.A. and Semikhatov M.A. Geochronology of Upper Proterozoic of the USSR. In book: Methods of izotope geology and geochronological chart. M.: Nauka. 1986. P. 159-183 (in Russian).

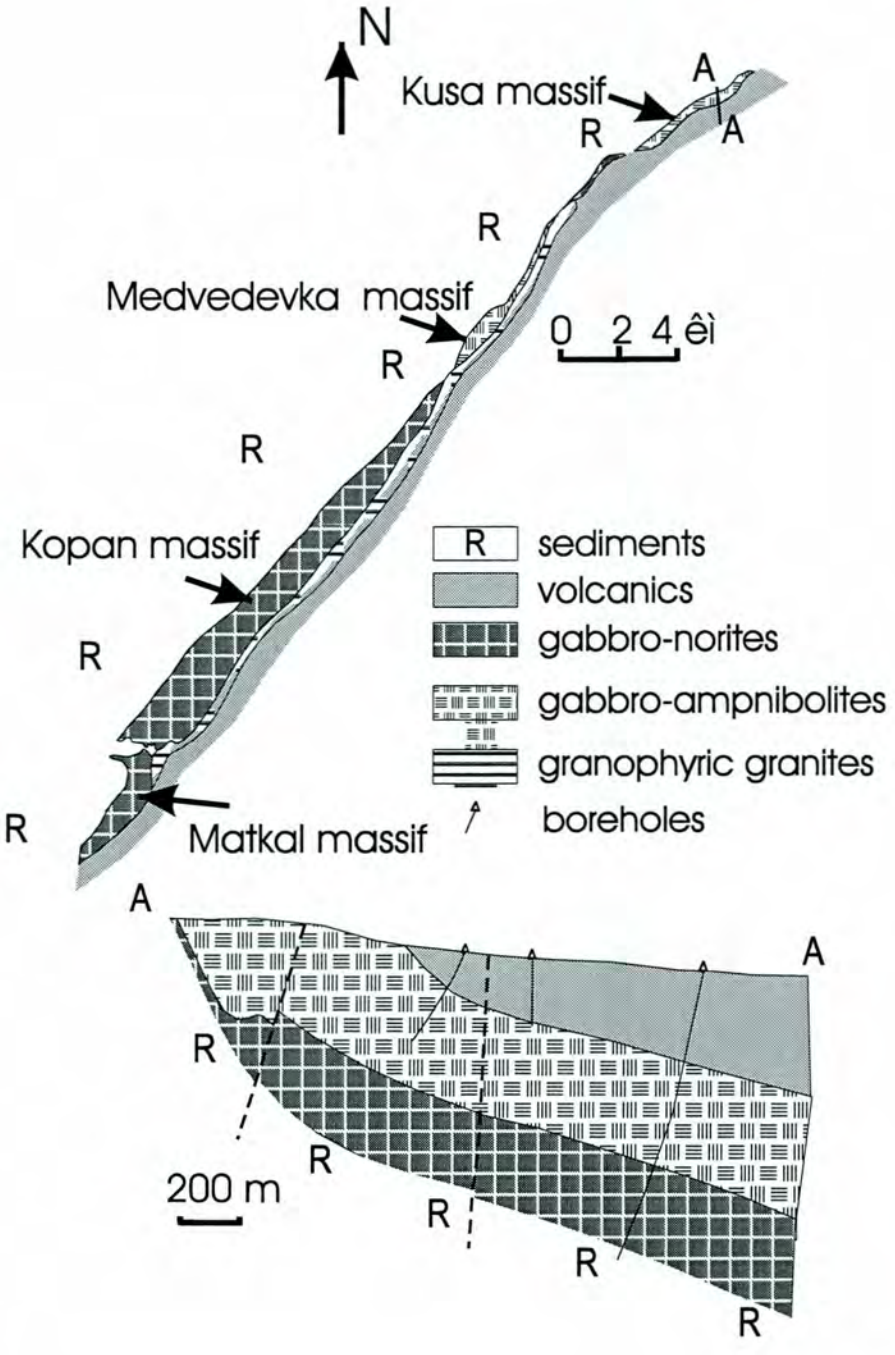

Fig. 1: Geological position of gabbro intrusions and section A-A (after Alekseev and Alekseeva) of Kusa massif.

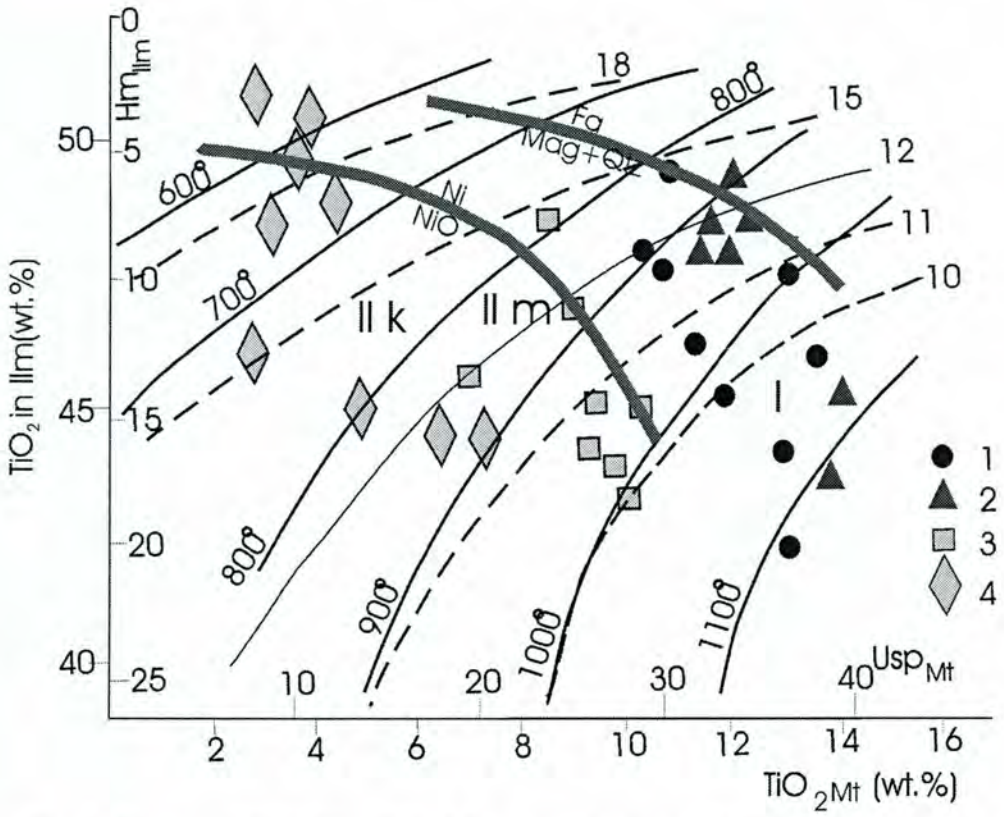

Fig. 2: Diagram Al/Si hbl - Al/Si pl for determination of P H_2O conditions of plagioclase-hornblende equilibrium. Numbers in circles are the pressure, in kbars (after Fershtater, 1990).

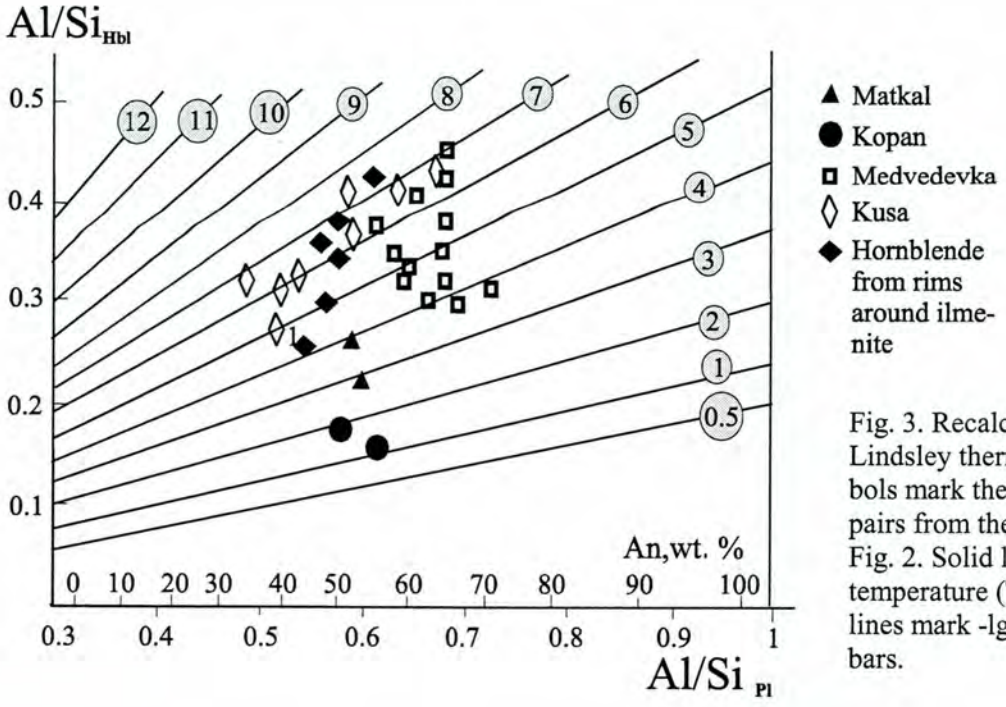

Fig. 3. Recalculated Baddington-Lindsley thermometer. 1- 4 symbols mark the magnetite-ilmenite pairs from the same massifs as in Fig. 2. Solid lines represent the temperature (°C) and dashed lines mark -lg of fO_2 fugacity, bars.

Gauthier M:

Cambrian titaniferous paleoplacers deposited on an Iapetus ocean's shoal at the margin of the Grenville Province (Canadian Shield) and, then metamorphosed during the Taconian Orogeny of the Quebec Appalachians

Michel Gauthier
Département des Sciences de la Terre, Université du Québec à Montréal, c.p. 8888, succ. 'Centre-Ville', Montréal (Qc) Canada H3C 3P8 (gauthier.michel@uqam.ca)

Key words: Grenvillian source rocks, weathering under low paleolatitude, transport, deposition, Taconian metamorphism.

Force (1991) noticed that only two types of ore deposit account for more than 90% of the world production of titanium minerals: 1) magmatic ilmenite deposits and (2) young shoreline placer deposits. He further notice that the placer resources are declining while the consumption of titanium minerals is increasing. Force (1991) concluded that' by the year 2010, we are likely to see titanium minerals being produced from deposits types not currently exploited. This means a challenge for economic geologists to define these new ore deposit type'. The purpose of our scientific communication will be to address this challenge from a northeastern North American perspective. Regional metallogeny concepts are first applied (e.g. 1) nature and extend of the proper source rocks, 2) weathering history (actual (Quaternary) and, past (EoCambrian)). Then a specific location were these favourable conditions seem to have occurred (e.g. Sutton (Qc)) will be examplified in further details

The Grenville Province is a Mesoproterozoic orogenic belt flanking the southeastern margin of the Canadian Shield. It outcrops in a 500 km wide and 2 000 km long high-grade metamorphic belt in the Canadian Shield as well as outliers in the Paleozoic Appalachians orogenic belt of New Jersey, Vermont, Maine and Quebec. The Grenville Province is known for its large anorthosite massifs and for its numerous magmatic titaniferous deposits. The most important are Lac Allard in Québec and Sanford Lake in the Adirondacks Mountains of New York (Fig. 1). Considering all this, the Grenville Province appears to be a very prospective source-region for younger titaniferous placers. As a matter placers are known to occur in Quaternary alluvial and deltaic deposits. The most important is Natashquan, a large deposit occurring in the Natashquan river delta on the St. Lawrence North Shore. An other Quaternary placer occurs were the Peribonka river form a delta in lake St. Jean. Both Natashquan and Peribonka placer deposits have been evaluated in recent years (e.g. Natashquan by Tiomin in the 1990's and Peribonka by SOQUEM in the 1970's). Both deposits are large but do not seem to be economic at this time.

Proper weathering of primary titanium minerals seems to be a prerequisite for the formation of economic placer deposits. Low-latitude (below 30^0) weathering is especially important in increasing the percentage of TiO_2 in ilmenite concentrate (Force, 1991). The duration of weathering under favourable paleolatitude is another important factor. Australia is quite favoured from that perspective. On the contrary, Natashquan and Peribonka, as well as the other Quaternary placers deposited in the Grenvillian region, lack these two prerequisites (e.g. the main weathering process involved was a continental glaciation and the deposition occured above 45^0N).

In the search for new titanium minerals resource, the next question is: if modern conditions were unfavourable for the formation of economic placer deposits in the Grenvillian region, is there any geologic period in which the conditions were more favourable? Such an approach has been succesfully applied to other ore deposit types (e.g. Stratiform copper deposits, cf. Kirkham, 1989).

In EoCambrian time, the Grenvillian cratonic region underwent deep weathering under low-latitude climate (Fig. 2). The widespread occurrence of red-bed sediments in rift facies of the early Iapetus ocean testify of such a paleoenvironment in the Quebec Appalachians (Gauthier et al. 1994). If paleoplacers of this age are preserved in Cambrian stratas, they might be of better grade than their Quaternary equivalent. During the 1980's, such paleoplacers have been identified near Sutton (Fig. 2) in the Quebec Appalachians.

The Sutton paleoplacers occur at the base of the Pinnacle Formation, in wacke and sandstone overlying alkaline volcanic rocks of the Tibbit Hill Formation. These heavy mineral deposits are marine placers that were deposited on an extensive shoal with strong drift currents at the mouth of the Proto-Ottawa river (Marquis and Kumarapeli, 1993). Extending laterally for several kilometers, the horizon comprise titaniferous magnetite and ilmenite replaced by hematite-leucoxene assemblage as well as.primary rutile, zircon and tourmaline as the heavy minerals. Massive heavy mineral horizons average 3 m and locally are 7 m thick. Together, the opaque minerals comprise 10 to 50 percent, and locally 95 percent, of the black sand paleoplacers.

The paleoplacer horizons were folded during the Mid-Ordovician Taconian orogeny. Detrital titanium minerals were sheared and dispersed along schistosity plane and formed fine-grained leucoxene dissemination. These leucoxene grains are finely intergrowth with chlorite. Local recrystallization of the detrital hematite-leucoxene assemblage to low Ti magnetite took place along Taconian thrust faults, producing an assemblage of euhedral magnetite and rutile with detrital rounded grains of zircon.

The rutile potential of these plaeoplacers was evaluated by SOQUEM in the early 1990's. Although tonnages and grades were impressive, rutile fineness and its intimate intermixing with hematite renders commercial extraction of the rutile uneconomic at that time. Although a major source-region and favourable climate prevaled during the deposition of these paleoplacers, subsequent deformation under greenschist facies metamorphic conditions proved to be deleterious. However, recrystallization along Taconian thrust faults was beneficial for rutile recovery.

The Sutton case history suggests that the search for new titanium mineral resources may need the interplay of different disciplines of the Earth Sciences (eg. Igneous petrology, paleo-climatology, sedimentology, metamorphic petrology and structural geology), a combination we are not accustomize to use in economic geology. The deleterious effects of low-grade metamophism and the positive effect of higher grade recrystallization on the Sutton titanium mineral deposits is a reminiscence of the Lake Superior type of iron deposits in which the iron-ore industry make a break-through in the 1950's combining a metamorphic petrology approach to sedimentology (James, 1954 and 1955). This may be one of the way to address the challenge to economic geologists pointed out by Force (1991)

References

Force E.R. (1991). Geology of titanium-mineral deposits. Geological Society of America, special paper 259, 112 pages.

Gauthier, M., Chartrand, F. and, Trottier, J. (1994). Metallogenic Epochs and Metallogenic Provinces of the Estrie-Beauce Region, Southern Quebec Appalachians. Economic Geology, Vol. 89, 1322-1360.

James H.L. (1954). Sedimentary facies of iron formation. Economic Geology, Vol. 76, 146-153.

James H.L. (1955). Zones of regional metamorphism in the Precambrian of northern Michigan. Geological Society of America bulletin, Vol. 66, 1455-1488.
Kirkham, R.V. (1989). Distribution, settings and genesis of sediment-hosted stratiform copper deposits in Sediment-hosted Stratiform Copper deposits, (ed) R.W. Boyle, A.C. Brown, C.W. Jefferson, E.C. Jowett and R.V. Kirkham. Geological Association of Canada, special volume 36, 3-38.
Marquis, R. and, Kumarapeli, P.S. (1993). An Early Cambrian deltaic model for an Iapetan rift-arm drainage system, southeastern Quebec. Canadian Journal of Earth Sciences, Vol. 30, 1254-1261.

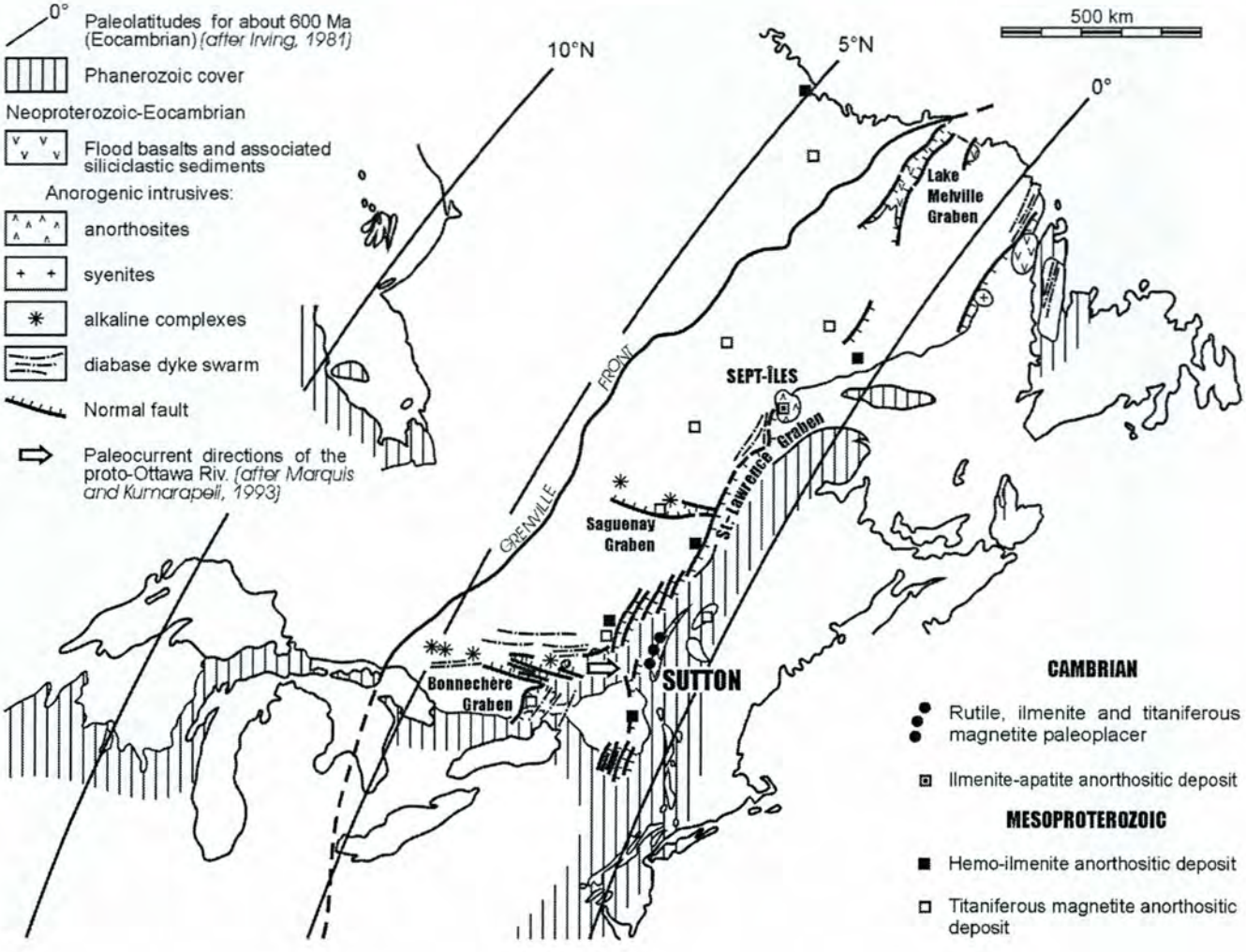

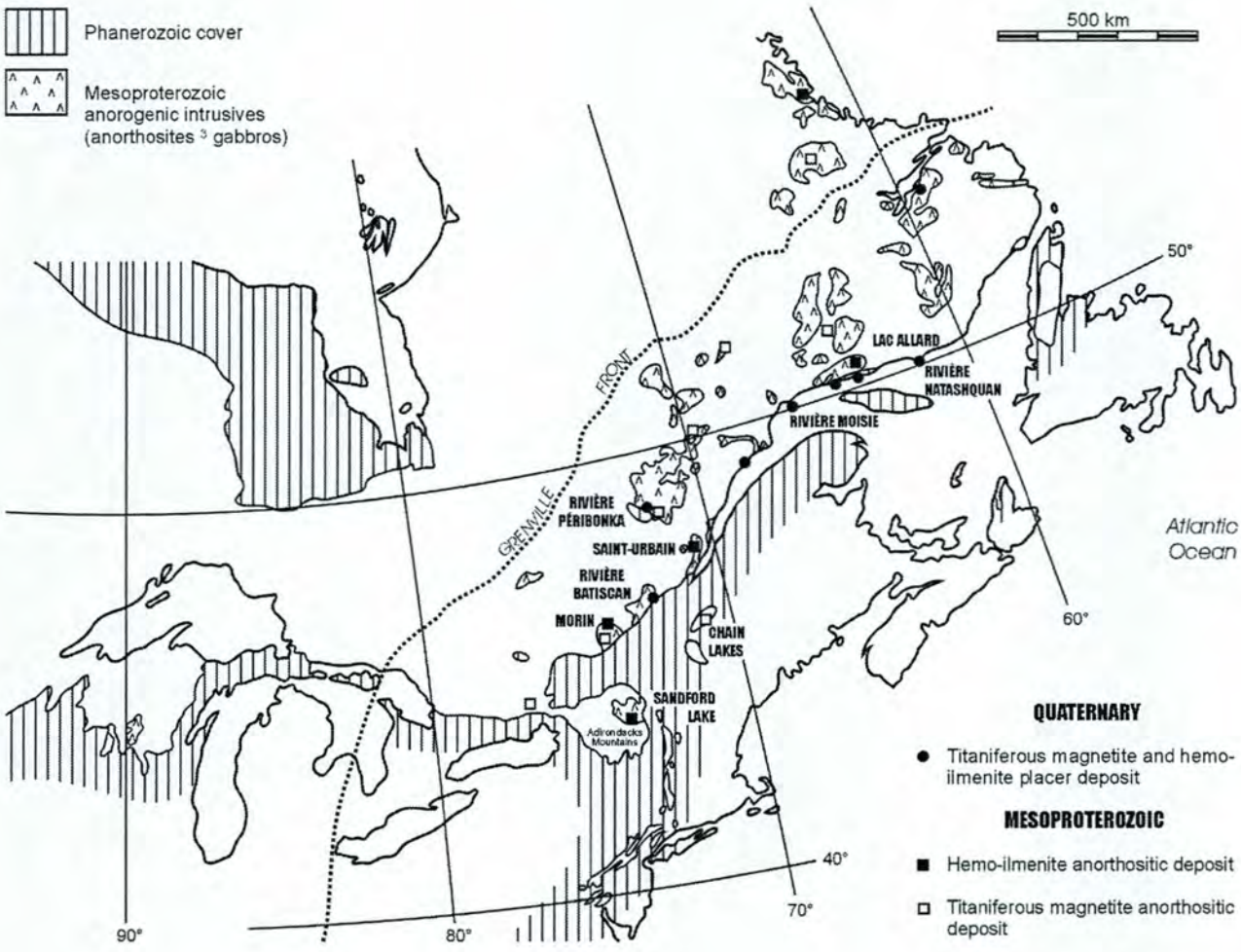

Gautneb H:

SEM elemental mapping and characterisation of ilmenite, magnetite and apatite from the Bjerkreim-Sokndal layered intrusion

Håvard Gautneb
Department of Mineral Resources, Geological Survey of Norway, N-7491, Trondheim, Norway.

Introduction

The grade and grain-size distribution of ore minerals are key factors in evaluating economic mineral deposits. The poster shows the results of mineral characterisation based on SEM elemental mapping and image processing. The work is part of Geological Survey of Norway's ongoing exploration for apatite, ilmenite and vanadium-bearing magnetite in the Bjerkreim-Sokndal layered intrusion.

Materials and Methods

The samples for this study was collected by several co-workers. The stratigraphical and petrogenetic interpretations of the samples are reported in other contributions in this conference. Selected thin sections was measured by SEM using EDS X-RAY elemental mapping. With our SEM instrumentation, we obtain picture files for up to 16 different elements, (one picture for each element). The images was recorded with a magnification of 16 times and the mapped area covers about 1/3 of a standard thin section. The x-ray element maps were processed using the KS300 image processing software. The X-ray images are converted to binary images which again are improved by morphological operations (several steps combining erosion and dilation) to remove noise, artificial grain contacts etc. Finally, by some steps of BOOLEAN image combination, new images are generated which represents the area distribution of selected minerals.

The image processing software automatically measures the morphological features (such as area, longest and shortest axis, axis of enclosing ellipse of each mineral grain etc.). In addition the total modal % of all minerals in the rock and the modal % of ilmenite magnetite and apatite within selected size fractions where calculated. Tables and figures are presented that show the total content of ilmenite, magnetite and apatite and the content within selected grain size classes. The results are shown on the figures and table below.

Grain-size distribution for apatite, ilmenite and magnetite measured by SEM imaging and processing.

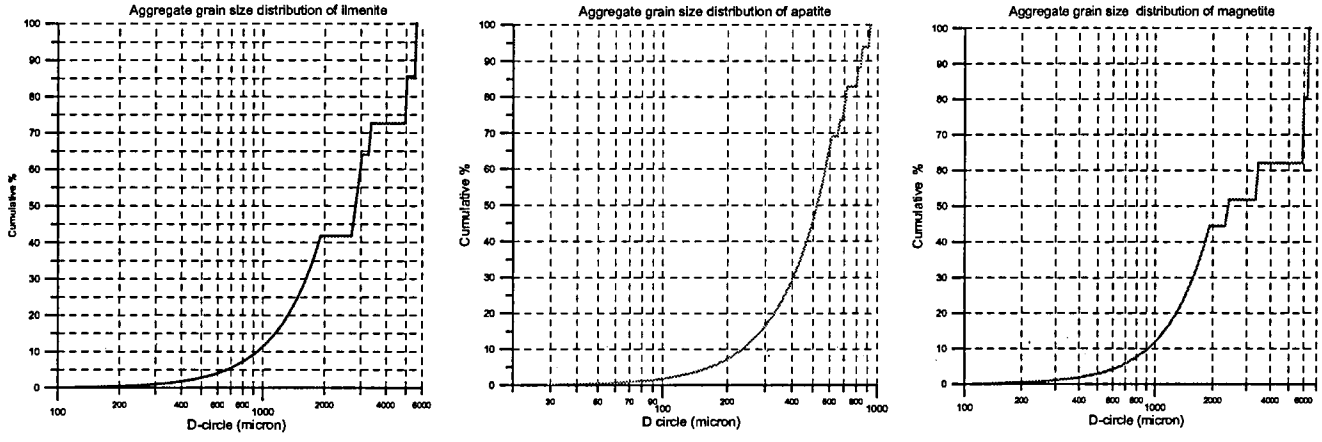

Conclusions

Our 35 analysed samples have the following modal and statistical data:

Ilmenite: The average mode is 14.17% the maximum value 54.71%. 2.7% of the total ilmenite in a sample is on average less than 50 micron. The D_{50} grain size (D-circle) is 2850 microns in diameter.

Magnetite: The average mode is 11.44% the maximum content is 51.95%. 4.50% of the total magnetite are on average less than 50 micron. The D_{50} d-circle length is 2400 microns.

Apatite: The average mode is 5.74%, the maximum content 12.78% 16% of the samples total apatite is in grains on average less than 50 micron. The D50 d-circle length is 523 microns

The sample that contains the highest content of apatite (12.78%) also contains 11.46 % of ilmenite and 6.56% of magnetite. This is a sample from the mega-cyclic unit 3e north of Vasshus.

Table 1: Content of apatite, ilmenite and magnetite in Bjerkeim-Sokndal rocks (unit, refers to the syclic units of the intrusion)

			% apatite in size class (microns)							% Ilmenite in size classes (microns)							% magnetite in size classes (microns)						
Sample no.	Locality	Unit	% total ap.	%ap <50	%ap <50	%ap 100 - 150	% ap 150 - 200	% ap 150 - 200	% ap >250	% total ilm.	% ilm < 50	% ilm 50 - 100	% ilm 100 - 150	% ilm 150 - 200	% ilm 200 - 250	% ilm >250	% total mt	% mt < 50	% mt 50 - 100	% mt 100 - 150	% mt 150 - 200	% mt 200 - 250	% mt >250
BJ9901	Orrestad	MCUIV	7.22	0.04	0.19	0.4	0.82	0.79	4.97	5.12	0.1	0.23	0.24	0.4	0.74	3.43	1.77	0.16	0.21	0.17	0.1	0	1.12
BJ9902	Orrestad	MCUIV	8.15	0.05	0.24	0.71	1.11	0.72	5.32	4.65	0.1	0.1	0.29	0.2	0.24	3.69	4.64	0.04	0.11	0.16	0.31	0.19	3.82
BJ9903	Orrestad	MCUIV	10.72	0.06	0.16	0.39	0.69	1.13	8.29	4.07	0.14	0.15	0.23	0.2	0.56	2.85	3.01	0.1	0.28	0.17	0.38	0.09	2
Bj9905	Orrestad	MCUIV	4.52	0.05	0.14	0.3	0.43	0.39	3.2	1.96	0.16	0.1	0.14	0.2	0.15	1.26	1.96	0.16	0.1	0.14	0.16	0.15	1.26
BJ9907	Orrestad	MCUIV	5.28	0.02	0.1	0.28	0.6	0.46	3.82	4.44	0.13	0.15	0.33	0.3	0.14	3.33	4.72	0.12	0.29	0.23	0.18	0.31	3.58
BJ9909	Orrestad	MCUIV	8.32	0.11	0.65	1.07	1.35	0.93	4.22	2.91	0.34	0.29	0.36	0.2	0.64	1.12	2.91	0.34	0.29	0.36	0.17	0.64	1.12
BJ9910	Orrestad	MCUIV	6.39	0.04	0.17	0.58	0.81	0.66	4.14	4.71	0.33	0.17	0.1	0.2	0.19	3.75	6.86	0.22	0.32	0.36	0.23	0.16	5.56
BJ9912	Orrestad	MCUIV	8.41	0.06	0.24	0.58	0.68	0.99	5.86	13.4	0.22	0.21	0.15	0.2	0	12.64	6.21	0.34	0.32	0.16	0.08	0.44	4.87
K320a	Svalestad	MCUIII	10.62	0.42	1.05	1.56	1.99	1.85	3.75	9.05	0.30	0.35	0.76	0.78	1.22	5.64	9.74	0.14	0.50	0.53	0.45	0.71	7.41
K320b	Svalestad	MCUIII	11.28	0.41	0.91	1.28	1.33	0.89	6.46	6.11	0.15	0.26	0.19	0.3	0.56	4.7	13.7	0.2	0.37	0.31	0.33	0.32	12.2
K322a	N Vasshus	MCUIII	11.35	0.61	1.99	2.37	2.58	2.47	1.33	8.28	0.48	0.78	0.99	1.1	1.2	3.77	10.61	0.2	0.65	0.66	0.74	0.88	7.47
K323a	N Vasshus	MCUIII	12.78	0.22	0.91	1.4	1.8	1.77	6.7	11.5	0.26	0.32	0.46	0.5	0.39	9.52	6.56	0.37	0.36	0.44	0.35	0.47	4.56
K324a	Orrestad	MCUIV	11.97	0.15	0.81	1.16	1.39	1.22	7.24	9.2	0.07	0.14	0.38	0.5	0.32	7.79	9.8	0.18	0.5	0.4	0.55	0.4	7.77
LPN088	Bakka	MCUIV	10.15	0.32	1.24	1.32	1.24	1.47	4.57	16.5	0.07	0.09	0.2	0.5	0.49	15.18	14.9	0.08	0.37	0.55	0.6	0.67	12.6
LPN085	Bakka	MCUIV	11.24	0.38	1.49	2.77	1.67	1.93	2.99	18.9	0.03	0.16	0.27	0.2	0.51	17.75	23.58	0.13	0.56	0.56	0.41	0.56	21.4
LPN090	Mydland	MCUIV	7.36	0.21	0.59	0.8	0.85	1.08	3.82	7.32	0.02	0.07	0.15	0.2	0.14	6.76	9.69	0.11	0.26	0.34	0.29	0.32	8.36
LPN144	Hauge	MCUIV	0.27	0.09	0.17	0.02	0	0	0	54.7	0.31	0.16	0.07	0	0	54.17	31.39	0.05	0.13	0.04	0.04	0.34	30.8
LPN148	Årstad 01	MCUIV	0	0	0	0	0	0	0	27.6	0.46	0.22	0.16	0.2	0.26	26.32	64.3	0.06	0.06	0.02	0.04	0.1	64
LPN166	Sokndal 111	MCUIV	0.06	0.03	0.02	0	0	0	0	51.3	0.01	0.08	0.09	0.2	0.25	50.62	0	0	0	0	0	0	0
LPN167	Sokndal 112	MCUIV	0.04	0.04	0	0	0	0	0	18	0.08	0.2	0.31	0.4	0.78	16.25	8.39	0.07	0.07	0.22	0.19	0.43	7.42
LPN167	Sokndal 112	MCUIV	0.04	0.04	0	0	0	0	0	18	0.08	0.2	0.31	0.4	0.78	16.25	8.39	0.07	0.07	0.22	0.19	0.43	7.42
LPN184	Sokndal 121	MCUIV	0.04	0.04	0	0	0	0	0	24.3	0.13	0.37	0.63	0.7	1.01	21.55	6.05	0.14	0.19	0.4	0.45	1.2	3.66
LPN187	Sokndal 123	MCUIV	0.07	0.03	0.01	0	0.04	0	0	20.6	0.18	0.12	0.15	0.2	0.15	19.85	51.95	0.09	0.09	0.08	0.06	0.1	51.5
LPN192-19	Sokndal	MCUIV	1.67	0.2	0.46	0.59	0.24	0.07	0.12	31.8	0.07	0.07	0.12	0	0	31.53	24.9	0.06	0.17	0.22	0.34	0.14	24
LPN192-23	Sokndal	MCUIV	2.42	0.25	0.73	0.6	0.46	0.24	0.14	25	0.09	0.2	0.13	0.1	0.34	24.07	29.92	0.39	0.33	0.33	0.41	0.67	27.8
LPN223	Mydland	MCUIV	2.14	0.17	0.27	0.38	0.49	0.24	0.59	16.1	0.1	0.29	0.43	0.9	0.99	13.47	1.81	0.19	0.29	0.24	0.25	0.49	0.35
LPN227	Åmdal	MCUIV	9.22	0.16	0.97	1.57	1.93	1.55	3.03	11.7	0.13	0.25	0.08	0.2	0.25	10.79	4.6	0.24	0.22	0.27	0.55	0.33	3
LPN231	Rekefjord	Eia-Rekfj.	5.3	0.13	0.75	1.1	0.98	0.4	1.94	3.98	0.07	0.19	0.56	0.3	0.44	2.47	2.27	0.04	0.12	0.13	0.04	0.37	1.57
LPN236	Eia	Eia-Rekfj.	2.48	0.33	0.92	0.67	0.32	0.23	0	2.04	0.12	0.3	0.31	0.5	0.07	0.78	1.94	0.24	0.25	0.34	0.4	0.29	0.42
LPN238	Teksevatn 02	MCIII	8.25	0.32	1.16	1.82	2.04	1.4	1.51	8.66	0.21	0.65	0.83	1	0.74	5.28	2.52	0.23	0.45	0.42	0.13	0.39	0.91
LPN248	Eigeland 1	Anorth.	2.11	0.81	0.91	0.33	0	0.07	0	2.6	0.39	0.54	0.36	0.3	0.08	0.93	8.57	0.29	1.18	1.51	1.2	0.88	3.52
LPN252	Dragland 252	MCUIV	0.37	0.08	0.08	0.06	0.06	0.08	0	24.4	0.08	0.24	0.53	0.6	1.22	21.8	3.61	0.05	0.08	0.19	0.31	0.32	2.66
LPN255	Bilstad 255	MCUIV	0.65	0.14	0.17	0.09	0.14	0	0.1	3.47	0.18	0.45	0.68	0.7	0.38	1.11	5.66	0.5	0.71	0.65	0.37	0.06	3.37
LPN256	Bilstad 256	MCUIV	10.91	0.31	0.95	1.42	1.96	1.42	4.85	9.02	0.21	0.44	0.61	0.6	0.54	6.66	0	0	0	0	0	0	0
LPN260	Bakka 260	MCUIV	9.19	0.28	1.13	1.45	1.67	1.64	3.02	14.4	0.08	0.33	0.46	0.2	0.38	13.02	13.61	0.16	0.23	0.22	0.33	0.37	12.3
Averages			5.74	0.19	0.56	0.77	0.85	0.75	2.63	####	0.17	0.25	0.34	0.37	0.46	12.57	11.44	0.16	0.29	0.32	0.30	0.38	9.99

Gongalsky BI & Sukhanov MK:

On the position of Chinites (plagioclase-titanomagnetite rocks) in the Chiney Layered Pluton (North Transbaikal)

B. I. Gongalsky & Sukhanov M.K.
Institute of geology of ore deposits, petrography, mineralogy and geochemistry, Russian Academy of Sciences, Russia.

High-Ti gabbroids with layering on different scales occur in the 100 km^2 Chiney layered pluton in North Transbaikal. They form series (1-1,5 km thick), members (70-200 m thick) and rhythms (< 3 m). They contain titanomagnetite as one of the main rock-forming minerals as well as monomineralic titanomagnetite rocks. Titanomagnetite-plagioclase rocks showing wide variations in modal proportions form 10 to 90% of layered units and they have been called chinites from the China River which cuts across the massif. Chinites form a large titanomagnetite ore deposit situated near the Baikal-Amur railroad that is ready for mineral extraction. There are some other names in geological publications for the rocks enriched in titanomagnetite: kosvite (titanomagnetite-clinopyroxene rock) or kazanskite (magnetite-troctolite). Chinites are tinanomagnetite gabbros or titanomagnetite anorthosites. In the lower parts of the layered members of Chiney massif there are kosvites but in the upper parts there are chinites associated with anorthosites. The thickest layer (about 60 m) composed of gabbro-chinites and massive ore is situated in upper part of the massif. Plagioclase (An50-55) forms grains 0,3 - 5 mm, titanomagnetite is situated in the interstices and surrounded by thin rims of biotite (0,1 mm) which forms a coronite-like structure. Apatite, pyrite and fluorite are typical accessories. Modelling of the fractional crystallization of average compositions of layered units displays a great similarity with compositions of real layered sequences. The formation of chinites end the process of bulk liquid crystallization, and volatile and alkaline metal enrichment led to liquation of the residual liquid with the formation of anorthosite and titanomagnetite layers. This research was supported by the Russian Foundation for Basic Research, grant 00-65-65000.

Typical chemical compositions of chinites:

SiO_2	TiO_2	Al_2O_3	Fe_2O_3	FeO	MnO	MgO	CaO	Na_2O	K_2O	P_2O_5
44,77	2,83	18,62	17,34	9,48	0,13	2,82	8,62	3,55	0,47	0,06
33,36	4,69	16,49	32,79	14,72	0,12	1,70	7,47	3,68	0,39	0,03
41,26	3,28	13,92	21,70	10,92	0,17	4,94	10,42	3,61	0,44	0,06
26,04	7,51	14,99	39,93	16,38	0,17	1,52	5,51	2,96	0,39	0,03
33,40	6,20	16,44	34,24	19,97	0,14	2,07	6,69	4,16	0,51	0,05
12,26	11,52	8,26	61,62	29,53	0,26	2,94	2,68	3,31	0,21	0,03

Gursky D, Nechaev S & Bobrov A:

Titanium deposits in Ukraine focussed on the Proterozoic anorthosite-hosted massives

Dmitry Gursky, Sergey Nechaev, Alexander Bobrov
Department of Geology, Ukrainian State Geological Research Institute, Avtozavodskaia St. 78. UA-04114 Kiev, Ukraine

Titanium deposits and prospects in Ukraine are related to Proterozoic and Palaeozoic magmatic basic rocks, Mesozoic and Cenozoic weathering crusts of basic rocks and alluvial placers, and Cenozoic littoral placers. The reserves and resources of Ti-ores are a stable basis for the Ukrainian titanium industry. The basis for the latter are the exogenic deposits of Ti-ores, whereas endogenic ores are not presently mined. Nevertheless the main Ti resources are hosted by gabbro-anorthosite massives.

The Ukrainian Ti-ore province as determined by J.J.Malyshev (1957) coincides spatially with the outlines of the Ukrainian Shield (USh) Precambrian complexes and its Mesozoic and Cenozoic cover. Later, the borders of the province were enlarged into the Dnieper-Donets aulacogen (Fig.1).

During the former USSR a large Ti-mineral industry was created in the Ukraine. The share of the Ukrainian TiO_2 industrial reserves in the USSR total was 42%, including more than 90% in the European part of the country. The basis of the industry includes more than 40 Ti-deposits, of which 11 are explored in detail. However, only 5 of them, of exogenic origin, are being exploited. The other Ti-deposits are reserves.

TiO_2 production in the Ukraine is considerable (Table 1).

Table 1. Overall production of ilmenite and rutile concentrates in Ukraine during 1988-1992 (thousands of tons recalculated as TiO_2, after Belous, 1998).

Form of production	1988	1989	1990	1991	1992
Ilmenite concentrate	263.0	249.3	229.6	217.2	221.4
Rutile concentrate	118.2	130.4	123.6	108.0	108.7
Total	381.2	379.7	353.2	325.2	330.1

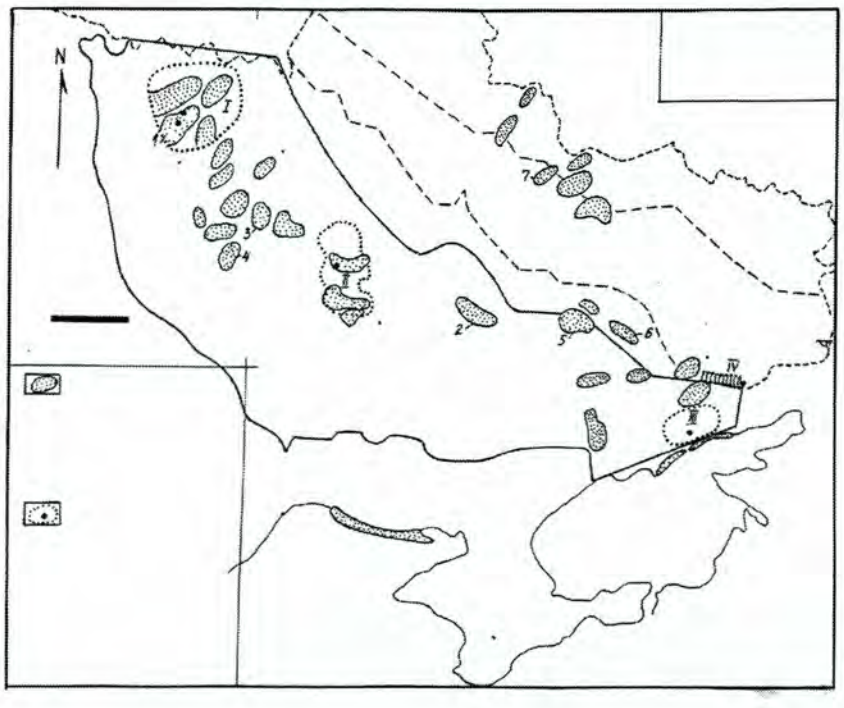

Ti-deposits are worked by the Irshansk Integrated Mining and Dressing and Verkhnedneprovsk State Mining and Metallurgical Combines. Since the active Ti mines in the Ukraine are in exogenic deposits, these are dealt with first.

Fig. 1 Sketch map showing the location of titanium deposits and prospects within the Ukrainian province

Table 2. The principal geological-industrial types of exogenic Ti-deposits (after Belous, 1998)

Deposit	Geological setting	Host rocks and their age	Ore bodies morphology	Ore mineral composition	Simultaneously useful component
Irsha group deposits	Sedimentary cover of the Ush	Alluvial and alluvial-deluvium deposits (secondary kaolin and kaolin clay), Mesozoic and Cenozoic	Layered	Ilmenite	Apatite
Malyshev, Volchansk, Tarasov, Zelenoyar	Sedimentary cover of the Ush, littoral placers	Sandy-clayey deposits, Neogene	Layered and lens-like	Ilmenite, rutile, leucoxene	Zircon, kyanite, staurolite, xenotime, sillimanite, diamonds
Krasnokut	The Dnieper-Donetz aulacogen, deltaic placers	Sandy-clayey deposits, Neogene	Layered and lens-like	Ilmenite leucoxene	Zircon

Exogenic deposits of Ti-ores are of residual and placer types. Residual deposits are spatially related to Mesozoic weathering of Ti-bearing gabbro-anorthosite massives in the northwest part of the USh. Average thickness of the weathering crust is between 10-15 m, but within linear tectonic zones it reaches 50-70 m and in places even more. The content of ilmenite in the weathering crust depends on its content in the primary crystalline rocks and normally fluctuates from 30 kg/m^3 up to 130 kg/m^3, reaching 200 kg/m^3 in productive horizons of weathered crust. According to V.S.Tarasenko (1992) layered ore bodies consist of kaolinite, montmorillonite and hydromica, and contain between 6.0-10.8% TiO_2 and 0.5-2.6% P_2O_5 related to ilmenite and apatite respectively. Placer deposits are the main industrial Ti-ores in Ukraine and complex Ti-Zr littoral placers in particular, although continental alluvial ilmenite placers are also important. The latter are developed to the northwest of Ush and are related to intense Upper Jurassic-Lower Cretaceous weathering and erosion. There are both ancient as well as modern continental placers. All of the ancient placers are buried. These are the largest and richest: ores have extents up to 5 km, widths up to 1 km, thicknesses up to 10 m, and ilmenite contents between 150-300 kg/m^3 (Belous, 1998).

Alluvial placers of the northwest USh are monomineralic, and contain alterated ilmenite (leucoxene). The modern placers are small as a rule and contain fresh ilmenite.

Ore bodies in alluvial placers usually are meandering, ribbon-like and coincide with river valleys. Ore minerals are concentrated in the lower parts of placers.

Both residual and alluvial placer deposits, are represented by the Irsha group located to the northwest of USh, and are worked by the Irsha Integrated Mining and Dressing Combine.

Littoral placers are developed in the central and southern regions of the Ukraine and represent ancient and modern sandy beaches and shallow shelfs. The former are buried, and the latter exposed.

The ancient placers coincide with sandy-clayey sediments of the Oligocene-Miocene seas, and the modern ones formed on the spits of land along comparatively short parts of the Azov and Black Seas northern coastlines by long-range drift. The industrial value of the modern placers is rather small, and the ancient are the main industrial type of Ti deposits. The latter are presented by a number of deposits (se table 2), of which only the one at Malyshev is being mined.

The Malyshev deposit (2 in Fig.1), also known as the Samotkan deposit, is a typical littoral placer. Its industrial part is 19 km long, and includes two horizontal layers of ore-grade, fine-grained sands. The average thickness of the upper bed is 11.5 m and the lower one 4.5m. Both of the beds are separated from each other by a barren layer 6-7 m in thickness. The industrial minerals in both of the ore-grade beds are ilmenite, rutile, leucoxene and zircon, as well as kyanite, sillimanite, xenotime and anatase. These minerals are found throughout the upper bed, but only in top part of the lower bed. The average contents (in kg/m^3) of heavy minerals are from 10-15 up to 100-150 including 22-45 ilmenite, 8-13 rutile, 2.5-7 zircon. Grains of ilmenite are 0.07-0.25 mm in

size and rutile 0.07-0.15 mm. The average content of TiO_2 in ilmenite is 67.7% due to leucoxenisation. The Malyshev deposit is worked by the Verkhnedneprovsk State Mining and Metallurgical Combine and the principal products are concentrates of rutile, ilmenite, zircon, kyanite-sillimanite and staurolite as well glass, moulding and building sands. The kyanite-sillimanite concentrate contains diamonds 0.01-0.03 mm in size and as much as 1 carat / t of concentrate.

As reserve for the Combine is the Volchansk deposit (6) located to the east. The average thickness of the ore-grade bed is 6 m, and the average contents (in kg/m^3) are 77 of ilmenite, 25 of rutile and 5.5 of zircon. Discovered not far from the Volchansk deposit, the Voskresenov placer (5) is 8 km long and 2 km wide. The thickness of the economic bed is 7 m, and the average contents (in kg/m^3) are 77 of ilmenite, 12 of rutile, and 3.7 of zircon. Ores both of the Volchansk and Voskresenovsk deposits contain sillimanite, kyanite and staurolite.

The Krasnokut (7) placer deposit, located within the Dnieper-Donetz aulacogen, is 6.6 m thick, and contains on average 10.5 (kg/m^3) of ilmenite, 7.7 of rutile, 8.1 of zircon.

The peculiarity of the Miocene littoral placer deposits of the Ukraine is a large number of fine diamonds of the kimberlite, lamproite eclogite and impactite types, as well as indeterminate origin (Kvasnitsa and Tsymbal, 1998). The latter, possibly, are pyroclastic konatiite diamonds. These placers were formed as a result of erosion and redeposition of sands older in age than ones hosting diamonds, the native sources of which remain unknown.

There are four areas with endogenic Ti-ores in Ukraine (se Fig.1). Three of them (I, II, III) are related to anorthosite massives and bodies within the Proterozoic large-scale and composite plutons in the USh: the Korosten, Korsun-Novomirgorod and East Azov. The fourth area, South Donbass, coincides with Devonian volcano-plutonic rocks situated in the border zone between the Azov block of the USh and Dnieper-Donets aulacogen.

There are a number of Ti-deposits/prospects, related to gabbroanorthosite within the Korosten and Korsun-Novomirgorod plutons. These were studied in detail by V.S. Tarasenko, who proposed the classification shown in table 3.

Three deposits may serve as examples: The Stremigorod, Krapivnia and Nosachev deposits.

(a) The Stremigorod Ti-deposit is situated within the Korosten pluton, and related to the monzonite-peridotite complex of the 830 km^2 Chepovichi gabbro-anorthosite massif. The ore body has an irregular oval form (2.3 x 1 km in size) and elongated in northwest direction along the Central Korosten fault. In cross section the ore body is conical with rather steep and sharp contacts with the host rocks. It is traced to a depth of 1200m and is characterized by a concentric structure: the central part represented by plagioclase peridotite and melanocratic troctolite, which are replaced gradually to the peripheral part by increasingly leucocratic troctolite, olivine gabbro, gabbro-monzonite, and gabbro-pegmatite (Fig.2). Troctolite is the main rock type in ore body.

Ores of the Stremigorod deposit are characterized by uniform compositions and distributions of apatite and ilmenite. Concentration of ore minerals increases from the peripheral to the central parts of the ore body (Table 4).

The richest apatite-ilmenite ores in central part of deposit contain 6.9-8.17 % TiO_2 and 2.8-4.9% P_2O_5 whereas the peripheral part contains 3.36-5.9% and 0.65-1.5`% and andesinite and monzonite contain no more than 1% TiO_2 and 0.5 % P_2O_5.

The weathering crust above the Stremigorod deposit contains between of 8-10% TiO_2 and 2.5% P_2O_5.

Table 3. Types of phosphate-titanium ores in gabbro-anorthosite massives in the Ukrainian Shield (after Tarasenko,1992)

Industrial type of ores	Settings		Morphology of ore bodies	Mineral composition		Content in ore (%)		Technological parameters of ores			
	Regional	Local		Ore minerals	Rock-forming minerals	TiO_2	P_2O_5	Extraction of the concentrate (%)		Content in the concentrate (%)	
								TiO_2	P_2O_5	TiO_2	P_2O_5
Apatite-ilmenite in troctolite	Anorthosite-granite assem-blage of the Korosten pluton	Monzonite-peridotite complex of the Chepovichi massif	Stock-like	Ilmenite, apatite	Olivine, plagioclase, pyroxene	4.1-8.2	0.52-4.95	70-75	75-80	45.3	37.39
Apatite-ilmenite-titanomagnetite with ulvospinel in peridotite and pyroxenite	Anorthosite-granite assem-blage of the Korosten pluton	Monzonite-peridotite complex of the Volodarsk-Volynsk massif	Layer-, lens-like	Ilmenite, apatite, titanomagnetite, magnetite	Olivine, plagioclase, pyroxene	5.0-8.0	0.3-3.5	65-70	68-70	40-42	35-37
Apatite-ilmenite and ilmenite in gabbro-norite	Anorthosite-granite assem-blage of the Korosten pluton and Korsun-Novo-mirgorod plutons	Monzonite-norite com-plex of the Volodarsk-Volynsk, Smela, Novo-mirgorod and ather massifs	Layer-, dyke-like	Ilmenite, apatite	Plagioclase, ortho- and clinopyro-xene, olivine	4.0-4.5, up to 36	0.5-2.5	70-84	70-80	48-50	35-37

Table 4. Modal and chemical characteristic of apatite-ilmenite ores of the Stremigorod deposit (after Tarasenko, 1992)

Mineral and chemical composition (%)	Host rock		
	gabbro	troctolite	peridotite
Plagioclase (An_{40-55})	60.6-64.4	37.1-46.0	25.5-31.6
Pyroxene (salite of augite series)	0.6-3.2	0.4-1.4	i.g*-0.7
Olivine (hyalosiderite Fa_{35-45}-hortonolite Fa_{50-58})	3.3-8.4	17.5-22.7	20.1-26.4
Ilmenite	4.95-11.4	11.6-12.6	11.6-15.1
Titanomagnetite	0.4-0.85	1.2-1.9	0.55-3.87
Apatite	1.1-3.0	4.5-6.0	8.1-10.1
Amphibole, talc, chlorite	15.1-19.8	17.9-21.7	16.8-21.7
TiO_2	3.36-5.99	6.8-7.2	6.9-8.17
P_2O_5	0.65-1.5	2.8-3.1	3.58-4.5
FeO	8.97-12.3	14.0-16.47	15.0-21.82
Fe_2O_3	2.82-4.35	5.27-5.86	4.56-6.31
MgO	3.38-6.02	7.37-8.17	6.87-9.01

* Individual grains

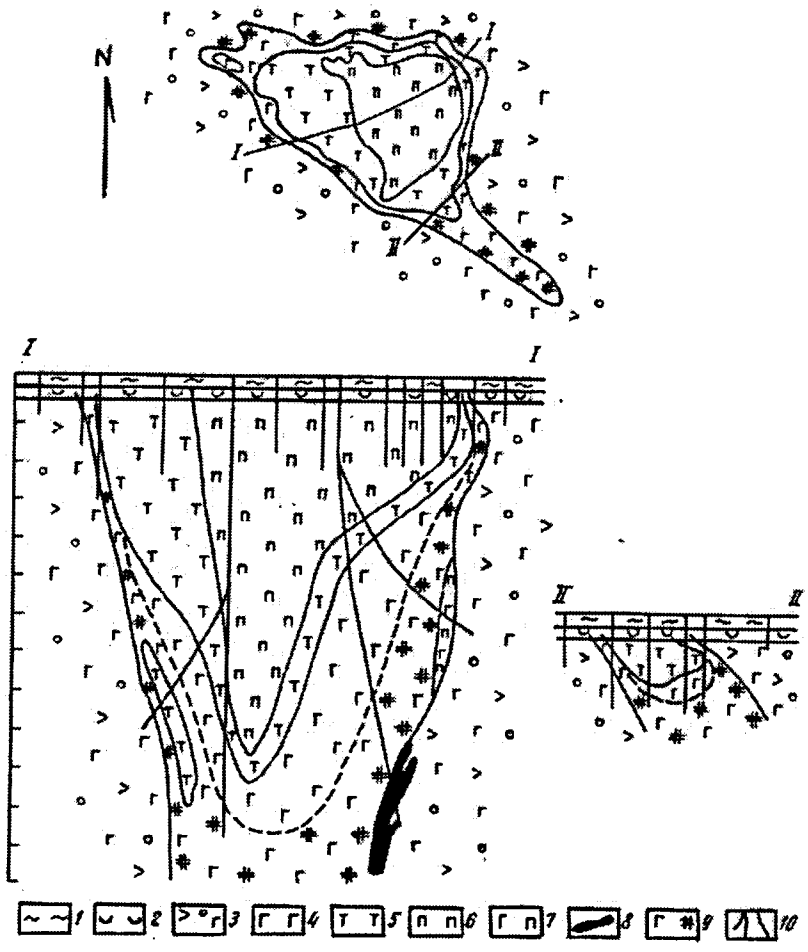

Fig.2 Schematic geologic map and cross sections of the Stremigorod deposit (after Tarasenko, 1990). 1 - sedimentary cover rocks, 2 - weathering crust, 3 - gabbroanorthosite, 4 - gabbro, 5 - ore-bearing troctolite, 6 - ore-bearing plagioclase peridotite and melanocratic troctolite, 7 - gabbropegmatite, 8 - olivine gabbro pegmatite, 9 - gabbromonzonite and quartz andesinite, 10 - exploratory bore hole.

Three varieties of apatite-ilmenite ores are distinguished: (1) poor, disseminated in olivine gabbro, (2) medium-rich, disseminated in leucocratic troctolite, (3) medium-rich ore disseminated in troctolite and plagioclase peridotite.

In the ore-bearing troctolite, 80-84% of all the TiO_2 is concentrated in ilmenite, and 90-93.8% of the P_2O_5 is in apatite. The ores are characterized by a rather high extraction of ilmenite and apatite and high contents of TiO_2 and P_2O_5 in the concentrates (Table 4).

(b) The Krapivnia Ti-deposit is located in central part of the Volodarsk-Volynsk gabbro-anorthosite massif within the Korosten pluton. The area of the massif is 1250 km^2.

The ore body has an oval lens-like shape about 350 m in thickness, and is characterized by zonal structure. From the peripheral part of ore body in the direction of the centre the host rocks change from gabbro-anorthosite to andesinite, leucotroctolite and gabbro, ore-bearing olivine gabbro, ore-bearing olivine pyroxenite and plagioclase peridotite.

The ore minerals, ilmenite, magnetite, titanomagnetite and ulvospinel, are concentrated in the interstices between silicates, forming a sideronitic texture. Of the whole-rock content of TiO_2 in ores, 27.8% is concentrated in ilmenite and 60% in titanomagnetite. The latter also contains 0.41% V_2O_5. Mineral and chemical compositions are given in Table 5.

Table 5. Mineral and chemical characteristics of apatite-ilmenite-titanomagnetite ores of the Krapivensk deposit (after Tarasenko, 1992).

Mineral and chemical composition (%)	Host rocks		
	gabbro	peridotite	pyroxenite
Plagioclase An_{45-47} and An_{50-55}	22	6	i.g.
Pyroxene (titanaugite)	29	40.5	45.0
Olivine	14	21	19
Ilmenite	4	6	3.5
Titanomagnetite	17	21.5	25.5
Apatite	4	5	7
Amphibole, talk, chlorite	0.5	i.g.	i.g.
TiO_2	5.84	6.69	7.84
P_2O_5	2.58	2.79	3.17
FeO	20.55	24.66	29.34
Fe_2O_3	4.03	5.44	5.44
MgO	5.96	7.01	7.82

(c) The Nosachev Ti-deposit is situated within the Korsun-Novomirgorod pluton, and located in the southern part of the Smela gabbroanorthosite massif. The deposit has a lens-like form, an overall length of 1.5 km, and a conical form in section.

Ore-bearing gabbronorite is bordered by gabbronorite, monzogabbronorite, quartz andesinite and intensly K-feldspathized gabbroanorthosite (Fig. 3). The zoned structure of the deposit is emphasized by variations in the chemical composition of the host rocks, including their TiO_2 contents: quartz andesinite (no more than 1% TiO_2), gabbronorite (between 3.68-4.58%), ore-bearing gabbronorite (more than 7%).

In gabbronorite forming the outer part of deposit, plagioclase is the dominant mineral (50-60%). The plagioclase is characterized by granulation as well as de-anorthization and very fine segregation of K-feldspar. The content of disseminated ilmenite reaches no more than 7-10%.

Ore-bearing gabbronorite is characterized by medium-rich disseminated and massive ores (Table 6).

Table 6. Mineral and chemical characteristics of ilmenite ores of the Nosachev Ti-deposit (after Tarasenko, 1992).

Mineral and chemical composition	Type of ores		
	Disseminated	Rich disseminated	Massive *
Plagioclase	30-40	25-30	5-10
Pyroxene (ortho-and clino)	20-30	20-30	10-15
Olivine	10-20	i.g.	i.g.
Ilmenite	15-20	30-50	70-80
Titanomagnetite	-	-	-
Apatite	1-3	1-3	i.g.
Amphibole, talk, chlorite	4-7	3-5	5-7
TiO_2	7.0	16.08	34.2
P_2O_5	≤0.26	≤0.25	0.06
FeO	14.89	17.77	29.32
Fe_2O_3	0.9	1.43	1.94
MgO	4.45	3.41	3.95

* Ores of massive type contain 0.24-0.28 V_2O_5 and 0.08-0.12% Cr_2O_3.
Ores are high-technological: TiO_2 extraction in concentrates reaches 84%.

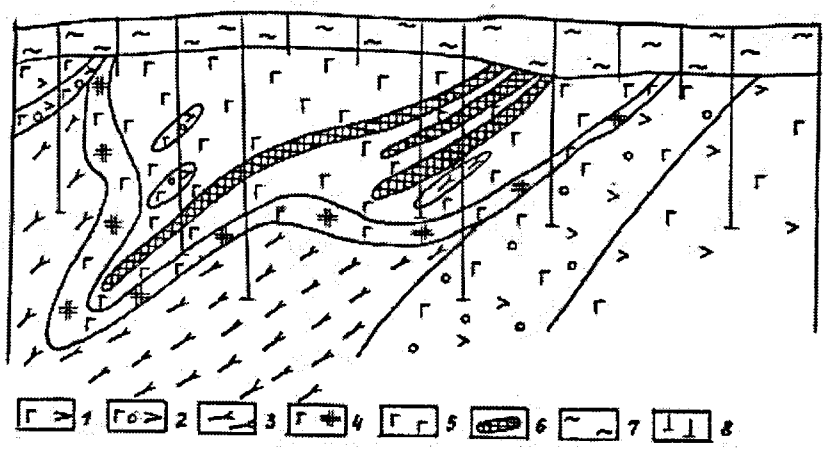

Fig.3. Schematic geologic section of the Nosachev deposit (after Tarasenko, 1990). 1 - gabbroanorthosite, 2 – K-feldspathized gabbro-anorthosite, 3 - quartz andesinite, 4 – monzogabbro-norite, 5 - gabbronorite with disseminated ilmenite ore, 6 - rich, disseminated and massive ilmenite ore, 7 - sedimentary cover rocks, 8 - prospect drill hole.

As distinct from deposits of Ti-ores in the Korosten and Kjrsun-Novomirgorod plutons relationships with gabbro-syenite assemblage are displayed in the East-Azov pluton. An example is the Kalchic prospect (d).The latter is situated in the southern part of the East-Azov pluton for which syenites including one hosting deposits of REE-Zr and Ta-Nb ores are more typical. Anorthosite and rapakivi granite are less characteristic though the East-Azov pluton is synchronous with the Korosten and Korsun-Novomirgorod plutons. According to Tarasenko et al. (1989) the Kalchik Ti-ores are enveloped by steeply-dipping bodies of gabbroid varying from a few dozens of metres up to hundreds in thickness and from a few hundreds of metres up to 4 km and more in length. Ore-bearing gabbroid is represented by layered lenses and schlieren which have indistinct contacts with the host rocks (composite layering of gabbropyroxenite, wehrlite, andesinite, gabbrodiorite and diorite. Ore bodies from a few up to tens of meters in thickness and up to a few hundreds of meters in a length are characterized by small and moderate amounts of ilmenite (6-10%), titanomagnetite (5-7%) and apatite (5-7%). Richer mineralization, but limited in thickness, are within wehrlite and pyroxenite in which the ratio titanomagnetite: ilmenite is 1:2 and 1:1respectively. In spite of the poorness of the ores economic products of apatite and ilmenite were obtained by concentration.

(d) The Palaeozoic Ti-bearing volcano-plutonic assemblag

The setting of this assemblage is determined by the Volnovakha fault zone in the eastern part of the Ukraine, on the boundary of the Azov block and Variscides of the Donets basin. The latter is the southeastern part of the Dnieper-Donets aulacogen, separating the Ush from the Voronezh massif in Russia.

The Palaeozoic volcano-plutonic assemblage is developed between the North- and South-Volnovakha faults as a strip 60 km long and 5 km wide, and the rocks of the assemblage are regarded as initial Ti-bearing formation (Nechaev, 1970).

The assemblage includes three successive complexes (Buturlinov at al., 1972):

1. Intrusives of alkaline-ultrabasic character (390-380±20 Ma),
2. Extrusives of basaltoid (365-335 Ma),
3. Intrusiions of nepheline syenite (330 Ma).

The first and third complexes are developed to the east of the Volnovakha fault zone, where they intruded the Precambrian basement and form the Pokrovo-Kireyevo massif, whereas the second is distributed all over the Volnovakha zone. 1 and 2 are Ti-bearing, but richer concentrations of TiO_2 are related to the alkaline massifs.

(e)The Pokrovo-Kiryevo massif is oval in form and covers 10 km^2. It consists of plagioclase pyroxenite and leucocratic gabbro. In pyroxenite along the massif's border zone there are bodies of ore-bearing pyroxenites 400-600 m long, containing on average 9.05% TiO_2, 0,049% V and 0,15% P. Ti-bearing minerals are titanomagnetite and ilmenite, as well as titanaugite. Titanomagnetite is the main ore mineral.

(f) The Ti-bearing Devonian basaltoid complex forms a cover, with a maximum thickness of 500 m. Typical rocks are shown in Table 7.

Table 7: Chemical composition of basaltoid rocks of the Volnovakha fault zone (after Buturlinov et. al., 1972).

Rock	Oxydes (%)								
	SiO_2	TiO_2	Al_2O_3	Fe_2O_3	FeO	MgO	CaO	Na_2O	K_2O
Picrite-basalt (30)*	41.85	5.18	9.61	7.0	7.09	11.42	10.84	1.72	0.69
Basalt (197)	43.85	5.27	13.18	9.04	5.09	6.40	7.71	2.70	1.99
Andesite-basalt (74)	48.60	4.45	14.63	9.43	3.46	4.50	5.13	3.48	2.21
Trachybasalt (10)	49.79	3.85	15.89	9.10	2.97	3.66	4.08	3.23	4.32
Ore-bearing gabbro-norite of the USh anorthosite massif (after Tarasenko, 1987	49.22	4.60	15.44	1.78	11.67	4.33	7.37	2.70	1.58

* in brackets- number of analyses

Ti-bearing minerals in the main basaltoid rocks are titanaugite, titanomagnetite and ilmenite, but in hydrothermally-altered rocks there are titanite and leucoxene.

There are no known economic Ti-ores related to the basaltoid rocks. However it may be seen (Table 7) that ore-bearing gabbronorite from anorthosite massifs is similar to andesite-basalt in content of oxides Si, Ti,Al, Mg and total Fe, as well to basalt in content of oxides Ca, Na and K.

Conclusion

Ukraine possesses many deposits of Ti-ores, which the presently active are placer and residual deposits, related to the weathering of Ti-bearing anorthosite massifs. Placer deposits are the main industrial type of Ti-ores, and contain considerable resources. The peculiarity of the Miocene littoral placer deposits is a large number of fine diamonds, the source of which remains undetected.

The greatest resources of Ti-ores are related to the Proterozoic anorthosite massifs in the USh. The Devonian Ti-bearing volcano-plutonic complex is interesting from the standpoint of the origin of the geochemical peculiarities of the Proterozoic anorthosite suite.

The elements of metasomatic zonation in the Ti-deposits in anorthosite-rapakivi granite plutons of the Ukrainian Shield illustrate links between the emplacement of the plutons and ore-forming events.

References
Belous, Ya.T., 1998, Titanium (geology-economic review). Geoinform, 48p. (in Russian).
Bochai, L. V., Gursky, D.S., Veselovsky,G.S., and Lasurenko, V.I., 1998, The main geological-industrial types of Ti and Zr alluvial deposits of Ukraine and their formation creation. Mineralni Resursy Ukrainy, №3, p.p. 10-13. (in Ukrainian).
Buturlinov, N.V., Kobelev, M.V., Nechaev, S.V., and Panov, B.S., 1972, Geological structure, volcanism and metal potential of joint zone between theDonets ridge and Azov block of the Ukrainian shield, In: The Ukrainian shields frame platform structures and their metal potential. Kiev: Naukova Dumka, p.p. 158-187. (in Rassian).
Kvasnitsa, V.N., and Tsymbal, S.N., 1998, Diamonds of Ukraine and prospects of surveying their deposits. Mineralogicheskii Zhurnal, 20, №1.p.p. 118-129. (in Ukrainian).
Malyshev, J.J., 1957, Regularities of formation and location of titanium ore deposits. Moscow: Gosgeoltekhizdat, 167p. (in Russian).
Nechaev, S.V., 1970, Mineralization in the Volnovakha fanet-zone. Kiev: Naukova Dumka, 172p. (in Russian).
Tarasenko, V.S., 1987, Petrology of anorthosites in the Ukrainian shield, and geological-genetic model of phosphate-titanium ore-formation. Geologicheskii Zhurnal, № 4, p.p. 43-52. (in Russian).
Tarasenko, V.S., 1990, Rich titanium ores in gabbroanorthosite massives of the Ukrainian Shield. Jzvestiya Akademii Nauk SSSR, №8, p.p. 35-44. (in Russian).
Tarasenko, V.S., 1992, Mineral-raw-material base of titanium ores in Ukraine. Geologicheskii Zhurnal, № 5, p. p. 92-103. (in Russian).
Tarasenko, V.S., Krivonos, V.P., and Zhilenko, L.A., 1989, Petrology and ore potential of the South-Kalchik massif gabbroids (East-Azov area). Geologicheskii Zhurnal, № 5, p.p. 78-88. (in Russian).

Hannah JL & Stein HJ:

Evidence from Re-Os for the origin of sulfide concentrations in anorthosites

Judith L. Hannah & Holly J. Stein:
AIRIE Program, Colorado State University, Fort Collins, CO 80523-1482, USA.
jhannah@cnr.colostate.edu

Recent Re-Os studies of sulfide concentrations in anorthosite-dominated plutonic suites consistently yield high initial $^{187}Os/^{188}Os$ ratios in sulfide minerals, indicating a major component of crustal Os. These studies have led to three distinct hypotheses for the origin of the sulfide mineralization, with implications for the genesis of the hosting plutonic rocks: (1) the source of the parental magmas is mafic continental crust; (2) mantle-derived melts achieve sulfide saturation and acquire crustal Os through bulk assimilation of silicate crust; or (3) mantle-derived melts achieve sulfide saturation and acquire crustal Os through selective assimilation of crustal sulfur and metals by volatilization and/or melting of crustal sulfides. We favor the third hypothesis on the basis of modeling of Re-Os data together with other geologic and geochemical constraints (Hannah and Stein, accepted). Nevertheless, the available data sets are limited, and we cannot yet preclude the possibility that real differences exist among the complexes examined to date.

Presently available Re-Os studies of anorthosite-dominated plutonic suites have focused on those with significant sulfide concentrations, including the major ore deposits at Voisey's Bay, Nain plutonic suite, Labrador (Lambert et al. 1999, 2000), and less well-defined deposits in the Suwalki complex, Poland (Stein et al. 1998, Morgan et al. 2000), and the Rogaland complex, Norway (Schiellerup et al. 2000). In each case, initial $^{187}Os/^{188}Os$ ratios in sulfides are

extremely high, indicating a crustal source for the Os. Re-Os data for two additional anorthosite-bearing plutonic complexes also indicate crustal input: the 1845 Ma Sally Malay mafic-ultramafic intrusion in East Kimberly, Western Australia (γ_{Os} of abundant, disseminated sulfides = +950 to +1300; Sproule et al. 1999), and the 1100 Ma Duluth layered igneous complex in Minnesota, USA (γ_{Os} of massive sulfides = +500 to +1200; Ripley et al. 1998).

In two cases, Suwalki and Rogaland, the high initial Os ratios have been attributed to a crustal source for the magmatic complex as a whole (Stein et al 1998, Morgan et al. 2000, Schiellerup et al. 2000). This hypothesis is supported by a variety of field and mineralogic observations (Taylor et al. 1984, Duchesne 1999), oxygen isotope data (Peck & Valley 2000), and experimental constraints (Longhi, et al. 1999). On the other hand, Re-Os data from Suwalki are limited to zones of massive titanomagnetite containing up to a few percent sulfides; modeling demonstrates that observed Re-Os concentrations and isotopic ratios can be explained by selective contamination of a mantle-derived melt by crustal sulfides. In a subsequent and similar study at Rogaland, Schiellerup et al. (2000) call upon a crustal source for the parental magma based on initial $^{187}Os/^{188}Os$ derived from a 10-point Re-Os isochron of 917 ± 22 Ma in agreement with zircon and baddeleyite ages. While an isochron initial $^{187}Os/^{188}Os$ of 0.63 ± 0.25 broadly supports this conclusion, the isochron has an extremely high MSWD (517) indicating variation in initial $^{187}Os/^{188}Os$ for the samples analyzed. That is, the samples analyzed do not form a perfectly coherent genetic suite. Moreover, the data table shows consistent variations in γ_{Os} for individual samples, with sulfides generally higher than oxides. It is conceivable that, as at Suwalki, a larger data set would document selective and variable crustal contamination.

At Voisey's Bay, chondritic γ_{Os} values for silicates lead to a model of selective assimilation of crustal sulfide (and Os) into an otherwise mantle-derived magma (Lambert et al. 2000). Similarly, both the Duluth and Sally Malay complexes show contrasts between the isotopic compositions of massive sulfide bodies and minor disseminated sulfide occurrences. The massive sulfides of the Babbitt deposit (Duluth) are strongly crustal, while troctolites with only disseminated sulfides yield epsilon Nd and $\delta^{34}S$ of -0.2 to +0.2 and -2.5 to +2.5, respectively (Ripley et al. 1998), typical of chondritic values. Similarly, for Sally Malay, Sproule et al. (1999) report γ_{Os} of +450 to +470 for sulfides from ore-bearing troctolite, and only +60 to +369 for sulfides from weakly mineralized troctolite and peridotite. These data support a model for selective contamination by crustal sulfides, with crustal Os sequestered in an immiscible sulfide melt and not mixing broadly with the complex as a whole.

References

Duchesne, J.-C. 1999. Fe-Ti deposits in Rogaland anorthosites (South Norway): geochemical characteristics and problems of interpretation. *Mineralium Deposita* 34: 182-198.

Hannah, J.L. & Stein, H.J., accepted. Re-Os model for the origin of sulfide occurrences in Proterozoic anorthosite complexes. *Economic Geology*.

Lambert, D.D., Foster, J.G., Frick, L.R., Li, C. & Naldrett, A.J. 1999. Re-Os isotopic systematics of the Voisey's Bay Ni-Cu-Co magmatic ore system, Labrador, Canada. *Lithos* 47: 69-88.

Lambert, D.D., Frick, L.R., Foster, J.G., Li, C. & Naldrett, A.J. 2000. Re-Os isotope systematics of the Voisey's Bay Ni-Cu-Co magmatic sulfide system, Labrador, Canada: II. Implications for parental magma chemistry, ore genesis, and metal redistribution. *Economic Geology* 95: 867-888.

Longhi, J., Vander Auwera, J., Fram, M.S. & Duchesne, J.C. 1999. Some phase equilibrium constraints on the origin of Proterozoic (massif) anorthosites and related rocks. *Journal of Petrology* 40: 339-362.

Morgan, J.W., Stein, H.J., Hannah, J.L., Markey, R.J. & Wiszniewska, J. 2000. Re-Os study of Fe-Ti-V oxide and Fe-Cu-Ni sulfide deposits, Suwalki anorthosite massif, northeast Poland. *Mineralium Deposita*. 35: 391-401.

Peck, W.H. & Valley, J.W. 2000. Large crustal input to high $\delta^{18}O$ anorthosite massifs of the southern Grenville Province: new evidence from the Morin Complex, Quebec. *Contributions to Mineralogy and Petrology* 139: 402-417.
Ripley, E.M., Lambert, D.D. & Frick, L.R. 1998. Re-Os, Sm-Nd, and Pb isotopic constraints on mantle and crustal contributions to magmatic sulfide mineralization in the Duluth Complex. *Geochimica et Cosmochimica Acta* 62: 3349-3365.
Schiellerup, H., Lambert, D.D., Prestvik, T., Robins, B., McBride, J.S. & Larsen, R.B. 2000. Re-Os isotopic evidence for a lower crustal origin of massif-type anorthosites. *Nature* 405: 781-784.
Sproule, R.A., Lambert, D.D. & Hoatson, D.M. 1999. Re-Os isotopic constraints on the genesis of the Sally Malay Ni-Cu-Co deposit, East Kimberly, Western Australia. *Lithos* 47: 89-106.
Stein, H.J., Morgan, J.W., Markey, R.J. & Wiszniewska, J. 1998. A Re-Os study of the Suwalki anorthosite massif, northeast Poland. *Geophysical Journal* 4(T20): 111-114.
Taylor, S.R., Campbell, I.H., McCulloch, M.T. & McLennan, S.M. 1984. A lower crustal origin for massif anorthosites. *Nature* 311: 372-374.

Hellström F:

Accumulation of ilmenite in the post-Sveconorwegian Tuve Dyke, SW Sweden

Fredrik Hellström
Department of Geology, Earth Sciences Centre, Göteborg University, Box 460, 40530 Göteborg
fredrikj@gvc.gu.se

The Tuve dyke is the largest of young WNW-trending dolerites in the area of Göteborg, on the Swedish west-coast, herein referred to as the Göteborg dolerites. The dykes are high Ti-P-K, within-plate, plagioclase-rich (57-78%) olivine-tholeiites to tholeiites, with Mg# (Mg/(Mg+Fe)) of 0.41-0.62. Their Post-Sveconorwegian setting is demonstrated by their sharp, chilled margins, which are discordant to all ductile structures in the wall rock, and their undeformed primary mineralogy and igneous intergranular texture. The dolerites are sometimes affected by hydrothermal alterations, especially close at their margins. Baddeleyite of the Tuve dyke gives an U-Pb intrusive age of 935 ± 3 Ma, which is suggested to be representative for the whole dyke swarm (Hellström and Johansson in prep.). The Göteborg dolerites are thus similar in age to e.g. the ca. 930 Ma Rogaland Anorthosite Complex in SW Norway (Schärer, 1996) and the 916 ± 11 Ma E-W trending Hakefjorden norite-anorthosite Complex on the Swedish west coast 20 km north of Göteborg (Scherstén *et al.*, 2000).

The Tuve dyke is found 10 km north of Göteborg and is marked by a positive anomaly on the aero-magnetic map, where it can be followed over a distance of 14 km. The strike of the dyke is N60-70°W, with a steep, near vertical dip. It can be divided into two parts, split by a ca 500 m dextral offset where the dyke passes the NE-trending Nordre Älv Shear Zone. The western part is 200 m wide and 6 km long, whereas the eastern part is about 100 m wide and 8 km long. The western part has accumulated up to a maximum of ca. 17 % ilmenite in the dyke centre.

The Tuve dolerite is even, fine-medium grained, fine-grained at the contacts, and has a subhedral intergranular texture. Diffuse cm-wide dyke-parallel plagioclase-rich bands illustrating flow banding are seen in the centre of the dyke. The dolerite can petrographically be classified as leuco-olivine-gabbronorite, with plagioclase (58-73 %), olivine (0-25 %) and Fe-Ti oxides (5-18 %). Orthopyroxene and clinopyroxene are minor phases, that together usually have a modal content below 10 % down to a few percent, then giving the rock an almost troctolitic composition. Ilmenite is much more abundant than magnetite. The magnetite grains

contain exsolution lamella of ilmenite and is usually found within the margins of ilmenite, suggesting that magnetite crystallised later than magnetite. The amount of k-feldspar is estimated to be less than 2-3 % and the content of biotite vary between 0.4-4.2 %. The modal quartz content increases in the marginal zone up to 1.7 %, but is elsewhere generally below 0.2 %.

Granular olivine was the first mineral to crystallise together with early subhedral albite-twinned labradoritic plagioclase. The plagioclase is normal zoned and has andesitic rims against interstitial phases. Excess silica in the intercumulus liquid reacted with the olivine to form rims of unzoned bronzite-hypersthene. In the central, ilmenite-rich western part of the dyke, rounded ilmenite grains are poikolitically enclosed in the hypersthene and must have crystallised before or simultaneously with the orthopyroxene. Ilmenite is also found at the margins of olivine, as rounded inclusions in augite and between plagioclases, but is usually associated with the orthopyroxene. At the margins the oxides have a more skeletal, tabular habit growing over plagioclase and ferromagnesian minerals. Where the oxide content is less, as in the eastern part of the dyke the oxides tend to have a more interstitial character floating out around subhedral plagioclase. Anhedral, undulating plagioclase with oscillatory zoning and minor inclusions of olivine crystallised next, followed by augite that crystallised late, filling the interstices between plagioclases. Apatite, k-feldspar, oligoclase-albit, quartz and baddeleyite represent that last liquid and is also found interstitially between plagioclase.

Major elements have been analysed from samples taken in two profiles across the Tuve dyke to investigate modal variations across the dyke and differences between the eastern and western parts. Calculated normative compositions give an estimate of the actual modal composition and generally agree with results from point counting. Though the normative hypersthene content seems somewhat overestimated and the normative plagioclase content is underestimated, but this does not change the trends seen. The total feldspar (an+ab+or=plagioclase) content is plotted together with normative olivine, hypersthene, and ilmenite in the two profiles (Fig. 1-3).

In the marginal zones the normative hypersthene content increases rapidly by the effect of increasing amount of interstitial quartz and decreasing amount of olivine possibly caused by contamination from the gneissic wall rock (Fig. 1, 2). Both profiles have a similar contents of diopside (2-6 %; not shown) and magnetite (2-4 %). The main difference between the eastern and the western part of the dyke is the accumulation of ilmenite in the western part. The general trend here is an increase of ilmenite from 8 % at the margins to 15 % in the centre (Fig. 3). The eastern part show similar concentrations at the margins (8 %), but is then gradually depleted in ilmenite down to 5 % in the centre. In both profiles olivine is gradually concentrated towards the centre, most clearly seen in the eastern profile, were the amount of olivine increase from 3 to 29 %. Plagioclase shows the opposite pattern with increasing amounts towards the margins.

The composition of olivine can be related to the mole fractions of Mg and Fe^{2+} in the melt by the partition coefficient $k_d = (X_{Mg}/X_{Fe})_{liq}/(X_{Mg}/X_{Fe})_{ol}$. The distribution coefficient has a value of 0.30 ± 0.03 and is relatively independent of temperature and melt composition (Roeder and Emslie, 1970). The calculated $(X_{Mg}/X_{Fe})_{liq}$ in equilibrium with the olivine compositions of the dyke is much less than the $(X_{Mg}/X_{Fe})_{whole\ rock}$ and the difference increases towards the centre of dyke (Fig. 4, 5). The whole-rock does thus not represent liquid composition but accumulation of cumulus olivine towards the centre of the dyke.

Early crystallised minerals could have accumulated towards the centre of the Tuve dyke during flow differentiation explaining the gradual increase in the olivine content towards the centre. Grain dispersive pressures during laminar flow causes moving phenocrysts and xenoliths to concentrate toward the centre of the dyke (Komar, 1972). In the centre of the western, ilmenite-rich part of the Tuve dyke, rounded ilmenite grains are usually poikolitically enclosed in orthopyroxene and are suggested to have crystallised before the orthopyroxene that rims olivine. The early formed ilmenite could also have been accumulated towards the centre by flow, but other explanations is also possible, e.g. gravitative separation of early formed

crystals in a magma chamber followed by injection of the crystal-stratified magma into the dyke giving plagioclase rich margins and a olivine-ilmenite rich central part.

Accumulation of ilmenite in the western part of the Tuve dyke seems to have depleted the eastern part in TiO_2, alternatively the eastern and western parts are different depths of exposure and the differences in ilmenite content is caused by a vertical fractionation mechanism. The 500 m horisontal offset separating the eastern and western parts of the dyke at the Nordre Älv Shear Zone, could be an effect of a vertical displacement of the steep south dipping dyke. Geophysical modelling of the shape of the dyke is in progress.

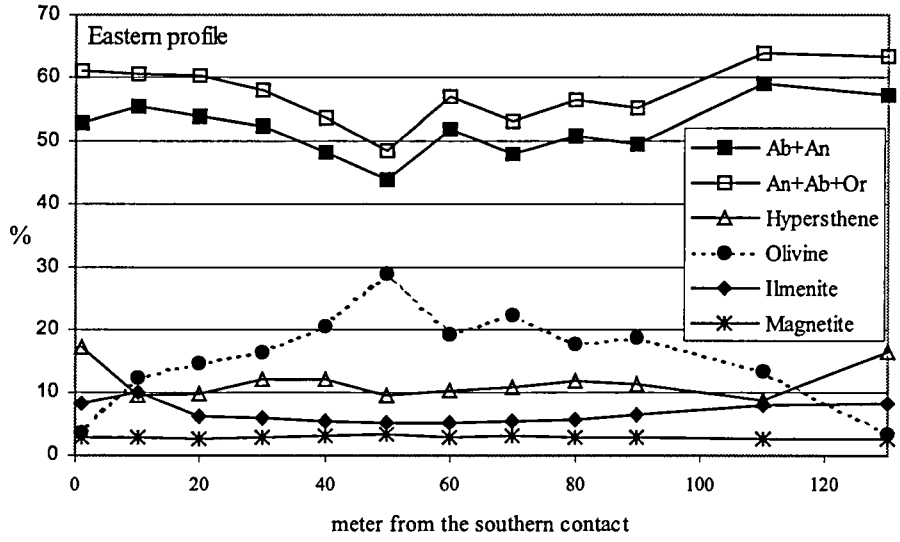

Figure 1. Normative compositions in a profile across the eastern part of the Tuve dyke.

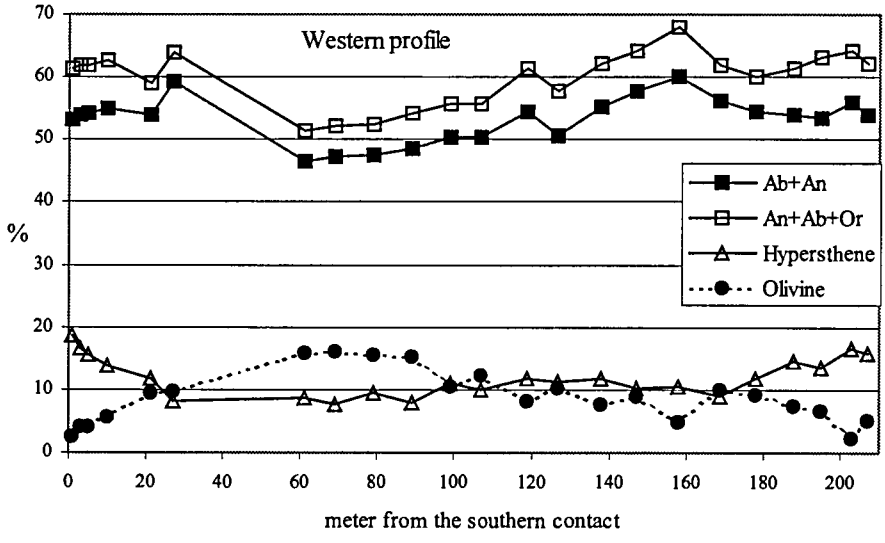

Figure 2. Olivine, hypersthene and plagioclase normative compositions in a profile across the western part of the dyke.

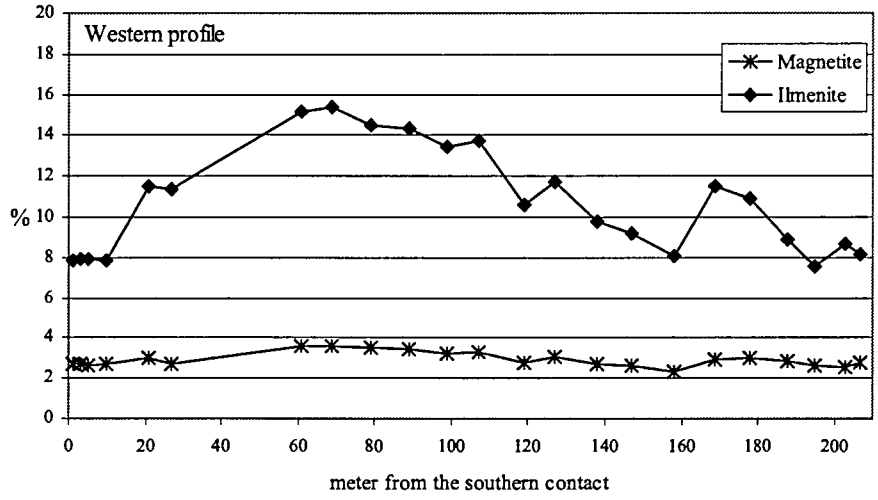

Fig. 3. Ilmenite and magnetite normative compositions in a profile across the western part of the Tuve dyke.

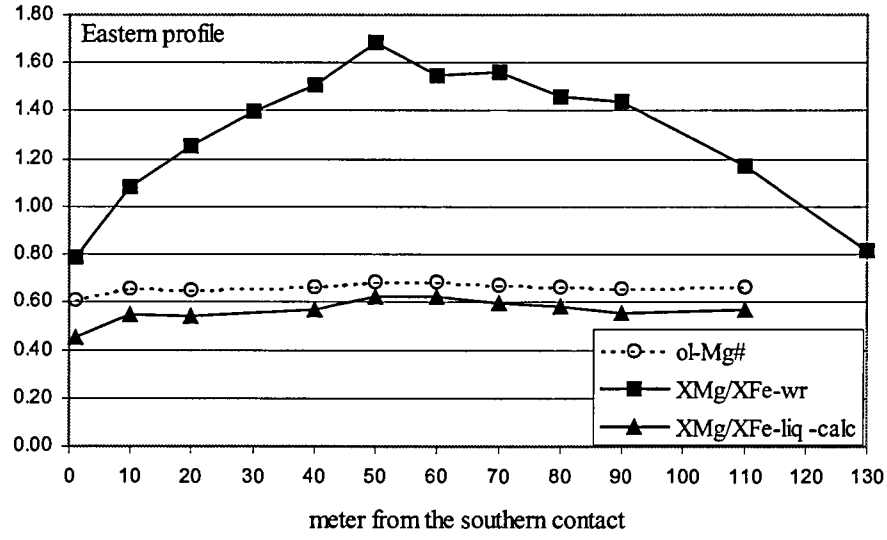

Fig. 4. Calculated $(X_{Mg}/X_{Fe})_{liq}$ in equilibrium with the olivine compositions (ol-Mg#) of the Tuve dolerite compared with $(X_{Mg}/X_{Fe})_{whole\ rock}$ in the eastern profile.

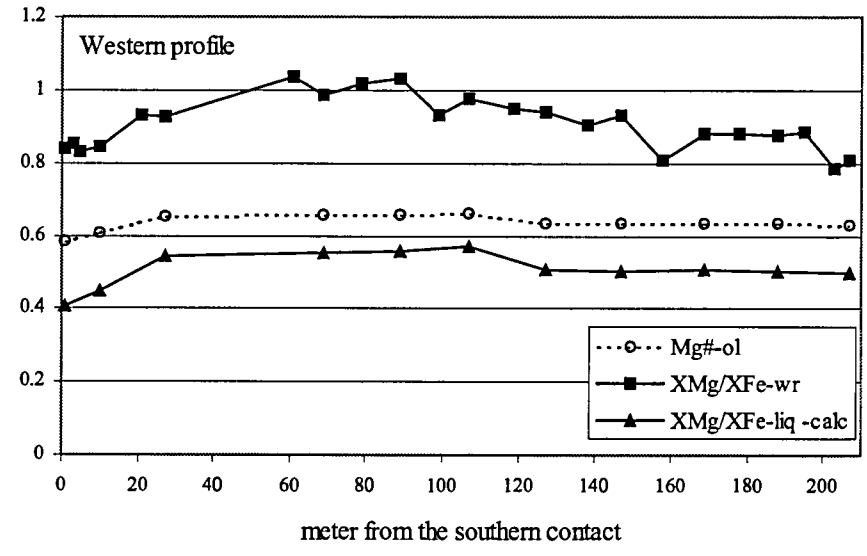

Fig. 5. Calculated $(X_{Mg}/X_{Fe})_{liq}$ in equilibrium with the olivine compositions (ol-Mg#) of the Tuve dolerite compared with $(X_{Mg}/X_{Fe})_{whole\ rock}$ in the western profile. The high ilmenite content in the centre of the dyke lower the $(X_{Mg}/X_{Fe})_{whole\ rock}$.

References

Komar, P.D., 1972. Flow differentiation in igneous dikes and sills: profiles of velocity and phenocryst concentration. *Geol. Soc. Am. Bull.*, **83**, 3443-3448.

Roeder, P.L. and Emslie, R.F., 1970. Olivine liquid equilibrium. *Contrib. Mineral. Petrol.*, **29**, 275-289.

Scherstén, A., Årebäck, H., Cornell, D., Hoskin, P., Åberg, A., and Armstrong, R., 2000. Dating mafic-ultramafic intrusions by ion-microprobing contact-melt zircon: examples from SW Sweden. *Contrib. Mineral. Petrol.* **139**, 115-125.

Schärer, U., Wilmart, E., and Duchesne, J.C., 1996. The short duration and anorogenic character of anorthosite magmatism: U-Pb dating of the Rogaland complex, Norway, *Earth Planet Sci Lett*, **139**, 335-350.

Kärkkäinen N:

Gabbro hosted ilmenite deposits in Finland

Kärkkäinen, Niilo
Geological Survey of Finland, 02150 Espoo, Finland

Ilmenite rich gabbros in the Kälviä and Kauhajoki areas, the ilmenite-magnetite deposit in Kolari, and the Otanmäki Fe-Ti-V mine (closed 1985) indicate high Ti potential of small mafic intrusions in Finland. Since 1993, when the Geological Survey of Finland began exploration for ilmenite from the Svecofennian bedrock, four economically interesting deposits have been reported from the Kälviä area, western Finland (Kärkkäinen et al., 1997, Sarapää et al. 1999, 2001). Ilmenite concentrates of commercial quality (44 - 45.6 % TiO_2) have been processed from the Koivusaarenneva and Peräneva ilmenite deposits by traditional beneficiation methods (Chernet 1999). The feasibility study of the Koivusaarenneva deposit is currently on-going by a private company, Kalvinit Oy. The apatite rich ilmenite-magnetite deposit in the Kauhajärvi gabbro, 300 km south from the Kälviä area, is another recently studied, but clearly subeconomic type of ilmenite occurrences (Fig. 1).

Kälviä area

In the Kälviä area several ilmenite-rich gabbros have been located in a chain of gravity and magnetic anomalies. The mafic intrusions were emplaced at 1881 Ma into tonalitic bedrock, and belong to a large gabbro province interpreted to have been formed in tensional zones in the vicinity or margin of convergent plate boundaries.

The largest ilmenite deposit (44 Mt with 15% ilmenite, 6 % magnetite) occurs in the Koivusaarenneva gabbro that is an elongated, 0.5 to 1 km thick and 3 km long sill-like intrusion. It can be divided into three different zones, lower, middle and upper, and the main rock type in all zones is a metamorphosed gabbro or gabbronorite (Kärkkäinen, 1997). The characteristic minerals in theses zones are ilmenomagnetite, ilmenite and apatite, respectively. The lower zone contains minor ilmenite rich layers with much ilmenomagnetite, and the TiO_2 /Fe_2O_3TOT ratio 0.2 is constant for all rock types in the lower zone. The middle zone contains a 1.5 km long and 50 to 60 m thick mineralized layer that grade between 8 and 48% ilmenite, 2 to 25 % magnetite and minor ilmenomagnetite. The average ratio of ilmenite to magnetite is 4:1. The TiO_2/Fe_2O_3TOT ratio of the middle zone is between 0.23 and 0.50. Ilmenite is the dominant Fe-Ti oxide in the upper zone that consists of P-rich gabbro and leucogabbro.

The three zones are interpreted to have crystallized from successive pulses of Ti-rich tholeiitic magma. The parent magmas for the lower and middle zones are similar. The lower zone is interpreted to have been generated by relatively closed system fractional crystallization, and based on the common ilmenomagnetite, under relatively high oxygen fugacity. Also the

upper zone has been generated by relatively closed system fractional crystallization, but the parental magma was more evolved.

The genesis of the Fe-Ti oxide rich layers in the middle zone can be explained by deposition from several magma pulses in an open system, because of the small volume of the rock in the middle zone. The middle zone may represent a channel for magma flow and the large mass of oxides was accumulated from multiple magma pulses. Ti-rich melt droplets or suspended oxides were removed from a Ti-saturated magma and sank to the floor of a shallow magma chamber to form the mineral deposit, composed of a Fe-Ti oxide rich matrix between a silicate framework. The Ti and Fe depleted magma flowed out of the poorly crystallized intrusion and was replaced by a new pulse of Ti-saturated parent magma.

Kauhajärvi area

Kauhajoki gabbro is one of the several Fe-, Ti-, and P-rich mafic intrusions within a granitoid area in mid-southwest Finland (Kärkkäinen & Appelqvist, 1999). It is composed of two different zones, a relatively thin basal zone and the main zone. Ti- and P-rich gabbro is the most voluminous rock type in the 800 m thick main zone that is differentiated, and its composition varies from peridotite to anorthosite. Layers with an average of 20 wt % combined ilmenite, apatite and ilmenomagnetite form a low-grade apatite-ilmenite-magnetite deposit (about 10 Mt mineralized rock). Apatite and Fe-Ti oxides are concentrated together with Fe-Mg silicates.

Early crystallization of magnetite supports the interpretation that the main zone crystallized under conditions of relatively high oxygen fugacity. There are three main factors controlling the concentration of the Fe-Ti oxides and apatite in the Kauhajärvi gabbro: 1) an Fe-, Ti- and P-rich parental magma; 2) a relatively high f_{O2} during crystallization that kept the solubility of Fe and Ti low so these elements could not be enriched during crystallization; and 3) high P in the magma enabled the crystallization of individual ilmenite coevally with Ti-bearing magnetite (ilmenomagnetite).

Based on current data, the Kauhajärvi intrusion hosts a smaller and lower grade Fe-Ti oxide deposit than the Koivusaarenneva gabbro. The Kauhajärvi intrusion is interpreted to have crystallized under relatively closed system conditions and the lack of dynamic magma flow through the intrusion prevented accumulation of a large mass of Fe-Ti oxides.

Summary

Gabbroic intrusions with ilmenite-dominant Fe-Ti oxide-rich rocks occur within variable geotectonic settings of the lower Proterozoic age between 2.1 Ga to 1.9 Ga (Table 1). The common features are the small size of the intrusions, and the occurrence of ilmenite and magnetite mainly as individual grains. The primary source of the magma (geotectonic environment) is probably less important in generation of a Ti-rich intrusion than the generation of a Ti-enriched parent magma by fractionation in a deep crustal reservoir. Fractionation under low oxygen fugacity conditions favors generation of a Ti-rich parental magma. Shallow magmatic processes concentrate ilmenite from the Ti enriched parent magma, and furthermore low f_{O2} environment favors ilmenite crystallization relative to Ti-magnetite. High P in magma may allow the crystallization of ilmenite under relatively oxidizing conditions (Toplis et al., 1994), as is suggested in the Kauhajärvi gabbro.

A magma-flow-through system in the shallow upper crustal environment is the critical process that enables the concentration of large volumes of oxides within small intrusions. In a magma flow system the oxides, or oxide rich melt, was trapped in favorable localities within the channelways. This is suggested to have produced the ilmenite deposits in the Kälviä area (Kärkkäinen and Bornhorst, 2000). A similar magma-flow-through model has been proposed to generate gabbro-hosted Ni-PGE sulfide mineralization at Norilsk, Russia (Naldrett et al., 1996), and the Ni-sulfides of the Voisey's Bay, Canada (Evans-Lamswood, 2000). Economically the most favorable intrusions are those among several interconnected intrusions. The magma-flow

genesis is supported by the fact that the Koivusaarenneva gabbro is a member in a chain of small intrusions, three of which, Lylyneva, Peräneva, and Kairineva also host ilmenite deposits.

Given the correct combination of magmatic processes, large volumes of ilmenite may be concentrated with or without large amount of iron oxides. Ti deposits hosted in small mafic intrusions are distinguishable from other types of Ti deposits. Quite large ilmenite deposits (50 to over 100 Mt) can be hosted by relatively small intrusions.

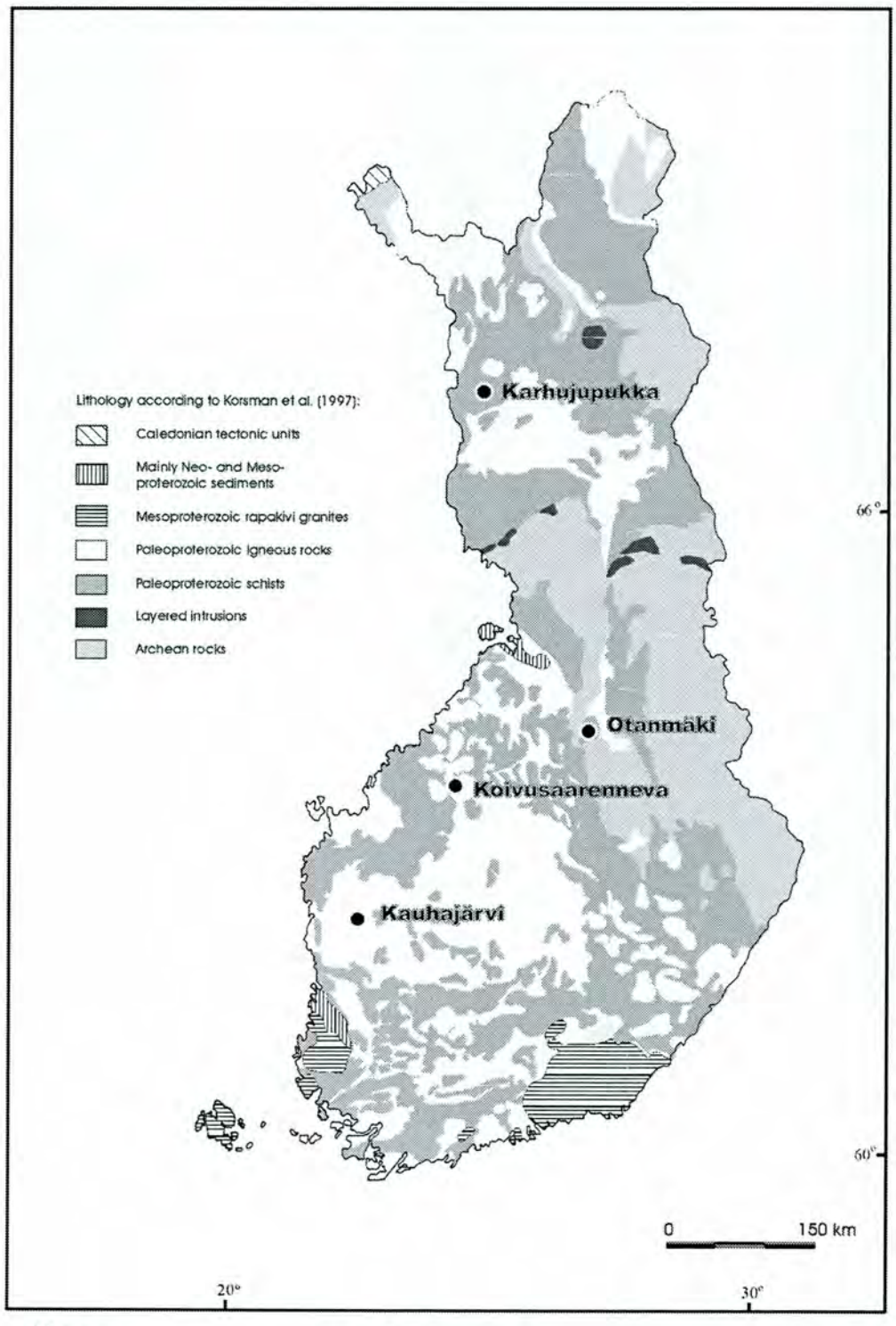

GTK *Geological Survey of Finland* *www.gsf.fi*

Table 1 Characteristics of some Finnish and other Fennoscandian gabbro-hosted ilmenite-rich deposits. (MT = magnetite, I=ilmenite).

	Koivusaarenneva, Kälviä	**Kauhajärvi Kauhajoki**	**Otanmäki Vuolijoki**	**Karhujupukka Kolari**	**Rödsand Norway**	**Akkavaara Sweden**
Intrusion	multistage gabbro with 3 zones	2-stage well-differentiated gabbro	differentiated gabbro-anorthosite	differentiated sill-like gabbro	gabbro (amfibolite)	noritic gabbro
Dimensions km^2	0.8 x 3 km^2	>1 x 6 km^2	15 x 1 km^2	0.5 x 1 km^2	> 700 m	6 x 1
Age Ga	1.881 Ga	1.875 Ga	2.06 Ga	2.1 Ga	>1.7 Ga	>1.7
Country rock	Tonalite	granodiorite	granite-gneiss	granitized metasediments	granite-gneiss quartz-diorite	granite
Geotectonic setting	arc near plate margin	intracratonic rift	shield (conti-nental margin)	cratonic basin	?	?
Deposit:						
% TiO_2 [1]	7.5	5	14	9	5.2	4.5
wt-% ilmenite	15 (8 to 48)	10	28	18	4	total ox.
wt-% magnetite	6 (-30)	2 - 8	35	66	25 to 30	10 -29%
I / MT	4 : 1	1.5 : I	1 : 2	1 : 2 (varies)	low	low?
% V in MT	0.7	0.3	0.6	0.57	0.5	< 0.15
Special		apatite	Co in Fe-sulfides Mined until1985		strongly foliated; mined until1981	Apatite
Source	Kärkkäinen et al. 1997	Kärkkäinen and Appelqvist 1999	Pääkkönen 1956 Paarma 1954	Karvinen et al. 1988	Sanetra, 1985 Korneliussen et al 1985	Grip and Frietch 1973

1) averaged TiO_2 content in mineral resource estimates

References

Chernet, T., 1999. Applied mineralogical studies of the Koivusaarenneva ilmenite deposit, Kälviä, western Finland, with special emphasis on the altered part of the ore. Chronique de la Recherche Minière 535, 19-28.

Evans-Lamswood, D.M, Butt, D.P., Jackson, R.S. Lee, D.V., Muggridge, M.G., Wheeler, R.I. and Wilton, D.H.C., 2000. Physical Controls Associated with the Distribution of Sulfides in the Voisey's Bay Ni-Cu-Co Deposit, Labrador. Economic Geology vol. 95, 749-770.

Grip, E. & Frietsch, R., 1973. Malm i Sverige 2, Norra Sverige. Almqvist & Wiksell Läromedel. Stockholm, 295 p.

Kärkkäinen, N. and Bornhorst, T. J., 2000. Magma flow genetic model for titanium ore in a small mafic intrusion. In: Geological Society of America 2000 Annual Meeting and Exposition, Reno, Nevada, November 13-16, 2000. Geological Society of America. Abstracts with Programs 32 (7), A-426.

Kärkkäinen, N., and Appelqvist, H., 1999. Genesis of a low-grade apatite-ilmenite-magnetite deposit in the Kauhajärvi gabbro, western Finland. Mineralium Deposita vol. 34, 754-769.

Kärkkäinen, N., 1997. The Koivusaarenneva gabbro, Finland, *In:* Papunen, H., (ed.) Mineral deposits: research and exploration - where do they meet? Proceedings of the Fourth Biennial SGA Meeting, Turku/Finland/11-13 August 1997. Rotterdam: A. A. Balkema, p. 443-444.

Kärkkäinen, N., Sarapää, O., Huuskonen, M., Koistinen, E., and Lehtimäki, J., 1997. Ilmenite exploration in western Finland, and the mineral resources of the Kälviä deposit. Geological Survey of Finland Special Paper 23, p. 15 -24.

Karvinen, A., Kojonen, K., and Johanson, B., 1988, Geology and mineralogy of the Karhujupukka Ti-V-Fe deposit in Kolari, Northern Finland. Geological Survey of Finland Special Paper 10, 95-99.

Kornelliussen, A. & Robins, B., 1985. Titanifrous magnetite, ilmenite and rutile deposits in Norway. Norges Geologiska Undersökelse (NGU) Bulletin 402, 98 p.

Naldrett, A.J, Fedorenko, V.A., Asif , M., Shushen, L., Kunilov, V.E., Stekhin, A.I., Lightfood, P.C., Gorbachev, N.S., 1996. Controls on the composition of Ni-Cu sulfide deposits as illustrated by those at Noril'sk, Siberia. Economic Geology vol. 91, 751-773

Pääkkönen, V., 1956, Otanmäki, the ilmenite - magnetite ore field in Finland: Geological Survey of Finland Bulletin 171, 71 p.

Paarma, H., 1954, The ilmenite-magnetite ore deposit of Otanmäki: Geological Survey of Finalnd, Geoteknisia Julkaisuja vol. 55, 36-42.

Sanetra, S., 1985, The Rödsand Fe-Ti-V deposits, Möre, western Norway. Norges Geologiske Undersökelse (NGU) Bulletin 402, p. 51-64.

Sarapää O., Kärkkäinen N., Reinikainen, J., Ahtola T., Appelqvist H., Seppänen H., 1999. New results from calcite and ilmenite exploration in Finland. Geological Survey of Finland, Special Paper 27, 25-34.

Sarapää O., Reinikainen J., Seppänen H., Kärkkäinen N. and Ahtola T., 2001. Industrial minerals exploration in southwest and western Finland. Geological Survey of Finland, Special Paper/Current Research 1999-2000 (in press)

Toplis, M.J., Libourel, G., and Carroll, M.R., 1994, The role of phosphorus in crystallization processes of basalts: An experimental study: Geochimica et Cosmochimica Acta, vol. 58, 797-810.

Korneliussen A:

On ilmenite and rutile ore provinces in Norway, and the relationships between geological process and deposit type

A. Korneliussen
Geological Survey of Norway, N-7491 Trondheim, Norway. Are.Korneliussen@ngu.no

There are a considerable variety of different types of titanium ore found in Norway (Korneliussen et al. 1985, 2000a). There is also a close link between geodynamics, at all scales, and the evolution of titanium deposits. At a regional scale, the distribution and character of the Ti-deposits are linked to distinct geological events at the western and south-western margin of the Fennoscandian Shield, ranging in age from the Proterozoic to Permian. The magmatic, metamorphic and structural processes involved, place distinct fingerprints on the individual Ti-deposits.

From an economic-geological point of view, the mineralogical variations are of overall importance, since mineralogy to a large extent defines the mineability of a Ti deposit. Mineralogy is a function of the geological evolution of the deposit, which is often very complex. In fact, a major task in continued investigations of Ti mineral deposits is to identify those that have ore-mineral qualities that will make it practically-economic possible to produce titanium mineral concentrates of ilmenite and rutile, of sufficient quality particularly for the Ti-pigment industry.

The dominant Ti-ore category is magmatic deposits of ilmenite, titanomagnetite and apatite in various proportions, and variably affected by secondary, metamorphic processes. The major ilmenite province is the Rogaland anorthosite province in southern Norway. It was emplaced in a Middle Proterozoic, migmatised, metamorphic terrain at intermediate crustal levels. Titanium deposits are widespread in the province, principally as ilmenite-magnetite rich cumulates, or as ilmenite - magnetite rich dykes. There is a wide variety in chemical characteristics and mineral textures in these deposits.

In some regions metamorphic processes related to major crustal events have transformed ilmenite-baring rocks into rutile-bearing rocks. Since rutile is a much more valuable mineral than ilmenite, such transformation processes are of significant economic interest.

In Western Norway, including the Sunnfjord province, Proterozoic mafic and felsic igneous rocks were strongly affected by the Caledonian orogeny. Two types of Ti deposits occur in this region: magmatic ilmenite-magnetite deposits associated with Proterozoic mafic intrusions, and rutile-bearing Caledonian eclogitic rocks. The rutile-bearing eclogites are Proterozoic basic rocks that were transformed into eclogite at high pressure during the collision between a Baltica (Fennoscandian Shield) and Lauretia at ca. 400 Ma. During this process, ilmenite in the protolith broke down, with the Fe entering garnet and Ti into rutile. Large volumes of ilmenite-bearing mafic rocks were transformed into rutile-bearing eclogitic rocks with the same TiO_2 content. From a mineral resource perspective, the ilmenite deposits within the eclogite regions in W. Norway are of only minor interest, while the rutile-bearing eclogites represent a major mineral resource, particularly the Engebøfjell deposit (McLimans et al. 1999).

The third orecategory is a variety of the Proterozoic rutile-bearing, scapolitised and albitised rocks in the Bamble - Arendal province (also called the Bamble Sector of the Fennoscandian Shield). Mafic rocks were extensively affected by alkali-metasomatism in the form of scapolitisation and albitisation. In this process ilmenite in the gabbroic or amphibolitic protolith breaks down to rutile during the metasomatic process while iron is removed from the system by the fluids. Thus, the metasomatism creates rutile ores.

References

Korneliussen, A., McEnroe, S. A., Nilsson, L.P., Schiellerup, H., Gautneb, H., Meyer, G.B. & Størseth, L.R., 2000 a: An overview of titanium deposits in Norway. Norges geologiske undersøkelse Bulletin 436, 27-38.

Korneliussen, A., McLimans, R., Braathen, A., Erambert, M., Lutro, O. & Ragnhildstveit, J., 2000 b: Rutile in eclogites as a mineral resource in the Sunnfjord region, western Norway. Norges geologiske undersøkelse Bulletin 436, 39-47.

McLimans, R.K, Rogers, W.T., Korneliussen, A., Garson, M. & Arenberg, E.: Norwegian eclogite: An ore of titanium. In: Mineral Deposits: Processes to Processing. Proceedings of the fith biennial SGA meeting and the tenth quadrennial IAGOD symposium, London 22-25 August 1999.

Kozlowski A & Wiszniewska J:

The Nelsonite problem: the origin by melt immiscibility

Andrzej Kozlowski, Faculty of Geology of the Warsaw University, Poland; akozl@geo.uw.edu.pl
Janina Wiszniewska, Polish Geological Institute, Warsaw, Poland; jwis@pgi.waw.p

Abstract

The origin of ore-bearing apatite rock (nelsonite) from the Suwalki anorthosite massif and Fe-Ti-P-rich monzodiorite (jotunite) from the Sejny massif, both of Proterozoic age and occurring within the ranges of the Mazury crystalline complex in NE Poland, was investigated by means of melt inclusion studies. Melt inclusions in apatite are filled by pyroxene, apatite, calcite, plagioclase, biotite, halite sylvite, ore mineral plus aqueous solution and gas bubble. At 880°C two melts (silicate and phosphate) were observed in the inclusions, which neither homogenised nor changed their proportions up to 1080°C. This evidences the formation of nelsonite from an immiscible, two-phase melt. Inclusions in pyroxene from jotunite are filled by an aggregate of pyroxene, feldspar, apatite, carbonate and ore mineral with gas bubble. The homogenisation temperatures spread from 1090 to 1180°C; at 1000 to 1030°C small droplets of carbonate and phosphate melt were visible in the silicate melt, homogenising subsequently in one melt phase.

Introduction

The exact determination of the origin of many rocks is by far not a trivial problem. There are three modes of solution of this question: thorough petrologic investigations, experimental modelling of the natural processes and studies of the parent environment in which the rock formed. Certain rare rock types require especially careful studies to establish their origin, because the comparative material is usually scarce. The apatite-ore rocks with variable but low contents of silicate minerals, called nelsonites, have been found up to now in a few places, and they needed special studies to recognise their genetic nature. The name *nelsonite* was used for the first time by Watson & Taber (1913) for the ilmenite-apatite rocks from Nelson County in Virginia, USA, related to the Proterozoic anorthosite suite. These peculiar nelsonites form fine-grained dikes composed mainly of ilmenite (60%) and apatite (30%) with a small amount of rutile. Most of the vein ore-apatite rocks (i.e. containing magnetite, magnetite and sulphides, or magnetite, ilmenite and rutile) or even biotite-apatite ores, if related to the basic magmatic rocks, have been since then called *nelsonites* (Anderson, 1966, Philpotts, 1967, Roelandts & Duchesne, 1979, Kolker, 1982). However, their origin was not recognised unambiguously. Essentially the world nelsonite occurrences are believed to be of magma-related origin but formed in different processes: hydrothermal (Ross 1941), crystal settling (Emslie 1975), or liquid immiscibility (Philpotts 1967). Important field, petrographic and experimental data indicate that nelsonites formed from a melt, separated from a diorite-type parent magma as an immiscible residual liquid at a late stage of the anorthosite massif magmatic evolution (Bolshover & Lindsley, 1983, Darling & Florence, 1995). Nevertheless, there is no direct evidence of a nelsonite origin in connection with the immiscibility process. Any ambiguity in this case could be removed by investigation of the parent environment of the nelsonites. Roedder (1979) showed the usefulness of fluid and melt inclusions in investigation of any kind of immiscibility in magmas, because such inclusions contain portions of the parent mineral-forming medium, thus delivering direct evidence of its two- or multiphase state at the time of a mineral crystallisation.

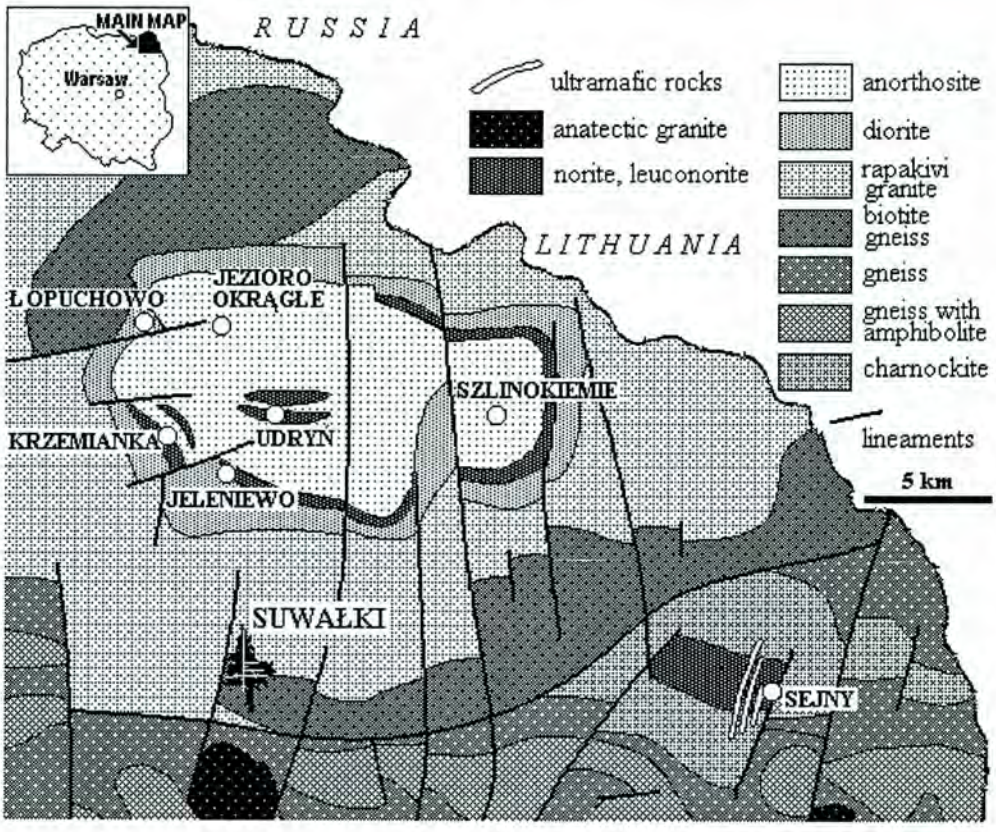

Fig. 1. Geological map of the Suwalki anorthosite intrusion (after Kubicki & Ryka, *Geological atlas in Polish part of the East European Platform*, Warszawa, 1982, modified).

Geological setting

The investigated specimens come from a Precambrian crystalline rock suite in NE Poland, belonging to the East European Craton (Fig. 1). E-W trending shear zones of post-collisional origin or rejuvenation of a previously formed lineament or terrane boundary were controlling the occurrence of the Meso-Proterozoic intrusions of bimodal composition: rapakivi type granite and anorthosite-norite massifs, called the Mazury Complex. Three anorthosite massifs: Ketrzyn, Suwalki and Sejny, have been recognised within a 200 km long and 40 km wide zone of the Mazury Complex. Their geochemical characteristics are similar to other massif-type anorthosite intrusions world-wide (Wiszniewska et al. 1999). The Suwalki anorthosite massif is the best documented intrusion due to occurrence of the titanomagnetite ore deposits, recognised in about 100 boreholes. The massif represents a Proterozoic anorthosite – mangerite – charnockite – rapakivi granite (AMCG) suite of rocks (Wiszniewska et al. 1999), known only from extensive drilling and magneto-gravimetric surveys, because these rocks and the associated Fe-Ti-V ores occur at the depth of nearly one kilometre beneath a Phanerozoic sedimentary cover. The Suwalki and Sejny intrusions are classified as typical Proterozoic "massif-type anorthosites" (Table 1) based on their geochemical and mineralogical characteristics. The ore-bearing apatite dikes (nelsonites) were found for the first time in Poland, in the north-west part of the Suwalki anorthosite massif, in the Lopuchowo IG-1 borehole (Fig.1). Complementary field, petrologic and experimental data indicate that a melt immiscibility process of two components: silicate melt of diorite composition and Fe-Ti oxide-apatite-rich melt with subsequent eutectic crystallisation

Table 1
Chemical compositions of nelsonite and associated rocks from the Suwalki massif (*wt. %*)

Component	Nelsonite	Anorthosite	Diorite
SiO_2	33.80	54.50	59.00
TiO_2	0.36	0.09	1.70
Al_2O_3	18.60	27.80	15.20
Fe_2O_3	9.29	0.73	6.41
FeO	2.89	0.20	3.41
MnO	0.08	0.01	0.16
MgO	0.37	0.27	2.28
CaO	19.80	11.00	5.18
Na_2O	2.14	4.78	2.93
K_2O	0.46	0.67	3.53
P_2O_5	8.71	0.01	0.57
S	1.69	0.04	0.18
Total	98.19	100.10	100.55

of apatite and magnetite, are responsible for the nelsonite origin. Orthopyroxene monzodiorite (jotunite) rocks of high Fe, Ti and P contents with chilled facies have been found in the Sejny noritic intrusion (borehole Sejny 2) and as a fine-grained dikes in the Suwalki anorthosite massif. This type of rocks found in the Mazury complex resembles the monzodioritic rocks of the Rogaland province, which have been suggested as a possible parent rock for anorthosites (Duchesne 1999).

Methods

Quantitative chemical analyses of the whole rocks and pure apatite fractions were performed by ICP-AES (at the Polish Geological Institute in Warsaw) and ICP-MS (in LAGPG at the University of Liège). Electron microprobe analyses of the minerals were carried out in the EDS

regime by use of the Jeol JSM 0035 microscope in Polish Geological Institute in Warsaw. Cathodoluminescence (CL) observations were made by means of the CCL 8200 mk3 device (Cambridge Image Technology Ltd.) combined with the polarising microscope Optiphot 2 (Nikon). The used voltage ranged from 12 to 18 kV.

The fluid inclusions were investigated in double polished slides 0.3–0.5 mm thick. Low-temperature heating measurements (±1°C) and freezing runs (±0.1°C) were performed by use of the Fluid Co. heating/freezing gas-flow stage mounted on a Leitz microscope. For moderate temperatures (to 900°C; ±5°C) the quenching method was applied (Kozlowski, 1981) and some observations at 800–1200°C (±10°C) were made on a high-temperature microscope heating stage. The inclusions were opened in a microscope crushing stage and analysed by electron microprobe in EDS and WDS regimes.

Investigated rocks

The samples for the present study were collected from two drilling cores coming from two neighbouring massifs of the Mazury complex. The ore-apatite rocks were sampled in the Lopuchowo-1 borehole in the Suwalki anorthosite massif, and the jotunite (monzodiorite) was taken from the norite-anorthosite Sejny intrusion (Fig. 1), Sejny 2 borehole. The fabrics of the anorthosites is dominated by coarse tabular calcic andesine crystals deformed in various degree due to diapiric emplacement of the massif. They are typically associated with noritic, charnockitic and granitic rocks, forming a bimodal magmatic suite (the so-called AMCG suite), considered as related to active or reactivated deep-crustal structures. The ore-bearing apatite rocks has been found in the western, marginal part of the Suwalki massif in the Lopuchowo PIG-1 borehole performed by Polish Geological Institute. The following rocks have been distinguished:

0–1241 m: sedimentary rocks
1241–2105 m: quartz monzodiorite and quartz diorite
2105–2227 m: leuconorite and leucogabbronorite
2227–2300 m: anorthosite.

Below the contact of diorite with the leuconorite – anorthosite complex, several dikes of ore-apatite composition have been found. These rocks form fine-grained vein bodies 0.3 to 1.5 m thick, with a sharp but strongly undulated contact with the host rocks. A linear arrangement of coarse sulphide, oxide and biotite grains have been observed. Nine zones of such rock with a total thickness of about 6 meters have been distinguished within the depth interval 2100 -2208 m.

Ore-bearing apatite rocks from the Suwalki anorthosite massif show dark grey-green, fine-grained, sideronite texture with a relatively uniform distribution of opaque minerals (Fig. 2). The contacts of these rocks with anorthosites and norites are locally underlined by streaks of coarse sulphide and oxide grains within the veins.

The rocks in question consist mainly of fluorapatite (up to 50-70 vol. %), magnetite (5-20 vol. %), ilmenite (2-5 vol. %), pyrrhotite (2-10 vol. %), pyrite (1-2 vol. %) and chalcopyrite (ca. 1 vol. %), whereas the silicate contents are relatively low, a character which differentiates the Lopuchowo rocks from other known nelsonites. The oxide/sulphide ratio in nelsonites is variable, ranging from 4:1 to 0.7:1. Minerals of a sulphidisation phase, such as bravoite, linnaeite, millerite, sphalerite, cubanite, pyrite and chalcocite, occur in traces as exsolution or substitution products in the magmatic stage minerals. Ce,Nd-allanite was sporadically found in association with titanite as rims around oxide minerals. Very fine grains of pleonaste and hoegbomite found as intergrowths within oxides are very rare. Anhydrite and calcite of the hydrothermal phase partly filled intergranular spaces between apatite and oxide grains (Fig. 3, see also Wiszniewska, 1997).

The ore-apatite rocks from Lopuchowo are enriched in Cr, Ni, Cu, Co and REE, when compared to other types of the rocks of the Suwalki intrusion. High contents of LREE, e.g. Ce, Nd and La, were found in nelsonites, however, the total REE in pure apatites amounted 8000 to 9000 ppm, as compared to 5500 ppm in whole nelsonites. This high content of REE was partially related to the presence of Ce,Nd-rhabdophane, very well visible in CL images.

The CL images of apatite show strong to medium yellow luminescence, indicative for La and Ce structural admixtures. Apatite, apparently homogeneous in the SEM images, was revealed to be zoned by the CL observations. Moreover, the latter method enabled identification of the late minerals such as anhydrite, allanite, rhabdophane and calcite (Wiszniewska, 1996, 1997).

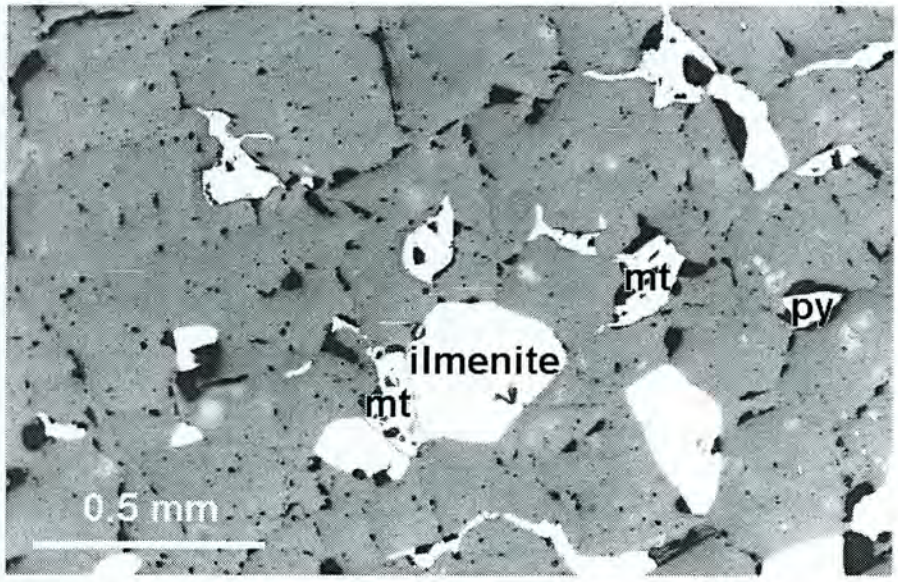

Fig. 2. Nelsonite in reflected light: grey apatite with interstitial ore minerals (mt-magnetite, py - pyrite).

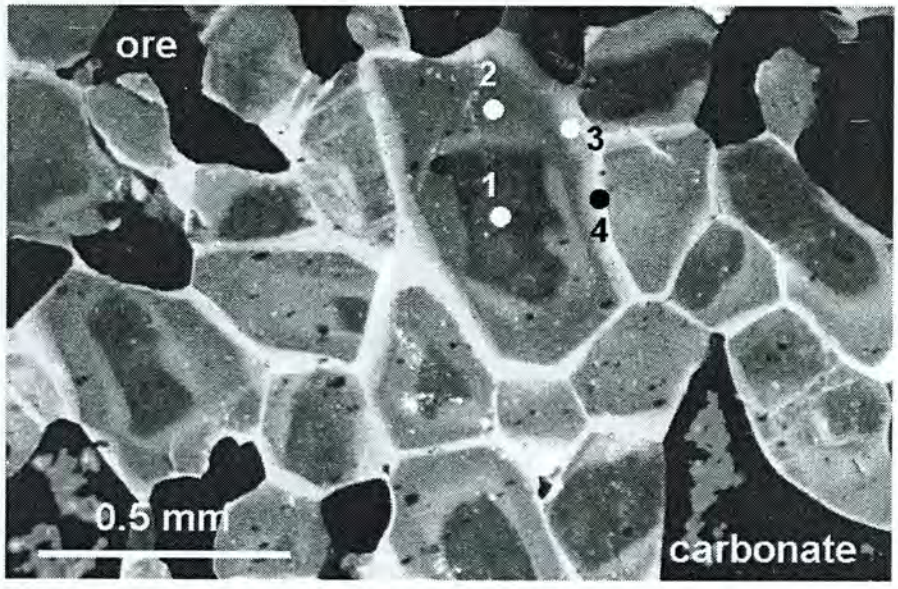

Fig. 3. Cathodoluminescence zoning of apatite from the Suwalki nelsonite; the numbers refer to the fluid inclusion types in apatite in individual growth zones, the circles indicate the typical inclusion positions.

Microprobe analyses evidenced the enrichment of apatites in REE, especially in the LREE. The presence of other REE-bearing minerals, such as Ce,Nd,La-allanite and rhabdophane $(Nd,Ce,La)PO_4 \cdot H_2O$, was recognised either in rims around apatite grains or in the interstitial neoplasms.

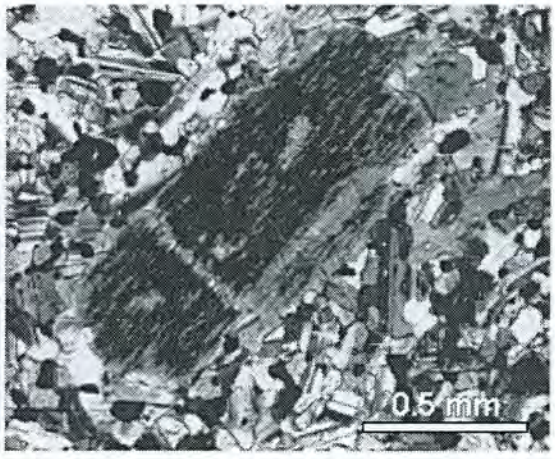

Fig. 4. Hypersthene porphyrocryst in the plagioclase-rich matrix, chilled margin of jotunite body from the Sejny 2 drilling core, depth 836,0 m; crossed nicols.

The jotunite dikes consist of orthopyroxene (Fig. 4), calcic plagioclase, biotite, apatite and Fe-Ti oxide ores as the essential components, with local porphyritic structure. The jotunite dikes from the Suwalki massif and „chilled rocks" from the Sejny intrusion have a very high content of iron (from 16.3 to 18.8% Fe_2O_3), titanium (from 2.26 to 3.45% TiO_2) and phosphorus (from 0.18 to 1.2% P_2O_5), and low magnesium number (# mg = 0.22), the latter lower than the values for jotunites of Canada (Owens et al. 1993) and for those of Rogaland. The REE distribution for the Suwalki and Sejny jotunites are medium differentiated with $(La/Yb)_{CN}$ ca.10 and without Eu anomaly. These geochemical characteristics are very similar to those of the Rogaland jotunites (Duchesne, 1990, Vander Auwera et al. 1998).

Fluid inclusions

Inclusions in apatite from nelsonite

Fluid inclusions were found in apatite grains in three zones: in the inner cores, in the intermediate zones and in the outer rims (Fig. 2). The inclusions in each zone differ in the type of filling and in the homogenisation temperatures.

1. The inner cores contain tubular inclusions up to 14 µm long and up to 5 µm thick, filled mainly by an aggregate of crystals, which comprise (in vol. %) pyroxene 20-25, apatite ca. 25, carbonate, probably calcite, ca. 25, plagioclase ca. 5, biotite 0-5, halite 5-7, sylvite 1-4 and aqueous solution 9-12. The minerals were identified by means of an electron microprobe in opened inclusions. The inclusions homogenised at 890-870°C in liquid phase after several hours of careful heating; the liquid was supposed to be in fact a complex hydrous melt of silicate-carbonate-phosphate-halide composition.

2. The intermediate zones of the apatite grains contain inclusions, poorer in pyroxene (ca. 10), plagioclase (0-3), without biotite and sylvite, but containing carbonate and apatite contents similar to the inclusions in the inner cores as well as an increased amount of aqueous solution up to 17-26 vol. %. Their homogenisation temperatures range from 820 to 770°C.

3. The outer rims contain inclusions rich in solution (30-53) and in halite (9-17), poor in carbonates (3-20) and devoid of silicates. These inclusions homogenised at 690-550°C. Most inclusions have small opaque daughter crystals, which dissolved on heating.

4. Gas-liquid inclusions were found as primary inclusions in the thin outermost parts of the apatite grains, and as secondary ones elsewhere in apatite. They are filled with aqueous solution, sometime containing halite (up to 10 vol.%) and calcite (up to 5 vol.%) daughter minerals, rarely single needles of an apparently trapped Fe-Mg-Ca silicate (pyroxene?). The homogenisation temperatures range from 480 to 230°C.

Thus, the inclusion study of the nelsonite apatite crystallisation indicates a distinct continuous transition from magmatic conditions to high- / moderate-temperature hydrothermal conditions.

The high-temperature melt inclusions in apatite of the types (1) and (2), when investigated by the quenching method, appeared completely homogeneous after quenching, with a rough surface and granular interior. One of the quenched inclusions, inclined to the preparation surface, showed, despite this roughness, a very poorly visible pale grey band across the vacuole in the middle of the inclusion. Thoroughly continuous observations of the homogenisation process on the high-temperature microscope heating stage revealed formation of two melts during the temperature increase, one from the silicate components, another from

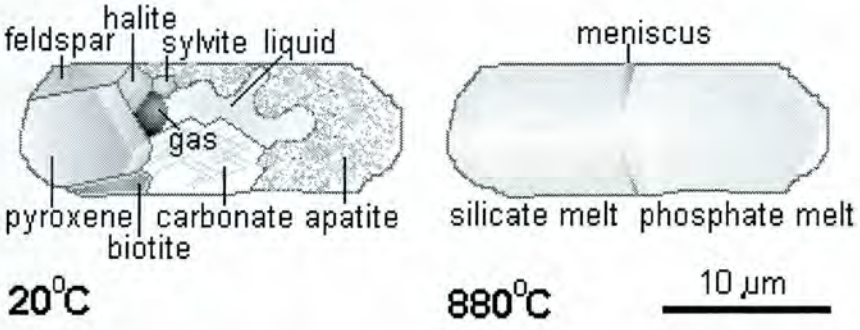

Fig. 5. Crystallised melt inclusion from the inner core of apatite from nelsonite at room temperature (*left*) and after homogenisation of the crystals and gas phase, with two immiscible melts (*right*).

the phosphate component (Fig. 5). These two melts were separated by a meniscus, which was observed as the grey band. Probably the carbonate substance was mainly dissolved in the phosphate-rich melt. The qualitative composition of the crystal phases in the untreated open inclusion and in the open inclusion with the originally completely melted filling was checked by electron microprobe. This indicated, that the aggregate described as "apatite" in fact contained also dispersed small grains of silicates and that both silicate and phosphate melts were containing carbon (i.e. carbonate component). The carbon content in the phosphate melt, however, was distinctly higher than in the silicate melt. Both melts contained also chlorine with a patchy distribution, what might be in part due to the uneven surface of the opened inclusion. Nevertheless, the variation was too strong to be explained only by the surface morphology and it should be related to the chemical inhomogeneity of the melted inclusion filling. Also the "roughness" observed in the quenched inclusions was most probably caused by initial heterogenisation of the melt despite very quick quenching. Moreover, it is impossible to define the state of the quenched phosphate melt, whether it was glassy or cryptocrystalline. The above presented results indicate that apatite and probably also other minerals of nelsonite largely crystallised from two immiscible melts, which neither homogenised in the studied inclusions up to temperature of 1080°C, nor even changed distinctly their volume proportions.

Inclusions in pyroxene from jotunite

1. Pyroxenes from the coarse-grained jotunite in the central parts of the dikes contain melt inclusions up to 20 µm long with crystallised filling, consisting of pyroxene, feldspar,

magnetite, calcite and apatite plus gas bubble (Fig. 6). The crystal aggregate started to melt in an observable degree at 800–820°C. The last crystals disappeared at 980–1040°C and small droplets of phosphate and carbonate melt formed. Complete homogenisation of all phases occurred at 1090–1170°C.

2. Fine-grained pyroxene from the chilled facies contain melt inclusions up to 12 μm long with a filling being an aggregate of tiny grains of non-recognisable minerals with gas bubble (Fig. 7). These fillings started to melt at 770–780°C. The last crystals disappeared at 1000–1060°C and small droplets of phosphate and carbonate melt formed. Complete homogenisation of these droplets and gas bubble with the silicate melt occurred at 1090–1180°C. In this case the amount of the phosphate and carbonate (10 to 15 vol.%) was too low to form a stable immiscible phase, though local, maybe metastable, immiscibility at sufficiently low temperature was observed.

Fig. 6. Crystallised melt inclusion in coarse crystal of pyroxene from the Sejny 2 jotunite, inclusion length 14 μm.

3. Pyroxenes contained also rare inclusions filled with carbon dioxide, probably in a liquid state (Fig. 8). These inclusions were difficult to observe because of their small size (3 to 4 μm); a few crushing stage investigations indicated either pure carbon dioxide filling, or a small admixture of nitrogen (ca. 10 vol.%) (prelininary determinations).

Fig. 7. Melt inclusion in pyroxene from chilled facies of the jotunite body, Sejny intrusion; the pictures show the course of melting of the inclusion filling (*from left to right*), note the formation of the phosphate and carbonate melt droplets.

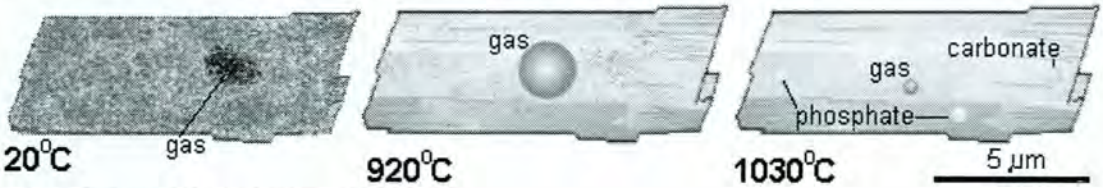

Fig. 8. Carbon-dioxide filled inclusion in pyroxene from the Sejny jotunite, inclusion length 4 μm.

Conclusions

Geochemical features of the investigated rocks, especially the REE concentrations in apatites from nelsonite veins , which show considerable amounts of LREE: La, Ce, Nd, with the typical flat or slightly increasing plotting line, indicate a relatively advanced stage of magma differentiation (Fig. 9). High contents of sulphides, that differ Suwalki nelsonites from other occurrences in the world, might suggest that sulphur acted as one of the fluxing agents in the immiscibility process (Duchesne, 1999). Homogenisation temperature of fluid inclusions in apatite distinctly indicate that nelsonites formed at the final magmatic stage

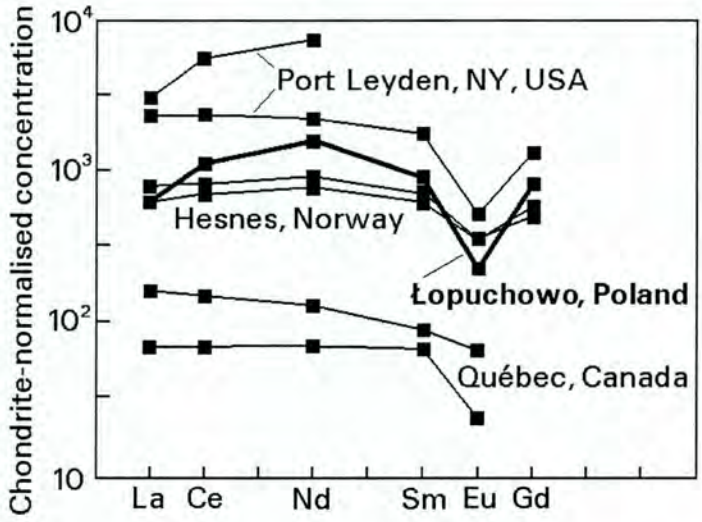

Fig. 9. Rare-earth-element contents in the Suwalki nelsonite compared to the characteristics of several world nelsonites.

mainly from a melt, which probably gradually and smoothly changed to a very saline high-temperature aqueous solution and subsequently to moderate-saline medium-temperature aqueous solution. These solutions produced the latest outer rims of the apatite grains.

Most nelsonite occurrences in the world are believed to be of magmatic origin, formed through a liquid immiscibility mechanism of two components: silicate melt of diorite composition and Fe-Ti oxide (± apatite)-rich melt. The possibility of an eutectic crystallisation of magnetite-apatite(F) and magnetite-apatite(F-Cl) systems was experimentally confirmed (Philpotts, 1967). The existence of an immiscibility gap in a diorite residual liquid enriched in Fe, Ti and P during the differentiation of magma was also observed by several authors (e.g. Roedder, 1979).

The nelsonite from the Suwalki massif formed from melt consisting of two immiscible phases: silicate one and phosphate one with carbonate admixture. As inferred from the melt inclusion fillings, the proportion of these two melts was close to the 1:1 ratio. Relatively uniform mineral-forming average compositions and its two-phase state may be explained as a kind of suspension of small droplets of one melt into the other. However, it is impossible to determine which melt was the background phase and which was the dispersed phase. The experiments of Philpotts (1967) in the system apatite – diorite – magnetite at 1420°C predicted the existence of two-phase melts along the apatite–diorite joint (Fig. 10). The composition 50% apatite–50% diorite, typical of the inclusion fillings in apatite from the Suwalki nelsonite, is quite far within the miscibility gap, thus in the two-phase region. Although the carbonate admixture may influence to some degree the extension of the miscibility gap, the latter should not be strongly modified. On the other hand, temperatures lower than in Philpotts's experiment should broaden the miscibility gap .

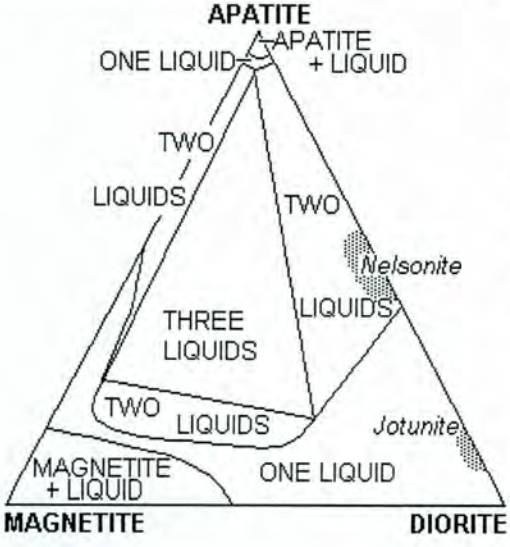

Fig. 10. Phase equilibria in the apatite – magnetite – diorite system, isothermal section at 1420°C (Philpotts, 1967), with the approximate fields (dotted) for melt inclusion compositions from the Suwalki nelsonite and the Sejny jotunite.

The earlier experimental studies indicated that the parent magma for nelsonites can exist at approximately 800-1000°C in the presence of phosphorus and carbonate (Philpotts 1967, Weidner, 1982). This reasonably supports the results of our melt inclusion studies.

Parent melt of jotunite from Sejny is already in the one-phase silicate melt area. and silicate and phosphate melts immiscibility apparently appeared locally at high temperature, though possibly in a metastable state. This may indicate crystallisation of apatite in jotunite from a separated phosphate melt, though in general the melt was homogeneous at the initial stage of the rock formation. Nevertheless, the type of inclusion filling with phosphate (and carbonate) melt droplets floating in silicate melt indicates the affinity between the jotunite parent melt and the melt which produced the Suwalki massif nelsonites.

It is noteworthy that the present melt inclusions studies in apatite from nelsonite of the Suwalki massif and in part in pyroxene from jotunite of the Sejny intrusion yielded the first direct evidence of crystallisation of nelsonite from a phosphate melt immiscible with a silicate melt.

Acknowledgements. The study was financed by the KBN grant No. 6PO4D027 (J.W.) and by the Faculty of Geology of the Warsaw University grants Nos. BW1419/33 and BW1484/30 (A.K.), what is graciously acknowledged?

References

Anderson A.T. Jr. 1966 — Mineralogy of the Labrieville anorthosite, Quebec: Amer. Miner., 51: 1671–1711.

Bolshover L.R. & Lindsley D.H. 1983 — Sybille oxide deposit: Massive Fe-Ti oxides intrusive into the Laramie anorthosite complex, (LAC) Wyoming (abs.): EOS, Trans. Amer. Geoph. Union, 64: 328.

Darling R.S. & Florence F.P. 1995 — Apatite light rare earth element chemistry of the Port Leyden nelsonite, Adirondack Highlands, New York: Implications for the origin of nelsonite in anorthosite suite rocks. Econ. Geol., 90: 964–968.

Duchesne J.C. 1990 — Origin and evolution of monzonorites related to anorthosites. Schweiz. Mineral. Petrogr. Mitt. 70, 189-198.

Duchesne J.C. 1999 — Fe-Ti deposits in Rogaland anorthosites (South Norway): geochemical characteristics and problem of interpretation. Mineralium Deposita, 34: 182-198.

Emslie R.F. 1975 — Major rock units of the Morin Complex, Southwester Quebec. Can. Geol. Survey Paper 74-48: 1-37.

Kolker A. 1982 — Mineralogy and geochemistry of Fe-Ti oxide and apatite (nelsonite) deposits and evolution of the liquid immiscibility hypothesis. Econ. Geol., 77: 1146–1158.

Kozlowski A. 1981 — Melt inclusions in pyroclastic quartz from the Carboniferous deposits of the Holy Cross Mts, and the problem of magmatic corrosion. Acta Geol. Polon., 31: 273-284

Krzeminski L., Tyda R. & Wiszniewska J. 1988 — Mineralogic and geochemical study of ore–bearing apatite rochs (nelsonites) from the Suwalki Massif (NE Poland). Miner. Pol., 19. 2: 35–55.

Philpotts A.R. 1967 — Origin of certain iron-titanium oxide and apatite rocks: Econ. Geol., 62: 303–315.

Roedder E. 1979 — Silicate liquid immiscibility in magma. In: Yoder HS (ed). The evolution of the igneous rocks. Fiftieth Anniversary Perspectives. Princeton University Press, Princeton, pp 15-57

Roelandts I. & Duchesne J.C. 1979 — Rare-earth elements in apatite fro layered norites and iron-titanium oxide ore-bodies related to anorthosites (Rogaland, S.W. Norway). Phys. Chem. Earth, 11: 199–212.

Ross C.S. 1941 — Occurrence and origin of the titanium deposits of Nelson and Amherst Counties, Virginia. U.S. Geol. Survey Prof. Paper 198: 1-38.

Vander Auwera J., Longhi J., Duchesne J.C. 1998 — A liquid line of descent of the jotunite (hypersthene monzodiorite) suite. Journ. Petrol. 39, 439-468.

Watson T.L. & Taber S. 1913 — Geology of titanium and apatite deposits of Virginia. Virginia Geol. Surv. Bull., 3–A: 308.

Weidner J.R. 1982 — Fe oxide magma in the system Fe-C-O. Can. Miner. 20: 555-566.

Wiszniewska J. 1996 — Application of cathodoluminescence method to ore-apatite rocks from the Suwalki basic massif (NE Poland). "International Conference on Cathodoluminescence and Related Techniques in Geosciensces and Geomaterials" Abstracts, 2–3 September 1996. Nancy. France.
Wiszniewska J. 1997 — Suwalki nelsonites - new mineralogical and geochemical data. Przegl. Geol., 45: 883-892.
Wiszniewska J., Duchesne J.C., Claesson S., Stein H., Morgan, J.W., 1999 — Geochemical constraints on the origin of the Suwalki anorthosite massif and related Fe-Ti-V ores, NE Poland. Journal of Conference Abstracts, 4: 686.

Kryvdik SG:

Ilmenite deposits and mineralization in alkaline and subalkaline magmatic complexes of the Ukrainian Shield

Kryvdik S.G.
Institute of Geochemistry, Mineralogy, and Ore Formation of Ukrainian NAS, Kyiv, Ukraine

There are known in the Ukrainian shield (US) some ilmenite deposits related to alkaline and subalkaline complexes. They usually consist of combined apatite-ilmenite-magnetite ores with variable contents of these minerals.

On the territory of this region the Proterozoic alkaline and subalkaline complexes with ilmenite mineralization predominate. There is also the Devonian alkaline complex (Pokrovo-Kyreyevo) in the border zone of US and Donbass folded structure.

Ilmenite-bearing Proterozoic alkaline and subalkaline complexes are subdivided into two formations (ensembles): alkaline-ultrabasic (with carbonatites) and gabbro-syenitic. These formations have different geological age: about 2.1 Ga for the first and 1.7-1.8 Ga for the second.

Ore concentrations of ilmenite related to alkaline-ultrabasic formations are found for the present only in the Chernigovka (Novo-Poltavka) complex situated in West Azov area. Ore-bearing rocks are represented here by alkaline pyroxenites (nepheline-free jacupirangites), which mainly consist of alkaline pyroxene (aegirine-diopside, aegirine-sahlite), ilmenite and magnetite, and subordinate amphibole, biotite, apatite, calcite, sphene etc. The ilmenite contents in these rocks vary 5-15%, average 10%. The ilmenite is enriched in Nb (to 0,3 %). Same varieties of carbonatites from these complexes have increased concentration of ilmenite that can be significant as one of useful accompanying minerals.

In the gabbro-syenitic formation the ilmenite-rich rocks are represented by ore gabbros, troctolites, cumulate peridotites and pyroxenites. In these formation two types of massifs are distinguished. In the first one gabbro-syenitic massifs associate with anorthosite-rapakivi granite plutons, spatially and genetically related to the latter. Thus, Davydky gabbro-syenitic massif lies on the north part of the Korosten anorthosite-rapakivi-granite pluton. The South-Kalchik massif (Azov area) represents an essentially syenitic analogue of such plutons. In the second type of gabbro-syenitic formation ore gabbroides and pyroxenites genetically relate to complex polyphasic massifs (Oktyabrsky, Pokrovo-Kyreyevo et al.), whose development is terminated by nepheline syenites (mariupolites, foyaites, juvites).

Among the ilmenite-bearing gabbroides and peridotites of gabbro-syenitic formation there are apatite-ilmenite and essentially ilmenite-ore varieties (contents of ilmenite amount to 20%, and apatite - 5-10%). These rocks are rather similar to ore troctolites of Stremygorod ilmenite-apatite deposit that is situated in the middle of Korosten pluton. In our view, gabbroides of this deposit are to be referred to gabbro-syenitic formation, because they differ essentially on their

increased alkalinity (present of titanaugite, potassic feldspar) from typical rocks of Korosten pluton.

All the above mentioned varieties of apatite-ilmenite gabbroides and peridotites have a magmatic ore-mineralization, formed mainly during the crystal accumulation of ilmenite, magnetite and apatite. Their initial magmas were enriched in titanium and/or phosphorus yet on the mantle level of their generation (nephelinites for alkaline-ultrabasic formation and alkaline basalts for gabbro-syenitic one) or by the differentiation process in the intermediate magmatic chambers.

Kullerud K:

Geochemistry and mineralogy of the Tellnes ilmenite ore body

Kåre Kullerud, Department of Geology, University of Tromsø, N-9037 Tromsø, Norway

The Tellnes ilmenite ore body is one of the largest ilmenite deposits of the world and has been mined by Titania A/S since 1960. The ore body, which is of magmatic origin, appears as a sickle-shaped lens about 2700 m long and 400 m wide in the Åna-Sira anorthosite massive, belonging to the Rogaland anorthosite province.

Whole-rock geochemical analyses have been carried out on drill cores of the ore body since the initial prospecting of the mine in 1955. At present, the geochemical database consists of about 5000 analyses including TiO_2, P_2O_5, S, Cr and modal magnetite. Furthermore, more than 2000 samples have been analysed for the remaining major elements and a selection of trace elements. In addition, mineral compositional data have been analysed from a selection of drill cores.

The ore is characterised by the lack of modal layering. However, the ore body shows a strong compositional zoning. The TiO_2 content is generally high (>18 wt %) within the central parts of the ore body, and there is a gradual decrease in the TiO_2 content towards the contact to the host-rock. The variations in the ore chemistry reflect the variations in the modal contents of the ore forming minerals. Based on these variations, the ore body has been divided in four zones: the upper marginal zone (UMZ), the upper central zone (UCZ), the lower central zone (LCZ), and the lower marginal zone (LMZ). It should be noted that this division is approximate, because the transitions between the various zones are transitional. UMZ is characterised by high modal contents of plagioclase and Fe-Mg silicates (CPX, OPX, OL), but low contents of ilmenite. UCZ shows high modal contents of ilmenite and Fe-Mg silicates, and low contents of plagioclase. LCZ, which is the most ilmenite enriched zone, is characterised by low contents of Fe-Mg silicates (olivine is absent), and intermediate contents of plagioclase. Through the LMZ, the ilmenite content decreases, while the contents of plagioclase, CPX and OPX increase.

The ore-forming minerals show compositional variations that are highly correlated to the whole-rock chemistry. In general, the Mg/(Mg+Fe)-ratios of ilmenite and the Fe-Mg silicates are high in the central TiO_2-rich parts of the ore body (UCZ and LCZ). Towards the margins, however, Mg/(Mg+Fe)-ratios of the ore-forming minerals decrease gradually.

Lindsley DH:

Do Fe-Ti oxide magmas exist? Geology: Yes; Experiments: No!

Donald H. Lindsley
Department of Geosciences, State University of New York, Stony Brook, NY 11794-2100

Field evidence strongly suggests that many Fe- and Fe-Ti-oxide bodies were emplaced as liquids. The evidence is strongest for the deposits at El Laco, Chile, where magnetite bodies appear to have been extruded as lavas, and for which the experiments of Jerry Weidner in the system Fe-C-O provide convincing proof of oxide liquids at geologically reasonable temperatures (<1000°C). Thus it was very exciting when we discovered that the Fe-Ti-oxide bodies in the Laramie Anorthosite Complex contain graphite. Very importantly, however, Weidner's experiments lacked TiO_2 - and the El Laco iron-oxide lavas are nearly titanium-free.

Field evidence of a magmatic origin for Ti-bearing oxide bodies (ilmenite and magnetite-ilmenite ores) still seems strong: many are dike-like, crosscutting the country rock with sharp contacts. Many are associated with anorthosite complexes. Isotopic studies show that many are closely akin to the host anorthosites. Many of these bodies ("nelsonites") contain abundant apatite, and it has been suggested that apatite serves as a flux to stabilize Fe-Ti-O-(apatite) magmas, possibly as melts immiscible with a complementary silicate liquid.

Unfortunately, despite much effort there is no experimental evidence to support the concept of apatite-fluxed melts. Philpotts reported ilmenite-apatite melts at ~1400°C, but this is hardly compelling. The temperature is unrealistically high for crustal conditions, and in any case fluorapatite and ilmenite separately melt near that temperature, so there is little evidence for a eutectic or cotectic relationship between them. Kolker pointed out that while nelsonites broadly contain approximately 1/3 apatite and 2/3 oxide, the proportions in fact vary widely, further casting doubt on the existence of a eutectic relationship.

For many years my students and I have tried - unsuccessfully - to generate Fe-Ti oxide liquids in the laboratory at geologically reasonable temperatures. We have tried apatite and iron phosphate and graphite - separately and in combination - as well as chlorides as possible fluxes. Using graphite alone we have made small amounts of Fe-rich liquid - but importantly that melt is nearly Ti-free; most of the titanium remains in the residual crystals. Using graphite and apatite we again made small proportions of Fe-rich, Ti-poor melt - but that melt dissolved more strontium than phosphorus from the natural apatite used in the experiments! Despite the common association of apatite and oxides in nature, there is no experimental support for the existence of apatite-oxide melts.

The experiments of Epler on an oxide-rich troctolite pegmatite (MS thesis, Stony Brook) suggest a possible explanation. Although he failed to produce an immiscible oxide *melt*, he showed conclusively that phosphorus and iron *mutually enhance their solubilities* in the silicate melts coexisting with crystalline Fe-Ti oxides. For example, at 5 kbar, 1100°C he produced a silicate liquid with 26.2 weight% iron as FeO, 4.2% TiO_2, and 3.8% P_2O_5. At 1150°C the values go up to 32.7, 8.56, and 4.2%, respectively. Thus the close association of apatite and oxides probably reflects coprecipitation from a silicate parent: once the silicate melt becomes saturated with one of these phases, the other is likely to coprecipitate as well. Experiments suggest that the oxide bodies crystallize from Fe-Ti-P-rich silicate liquids and are emplaced either as crystal mushes or in the solid state.

McEnroe SA, Robinson P & Panish PT:

Aeromagnetic anomalies, magnetic petrology and rock magnetism of hemo-ilmenite- and magnetite-rich cumulates from the Sokndal region, South Rogaland, Norway

Suzanne A. McEnroe[1], Peter Robinson[1, 2] & Peter T. Panish[2]
[1]Geological Survey of Norway, N-7491 Trondheim, Norway
[2]Department of Geosciences, University of Massachusetts, Amherst, MA 01003, USA

Aeromagnetic maps of the Egersund Mid-Proterozoic igneous province show a spectacular range of positive and negative magnetic anomalies with a contrast up to 15,600 nT. The positive magnetic anomalies are over magnetite norites and overlying mangerites and quartz mangerites of the Bjerkreim-Sokndal layered intrusion. These rocks are dominated by MD magnetite. The negative magnetic anomalies are over, ilmenite-rich norites of the Bjerkreim-Sokndal layered intrusion, Tellnes ilmenite norite ore deposit and massif anorthosites. These rocks are dominated by hemo-ilmenite and/or by silicates with fine-grained oxide exsolution lamellae. Electron probe analyses of coexisting oxides in the layered intrusion confirm earlier observations that oxides in early magmatic rocks are dominated by hemo-ilmenite with minor end-member magnetite, followed by more reduced oxides dominated by titanomagnetite with minor near end-member ilmenite. What is not fully understood is the property of ilmenite with hematite exsolution lamellae, or, even more striking, hematite with ilmenite lamellae, to produce strong remanent magnetization of high coercivity and with a Néel temperature equal to or above the Curie temperature of magnetite. This property makes the rhombohedral oxides an important candidate to explain some high-amplitude deep-crustal anomalies on earth, or strong remanent magnetization on other planets. A remarkable feature in the Egersund province is that primitive magmas produced rocks rich in hemo-ilmenite causing negative magnetic anomalies related to magnetic remanence, and more evolved magmas produced rocks rich in magnetite related to positive induced magnetic anomalies, all in the course of crystallization-differentiation.

Meyer GB & Mansfeld J:

LA-HR-ICP-MS studies of ilmenite in MCU IV of the Bjerkreim-Sokndal intrusion, SW Norway

Meyer, G.B. & Mansfeld, J.
Geological Survey of Norway, N-7491 Trondheim, Norway
Gurli.Meyer@ngu.no, Joakim.Mansfeld@ngu.no

The layered Bjerkreim-Sokndal Intrusion (BSI) forms part of the Rogaland Anorthosite Province of South Norway. The province is known for its volumetric anorthosite bodies and ilmenite-rich noritic intrusions of which the Tellnes Dyke contributes to c. 6% of the present world Ti-production. Earlier studies of ilmenite compositions in the noritic bodies were primarily based on analyses by electron microprobe or analyses of ilmenite concentrates. These studies have given significant knowledge of the ilmenite compositions in many of the noritic

intrusions in the province. However, the need for high precision in situ analyses of ilmenite has grown during the last few years. Based on this need we have developed a method for analysing ilmenite by a Laser Ablation High Resolution Inductive Coupled Plasma-Mass Spectrometer (LA-HR-ICP-MS). Here we present the method based on 24 samples from a profile covering a 2400 m thick cumulate sequence. The profile is situated in the northern part of the Bjerkreim-Sokndal Intrusion.

The northern part of the Bjerkreim-Sokndal Intrusion consists of a c. 7 km-thick Layered Series, which is divided into megacyclic units (MCU) arranged in a syncline. Each MCU formed in response to magma replenishment in a bowl-shaped magma chamber. The megacyclic units are characterised by common crystallisation sequences of which the fourth and last (MCU IV) is the most complete. The profile we present in this poster covers the uppermost part of MCU III and a major portion of MCU IV.

The samples were analysed by UV-laser ablation in medium resolution ($M/\Delta M=3000$) on a Finnigan MAT ELEMENT® double focusing sector ICP-MS. Previous to the ablation, the ilmenite was analysed by electron microprobe. Continuous laser ablation of the samples was performed as a 100 by 100 µm raster, giving the bulk composition of ilmenite plus hematite exsolution in each grain. The elements Ti, Fe, Mg, Mn, Si, Ca, Al, V, Cr, Ni, Zr, Nb were analysed. The concentration of the major elements (Ti, Fe, Mg, Mn) was determined by stoichiometric calculations in combination with element calibration. Trace elements were calibrated against international and synthetic ilmenite and rutile standards that were manufactured from $TiFeO_3$ powders doped with trace elements in varying concentrations. The powders were melted by direct fusion in graphite electrodes resulting in fast melting and quenching. Two or more analyses of 10 different standards were used to establish the calibration curves, which allowed outliers caused by inhomogeneous standards or analytical noise, to be excluded. The analytical and calibration uncertainty is between 2-5% in total and the detection limits are 0.1-10 ppm for trace metals and less than 0.1 % for major oxides.

At the transition between MCU III and MCU IV ilmenite contains 10-20% hematite, increasing to 25% in the lower part of MCU IV. The haematite content gradually decreases to 5-10% in the central and uppermost part of the profile. The same trend is seen for the Geikielite component of ilmenite, which increases from 1% to 15 % in the lower part of MCU IV, and then decreases gradually throughout MCU IV to 1-2%. The pyrophanite component of ilmenite increases gradually through the entire profile, with only minor indications of a decrease in the lower part of MCU IV. The elements V, Cr and Ni all show an increase in concentrations at the lowermost level of MCU IV and then a decrease corresponding to increasing degree of fractional crystallisation; V being largely controlled by the onset of magnetite crystallisation. Both Zr and Nb show classic incompatible behaviour with increasing concentrations in response to increasing degree of fractional crystallisation. The trends described are in good agreement with the trends described in earlier work for the silicate minerals, which indicate a major replenishment event of magma reflected by the reversion in compositions in the lower part of MCU IV followed by fractional crystallisation of magma throughout MCU IV.

Mitrokhin AV:

The gabbro-anorthosite massives of Korosten Pluton (Ukrain) and problems evolution of parental magmas

A.V. Mitrokhin
Geological Fakulty of Kiev Taras Shevchenko National University, Ukrain.

Abstract: Recent field investigations have shown that large gabbro-anorthosite massives of Korosten pluton are composed several age associations of basic rocks: Early Anorthosite Suite, Main Anorthosite Suite, Early Gabbroic Suite, Late Gabbroic Suite and Dake Suite. Detailed studies of age suites of basites allow to trace evolution of mineral and chemical compositions with transition from early suites to later suites. There are concluded that depletion Mg, Cr, Ni, Sr and accumulation Ti, Fe, Mn, K, P, V, Sc, Ba, La, Ce, Zr, Y, Cu, Mo in row: Early Anorthosite Suite - Main Anorthosite Suite - leucodolerites of Dake Suite are conected with deep evolution of compositions of parental high-aluminous basalt magmas.

Introduction and geological setting

The massive anorthosites are one of the largest occurence of Precambrian basic magmatism. The proterozoic anorthosite complexes contain numerous Fe-Ti deposites of economic grade and therefor are studed extensively. The Korosten pluton occurs in the north-west part of Ukrain Shield into Volynia Block. The pluton is a multiple anorogenic intrusion that is composed by the classical association of gabbroids - anorthosites - rapakivi-granites [Velicoslavinsky et al., 1978], which were intruding in the Proterozoic 1737-1800 Ma. The rocks of Korosten Complex occupy an area of 12000 km^2. The lagest gabbro-anorthosite massives: Volodarsk-Volynscy (1250 km^2), Chepovichsky (830 km^2), Fedorovsky (104 km^2), Pugachevsky (15 km^2), Krivotinsky (30 km^2) occupy 18% of the area. The massives are subhorisontal flate form bodies whith thikness into 0.5-3 km [Bukharev, 1973a]. Gabbro-anorthosite varieties of basites predominate in the composition of the most massives. Anorthosites and mesocratic gabbroids are less sreaded. Ultrabasites are rare rocks. Long time there are considered that the anorthosites (gabbro-anorthosites) and gabbroids were intruded into two phase [Polcanov, 1948; Bukharev, 1973b]. Recent detailed field studies have shown that both the anorthosites and the gabbroids were inttruding repeatly [Mitrokhin, 2000]. On the base new field geological, mineralogical, petrographical and geochemical investigationes there have proved large gabbro-anorthosite massives are multiple intrusiones, which are composed several age associationes (suites) of the basic rocks. Into Volodarsk-Volynsky (VVM), Chepovichsky (CHM), Fedorovsky (FEDM) and Pugachovsky (PUGM) massives there are distinguished five age suites of the basic rocks: Early Anorthosite Suite, Main Anorthosite Suite, Early Gabbroic Suite, Late Gabbroic Suite and Dake Suite [Mitrokhin, 2000; Zinchenco et al., 2000; Zinchenko and Mitrokhin 2000].

Field relationshipes and petrography of the age suites of basites

Early Anorthosite Suite (A_1) concludes oldest basic formatines of the Korosten pluton. Among the rocks A_1 there are distinguished anorthosites, which contain less 10% mafic minerals, norite-anorthosites with 10-25% mafic, leuconorites with 25-35% mafic as well as amfibolizate varieties of anorthosite rocks. The magnesium anorthosites - leuconorites of A_1 are presented by xenolithes into ferric anorthosites, gabbro-anorthosites and gabbroids of the later phases as well as into korosten granites and basic dakes. U-Pb age of the xenolithes of the "old anorthosites" are constrained 1800-1784 Ma [Verhogliad, 1995]. Near the village Pugachovka and Vaskovichy there are proposed primary occurence of the rocks A_1. Now formationes A_1 have studed into CHM, FEDM, PUGM. Taking into account findes of ksenolites magnesium anorthosites into basic

dakes, which are intruding korosten granites, there are proposed presence formationes A_1 on the depth. The anorthosites, norite-anorthosites and leuconorites A_1 are coarse grained light-grey to white rocks. In exposures gigantic-coarse graned adcumulate anorthosites alternate with coarse grained mesocumulate norite-anorthosites. Main minerals are plagioclase (An_{42-57}), high-alumina orthopyroxen with f=22-46% (f=100*Fe/Fe+Mg) and content of Al_2O_3=2.3-4.9%. Secondary minerals are actinolite, chlorite, quartz. There are characteristic rarity to absence of apatite and Fe-Ti oxide minerals.

Main Anorthosite Suite (A_2) are presented anorthosites (<10% mafic), gabbro-anorthosites (10-25% mafic), leucogabbro-norites (25-35% mafic). The rocks of A_2, composing main voluie of gabbro-anorthosite massives, contain xenolithes A_1 but themselves are intruded by the later bodies of gabbroids and granites of korosten komplex. U-Pb age gabbro-anorthosites A_2 of VVM are estimated at 1760-1758 Ma [Verhogliad, 1995]. The anorthosites, gabbro-anorthosites and leucogabbro-norites A_2 are gigantic-coarse grained rocks with dark-grey to black coloure. Coarse-graned mesocumulate gabbro-anorthosites are most spreaded. Main minerals are plagioclase (An_{46-62}), inverted pigeonite (f=44-54%, Al_2O_3=0.5-0.7%), augite ($Wo_{32-41}En_{32-41}Fs_{23-28}$, f=38-46%), olivine (f=43-59%); minor and accesory are orthoclase, ilmenite, magnetite, apatite; secondary are sericite, biotite, amfibole, quartz, chlorite, epidote, calcite.

Early Gabbroic Suite (G_3) are presented leucogabbro-norites (25-35% mafic) and gabbro-norites (>35% mafic) which are exsposured in south part of VVM. In quarring Slipchicy the rocks G_3 include xenolithes of anorthosites A_2 but themselves are intruded by dake olivine microgabbro G_4. The gabbro-norites G_3 are grey colour medium-grained rocks with orthocumulate gabbro-ophitic texture and plane parrallel structure. Main minerals are plagioclase (An_{43-56}), inverted pigeonite (f=45-55%), augite ($Wo_{30-32}En_{57-58}Fs_{11-12}$, f=16-17%). Gabbro-norites G_3 are distingushed from the later gabbroids by rarity to absence olivine and low contentes Fe-Ti oxide minerals and apatite.

Late Gabbroic Suite (G_4) are presented numerrous varieties of olivine gabbroides and ultrabasites within layered bodies that are intruding the formationes A_2 but themselves are intruded by korosten granites. U-Pb age olivin gabbro-norites VVM (1759 Ma) [Verhogliad, 1995] are near to age gabbro-anorthosites which are belonged A_2. Intrusiones G_4 are spreaded into all massives of gabbro-anorthosites but especially in VVM where was considered how "side complex" [Polkanov, 1948] or independent phase [Bukharev, 1973b].

Among the rocks of G_4 there are most spreaded mesocratic meso-orthocumulate olivine gabbro (gabbro-norites) with medium-grained allotriomorphic-granular texture. The main minerals of the rocks are plagioclase (An_{34-57}), augite ($Wo_{34-44}En_{29-37}Fs_{22-37}$, f=39-56%), inverted pigeonite (f=56-64%), olivine (f=47-77%). There are characteristiced high contentes of ilmenite and magnetite as well as constant presence orthoclase.

The ultrabasites composing singenetic bends among olivine gabbro G_4 are rare rocks. There are distingushed olivine melagabbro, peridotites and pyroxenites. The main minerals of the ultrabasites are olivine (f=32-74%), augite ($Wo_{40-48}En_{26-37}Fs_{23-25}$, f=38-49%), ilmenite, magnetite. Minor and accessory minerals are plagioclase (An_{28-36}), biotite, orthoclase, apatite. The amfiboles, chlorite, epidote, talc, serpentine, calcite are secondary.

Dake Suite (D_5) are presented leucodolerites, trachydiabases, trachyandesibasaltes that complete formation of basic magmatism of Korosten pluton. The rocks D_5 form numerous dakes in gabbro-anorthosite massives, korosten granites and gneiss-migmatites of pluton's setting.

Subalkalic high-aluminous leucodolerites of Zvizdal-Zaleskaja, Skuratynskaja and Belokorovichscaja dakes have medium-coarse graned ophytic textures. The main ninerales are presented by plagioclase (An_{43-60}), augite, orthoclase; minor and rare are olivine (f=57-60%), apatite, ilmenite. The quartz, sericite, epidote, calcite, chlorite and actinolite are secondary.

Subalkalic moderate-aluminous trachydiabases and trachyandesibasaltes are characteristiced porphyric texture with ophitic or intesertal to hyalopilitic matrix. Phenocrystes are plagioclase (An_{47-52}). The matrix are composed by plagioclase (An_{23-30}), augite (f=41-72%), orthoclase, ilmenite, apatite and glass. The quartz, sericite, epidote, actinolite, biotite, chlorite are secondary.

The mineral and chemical evolution of basites

The new data about stages of formation of the gabbro-anorthosite massives allow to make preliminery conclusions about the evolution basic magmatism of Korosten pluton.

The Early Anorthosite Suite, Main Anorthosite Suite and leucodolerites of Dake Suite form consecutive row subalcalic high-aluminous basic rocks. Within of each suite the descent of contents plagioclase with addition of contents mafic minerals accompany by the regular descent SiO_2, Al_2O_3, CaO, Na_2O and addition of TiO_2, FeO, MgO (Table 1). The ratios FeO:MgO, TiO_2:FeO, within each suite are almost constant that is corresponded "anorthosite schem" of fractionation with essential accumulation of plagioclase with ascent on final level of emplacement. Within the row high-aluminous basites with transitione from anorthosite - leuconorites A_1 to anorthosite -leucogabbro-norites A_2 and to leucodolerites D_5 there are traced the change of mineral associationes: $Pl_{42-57} + Opx_{22-46}$ to $Pl_{45-62} + Pig_{44-54} + Aug_{38-45} \pm Ol_{45-59} \pm$ Fsp to $Pl_{45-60} +$ Aug + Fsp $\pm Ol_{57-60}$ with addition contents of Fe-Ti oxides and apatite. The change of mineral associations are accompaned by descent contents MgO, Cr, Ni, Sr and addition content TiO_2, FeO, MnO, K_2O, P_2O_5, V, Sc, Ba, La, Ce, Zr, Y, Cu, Mo with regular addition of ratios FeO:MgO, TiO_2:FeO.

The Early Gabbroic Suite, Late Gabbroic Suite and trachydiabase - trachyandesibasaltes of Dake Suite form consecutive row subalkalic moderate-aluminous basic rocks. Within each of suites the descent contents SiO_2, Al_2O_3, Na_2O, K_2O with regular addition TiO_2, FeO, MgO are accompaned noticeable change of ratios FeO:MgO, TiO_2:FeO (Table 1). This is corresponded to differentiation with essential separation of plagioclase and mafic minerals. Within row moderate-aluminous basites with transition from gabbro-norites G_3 to olivine gabbroides G_4 and to trachydiabases D_5 there are traced change mineral associations: $Pl_{43-56} + Pig_{45-55} + Aug_{16-17}$ to $Pl_{28-60} + Aug_{38-56} + Ol_{32-77} \pm Pig_{56-64} \pm$ Fsp and to $Pl_{25-62} + Aug_{42-72} +$ Fsp with sharp addition contents Fe-Ti oxides and apatite in G_4. The change of mineral associationes are accompaned by addition of contents TiO_2, FeO, K_2O, P_2O_5 with change ratios FeO:MgO, TiO_2:FeO.

Conclusion

1. Taking into account the "anorthosite schem" of crystalisation for high-aluminous basic suites there may proposed that the depletion Mg, Cr, Ni, Sr and accumulation Ti, Fe, Mn, K, P, V, Sc, Ba, La, Ce, Zr, Y, Cu, Mo with addition ratios FeO:MgO, TiO_2:FeO, in row: (anortorthosite - leuconorite A_1) -> (anorthosite - leucogabbro-norite A_2) -> (leucodolerite D_2) are conected with deep evolution of the compositions of parental high-aluminous basalt magmas.

2. The Main Anorthosite Suite and Late Gabbroic Suite have hereditery mineral and chemical compositions that make possible to consider them as cumulate (A_2) and complementary product of residium liquid crystalisation (G_4).

3. The estabblished features evolution of basic magmatism of Korosten pluton allow to propose the occurence of Ti-Fe-P magmatic deposites into formationes of G_4 and D_5.

References

Bukharev V.P., Stekolnikova A.V., Poliansky V.D. Tectonics and deep framework of anorthosite massives north-west part of Ukrain Shield // Geotectonics. -1973. -N4. -P.34-41.

Bukharev V.P., Kolosovska V.A., Hvorov M.I. The features of formation of the anorthosite massives north-west part of Ukrain Shield //Soviet geology.-1973.-N6. -P.125-132.

Bucharev V.P. Precambrian magmatic evolution of the western part of the Ukrainian Shield. -Kiev. - 1992. -152 p.

Zinchenco O.V., Mitrokhin A.V., Moliavko V.G. New data on stages of basic rocks formation of the Korosten pluton // Reportes of National Academy of Sciences of Ukraine. -2000. -N4. -P.128-130.

Zinchenco O.V., Mitrokhin A.V. Postgranite Dake Suite of the basic rocks of Korosten pluton // Mat. of Science Conference " The Actual Problems of Ukraine Geology".-2000.-P.18.

Mitrokhin A.V. Age relationships between basic rocks of the Korosten pluton // Visnyk of Kiev University. Geology. -2000. -Vol.16. -P.15-20.

Polkanov A.A. -1948. Gabbro-labbradorite pluton of Volyn area of the USSR. -Leningrad University. -1948. -80 p.
Verchogliad V.M. -1995. Age stages of Korosten pluton magmatism // Geochemistry and Ore Formation. -1995. -N21. -P.34-47.

Table 1. Average compositions of basic rocks of the Korosten pluton

Suites	A_1			A_2			D_5	
Rocks	1	2	3	4	5	6	7	8
SiO_2	54.92	54.46	52.99	53.74	52.55	51.89	48.98	49.52
TiO_2	0.13	0.25	0.34	0.29	0.86	1.11	2.2	2.6
Al_2O_3	26.36	23.86	20.37	26.93	22.86	20.16	18.89	18.2
Fe_2O_3	0.19	0.52	1.23	0.48	1.23	1.54	2.69	2.6
FeO	0.89	2.59	5.56	1.4	4.54	7.24	8.23	8.2
MnO	0.02	0.06	0.09	0.02	0.07	0.08	0.12	0.1
MgO	1.07	3.02	5.94	0.63	2.11	3.24	2.86	2.65
CaO	9.28	8.69	7.63	9.94	9.18	8.25	7.8	7.3
Na_2O	5.13	4.27	3.37	4.68	4.07	3.56	3.35	4.1
K_2O	0.9	0.81	0.74	0.81	0.98	1.14	1.68	1.8
P_2O_5	0.06	0.07	0.06	0.08	0.26	0.43	0.52	1.03
f%	35.2	36.26	38.83	61.83	60.11	60.06	67.44	69.0
ti %	15.3	9.21	5.0	14.41	14.96	13.24	20.11	24.07
n	10	19	6	24	91	17	9	4
Or	5.1	4.8	4.3	4.6	5.8	6.8	10.3	11
Pl	90	80.3	67.7	89.6	78	68.6	63.9	64.5
Opx	3.9	11.6	24	3.1	9.9	16.9	14.8	9.4
Cpx	-	-	-	-	2.1	2.1	3.5	3.5
Ol	-	-	-	-	-	-	-	3
Qu	0.2	1.9	1.7	1	1.1	1.5	0.3	-
Il + Mt	0.4	0.9	1.7	0.9	2.5	3.2	6.1	6.6
Wo	-	-	-	-	-	-	-	-
C	0.2	0.3	0.3	0.5	-	-	-	-
An %	49.8	52.7	55.4	53.7	52.9	52.8	51.2	41.4
fsil%	25.6	29.3	31.3	45.2	46.5	49.7	50.0	50.0
Il/Il+Mt%	50	44.4	23.5	44.4	48	50	52.5	57.6

Table 1 (continued):

Suites	G_3		G_4						D_5	
Rocks	9	10	11	12	13	14	15	16	17	18
SiO_2	52.38	50.81	49.45	47.52	40.75	33.67	30.96	28.23	52.09	55.17
TiO_2	0.92	1.35	2.37	2.93	5.4	6.21	7.52	7.4	2.54	2.13
Al_2O_3	18.51	16.03	18.77	14.52	12.23	6.79	3.81	1.74	14.28	13.97
Fe_2O_3	1.81	1.93	1.91	2.54	4.4	5.81	5.24	7.56	2.64	2.56
FeO	7.16	8.84	8.99	13.06	16.69	24.57	30.96	33.69	10.47	9.72
MnO	0.14	0.12	0.12	0.18	0.28	0.28	0.47	0.4	0.15	0.14
MgO	4.96	6.81	3.83	4.57	5.62	7.08	8.2	8.71	3.09	2.57
CaO	8.49	8.48	8.4	8.17	8.09	9.77	9.65	8.54	5.49	5.06
Na_2O	3.61	2.82	3.58	3.12	2.44	1.36	0.78	0.49	3.14	3.26
K_2O	0.74	0.83	0.95	1.04	0.78	0.48	0.3	0.17	2.44	2.84
P_2O_5	0.28	0.28	0.6	0.96	1.29	2.47	1.32	1.97	0.83	0.67
f%	49.92	46.3	61.54	64.8	67.15	69.83	71.0	72.08	70.0	72.33
ti %	10.5	12.4	21.85	19.2	27.37	20.72	21.25	18.42	19.5	17.37
n	12	10	41	98	59	46	4	12	20	30
Or	4.3	5	5.6	6.3	5	3.2	2	1.2	15.1	17.4
Pl	64.7	54.9	65.6	52.4	45	25.5	14.3	7.3	48.3	46.3
Opx	19.5	25.1	15.4	17.6	10.1	-	-	-	18.8	15.8
Cpx	6.7	9.6	4.8	10.4	10.6	17	-	10	4	5.1
Ol	-	-	2.1	4.3	13.7	31.2	47.9	48.4	-	-
Qu	1	0.8	-	-	-	-	-	-	5.4	8.1
Il + Mt	3.1	4.1	5.4	7	12.9	16.3	17.7	20.8	6.7	6
Wo	-	-	-	-	-	1.6	15	8	-	-
C	-	-	-	-	-	-	-	-	-	-
An %	49.8	53.2	50.2	44.7	48	47.5	46.2	31.5	38.5	34.1
fsil %	39.5	35.9	47.4	53.4	50.5	56.7	60.5	60.7	56.4	59.5
Il/Il+Mt%	38.7	48.8	63	60	62	58.9	65.5	56.7	56.7	53.3

Early Anorthosite Suite (A_1): 1 - anorthosites; 2 - norite-anorthosites; 3 - leuconorites. Main Anorthosite Suite: 4 - anorthosites; 5 - gabbro-anorthosites; 6 - leucogabbro-norites. Subalkalic leucodolerites of Dake Suite (D_5): 7 - Zvisdal-Zaleskaja dake; 8 - Belokorovichskaja dake [from Bukharev, 1992]. Early Gabbroic Suite (G_3): 9 - leucogabbro-norites; 10 - gabbro-norites. Late Gabbroic Suite (G_4): 11 - leucogabbro-norites; 12 - olivine gabbro-norites; 13 - ore olivine gabbroes; 14 - olivine melagabbroes; 15 - pyroxenites; 16 - peridotites. Dake Suite (D_5): 17 - trachydiabases; 18 - trachyandesibasaltes. The average number of petrochemical ratios: f%=100*Fe/Fe+Mg; ti=100*TiO_2/Fe_2O_3+FeO. n - number of analyses. The norm have calculated by method of Nigli. The norm ratios: An%=100*An/An+Ab; fsil%=100*Fa/Fa+Fo=100*En/En+Fs.

Morisset CE:

Mineralization in iron – titanium oxide minerals and apatite of the Lac Mirepoix ore deposit, Lac St-Jean Anorthosite Complex (Québec, Canada)

Caroline-Emmanuelle Morisset
Département des Sciences de la Terre, Université du Québec à Montréal, C.P. 8888, Succursale Cenre-Ville, Montréal, PQ H3C 3P8 Canada, and
L.A. Géologie, Pétrologie, géochimie, Université de Liège, Bat. B-20, 4000 Liège, Belgique

The Lac Mirepoix mineralization is within the Lac St-Jean Anorthosite Complex of the Grenville Province, 250 km north of Québec City (Canada). The Lac St-Jean Anorthosite Complex (20 000 km^2) have been dated by U/Pb on zircon at 1150 Ma (Emslie and Hegner, 1993). In Canada, the last deformation associated with the Grenville Orogeny is dated at 1035 Ma, 80 Ma after emplacement of the Lac St-Jean Anorthosite (Emslie and Hegner, 1993).

This Fe –Ti oxide minerals and apatite mineralization is contained in a small layered body of about 4 km^2. The lather is composed, form bottom to top, of anorthosites, norites, oxides-norites, and gabbronorites. The horizons of anorthosite are poor in oxides and the proportions of the latter grow with the proportion of mafics minerals. Some nelsonitic (1/3 apatite and 2/3 oxide minerals) horizons, 10 to 15 cm thick, can be found in the oxides-norites layers. These types of rocks can be classified as oxides-apatite gabbronorite (OAGN) as described by Owens and Dymek (1992) in the Anorthosite of St-Urbain, Canada. Pure hemo-ilmenite discordant veins can be found in some parts of the studied area. Metamorphic minerals like amphibole and biotite are present and some very important deformation (e.g., gneissosity) can be seen.

Micro-probe analyses have shown that there is no cryptic layering in the body (no variation in the composition of minerals). Plagioclases are andesine (An_{42-49}) and orthopyroxenes are hypersthene (En_{46-50}). Clinopyroxene appears later in the evolution of the complex and the oxides present a degree of fractionation. At the base, hemo-ilmenite (Hem_{20-30}) is the only oxide mineral. Then, with appearance of the magnetite the proportion of hematite in hemo-ilmenite drops (Hem_{10}). In the upper part of the sequence, magnetite is more abundant and ilmenite has display rare hematite exsolutions.

The genesis of those mineralizations is still enigmatic. A formation by fractional crystallisation process in a small magma chamber is supported by the structure of the body and the layered character of the rocks. The sequence of oxide minerals and the variation in their composition is very similar to that observed in the Bjerkrem-Sogndal layered intrusion (Duchesne, 1972). Pure hemo-ilmenite concentrations can however not be explained by this phenomenon. Deformation and recrystallization have affected the paragenesis and the composition of the minerals. Geochemical modelling and reconstruction of the subsolidus evolution will try to account for the actual composition of the Fe-Ti oxide minerals and apatite. In an economic perspective, deformation, recrystallization, and fractional crystallisation have to be regard as natural purifying mechanisms of ilmenite and magnetite (Duchesne, personal communication). This understanding can be very important for the exploitation and could help to develop new models of exploration of iron and titanium deposits.

References

Duchesne, J.C., 1972. Iron-Titanium Oxide Minerals in the Bjerkrem-Sogndal Massif, South-western Norway. Journal of Petrology, 13-1, p.57-81.

Emslie, R;f. and Hegner,E., 1993. Reconnaissance isotopic geochemistry of anorthosite-mangerite-charnockite-granite (AMCG) complexes, Grenville Province, Canada. Chemical geology, 106, p. 279-298.

Owens, B.E. and Dymek, R.F., 1992. Fe-Ti-P rocks and massifs anorthosite: problems of interpretation illustrated from the Labrieville and St-Urbain plutons, Québec. Canadian Mineralogy, 30, p.163-190.

Nechaev S & Pastukhov V:

Links between the Proterozoic anorthosite-rapakivigranite plutons and ore-forming events in the Ukrainian Shield (ores of titanium, uranium, rare metal and gold)

Sergey Nechaev & Viktor Pastukhov
Ukrainian State Geological Research Institute, Geological Survey of Ukraine, Avtozavodskaya st. 78,UA-04114 Kiev, Ukraine. Ukrdgri@geologiya.com.ua

Introduction

Two large Proterozoic anorthosite-rapakivigranite plutons situated within the Ukrainian Shield (USh) belong to the Palaeoproterozoic Kirovograd orogen/Central Ukrainian fold belt. Extensive reserves of Ti ores and all economic occurrences of pegmatite are located within these plutons. Numerous deposits and prospects in adjoining plutons contain major reserves of U and Be ores, considerable resources of REE-Zr, Li and accompanying rare metal ores including gold. The Palaeoproterozoic granititic plutons that are widespread within the orogen are traditionally regarded as the principal ore-forming factor. However, analysis of the UShís tectonic development, together with spatial and age relationships between magmatism and postmagmatic ore mineralization reveal the leading role of plutons as an energy/temperature factor for economic ore formation.

Geological setting of anorthosite-rapakivigranite plutons of the USh.

The Korsun-Novomirgorod (KNP) and Korosten (KP) plutons, belonging to anorthosite-rapakivi granite suite, are situated in the central and northwestern parts of the Ush respectively. The KNP coincides with the central part of the Palaeoproterozoic Kirovograd orogen (KO). The latter separates the Podol microcontinent (foreland) to the west from the Dnieper cratonic domain (hinterland) to the east. The KP is located at the intersection of the KO and the back-arc thrust belt of the Osnitsk-Mikashevichi orogen (Fig. 1).

According to the most complete U-Pb isotopic data of the USh rocks (Stepanyuk, 2000; Shcherbak and Ponomarenko, 2000), the Archaean domains mentioned above consist of enderbite-gneisses (from more than 3.4 Ga up to 2.6 Ga in age) within the Podol domain and granite-greenstones (from 3.2 Ga up to 2.6 Ga in age) within the Dnieper domain. Borders between the Archaean domains and the KO are represented by the Odessa-Zhitomir thrust zone in the foreland and a system of nappes in hinterland. The two Archaean domains plunge towards each other and join in the central part of the KO, which, in accordance with seismic deep sounding, is to be regarded as the Transregional fault (Chekunov, 1992).

Thrust zones in the foreland and hinterland and corresponding areas contain BIF, ophiolitic mafic-ultramafic rocks and flysch assemblages forming complexes of intercontinental rift, oceanic crust and passive continental margins. The interior part of KO comprises calc-alkaline associations of island arc affinity. Basal sedimentary sequence in the eastern part of the orogen are represented by coarse terrigenous Au-U-bearing deposits which are also found on the surface of eroded granite-greenstone structures in the Dnieper craton (Bobrov and Guliy, 1999).

Isotopic ages of U-mineralization in conglomerate and sandstone at the base of the Palaeoproterozoic Krivoy Rog Supergroup fall in the range 2.6-2.45 Ga (Belevtsev, 1995) and 2.68-2.31 Ga (unpublished data). The Archaean ages are of detrital radioactive minerals

(erosion products). The Palaeoproterozoic ages correspond to the first phase of the Palaeoproterozoic granitoids and fall in the range 2.45-2.31 Ga (Stepaniuk, 2000; Shcherbak and Ponomarenko, 2000).

Formation of the KO was completed about 2 Ga ago by collision of an island arc with the Podol domain. This explains why the Palaeoproterozoic granitization is most abundant in the northeastern part of the domain and adjacent to orogenic areas. In contrast to the Podol domain, the Dnieper domain was not affected by this granitization. Rocks related to the deformed Archaean basement (oceanic crust, forearc and backarc basins, and shelf) were also emplaced by nappe style tectonics toward the inner parts of both domains. In the northwestern part of the KO fragments of volcanic belt (island arc) were thrust over shelf and flysch complexes.

The largest KP occupies an area of about 10000km2. Gabbro and anorthosite (labradorite-bearing) form the main body, and occur in windows as separate massives among rapakivi and rapakivi-like granites in the central and marginal parts of the pluton. All massives are characterized by zonal structures. Their roof and base are formed by marginal complexes of massive and layered gabbro, while the middle part is represented by central complexes of anorthositic gabbrol and anorthosite. The ovoid and non-ovoid rapakivi-like and micropegmatitic/granophyric granites are the main members of the granitoid part of the anorthosite-rapakivi suite, and occupy the upper part of the pluton or its granitoid roof, including remnants of the Palaeoproterozoic cover. Rapakivi granites typically cut across gabbro-anorthositic bodies. A younger dyke complex is represented by diabase, andesite- and diabase porphyry, subalkaline olivine gabbro, gabbromonzonite and monzonite which cut across all rocks of the pluton and its envelope.

The KNP occupies area about 5000km^2. The pluton comprises anorthositic gabbro massives with marginal and central complexes, and these massives belong to a single body that outcrops in windows among granites. The pre- dominating rocks are large ovoid rapakivi granites in the central part of the pluton, which become less ovoid in the peripheral parts. Syenitic granites are also present, whereas subodinate micropegmatitic rapakivi-like granite is only represented along the eastern contact of the pluton.

The KNP and related massives of palingenetic K-granite to the south occur like pearls on a thread along the Transregional fault. The latter is characterised by a decrease in rock density (Chekunov, 1992) including ones identified as belonging to the upper mantle, as well as a decrease in depth to the Moho (between 45 and 35 km only), and a sharp reduction in thickness of the basaltic layer (up to 2 km).

These features (location of the pluton location within a double-sided orogen and well zonal distribution of mineral deposits and prospects (Nechaev and Naumov, 1998; Nechaev and Pastukhov, 2000)) could be explained from the standpoint of B. Wernicke (1985) by postcollisional strain of the orogen owing to deconsolidation/density decrease of rocks in the axial zone of the orogen, and overthrust nappes both ìwingsî of the orogen onto the Archaean domains.

Origin of the anorthosite-rapakivigranite suite

According to petrogical studies (Tarasenko, 1987) the anorthosite-rapakivi granite suite formed as multiphase intrusions as aresult of the emplacement of subcrustal high alumina basaltic magma (phase I), followed by crustal granite magmatism (phase II). Thermobarometric studies suggest that the highest temperature of formation of ovoidal rapakivi granite was in the range 980-1170∞C (Belevtsev, 1995).

A sequence of emplacement of the main rocks units of the suite is the folloving (Dovbush and Skobelev,2000):

(1) Early anorthosite unit 1800-1790 Ma;
(2) Rapakivi granite unit 1771-1767 Ma;
(3) Gabbronorite-anorthosite unit (gabbronorite, anorthosite, gabbro, ultramafic and mafic dyke rocks) 1761-1754 Ma;

(4) Non-ovoid biotite subalkaline leucogranite unit 1752 Ma;
(5) Granite-porphyry and rhyolite unit 1745-1737 Ma.

Spatially and temporally related to both plutons are small intrusions/stocks of REE-Zr-bearing syenite (Nechaev and Krivdik, 1989) with ages (K-Ar method (amphibole)) in the range 1780 – 1770 +/-30 Ma (Nechaev and Boyko, 1988). The youngest is a veined granite (1685+/-30 Ma; (biotite, microcline)) which cuts across rapakivi granite.

Gabbro of the marginal complex in the KP was interpreted by V.G. Pastukhov as a chilled facies of an anorthosite body; the chemical composition of gabbro is close to a moderately-subalkalian Al-basalt of island arc or active continental margin affinity. According to their chemical compositions, gabbro-anorthosite and anorthosite are similar to leucocratic Al-diorite and have a similar content of REE, compatible and incompatible elements to gabbros of the marginal complex. The coeval development of anorthosite and rapakivi, as well as their petrological peculiarities, are evidence of their comagmatic origin. The anorthosite-rapakivi granite suite forms a single magmatic assemblage, which is the plutonic equivalent of the basalt-andesite-liparite series (Pastukhov and Khvorova, 1994).

Sm-Nd isochrons obtained for the gabbronorite-anorthosite unit (Dovbush and Skobelev, 2000) give a calculated age of 1750 Ma, in good agreement with U-Pb isotopic ages of zircon and baddeleyite in the same samples. However, the value of eNd is negative (-0.8), and the same value of eNd has been calculated for anorthosite belonging to the early unit. The eNd for the rapakivi granites is below -1.8. Both mafic and felsic units therefore could not be derived directly from depleted mantle. They are most likely derivatives of partial melting of the lower crust and/or the upper mantle, enriched by oceanic crustal material due to previous subduction. Melting of high-alumina basalt could produce the initial magmas for mafic rocks belonging to the pluton. The rapakivi granites cannot be derived from the parental magma, as their isotopic signatures differ from those of the mafic rocks. It seems likely that anatexis of the upper crustal rocks stimulated rapakivi granite formation, and potentially ore-bearing peculiarities of syenite, related to anorthosite. Isotopeic data, supported by geophysical deep sounding, turn attention to the probability of the basaltic layer as a principal factor for formation of anorthosite and lateral tectonic transference within the orogen.

As has been noted by Dovbush and Skobelev (2000), K-Ar data on biotite and amphibole from rocks of the Korosten suite are numerous, and K-Ar ages of 1700-1800 Ma correspond to the same range of ages that have been obtained by other isotopic methods. This is important in connection with analysis of links between plutons and ore-forming events.

The spatial and age relationships between plutons and ore formation

Deposits of pegmatite, ores of Ti, REE and Zr are all closely related to the anorthosite-rapakivi granite plutons. Pegmatites contain quartz, topaz, beryl, phenakite, fluorite and Ta-Nb minerals. Only the first three are, however, economically important. REE-Zr and Ti-ores are located within REE-Zr-bearing syenite (which belongs to the gabbro-syenite intrusive complex; Nechaev and Krivdik, 1989), and Ti-bearing gabbro-anorthosite massives respectively. Deposits and prospects of these ores are epigenetic in character; this is evident from their coincidence with faults, in particular related to the Central fault of the northwest trend (Metalidi and Nechaev, 1983).

Rare earth element-zirconium ores

Deposit of these ores are located in the northwestern flank of the Central fault. Ore-bearing syenite is characterized by high concentrations of Zr (0.2-0.3%), and separate ore bodies contain more than 6% ZrO2. The zircon crystals have complex structures, typically including cores with an age of 1.79Ga surrounded by a new generation of overgrowth reflecting overprint of the ore-forming episode at 1.73-1.72 Ga (Nechaev et al., 1985). REE minerals are

represented by britholite, orthite and bastnaesite (accompanied by Y-fluorite) and there are two obvious generations of REE-mineralization. Similar ore prospects are located in the southeastern corner of the KNP.

Possible precursors of economic REE-Zr ores were preexisting concentrations of monazite and zircon within the Podol domain, as well as in the Archaean enderbite-gneiss basement. Such mineral concentrations in rocks of the Podol domain are represented by a number of small segregations, mainly of monazite. Monazite from different segregations have been U-Pb dated (207Pb/206Pb age) as 3.32, 2.52 and 2.29 Ga (Table 1).

Table 1. Results of the monazite isotope investigation, performed by G.D. Elisseyeva at the Department of Isotope Geochemistry, Institute of Geochemistry, Mineralogy and Ore Formation, Ukrainian Academy of Science

Probe number	Content, %			Pb- isotope content, %				Ages, Ma			
	U	Th	Pb	204Pb	206Pb	207Pb	208Pb	207Pb/206Pb	207Pb/235U	206Pb/238U	208Pb/232Th
2	0.041	9.53	0.96	<0.01	1.62	0.43	97.94	3320	2920	2350	2130
4	0.130	10.80	0.98	0.045	5.62	1.47	92.87	2520	2440	2340	1810
1	0.065	8.99	1.03	<0.01	2.74	0.39	96.86	2290	2460	2600	2380

Titanium ores

These ores are located directly within the initial Ti-bearing anorthosite massives 1.8 Ga in age, and Ti-deposits are coincident with the Central fault (Fig.1).

The principal Ti ore-bearing complexes 1.75 Ga in age are metasomatic in origin. They consist of monzonite-norite, monzonite-peridotite, and ìoligoclasite-andesiniteî (Tarasenko, 1987; 1990; 1992). They were formed as a result of the contact influence of granite on anorthosite during phase II (1.77Ga). These complexes are located within anorthosite massifs affected by extensive cataclasis and K- feldspatization, and have a zoned metasomatic structure in which ore- and rock-forming components have been redistributed. Ti, Fe and P were leached from the internal portions of metasomatic columns and deposited at the front of the columns, resulting in ore-mineralisation (i.e. not initially magmatic impregnation). The ìoligoclasite-andesiniteî complex represents essential chemical and mineral transformation of initial anorthosite, and zones of basification related to this complex include ilmenite ore containing up to 20-35% TiO_2.

According to V.S. Tarasenko (1987), zonation of Ti-bearing complexes is determined by their temperature of formation that depends on the distance from the rapakivi granite contact (Fig 2). The monzonite-norite complex represents the highest temperature (830∞C) located in the peripheral part of anorthosite massives near the contact with rapakivi granite, whereas monzonite-peridotite formed at 750-700∞C, some distance from the rapakivi granite. The ìoligoclasite-andesiniteî complex, remote from the rapakivi granite, was formed at 500-450∞C, and ore minerals are associated with hornblende, actinolite-tremolite, biotite, chlorite, calcite and quartz. PT-conditions of formation of these minerals formation to the border between epidote-amphibolite and greenschist facies.

The relationships between epigenetic Ti-ores on the one hand, and anorthsite and rapakivi granite on the other, imply that anorthosite provides the source of Ti and the rapakivi granite intrusion appears to be responsible for the metasomatism which caused redistribution and

concentration of Ti. K- metasomatism is prevalent at the high temperature conditions whereas Na-metasomatism is significant at lower temperatures. The richest Ti-ore is related to the ìoligiclasite-andesiniteî complex. Compared with the Ti-ores of monzonite-norite and monzonite-peridotite complexes, a high degree of oxidization and leucoxenisation of ilmenite is characteristic for the ìoligoclasite-andesiniteî complex. The presence of hydrous silicates indicates a transition to true hydrothermal processes.

Epigenetic Ti-ores within anorthosite massives are only one phase in a sequence of ore formation episodes which spread outside the plutons. The first of these concerns U-ores.

Uranium ores

Deposits of U-ores are widespread within the KO, and have been described in detail by Belevtsev (1995). These ores are represented by metasomatic U-K (K-feldspar) and hydrothermal fissure-vein types which are both subeconomic. They have an age of ca. 2Ga (2.19-1.93) and are located in the Palaeoproterozoic metamorphic rocks. A separate metasomatic U-Na (albitite) type (ca. 1.8Ga in age; U-Pb isochron age) occurs in the same rocks and in palingenetic K-granite massives. The latter, which adjoin the KNP to the south, have been U-Pb dated between 2.07 and 2.01Ga (Belevtsev, 1995). The U-Na ore type is also developed in the Palaeoproterozoic ferrigenous rocks of the Krivoy Rog supergroup

It is possible that the first two types of U-ores could be related to the K-granite whereas connection between the U-Na ore type and K- granite is unlikely in view of the fact that the time gap between ore- and granite-formation is more than 200Ma. Another distinction is that the U-K ore type contains relatively high concentrations of REE- and Th-bearing minerals, as well as molybdenite; these are absent in the U-Na ore type.

According to Belevtsev (1995), mineral assemblages of U-bearing albitite are represented by the following: moderate temperature epidote-chlorite (up to 350∞C) and riebeckite-aegirine (350-400∞C); high temperature garnet-actinolite (420-480∞C), garnet-diopside (450-480∞C) and garnet-wollastonite (ca. 500-550∞C). It is emphasized that metasomatic columns of high temperature albitite are only developed near the contact with the pluton. That is why, in our opinion, the so called high temperature albitite is actually calcareous skarn that has suffered Na-metasomatism. Two stages of albitisation of the of the U-Na type deposits are separated by a cataclastic (Belevtsev, 1995).

High temperature U-bearing albitite (420-550∞C) is close to the temperature formation of ìoligoclasite-andesiniteî Ti-ore-bearing complexes (450-500∞C) and the ìalbitite haloî of the pluton appears to be a continuation of Na-metasomatism within the pluton itself. The most the U-Na ore type formed at 250-300∞C.

A geochemical feature that links the Ti- and U-ores is the presence of accompanying elements such as P, Zr, V and Sc. Primary ilmenite in anorthosite contains an average contents of 750 ppm V and 56.5 ppm Sc, whereas ilmenite in Ti-ores contains average contents of 1550 ppm and 74 ppm respectively (Borisenko et al., 1980). The early mineral paragenesis of U-bearing albitite includes apatite, malaconite and U-titanates (brannerite and davidite). Andradite from garnet-diopside albitite contains up to 3% TiO2 as well as about 1% V, and this albitite also contains tortweitite with > 40% Sc2O3 and 7.6% ZrO2. The complex Sc-V-U ore of the Zheltaya Rechka deposit is related to Na-metasomatism of ferruginous rocks of the Krivoy Rog supergroup where aegirine-acmite contains 0.08-0.1% Sc and 2-9% V (Belevtsev, 1995). The U-Na ore type is spatially related to rare metal and gold deposits and prospects.

Rare metal ores

Deposits of rare metal ores situated in the framework of the plutons usually are located within microcline-albite pegmatite which predate the rare metal mineralization. In the southeastern part of the KP such a pegmatite is associated with magnesian skarn, both of which have ages near to the K-granite, i.e. ca. 2Ga. However, ore mineralization of pegmatite and skarn is

epigenetic in character: Ta-Nb minerals and cassiterite are concentrated in zones of greisenization (1.77Ga), and segregations of scheelite are located in zones of calcareous skarn (1.79 Ga) that developed after retrograde metamorphism (Table 2). Both the superimposed types of mineralization are accompanied by contrasting Be geochemical anomalies which may contain beryl or phenacite.

Table 2. K-Ar ages of rocks from the frame and contact zones of plutons (published author's data)

The setting	Rock	Mineral	Ages (Ma)
Southeastern frame of the KP	Pegmatite	Muscovite	2000+/-35
	Pegmatite Greisenizated hosting Ta-Nb and Sn mineralization	Muscovite	1770+/-30
	Skarn magnesian suffered by retograde metamorphism hosting accessory scheelite	Phlogopite	1930+/-35
	Skarn apomagnesian calcareous scheelite-bearing	Phlogopite	1790+/-30
Western frame of the KNP	Skarn apomagnesian calcareous scheelite-bearing (BaO content from 7.07 up to 17.62%)	Ba-phlogopite	1780+/-35
	Metasomatite tourmaline-biotite-cordierite	Biotite	1905+/-35
	Pegmatite brecciated and replased with Li minerals	Muscovite	1800+/-35
	Gneiss hosting scheelite- bearing tactite and Au-Bi-As mineralization	Biotite	1670+/-35
Western endocontact of the KNP	Granite vein hosting	Biotite	1685+/-35
	Au-Bi-As-Quartz mineralization and cut across rapakivi	Microcline	1685+/-35
Southern flank of the Zhitomir Odessa fault	Apoamphibolit gneiss/	Hornblende	1960+/-45
	Skarn suffered by retrograde biotite -diaphtorite metamorphism	Hornblende	1690+/-40
		Biotite	1670+/-35

The spatial association of ore-bearing skarns and pegmatites probably has a genetic significance because titanite + apatite assemblages typical for skarns could be a precursor for ore-forming elements: titanite contains: 500-983ppm Nb, 21-116ppm Ta, 50-61ppm Sn, 366-386ppm Y; and apatite contains 300-545ppm Ce, 175-231ppm La, and 107-169ppm Y.

Deposits of economic rare metal ores are spatially related to U-Na ore type deposits in the southwestern part of the KNP. Rare metal ores are superimposed onto extensively brecciated microcline-albite pegmatite, and considered to be similar to rare metal pegmatites corresponding to replacement dykes in which Li is the principal ore component (Nechaev et al., 1991). Li-ore deposits are characterized by the predominance of petalite over spodumene and other Li minerals, and average concentrations of Li_2O in ore is ca. 1.5%.

The complexity of these deposits is caused by extensive metasomatic transformations, not only in the initial pegmatite (ca. 2.3Ga in age; Voznyak et al., 1996), but also in the host rocks which consist of high-alumina gneiss. Along the latter contact pegmatite is replaced by albite and contains Ta-Nb minerals, chrysoberyl, uraninite, graphite, cassiterite and ilmenite; both the latter contain up to 2% Ta. Microcline-tourmaline-biotite-cordierite assemblages that are enriched apatite developed after the gneisses. There are subeconomic concentrations of Li, Rb and Cs in biotite, cordierite and microcline (Voznyak et al., 2000). The K-Ar age of gneissic metasomatite is ca. 1.9 Ga (Table 2). The first stage of rare metal mineralization was completed by regressive metasomatism involving the replacement of cordierite by a serizite-clorite assemblage.

The following stage at ca. 1.8 Ga, which related economic Li ore (quartz-albite-petalite assemblage) displayed as synchronous to the KNP emplacement, what was the cause of high temperature Li metasomatism: fine-grained petalite, typical of ore deposits, was formed by solutions at T<=680∞C (Voznyak et al., 2000). Rutile inclusions in quartz (in the form of a

sagenitic lattice) testify to initially high concentrations of Ti in hydrothermal solution (Voznyak et al., 2000).

The spatial connection between Li ores and tourmaline-bearing rocks as well as scheelite-bearing tactites and skarns allows comparison with deposits in the USA. Considerable resources of Li, B and W are present in the Neogene deposits of the Cordilleras (California, Nevada) as well as in brines and salt lakes (Silver Peak, Searls and others) (Kozlovskiy, 1989). A similar precursor is possible within the Palaeoproterozoic epicontinental depressions in the central part of the USh.

The Perga rare metal deposit, located in the northwestern part of the KP, contains economic Be-mineralization (genthelvite, phenacite). Ore formation in the period 1.74-1.62Ga (Shcherbak, 1978) is related to K-Na metasomatism with Li-F specialization (Metalidi and Nechaev, 1983; Buchinskaya and Nechaev, 1990). The Perga deposit is similar to rare metal deposits in the SW part of the KNP where there are concentrations of Li, Be, Ta, N b, Sn, W and superimposed sulphide mineralization associated with native gold (Nechaev, 1990; 1992). Unique ore combinations within the Perga area are supplemented by epigenetic Cu-Co-Ni mineralization (chalcopyrite, carrollite, pentlandite and violarite, all rich in Co), and coincided with mafic intrusions ca.1.96 Ga related to thermal influenceof the Korosten pluton.

Gold ores

The main deposits and prospects of Au ores known at present are situated in the southern part of the KNP and in the western overthrust zone (the southern flank of the Zhitomir-Odessa fault) of the Palaeoproterozoic orogeny. All of them are associated with U and rare metals as well tourmaline-bearing fields, and commonly contain scheelite.

Epigenetic Au ores formed after extensive deformation, including the mylonitization of the country rocks (amphibolite, gneiss, migmatite, granite, skarn, aplite and pegmatite). Au-bearing prospects are located within linear zones of brittle deformation. Pre-mineralisation alteration of the host rocks are involve metasomatism with different contents of hornblende, garnet, cordierite, biotite, plagioclase, tourmaline, sillimanite, quartz and magnetite which is replaced by pyrrhotite. The interior parts of linear zones are effected by oligoclase-quartz-biotite metasomatism and contain ore mineral assemblages with native gold and tellurides (far from the KNP) and maldonite without tellurides (close to the pluton).

Alterations of host rocks by hydrothermal ore-bearing solutions is displayed by minor albitization of plagioclase and formation of K-feldspar, carbonatesand mixed-layer silicates of illite-smectite type. According to Mudrovskaya (2000) transformation of hexapyrrot□i□n□e□ to clinopyrrotine was caused by hydrothermal solutions, and Au transference by hydrosulfide complexes became permissible. Liberation of Fe^{2+} during replacement of hexapyrrotine by clinopyrrotine led to destruction of Au-hydrosulphide complexes and deposition of late pyrite together with native gold. The upper temperature of Au-bearing assemblage formation corresponds to the transformation of hexapyrrotine to clinopyrrotine (273°C) and the lower temperature limit is fixed by the formation of mixed-layer silicates (<178°C).

The thermal parameters of Au-ore formation are similar to post-albitite assemblages of U-Na ore deposits located close to the KNP. These assemblages formed under the influence of hydrothermal solutions at temperatures lower than 300°C, which are characterized by high activity of K and CO_2 compared with U-bearing albitite (Belevtsev, 1995). The Au ore-forming processes therefore appear to be a continuation of the U-Na ore-forming event. However, Au- and U-ores are sharply divided spatially and geochemical antagonism between Au and U within united ore- bearing areas, ore fields and even deposits can be explained by the transference of Au as hydrosulphide complexes. The formation of Au-ores after U-ores agrees with the occurrence of Au-bearing assemblages accompanied by adularia-chlorite metasomatism which cuts across U-bearing albitite (Prokhorov et al., 1994).

The fall in temperature and development of proper hydrothermal processes was associated with an increase in S-activity, resulting in deposition of Fe, As, Sn, Bi, Cu, Zn, Pb sulphides. Native gold and bismuth accompany rare metal ores. Proceeding from the temperature of Bi crystallization (ca. 270°C) and a calculated estimate of the stannite-sphalerite paragenesis (213-294°C; Nechaev and Bondarenko, 1993) the beginning of native gold deposition in rare metal ores took place at temperature no more than 300°C. However, according to Yatsenko and Gurskiy (1998) Au-bearing mineral assemblages (T 550-250°) developed after tourmaline- and scheelite-quartz (T 420-330°) in the KNP region. This temperature inversion probably reflects the influence of the pluton. Au dispersed in Fe and As sulfides (T 550-380°) subsequently changes to an assemblages of native gold + chalcopyrite (T 450-370°C) and then to native gold + bismuth. (T ca. 270°C). This suggesats that Au mineralization + tellurides located far from the KNP appear to be a continuation of the higher temperature Au-bearing assemblages located close to the pluton.

Waning of magmatic activity in the KNP is fixed by granite veins at 1685+/-35Ma which cut across rapakivi granite, and also by nearly synchronous retrograde metamorphism (1670+/-30Ma) of gneiss surrounding the pluton (Table 2). Despite the fact that direct data for the age of Au ores is lacking, the latter can not be older than 1685+/-35Ma because quartz veinlets including Au-Bi-As mineralization occur in the granite veins. In Au deposits distant from the KNP to the southwest, and situated in rocks with an age og ca. 2Ga (amphibolite, aplite, pegmatite, gneiss, migmatite), retrograde metamorphism was displayed between 1.69 and 1.67Ga (Table 2), and the K-Ar age of biotite from Au-bearing oligoclase-quartz metasomatite is 1615+/-30Ma. The timing of events related to economic Au-mineralization indicates that the KNP was a significant thermal factor for ore formation.

Untraditional occurrences of Au related to REE-Zr-bearing syenite and Nb-Sn-bearing granite also occur in the northwestern part of the KP within the Perga rare metal ore field (Nechaev et al., 1983,; 1986). Both syenite and granite were drilled at depths of more than 1500m and the anomalous Au content in these rocks were established. The Au content in syenite varies between 0.01-0.1 g/ton with local concentrations up to 1.5g/ton. Native gold was not discovered as a result of mineralogical studies. However, heavy liquid mineral separation from hand specimens of syenite produced an amalgam of Au3Hg; elevated Au contents have also been found in biotite and amphibole. The gold is therfore believed to occur in a very fine grained state. The Au abundance in granite is similar to syenite, with a maximum Au content of 3.45g/ton per 1m of drill sample.

Precious metal mineralization (native silver and electrum) was also discovered in Be-bearing K-Na metasomatites of the Perga deposit, and in hand specimen impregnated by sulphides the Ag content reaches 3000g/ton and Au is up to 2 g/ton. Ore mineralization of the Perga ore field is considered to belong to a rare metal-polymetallic evolution series (Nechaev, 1990) in which the successive stages are as follows:

(1) Be-bearing K-Na metasomatite hostig zircon, magnetite, columbite and cassiterite;
(2) Quartz-muscovite greisens hosting cassiterite, ilmenorutile, wolframite and minor native indium;
(3) quartz veins and veinlets accompanied by molybdenite, chalcopyrite, wittichenite, galena, sphalerite and minerals of the wurtzite-greenockite series;
(4) hypogene enrichment of betekhtinite, bornite, chalcosite, hematite, native silver and electrum.

A geochemical peculiarity of the Perga deposit ore mineralization is the absence of arsenic. The Au mineralization could be a result of regressive hydrothermal processes caused by the influence of the KP (1.8-1.7Ga) because syenite, granite and Be-bearing metasomatism are synchronous and spatially related to the pluton.

The precursors of gold ores could be Au-bearing greenstone complexes of the Archaean basemet and potentially Au-bearing deposits within the Palaeoproterzoic epicratonic depression. Such intermediate collectors of Au have been established in the Krivoy Rog supergroup (Nechaev and Pastukhov, 2000) and in flysch-like sequences on both sides of the KNP (Kobzar, 1981), where Au-bearing prospects have recently been discovered. The sequence is represented by layering/sedimentation of metapelite and metamarl (biotite plagiogneiss and diopside-plagioclase taktite respectively), which initially were enriched in Au and W. The spatial relationship between the pluton and epigenetic native gold, as well as scheelite mineralization, is best explained by hydrothermal remobilization of these metals and deposition in minerals within fault zones. The Au-bearing syenite of the Perga ore field is anatectic in origin proceeding from the increased in Sn, W and Mo contents.

Discussion and conclusions

There are clear links between the anorthosite-rapakivi granite suite and ore formation within the central part of the USh. There appears to be a bilateral symmetry between ore mineral zonation in the Kirovograd orogen related to the Korsun-Novomirgorod anorthosite-rapakivi granite pluton. Formation of the latter completed the orogeny, and all the ore-types related to the pluton are post-orogenic. However, the early pegmatites (ca.2.3Ga) as well as K-Na metasomatism of the Palaeoproterozoic sequence, preceded the pluton. Hydrothermal U-mineralization of vein-fissure type (generally subeconomic) was deposited some time later (ca.2.2Ga).

The next phase of orogeny was displayed by extensive granitization and formation of anatectic K-granites (2.08-2.02 Ga) as well as K- and Mg- metasomatites (2.02-1.95 Ga) represented by microclinite, magnesian skarn, as well as cordierite- and tourmaline-bearing rocks. These phenomena were accompanied by remobilization of ore-forming elements to produce largely subeconomic deposits. As likely precursors were the Palaeoproterozoic rocks (including stratified horizons) comparatively enriched in U, Au, W, Mo, B and rare alkali elements as well as the Archaean basement rocks hosting REE, Zr, Th and Au mineralization. Sopme 200 Ma before the pluton formation, rocks within the orogen were retrograded to greenschist facies conditions.

The anorthosite-rapakivi granite suite formed as multiphase intrusions with emplacement of subcrustal high alumina basaltic magma during phase I (1.8 Ga), and subsequently phase II (1.77 Ga) involving crustal granite magmatism. The lower-crustal rocks of the Archaean basement may have caused contamination of the basaltic magma. The first phase resulted in large anorthosite massives and small syenite intrusions that were enriched in Ti (P, V, Sc) and REE, Zr, Nb respectively. The second phase represented by rapakivi-granite complex is enriched in rare metals and contains pegmatites with Be, Li, Ta and Nb. Mineralization. Emplacement of anorthosite caused Ca-Na metasomatism (1.8 Ga), the effect of which extended far from the massive anorthosite and caused formation of:

(1) Rare metal ore of the main quartz-albite-petalite type (T<680°C) located in the pluton contact;
(2) Scheelite-bearing calcareous skarn (T 550-420°C) and accompanying quartz-plagioclase veinlets located near the pluton;
(3) U-bearing albitite of the first generation enriched in Ti, V, Sc (±P, Zr) are superimposed onto skarn as well as onto ferrigenous rocks situated far from the pluton (T 300-250°C). Emplacement of rapakivi-granite (1.77 Ga) in initially Ti-bearing anorthosite accompanied by K-metasomatism (T 830-700°C) and related Ti concentrations up to ore level, whereas Na-metasomatism that took place at 500-450°C resulted in the formation of Ti-rich ores.

In Au-bearing prospects (less than 1.68 Ga in age) near the pluton, the first is Au dispersed within Fe and As sulphides (T up to 550°C), and the bulk of native gold is accompanied by

maldonite as well as native bismuth and was deposited at <270°C. Distant from the pluton native gold associated with Au- and Bi-tellurides were deposited (ca.1.62Ga) at between 270° and 180°C; this appears to be a continuation of the earlier Au-bearing assemblages. These events can be summarise as follows:

(1) 1.8 Ga, rare metal – uranium
(2) After 1.77 Ga, titanium (REE - Zr) - uranium – gold

Potentially ore-bearing mineral complexes formed before emplacement of the pluton. However, the spatial and age relationships between pluton and ore formation in surrounding rocks was not restricted to thermal energy activity for the regeneration of ores of economic grade. It may be presumed that Ti, V and Sc sources belonging to the in U-Na ore type were hydrothermal solutions related to the pluton paragenesis.

Thermal influence of the pluton determines the local zonal disribution of ore mineralization types. However, this zonation inherits an earlier regional one. The mineral-chemical ore types were established in those geological settings where their corresponding precursors were present. The most distinct dependence of this kind is displayed within the pluton itself, where Ti ores are located within Ti-bearing anorthosite massives and REE-Zr ores within syenite. In the plutonic framework, regeneration processes led to formation of contrasting ores of U (+/- Sc, V), including rare metals and gold.

References

Belevtsev, Ya. N.(chief editor), 1995: Genetic types and regularities of location uranium ore deposits in Ukraine. Naukova Dumka Press, Kiev, 396 p. (in Russian)

Bobrov,A.B., and Guliy,V.N., 1999: Auriferous conglomerates of terrigenous formation, Verkhovtsevskaya structure in the Precambrian, Ukrainian Shield. Precambrian gold in the Fennoscandian and Ukrainian Shields and related areas, Goldí99 Trondheim. Abstr. Vol., edited by N.J.Cook and K.Sundblad, 44-45.

Borisenko,L.F., Tarasenko,V.S., and Proskurin,G.P., 1980: Ore-bearing gabbroids of the Korosten pluton. Geologiya Rudnykh Mestorozhdeniy,no.6, 27-36. (in Russian)

Buchinskaya,K.M., and Nechaev,S.V., 1990: On the Perga granites problem. Mineralogicheskiy Zhurnal,no.3, 22-32. (in Russian).

Chekunov,A.V.(chief editor), 1992. Scheme of the deep lithosphere structure in the southwestern part of the East European Platform, scale 1:1 000 000. Goskomgeologiya Ukrainy, Kiev. (in Russian)

Dovbush,T.I., and Skobelev,V.M., 2000: Some remarks on the origin of the Korosten anorthosite-rapakivigranite complex as based on isotope data. Geophys. Journ., 22, no.4,84-85.

Kobzar,V.N., 1981:The Early Proterozoic sedimentation and metallogenic questions of the Ukrainian Shield central part. Naukova Dumka Press, Kiev, 104p. (in Russian)

Kozlovskiy, E.A.(chief editor), 1989: Mining Encyklopaedy, United States of America.Sovetskaya Encyklopaediya Press, Moscow, Vol.4, 580-614. (in Russian)

Metalidi,S.V., and Nechaev,S.V., 1983: The Sushchany-Perga zone: geology, mineralogy ore potential. Naukova Dumka Press, Kiev,136p. (in Russian)

Mudrovskaya,I.V., 2000: The mineralogical-genetic model of gold mineralization in the Savran-Sinitsovka ore zone (Ukrainian Shield). Thesis for a candidateís geol. sci. degree, Lviv State University, 23 p. (in Ukrainian)

Nechaev,S.V., 1990: Evolution of ore formation processes in the Ukrainian Shield structures.Geologicheskiy Zhurnal, no.2, 68-80. (in Russian)

Nechaev,S.V., 1992: Some peculiarities of gold and silver occurrences in the western part of the Ukrainian Shield. Geologicheskiy Zhurnal,no.4, 79-88. (in Russian)

Nechaev,S.V., Semka,V.A., Shirinbekov., and Chebotarev,V.A., 1983: The first find of native silver in the Ukrainian Shield. Doklady Akademii Nauk SSSR, v.270,no.2, 418-420. (in Russian)

Nechaev, S.V., Bondarenko,S.N., and Buchinskaya,K.M., 1986: Mineral state of gold and silver in intrusive syenite and metasomatite of the Ukrainian Shield. Doklady Akademii Nauk SSSR, v.289, no.6, 1483-1487. (in Russian)

Nechaev, S.V., and Boyko, A.K., 1988: Indication of the Proterozoic ore mineralization stages in the Ukrainian Shield. Visnyk Akademii Nauk Ukraine, no.5, 40-46. (in Ukrainian)

Nechaev,S.V., Krivdik,S.G., Krochuk,V.M., and Mitskevich,N.Yu., 1985: Zircon from syenite of the Yastrebets massif(Ukrainian Shield) ñ indicator of their crystallization conditions. Mineralogicheskiy Zhurnal,no.3, 42-56. (in Russian)

Nechaev,S.V., and Krivdik,S.G., 1989: Geological regularities in distribution of alkaline rocks in the Ukrainian Shield. Geologicheskiy Zhurnal,no.3,,113-120. (in Russian)

Nechaev,S.V., and Bondarenko,S.N, 1993: New ore minerals of the Ukrainian Shield. Mineralogicheskiy Zhurnal,no.4, 17-28. (in Russian)

Nechaev,S.V., Makivchuk,O.F., Belykh,N.A., Ivanov,B.N., Kuzmenko,A.V., and Prytkov,F.Ya., 1991: New rare metal district of the Ukrainian Shield. Geologicheskiy Zhurnal, no.4,119-123. (in Russian)

Nechaev,S.V., and Naumov,G.B., 1998: Zonation in ditribution of mineral deposits and occurrences on the Ukrainian Shield: modern pattern and paleotectonic reconstructions. Geology of Ore Deposits, v.40, no.2, 109-120.

Nechaev,S.V., and Pastukhov,V.G., 2000: Archaean and Proterozoic metallogeny of the Ukrainian Shield: the geodynamic aspect evolution. Research report 2nd GEODE- Fennoscandian Shield field workshop on Palaeoproterozoic and Archaean greenstone belts and VMS districts in the Fennoscandian shield, Gallivare-Kiruna, Sweden. Abstr. Vol., edited by P.Weihed and O.Martinsson, CTMG Lulea Univers. Technol., 29-31.

Pastukhov,V.G., and Khvorova,G.P., 1994:Paleogeodynamic of the Ukrainian Shield. In: Geological mapping of the Early Precambrian complexes, edited by N.V.Mezhelovskiy and G.S.Gusev. Geokart, Moscow, 318-373. (in Russian)

Prokhorov,K.V., Glagolev,A.A., and Kuznetsov,A.V.,1994: Gold-bearing metasomatites of the Yurievsk ore prospect in the Ukrainian Shield central part. Otechestvennaya Geologiya,no.6,17-25. (in Russian)

Shcherbak,N.P. (chief editor), 1978: Catalog of the isotope data. Naukova Dumka Press, Kiev, 223 p.

Shcherbak,N.P., and Ponomarenko,A.N., 2000: Age sequence of the volcanism and granitoid magmatism processes of the Ukrainian Shield. Mineralogicheskiy Zhurnal, no. 2/3,12-24. (in Russian)

Stepanyuk,L.M., 2000: Geochronology of the Precambrian of western part of the Ukrainian Shield (Archaean-Palaeoproterozoic). Thesis for a doctorís geol.sci. degree, Institute of Geochem., Mineral. and Ore Form., NAS of Ukraine, Kiev, 35 p. (in Ukrainian and Russian)

Tarasenko,V.S., 1987: Petrology of anorthosites of the Ukrainian Shield and geological-genetic model of phosphate-titanium ore formation. Geologicheskiy Zhurnal, no.4, 43-52. (in Russian)

Tarasenko,V.S.,1990: Rich titanium ores in gabbro-anorthosite massives of the Ukrainian Shield. Izvestiya Akademii Nauk SSSR, geol. ser., no. 8, 35-44. (in Russian)

Tarasenko,V.S., 1992: Mineral-raw material basis of titanium ores in Ukraine. Geologicheskiy Zhurnal, no.5, 92-103. (in Russian)

Voznyak,D.K., Pavlishin,V..I., Bugaenko,V.N., and Galaburda,Yu.A., 1996: The features, genetic and geochronologic sense of radiogenic halos in minerals of the Polokhov deposit (the Ukrainian Shield). Mineralogicheskiy Zhurnal, no.5, 3-17. (in Russian)

Voznyak,D.K., Bugaenko,V.N., Galaburda,Yu.A., Melnikov,V.S., Pavlishin,V.I., Bondarenko,S.N., and Semka,V.A., 2000: Peculiarities of the mineral composition and conditions of formation of rare-metal pegmatites in the western part of the Kirovograd block (the Ukrainian Shield). Mineralogicheskiy Zhurnal, no.1, 21-41. (in Ukrainian)

Wernicke,B., 1985: Uniform ñ sense normal simple shear of the continental lithosphere. Canad.J.Earth.Sci., v.22, 108-125.

Yatsenko,G.M., and Gurskiy,D.S.(chief editors), 1998: Gold deposits in the Precambrian gneiss complexes of the Ukrainian Shield. Geoinform Press, Kiev,256 p. (in Russian)

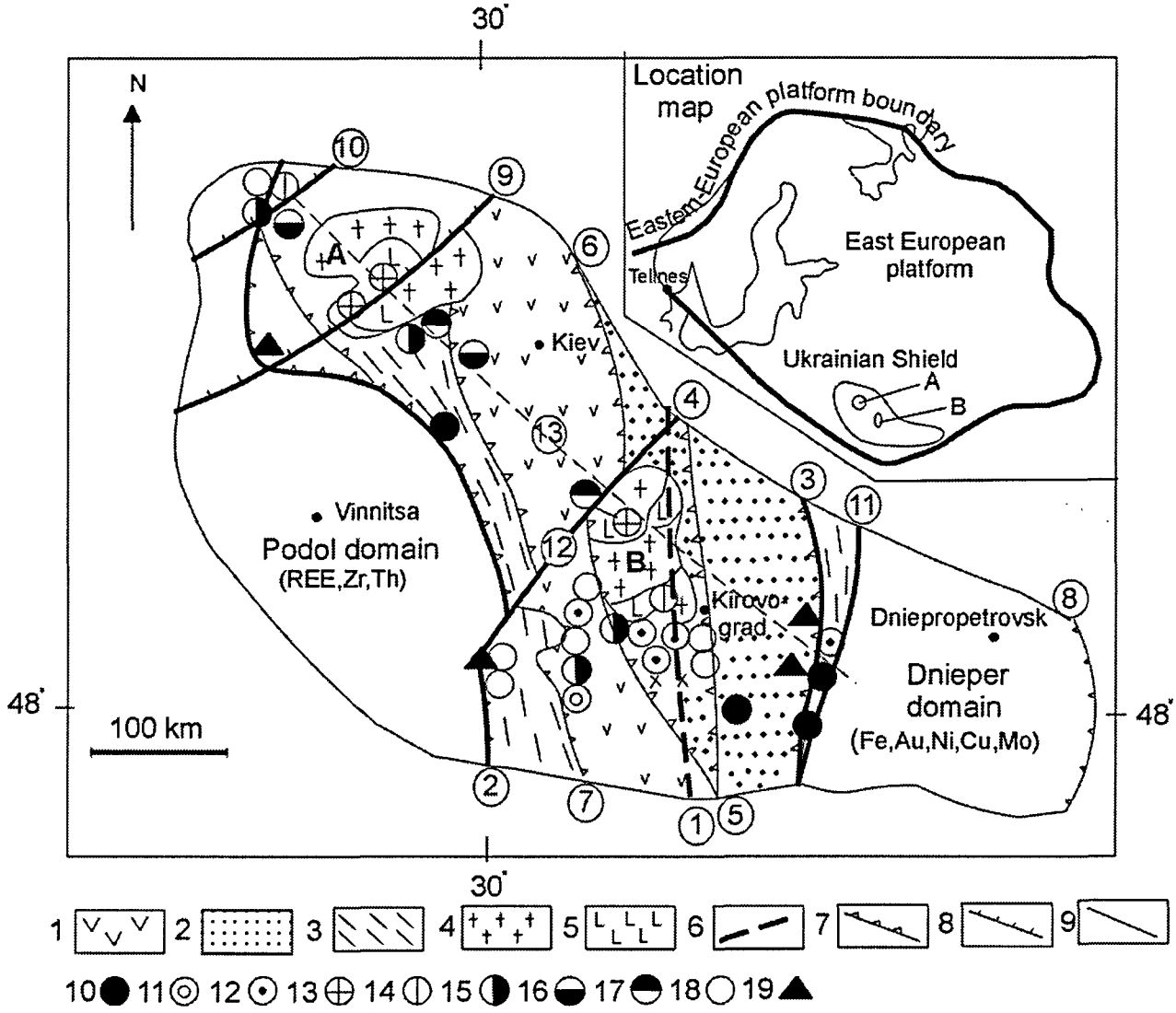

Fig.1 Tectonical division of Ukrainian Shield, location of anorthosite-rapakivigranite plutons and principal deposits and prospects (excluding numerous occurrences/manifestations of ore mineralisation). 1-3 – Kirovograd orogen: 1-volcanic belt, 2-backarc basin and shelf of hinterland, 3-frontal overthrust belt and paraautochtonous; 4-5 – plutons (A-Korosten, B-Korsun-Novomirgorod): 4-rapakivi-granite, 5-anorthosite; 6-9 – Faults: 6-Transregional (1); 7-Main overthrust zones of orogen: (2) Odessa-Zhitomir, (3) West Ingulets, (4) Kirovograd, (5) Zvenigorodka-Annovka, (6) Jadlov-Traktemirov, (7) Pervomaysk-Brusilov, (8) Orekhov-Pavlograd; 8 – Overthrust zones of backarc Osnitsk-Mikashevichi orogen: (9) Teterev, (10) Perga; (9) Shear Zones: (11) Krivoy Rog-Kremenchug megashear, (12) Talnov, (13) Central; 10-19 – Deposits/prospects: 10-U hydrothermal vein type, 11-K-U (REE±Mo) type, 12-Na-U type, 13-Ti (P,V,Sc), 14-REE-Zr, 15-Rare metal (Li,Be et all), 16-Mo, 17-W (skarn type), 18-Au, 19-graphite. Within the Archaean Podol and Dnieper domains is shown their metallogenic specialization.

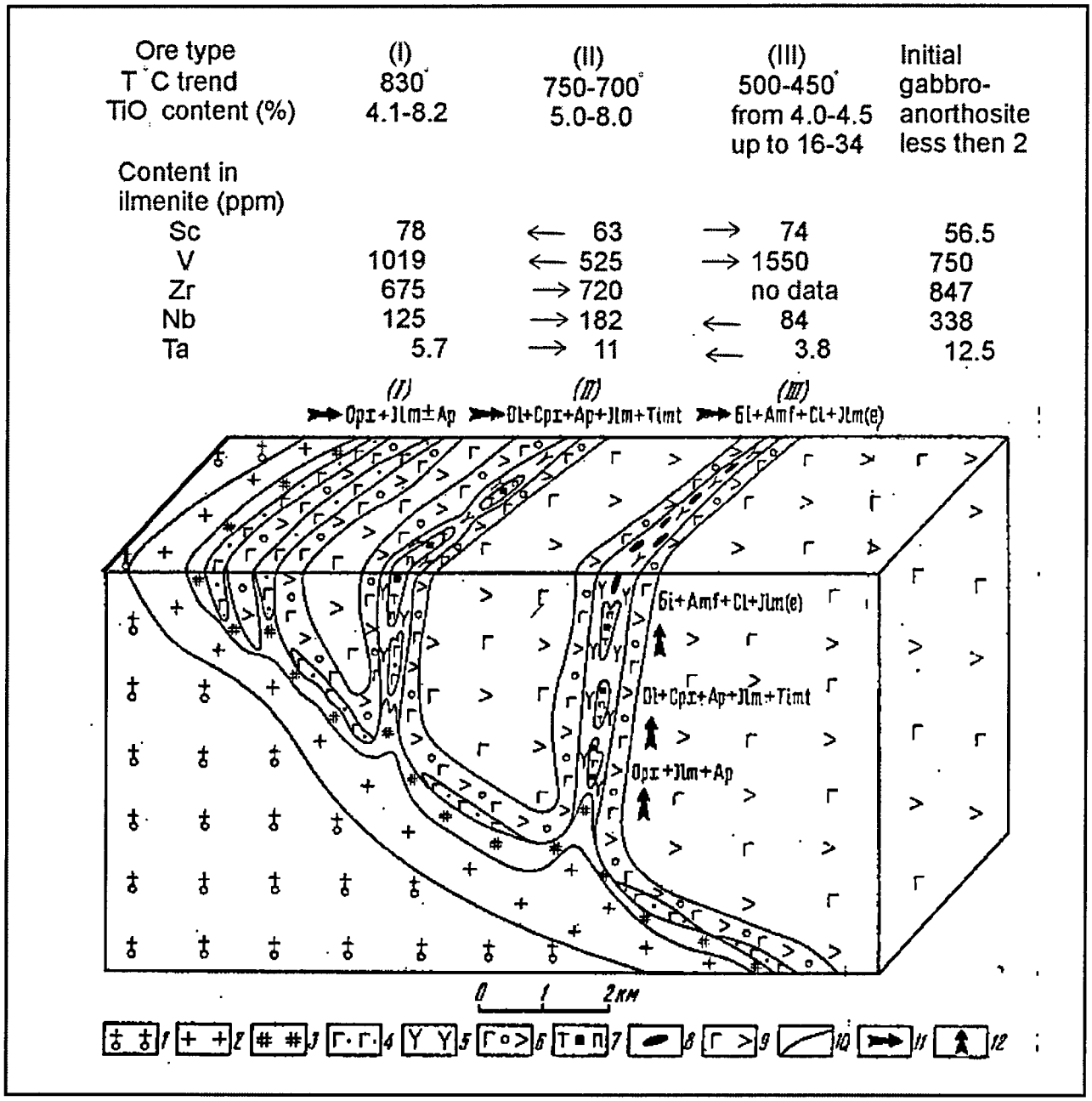

Fig.2 Summarized geological model of P-Ti ore formation in gabbroanorthosite massives of the Ukrainian Shield (after Tarasenko, 1987) and redistribution trend of some accompanying elements including in ilmenite after Borisenko et al., 1980). 1-rapakivi granite; 2-endocontact indistinct porphyro-like olivine-bearing granite; 3-quartz monzonite, monzonite, gabbro-monzonite; 4-gabbronorite of monzonitenorite copmplex (I) containing ilmenite and apatite-ilmenite ore; 5-andesitite, oligoclasite; 6-K-feldspatizated gabbroanorthosite; 7-gabbro, troctolite, plagioclase peridotite and pyroxinite of monzonite-peridotite complex (II) containing apatite-ilmenite and apatite-ilmenite-titanomagnetite ore; 8-embedded and massive apatite-ilmenite ore in gabbro-anorthosite oligoclasite-andesinite complex (III); 9-coarse- and giant-grained gabbroanorthosite; 10-boundaries of rocks and ores; 11-replaceability typomor-phic mineral assemblages along the lateral; 12-the same along the vertical. Opx-orthopyroxene, Cpx-clinopyroxene, Ol-olivine, Ilm-ilmenite, Ilm(e)-oxidized (leucoxenizated) ilmenite, Timt-titanomagnetite, Ap-apatite, Bi-biotite, Amf-amphisole, Cl-clorite/

Ponomarenko OM, Skobelev VM, Stepanyuk LM & Lesnaya I.:

Anorthosites of the Ukrainian Shield, morphology and composition of their accessory minerals

Ponomarenko Oleksandr M., Skobelev Vladimir M.,
Stepanyuk Leonid M., & Lesnaya Irina M.
Institute of Geochemistry, Mineralogy and Ore Formation, NAS, Ukraine, Kyiv;
pan@cki.ipri.kiev.ua

Three genetic groups of anorthosites may be distinguished within the Ukrainian Shield (UkS).

The first group is related to the Archaean granulite-enderbite-charnockite association of the Dniester-Bug region of the UkS. This region is the oldest domain of the continental crust within the UkS. As a rule, anorthosites occur there as small non-root bodies without sharp boundaries against enderbites and mafic granulites. Their composition is very fickle. Normative and modal quartz, and antiperthitic plagioclase are usual for anorthosites. The plagioclase composition varies from oligoclase to bytownite. Crystalloblastic textures are always characteristic for the anorthosites. Therefore, we can not regard them as initial magmatic cumulates, and these are metamorphic or metasomatic formations. The age of these type of anorthosites is not established. However, the U-Pb zircon ages of the country rocks correspond to the Early Proterozoic (2.31-2.02 Ga) [1, 2], and Sm-Nd model ages of anorthosites are always very old (3.8-3.3 Ga) [3]. Thus, they may be products of the Early Proterozoic metamorphic and metasomatic reworking of the Achaean substratum. Sometimes anorthosites observed as layer-like bodies in skarn contact zones between charnockites and carbonate-enriched rocks. Generally, the structure of these zones is, as following: charnockites – anorthosites – clinopyroxenites – calciphyres - ultramafic granulites. These anorthosites contain anorthite, which is associated with corundum.

The second genetic group of anorthosites (2.00-1.98 Ga [4]) is related to the layered nickel-bearing gabbroid intrusions, that occur within the North-Western region of the UkS (towards north from the Dniester-Bug region). During the period of 2.06-1.96 Ga [4] the region represented the active continental verge of the Sarmatian terrane. The diversity of magmatic complexes formed during this period is astonishing. Low-alkaline, sub-alkaline and alkaline ultramafic-mafic associations; temperate alkaline and sub-alkaline intermediate and acidic rock complexes; anatectic granite complexes, volcanic-plutonic rock associations all are observed there. With all this going on, the magmatic rock associations are generated synchronously both in zones of compression and extension. The layered nickel-bearing gabbroid intrusion [4], where the anorthosites occur, is related to a deep fault corresponding to the extension zones. The rocks have not been deformed, and have not been metamorphosed as the rocks in the compression zones. The anorthosites are related to the following rock assemblages: peridotite-gabbro-anorthosite, and troctholite-gabbronorite-gabbro. The anorthosites occur there as evident cumulative formations. The thickness of the anorthosite layers vary from some cm to 300 m. As a rule, the anorthosites lay in the upper parts of the layered intrusions.

The third genetic group (1.80-1.75 Ga) [5] is related to the rock association of the Korosten (the North-Western region) and the Korsun'-Novomirgorog (the Ingul-Ingulets region) gabbro-anorthosite – rapakivi granite plutons. Anorthosites and gabbronorite-anorthosites are predominant rocks in these gabbroid intrusions. In generally they compose central parts of the gabbroid intrusion massifs. The anorthosites have been generated during two intrusive events: 1) 1.8-1.79 Ga; 2) 1.76-1.75 Ga [5]. Rapakivi granites intruded in the period between the anorthosite intrusions (1.77 Ga [5]). In the quarries one can see cutting contacts between the anorthosites of the early and late phases. The formation of the gabbro-anorthosite – rapakivi

granite plutons was related to the collision stage of the geological history of the UkS (the collision of the Sarmatian and Fennoscandian terrains).

In our presentation the morphology and composition of the accessory minerals of anorthosites of the Ukrainian shield will also be considered.

References

Stepanyuk, L.M. Crystallogenesis and zircon ages of mafite-ultramafite rock association of the Middle Bug region // Mineralogical journal, 1996, v.18, N 4. – P.10-19 (in Russian).

Stepanyuk, L.M. The chronology of endogenic processes in granulite rock complexes of the Dniester-Bug megablock of the Ukrainian Shield (the Late Archean – Early Proterozoic) // Mineralogical journal, 1998, v.20, N 2. – P.68-73 (in Russian).

Dovbush, T.I., Skobelev, V.M., Stepanyuk, L.M. The results of study of the Precambrian rocks of the western part of the Ukrainian Shield by Sm-Nd isotopic method // Mineralogical journal, 2000, v.22, N 2/3. – P.132-142 (in Russian).

Skobelev, V.M., Jackovlev, B.G., Galiy, S.A. et al. Petrogenesis of the nickel-bearing gabbroid intrusions of the Volyn'megablock of the Ukrainian Shield. Kiev: Naukova Dumka, 1991.- 140 p. (in Russian).

Amelin, Yu.V., Heaman, L.M, Verkhogliad, V.M. and Skobelev, V.M. Geochronological constrains on the emplacement history of an anorthosite-rapakivi granite suite: U-Pb zircon and baddeleyite study of the Korosten complex, Ukraine // Contrib. Mineral. And Petrol. – 1994. – v.116, N 4. – P. 411-419.

Perreault S & Hebert C:

Review of Fe-Ti and Fe-Ti-P_2O_5 deposits associated with anorthositic suites in the Grenville Province, Québec

Serge Perreault, Géologie Québec, 456, avenue Arnaud, local 1.04, Sept-Iles, Quebec Canada G4R 3B1; serge.perreault@mrn.gouv.qc.ca

Claude Hébert, Géologie Québec, 5700, 4ième avenue Ouest, Charlesbourg, Québec, Canada G1H 6R1; claude.hébert@mrn.gouv.qc.ca

Anorthositic suites are a characteristic of the Grenville Province. Numerous deposits of titaniferous magnetite, of magnetite-ilmenite-apatite and of massive ilmenite are known since the mid 1850's. However, only few of them have been economically mined since 1870 and only the world class massive ilmenite deposit of the Tio Mine is mined since 1950. In the poster, we present a brief review of the most typical Fe-Ti and Fe-Ti-P_2O_5 deposits associated with anorthositic suites in the Grenville Province in Québec. It is a summary of works done by Rose (1969), compilation of deposit files done by several geologists at the Ministère des Ressources Naturelles du Québec and from assessment works from mining companies.

In general, the shape of these deposits varies from tabular intrusions, stocks, sills or dykes in the anorthositic rocks. Locally, some deposits are characterized by stratiform mineralization in layered anorthositic rocks. Four distinct styles of mineralization have been described (Gross, 1996) and only the first three styles are known in the Quebec's Grenville Province:

1) Syngenetic formation for disseminated Fe-Ti oxides in the host anorthosite.

2) Irregular to concordant injections or intrusions of massive ilmenite, massive titaniferous magnetite and oxide-rich norite or ferrodiorite, with clear cut or diffuse contact with the host rocks, in an older anorthosite or associated rocks. The emplacement of massive ilmenite

mineralization is attributed to an oxide-rich liquid derived from a parental oxide-rich norite or ferrodiorite emplaced during the crystallization and cooling of the anorthosite (Force, 1991).

3) Late injections, dikes or intrusions of magnetitite, ilmenitite or oxide-rich norite in an already cooled and solidified anorthosite (Gross, 1996).

4) Finally, Fe-Ti mineralization and ilmenite-rutile mineralization in skarns and alteration zones at the contact of the anorthositic rocks and the country rock (Force, 1991 and Gross, 1996).

Fe-Ti mineralizations in the Morin Anorthosite

Two deposits ilmenite were mined in the past in the Morin Anorthosite: Ivry and Desgrosbois (figure 1). These deposits form dykes and lenses of a hemo-ilmenite ore in the anorthosite. Disseminated ilmenite and magnetite are commonly observed in the host anorthosite around the massive mineralization. The main body of the Ivry Mine, composed of lenses of massive ilmenite with disseminated ilmenite in the host anorthosite, measure 228 m long by 18 m large and 56 m deep and was mine as an open pit. The deposit was mined between 1912 and 1918 (16 000 tons at 47 % Fe and 31.6 % TiO2) as an iron and titanium ore and between 1958 and 1959 for heavy aggregates (36 000 tons). Typical chemical analyse for the massive ore is 42.5 % Fe, 33.23 % TiO2, 7.54 % SiO2. Mineral reserves are estimated at 163 000 tons at 47 % Fe and 19 % TiO2.The Desgrobois deposit was in production for short periods in 1912 and 1949. The mineralization of titaniferous magnetite and ilmenite occurs as small masses and stratoid lenses in brecciated zones at the contact of leuconorite and anorthosite. Disseminated magnetite and ilmenite are also present in the host leuconorite. The ore consist of ilmenite and titaniferous magnetite with spinel, pyroxenes and plagioclase. The production in 1947 is estimated at 10 800 tons. Mineral reserves of 5.01 Mt at 40.8 % Fe and 11 % TiO2 were estimated by Pershing Co. between 1952 and 1953.

Between 1900 and 1960, numerous showing and small deposits of massive ilmenite or titaniferous magnetite – ilmenite were discovered. The Titanium Development deposit is composed of three massive zones of unknown shape of hemo-ilmenite associated with disseminated ilmenite in the host anorthosite. The deposit is not far from the Desgrobois. An estimated 2.59 Mt at 38.5 % Fe and 30.8 % TiO2 were calculated by Titanium Development Corp. in 1948. The Saint-Hippolyte deposit is composed of massive and disseminated hemo-ilmenite with estimated mineral reserve of 10 Mt at 27 % and 20 % TiO2. The Tamara deposit is composed of titaniferous magnetite and ilmenite in a leuconorite with estimated mineral reserves of 55 Mt at 22 % Fe and 6 % TiO2.

Fe-Ti mineralization in the Saint-Urbain Anorthosite

Several ilmenite deposits of the Saint-Urbain Anorthosite are known since 1666. As observed in other anorthositic suites, the massive ilmenite deposits occur as dykes, lenses and irregular masses associated with disseminated ilmenite in the host anorthosite. The main deposits included General Electric, Coulombe East and West, Bignell, Dupont, Fourneau, Bouchard, and Glen. The General Electric, between 1910 and 1925, for making iron and titanium alloy mined most of these deposits. Between 1939 and 1978, some of these deposits were mined as supply for heavy aggregates mainly by Continental Iron and Titanium Mining Ltd between 1957 and 1959.

The General Electric deposit is composed of an E-W vertical dyke of massive hemo-ilmenite of 120 m long by 20 m wide and 40 m thick in a massive to foliated anorthosite. Small lenses and smaller dyke of massive ilmenite and disseminated ilmenite in the anorthosite are associated with the main mineralization. The ore consist of hemo-ilmenite with minor pyrite, pyrrhotite, chalcopyrite and locally disseminated rutile. Veinlets of remobilize rutile have been noted. Typical chemical composition of the ore is 37 to 50 % Fe, 42 to 52 % TiO_2, 3 % Al_2O_3

and 0.4 % CaO. An estimated mineral reserves of 6.53 Mt at 27.3 Fe and 29.2 % TiO_2 has been calculated by SOQUEM. In 1918, 1300 tons of ore were mined.

The Coulombe East and West were mined between 1910 and 1911 with a production of 1 350 tons of ilmenite and in 1922 by the American Titanic Ore Co. Between 1939 and 1948 108 000 tons were produced as heavy aggregates. The main deposit is composed of a dyke of massive ilmenite of 240 m long by 30 wide in an anorthosite. Smaller dykes and veins of ilmenite and disseminated ilmenite are encountered in the host anorthosite. The mean grade is 36 % Fe, 39 % TiO_2, 4 % SiO_2, 4 % Al_2O_3 and 4 % CaO. In 1977 SOQUEM estimated the mineral reserves at 6.71 Mt at 26.6 % Fe, 29.7 % TiO_2 for Coulombe Ouest and 33 000 tons at 29.8 % Fe and 32.8 % for Coulombe East.

Between 1940 to 1946, 1957 to 1966 and in 1977 more than 397 000 tons of ilmenite were extracted from Bignell deposit for heavy aggregates. Bignell deposit is composed of a dyke of massive hemo-ilmenite of 160 m long by 60 m wide and 30 m thick, emplaced in anorthosite. SOQUEM estimated a total of mineral reserves at 3.44 Mt 34.1 % Fe and 34.7 % TiO_2 with 2.5 Mt at 35.7 % Fe and 36.4 % TiO_2 proven reserves.

The Furnace deposit close to the village of Saint-Urbain was the first massive ilmenite deposit to be mined in the Saint-Urbain Anorthosite. Between 1871 and 1875 the Canadian Titanic Iron Co. mined the Furnaced ilmenite to produced an iron slag. The deposit was subsequently mined periodically by different producers mainly as a supply for heavy aggregates after 1940. The deposit is composed of a massive hemo-ilmenite irregular band of 120 m long by 60 m wide, and oriented NW-SE with a vertical dip. It is associated with numerous smaller bands, lenses, pockets and veins of massive ilmenite in an ilmenite-bearing anorthosite. SOQUEM estimated mineral reserves of 2.09 Mt at 26 % Fe and 27 % TiO_2.

Finally, the Glen deposit is composed of a dyke of massive hemo-ilmenite of 40 m long by 4 to 6 meters wide. About 1270 tons of ilmenite was extracted in 1924 by the Baie Saint-Paul Titanic Iron Ore. A typical sample return values of 43.06 % Fe, 38.29 % TiO_2, 1.68 % SiO_2 and 0.04 % P.

The Morin showing (figure 1) is located in a jotunite sill emplaced at the contact between a mangerite and paragneiss at the western edge of the Saint-Urbain Anorthosite. The mineralization is composed of massive lenses and disseminated magnetite, ilmenite and apatite in the jotunite. Best values obtained from representative samples are 21.7 % Fe, 7.10 % TiO_2 and 4.14 % P_2O_5. Concentration test gave 11.98 % TiO_2 and 10.78 % P_2O_5 for non-magnetic concentrate and 70.56 % Fe and 0.31 % V_2O_5 for the magnetic fraction. This showing is located in a 12 km linear magnetic anomaly that corresponds to the jotunite.

Fe-Ti and Fe-Ti-P_2O_5 mineralization in the Lac-Saint-Jean Anorthosite

Since the late 1880's, only a few showings and deposits were known to be associated with the Lac-Saint-Jean Anorthosite (LSJA). However, recent mapping done by the Government of Quebec results in discovery of large numbers of showings of magnetite-ilmenite-apatite in nelsonite or jotunite. Some of them are presently working by mining companies. Few showings of hemo-ilmenite are known in the LSJA and most showings are titaniferous magnetite or magnetite-ilmenite-apatite mineralizations.

The Saint-Charles deposit, discovered in 1884, is located in the southern part of the LSJA (figure 1). The mineralization is composed of lenses of massive titaniferous magnetite with ilmenite, apatite, and spinel. Disseminated mineralization is also observed in the host leuconorite or leuco-gabbronorite and anorthosite. Typical chemical compositions from apatite-rich and apatite-poor mineralization are respectively 35 % Fe, 15 % TiO_2, between 3 and 5 % P and 46 % Fe, 19 % TiO_2 and 0,13 % P. The mineralized zones (massive + disseminated) extent over 1.8 km long by 336 m wide and extent to a depth of 31 to 61 meters. Estimated mineral reserves for the main deposit are 5.4 Mt at 29.47 % Fe, 10.12 % TiO_2 and 9.25 % P_2O_5, 0.10 % V_2O_5 and 0.10 % REE.

In the last 3 years, three junior mining companies had been working on several showings of magnetite-ilmenite-apatite mineralization following the geologic mapping done by the Government of Québec. The Buttercup showing is composed of vanadiferous titaniferous magnetite cumulates in a leuconorite or leuco-gabbronorite. Drilling on the property had indicated mineral reserves of 3.5 Mt at 49 % Fe, 19 % TiO_2 and 0.67 % V_2O_5. In the north central part of the LSJA, numerous showing of magnetite-ilmenite-apatite had return values of 6 to 14 % P_2O_5 and 6 to 21 % TiO_2. A zone discovered by drilling of 188 m wide had return 7.6 % P_2O_5 and 9.7 % TiO_2.

The Mine Canada Iron furnace deposit occurs at 4 km south of St. Charles deposit. The Canada Iron Furnace Company Ltd has exploited this deposit in 1901 for its iron. Only 272 tons have been extracted and shipped from the short-lived Radnor Mine. The ore is composed of magnetite, ilmenite, apatite, rutile and garnet. The mineralization occurs as lenses of massive and disseminated oxides in a gabbroic facies of the anorthosite. Best results from a massive mineralization are 39.99 % Fe and 18.38 % TiO_2. There are also three other showings near this deposit. It is important to note that no work has been ever done to evaluate the tonnage of the main deposit.

The La Hache-East deposit is located at the eastern margin of the LSJA. The mineralization occurs in three showings within a large monzonitic and jotunitic (ferrodioritic) intrusion. Following an airborne aeromagnetic survey and a ground magnetometric survey in 1952, a prospector found the first showing of massive magnetite and ilmenite of the La Hache-East. Later in 1967, Terra Nova Company carried out exploration works and concluded a partnership with the stated owned Société québécoise d'exploration minière (SOQUEM). After an aggressive drill program, the joint venture announced that the mineral reserves of the main showing were 20.32 Mt at 24.75 % Fe, 5.12 % TiO_2, 5.21 % P_2O_5. Works donned by SOQUEM showed that it was possible to recovered a magnetite concentrate at 66.5 % soluble iron with 2.5 % TiO_2 and a concentrate of ilmenite with 47.5 % TiO_2 and 0.3 % P_2O_5. Due to low prices of these two minerals at that time, the companies decided to abandon the project. The mineralization occurs as stratiform lenses of massive to disseminated magnetite, ilmenite and apatite in the jotunite.

Fe-Ti mineralization in the Labrieville Anorthosite

The Lac Brulé deposit is composed of massive hemo-ilmenite lenses. Bands of massive to disseminated ilmenite are also present in the host anorthosite. A nelsonite horizon is underlying the main mineralized zone. The largest lens measured 120 m long and its width vary from 3 to 12 meters. An estimated mineral reserves for massive and disseminated mineralization by Bersimis Mining in late 1950's gave 5.8 Mt at 42 % Fe and 35 % TiO_2.

Fe-Ti mineralization in the La Blache Anorthosite

The massive titaniferous magnetite mineralization occurs as a 10 to 25 meters thick dykes or sills emplaced in a labradorite-bearing anorthosite (figure 1). Best values for the three different deposits, distributed over 10 km, range from 38.6 to 36.7 % FeO, 31.3 to 33.7 % Fe_2O_3, 20.2 to 22 % TiO_2, 0.46 to 0.48 % V_2O_5, 7.11 to 8.15 % Al_2O_3 and 2.50 to 4.70 % MgO. Mineral reserves estimated by Bersimis Mining in late 1950's are 79 Mt at 48 % Fe and 20.1 % TiO_2 for the three mains deposits. In the southwest extension of the La Blache Anorthosite, the Lac Dissimieu deposit is characterized by bands of disseminated to massive ilmenite and apatite in the anorthosite. A mineralized zone of 4 km long by 250 m wide was the focus of a drilling program that gave 10 to 15 % ilmenite and with a grade of 45 % TiO_2 and 4.5 % P_2O_5.

Fe-Ti in the Pambrum Anorthosite

The Lac Pambrum deposit is characterized by lenses of massive titaniferous magnetite and ilmenite associated with layers of pyroxenite in an anorthosite. Small pockets of massive oxide are commonly observed in the anorthosite close to the main mineralization. The exact shape of

the mineralized is unknown. However, preliminary estimated of mineral reserves indicated 49 Mt at 47 % Fe and 11 % TiO_2. The ore is composed of magnetite-ilmenite intergrowths. Separation tests perform on the ore show that the metallurgy is to complex to be economically mined for neither its iron nor its titanium.

Fe-Ti mineralization in the Riviere-Pentecote Anorthosite

The Fe-Ti mineralizations in the Rivière-Pentecôte Anorthosite are usually composed of small showings. They consist mostly of small lenses of massive titaniferous magnetite in the anorthosite. Locally, pockets of massive ilmenite along with disseminated ilmenite and titaniferous magnetite are observed in the anorthosite and leuconorite. On the west margin of the anorthosite, in a sheared anorthosite, a showing, discovered few years ago, is composed of centimeter to a meter thick veins massive magnetite, with up to 25 % pyrite and pyrrhotite. This peculiar mineralization was the first time observed in the area. Magnetite-ilmenite-apatite mineralizations associated with nelsonite lenses are locally observed in the anorthosite and leuconorite.

Fe-Ti mineralizations in the Havre-Saint-Pierre Anorthosite

The world class Tio Mine deposit, exploited since 1950 by QIT, is the classic example of this type. The Tio Mine, located 42 km north of Havre-Saint-Pierre (figure 1), was discovered in 1946 by geologists of the Kennecott Copper Inc. following a regional airborne magnetic survey and extensive field works. Over 20 significant showings were discovered by J. Retty in 1941 and by Kennecott and QIT geologists between 1944 and 1950 near Lakes Allard and Puyjalon.

The Tio Mine is composed of a sub-horizontal, massive ilmenite intrusion separated into three deposits separated by normal faults. The main deposit measures 1097 m in the N-S direction and 1036 m E-W. Its thickness is estimated at 110 m and the deposit is inclined 10° to the east. The deposit is divided into 3 zones. The upper zone is composed of massive hemo-ilmenite, the intermediate zone of alternating layers of massive to semi-massive hemo-ilmenite and anorthosite, and the lower zone of massive hemo-ilmenite. The Northwest deposit forms a band of 7 to 60 meters in thickness of massive ilmenite alternating with anorthosite. The deposit is gently inclined to the east. The Cliff deposit forms a hill that overlooks the Tio Mine, and has an ellipsoidal shape. Both the Main and the Northwest deposits are mined. The ore is composed of a dense coarse-grained aggregate of hemo-ilmenite. Accessory minerals are plagioclase, spinel, pyrite, and chalcopyrite. Locally, the modal proportion of sulfides reaches 2 %. The mean composition of the ore is 34,2 % TiO_2, 27,5 % FeO, 25,2 % Fe_2O_3, 4,3 % SiO_2, 3,5 % Al_2O_3, 3,1 % MgO, 0,9 % CaO, 0,1 % Cr_2O_3, and 0,41 % V_2O_5. The Main deposit is estimated at 125 millions tons. The Northwest deposit contains 5 Mt at 37,4 % Fe and 32,32 % TiO_2, and the Cliff deposit 8,4 Mt at 39,2 %Fe and 33,9 % TiO_2. Since 1950, QIT has extracted an estimate of 60 Mt at 38,8 % Fe and 33,6 % TiO_2.

Other similar deposits occur around Lakes Allard and Puyjalon. The most promising deposits include Grader (which was mined in 1950 for a short period), Springer, and Lac-au-Vent. All these deposits and smaller showings are composed of massive ilmenite dykes emplaced in the andesine-bearing anorthosite. One exception worthy of mention is the Big Island deposit. This deposit is composed of a rutile and sapphirine-bearing massive hemo-ilmenite dyke with fragments of oxide-rich norite and anorthosite containing. Rutile can be as high as 15 %. Typical grab samples collected for assays gave values of 26 % FeO, 21,1 % Fe_2O_3, 40,3 % TiO_2, 3,12 % MgO, 0,36 % V_2O_5, 4,35 Al_2O_3, and 6,26 % SiO_2 for a sapphirine and rutile-bearing ilmenitite, and 29,1 % FeO, 29,8 % Fe_2O_3, 38,9 % TiO_2, 2,99 % MgO, 0,39 % V_2O_5, 1,54 % Al_2O_3, and 0,91 % SiO_2 for massive ilmenitite. The dyke is 15 m wide and outcrop over 500 m.

The Fe-Ti and Fe-Ti-P_2O_5 mineralization occurs in a jotunite ont the East Side of the HSPA. It is composed of 20 to 50 % magnetite, ilmenite and apatite and locally bands enriched in

oxides define a primary layering in the jotunite. The size of the deposit correspond to the jotunite itself, witch is 3 km long by 300 m wide. Gulf Titanium has estimated in the late 1950's a mineral reserve of 294 Mt at 16,2 % Fe, 9,75 % TiO_2 et 4 % P_2O_5. Titaniferous magnetite showings and small deposits are typically observed on the western margin of the HSPA in a labradorite-bearing anorthosite.

Fe-Ti mineralizations in the Lac Fournier Anorthosite

The Magpie deposit outcrop on a ridge that is located 160 km north of Mingan and 3 km west of Saint-Jean River (figure 1). It is composed of four zones of massive titaniferous magnetite with ilmenite and spinel associated with a leuconorite and an anorthosite of the Lac Fournier Anorthositic Suite. The deposit has been worked by Stramat Ltd between 1958 and 1965 and by SOQUEM between 1968 and 1978. The Magpie deposit can be classified as a world class deposit of titaniferous magnetite with an estimation of mineral reserve at 1.8 billions tons with 184 Mt of proven and 627 Mt of probable reserves at 43.1 % Fe, 10.6 % TiO_2, 1.55 % Cr and 0.19 % V.

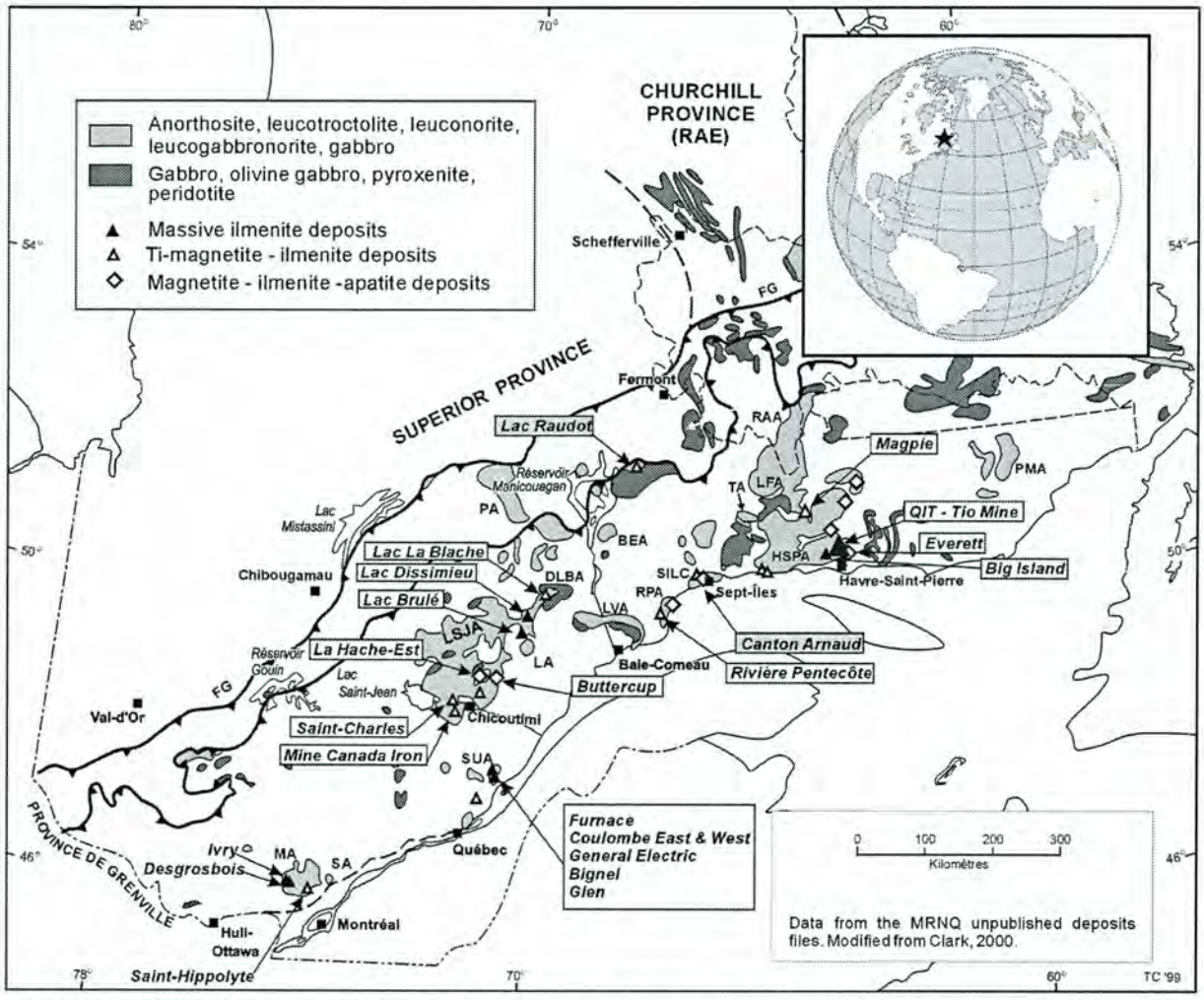

Figure 1. Location of the studied area in the Grenville Province. HSPA, Havre-Saint-Pierre anorthosite; LFA, lac Fournier anorthosite; LSJA, Lac Saint-Jean Anorthosite; RPA, Rivière Pentecôte Anorthosite; TA, Tortue Anorthosite; PMA, Petit-Mécatina Anorthosite; RAA, Atikonak River Anorthosite; BEA, Berté Anorthosite; LA, Labrie Anorthosite; LVA, Lac Vaillant Anorthosite; PA, Pambrun Anorthosite; MA, Morin Anorthosite; SUA, Saint-Urbain Anorthosite; SILC, Sept-Iles Layered Complex; FG, Grenville Front.

Fe-Ti mineralizations in large mafic layered complex

Other deposits worth to mention associated with mafic layered complex in the Grenville included the massive and disseminated titaniferous magnetite layers associated with an olivine-bearing layered gabbro in the Raudot Complex (figure 1) and the ilmenite-apatite-magnetite deposit of the Canton Arnaud in the Cambrian Sept-Îles Layered Complex. The oxide mineralization is present in nelsonite layers and associated magnetitite layers in the upper part of the Lower Layered Serie (Cimon, 1998). Detailed works by SOQUEM on the deposit has given proven and probable reserves of 107 Mt at 6.2 % apatite and 8.4 % TiO2. Other small titaniferous magnetite deposits in mafic igneous complexes are also known in isolated intrusions or closely related to anorthosite suites.

References

Cimon, J., Dion, D.-J., Authier, K., Feininger, T., 1998. Le complexe de Sept-Îles. I. L'unité à apatite de Rivière des Rapides, Complexe de Sept-îles : localisation stratigraphique et facteurs à l'origine de sa formation. II. Interprétation gravimétrique du Complexe mafique stratifié de Sept-Îles. Ministère des Ressources Naturelles, Québec ; ET 97-05.

Force, E., 1991. Geology of titanium-mineral deposits. Geological Society of America, Special Paper 259, 112 pages.

Rose, E.R., 1969. Geology of titanium and titaniferous deposits of Canada. Geological Survey of Canada, Economic Geology Report 25, 177 pages.

Perreault S & Heaman L:

The 974 Ma Vieux-Fort Anorthosite, Lower North Shore, Québec: the youngest anorthosite in the Grenville Province

Serge Perreault, Géologie Québec, 456, avenue Arnaud, Local 1.04, Sept-Îles, Québec G4R 3B1
Larry Heaman, Dept. of Earth & Atmospheric Sciences, University of Alberta, Edmonton, T6G 2E3

The Vieux-Fort Anorthosite is a small complex (~ 60 km^2) located in the northeastern Grenville Province, in Quebec's Lower North Shore area (figure 1). The complex is composed mostly of massive to weakly deformed anorthosite and leuconorite with small amounts of leucogabbro, pegmatitic gabbro, and gabbro; it is bordered to the north by mangeritic rocks (figure 2). South of the NE-trending Vieux-Fort fault, leuconorite at the contact of the pluton is foliated parallel to the regional foliation in the adjacent Pinware Terrane granitic gneiss.

Zircons recovered from a massive, pegmatitic, quartz-bearing, granophyric leuconorite are colourless to light tan, irregular fragments and shards, with a low uranium content (38-267 ppm U, usually <100 ppm U) and a high Th/U ratio (0.8-0.9), features typical of zircons crystallizing rapidly at a late stage from a mafic magma. Many grains have tiny, opaque or transparent mineral inclusions; a few grains are fractured. The U-Pb results show a slight scatter but the $^{207}Pb/^{206}Pb$ ages for all six analyses are clustered between 960 and 976 Ma; they are 0,6-0,9 % discordant except for two analyses at -1,1 % and 1,5 %. A best-fit regression yields an upper intercept age of 974.5 ±1.8 Ma, which is interpreted as a crystallization age (figure 2). Thus, the Vieux-Fort Anorthosite is the youngest known anorthosite in the Grenville, younger than the 1018 Ma Labrieville Anorthosite and the 1062 Ma Havre-Saint-Pierre Anorthosite.

The massive appearance of the anorthosite and of the related mangerite envelope, with tectonic foliation limited to the margin of the pluton, and the absence of metamorphic mineral

assemblages in the anorthositic rocks, suggest that the Vieux-Fort Anorthosite has escaped the major Grenvillian (1080-980 Ma) deformation and associated metamorphism that affected the eastern Grenville Province. The crystallization of the Vieux-Fort Anorthosite at 974 Ma was coeval with late- to post-Grenvillian gabbros, syenites, monzonites and granites (980-966 Ma) in the eastern Grenville. Pb loss at 950 Ma, suggested by a slight scatter in the distribution of the analyses, is coeval with a cluster of titanite U-Pb ages (970-930 Ma), which correspond to titanite U-Pb closure temperatures and to post-peak metamorphic cooling. We suggest that the Vieux-Fort Anorthosite was emplaced after the main Grenvillian deformation and metamorphism, in a partially cooled, thickened crust. The Vieux-Fort Anorthosite and its associated mangeritic rocks may be coeval with the earliest components of post-tectonic gabbroic and granitic magmatism resulting from melting at the base of the thickened Grenvillian crust.

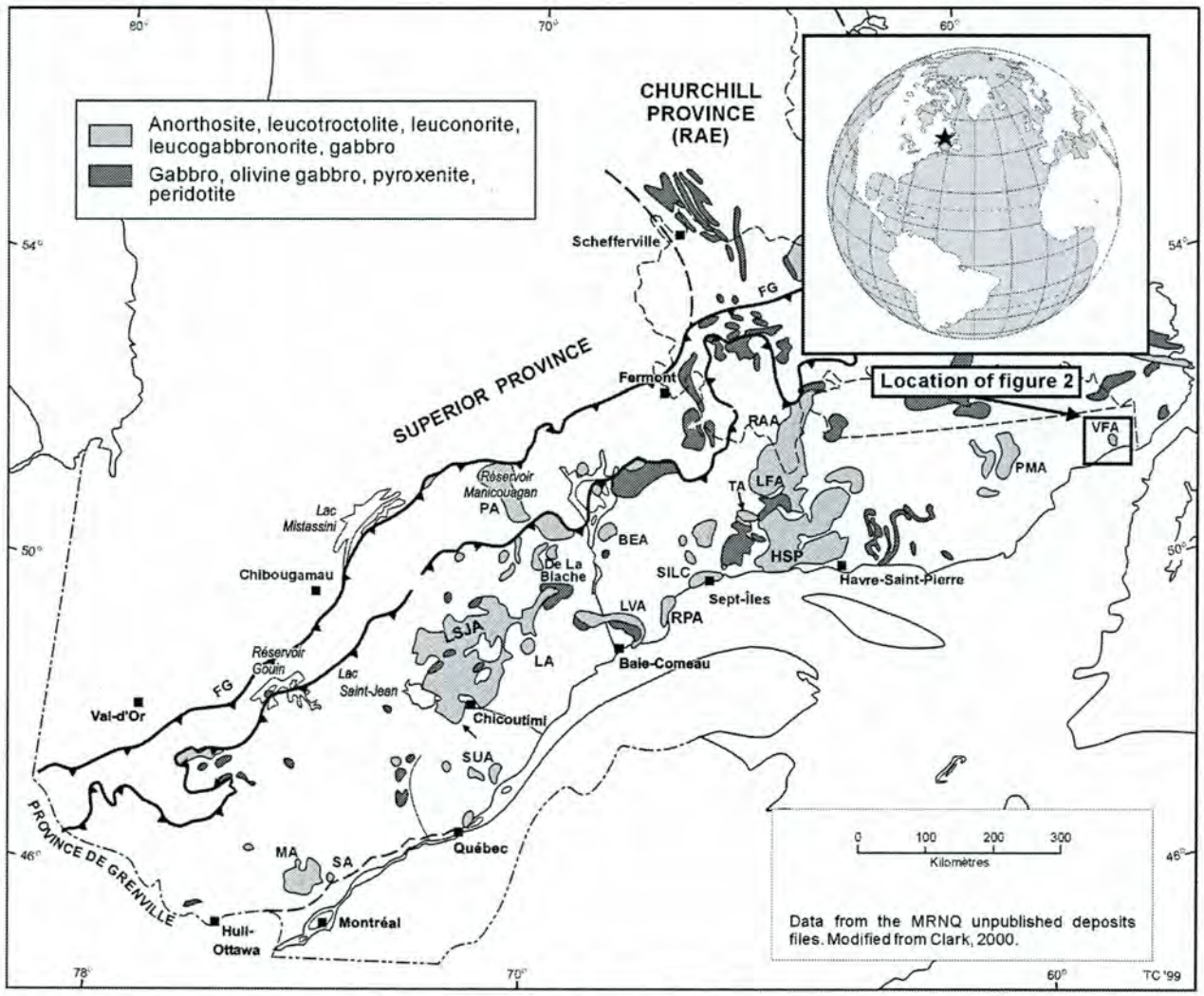

Figure 1. Location of the studied area in the Grenville Province. HSP, Havre-Saint-Pierre anorthosite; LFA, lac Fournier anorthosite; LSJA, Lac Saint-Jean Anorthosite; RPA, Rivière Pentecôte Anorthosite; TA, Tortue Anorthosite; PMA, Petit-Mécatina Anorthosite; RAA, Atikonak River Anorthosite; BEA, Berté Anorthosite; LA, Labrie Anorthosite; LVA, Lac Vaillant Anorthosite; PA, Pambrun Anorthosite; MA, Morin Anorthosite; SUA, Saint-Urbain Anorthosite; VFA, Vieux-Fort Anorthosite; SILC, Sept-Iles Layered Complex; FG, Grenville Front.

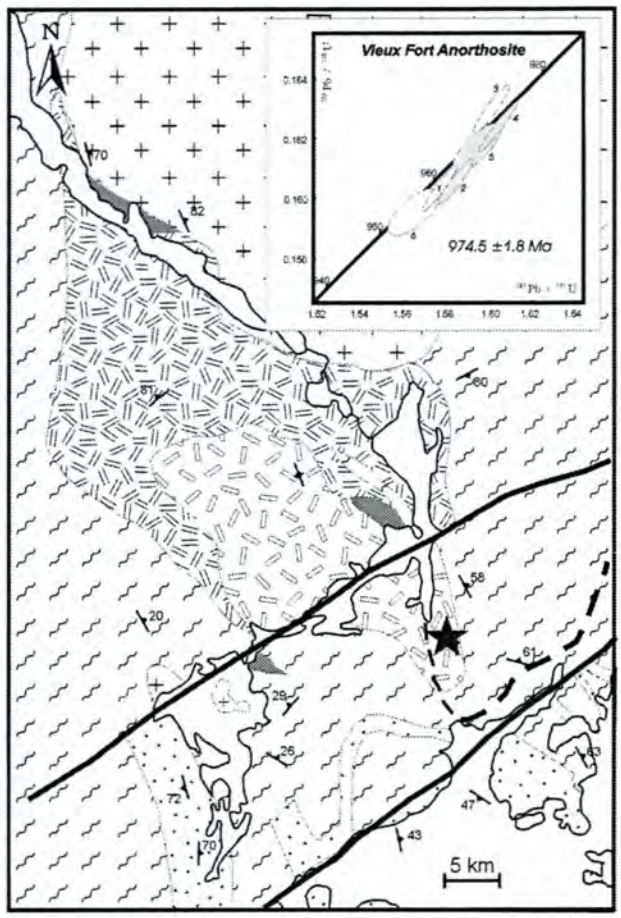

Figure 2. Simplified geological map of the Vieux-Fort area and U/Pb diagram.

Perreault S:

Contrasting styles of Fe-Ti mineralization in the Havre-Saint-Pierre anorthosite suite, Quebec's North Shore, Canada

Serge Perreault
Géologie Québec, 456, avenue Arnaud, local 1.04, Sept-Iles, Quebec Canada G4R 3B1
serge.perreault@mrn.gouv.qc.ca

The Havre-Saint-Pierre anorthosite suite (HSP) is located in the northeastern part of the Grenville Province (figure 1). It is composed of several massifs or lobes separated from each other by structural zones. It includes a wide range of rock units typical of AMCG suites. The HSP is composed of seven massifs: the well-known Lac Allard massif, as well as the Rivière Romaine, the Rivière Magpie-Ouest, the Nord-Ouest, the Sheldrake, the Brézel, and the Rivière-au-Tonnerre massifs. Most of the Fe-Ti mineralizations are associated with the lac Allard, the Rivière-au-Tonnerre and the Rivière Romaine massifs. The Nord-Ouest massif is characterized by Cu-Ni mineralizations associated with pyroxenite and melanorite in anorthositic rocks at the margin of the massif (Clark, 2000 and Verpaelst et al., 2001). The structural state of the HSP ranges from undeformed and weakly recrystallized anorthosite to highly deformed and recrystallized anorthositic gneiss. Close to the margins of the massifs, the

anorthosite is commonly mylonitic. Partially or totally deformed and recrystallized mangerite and charnockite envelop most of the anorthositic massifs. Slivers of deformed and highly metamorphosed supracrustal rocks are commonly found between the massifs. The emplacement of the HSP was complex: in the north, it was thrust over the country rocks; in places, one massif was thrust over another; and in the south, the relatively young Rivière-au-Tonnerre massif was intruded into an older massif. U/Pb zircon geochronology on various massifs shows a range in ages. A mangerite associated with the Allard Lake massif was dated at 1126 ± 6 Ma (Emslie and Hunt, 1990). An age of 1130 Ma was found for the Sheldrake massif (in Verpaelst et al., 2001), and an age of 1062 Ma was obtained for the Rivière-au-Tonnerre massif (van Breemen and Higgins, 1993).

Fe-Ti mineralizations

The Fe-Ti showings and deposits associated with the HSP are divided into four groups: veins and dykes of massive ilmenite associated with andesine-bearing anorthosite; dykes or intrusions of magnetite, ilmenite, and apatite-bearing jotunite (or ferrodiorite), generally emplaced at the interface of anorthosite-mangerite; dykes and intrusions of ilmenite and magnetite-bearing norite with ilmenite veins emplaced in labradorite-bearing anorthosite; horizons, dykes, and masses of semi-massive to massive titaniferous magnetite emplaced along the margin of labradorite-bearing anorthosite. Locally they are associated with oxide-rich jotunite.

Massive ilmenite dykes and veins

The world class Tio Mine deposit, exploited since 1950 by QIT, is the classic example of this type. The Tio Mine is located 42 km north of Havre-Saint-Pierre (figure 2) and was discovered in 1946 by geologists of Kennecott Copper Inc. Over 20 significant showings were discovered by J. Retty in 1941 and by Kennecott and QIT geologists between 1944 and 1950 near lakes Allard and Puyjalon.

The Tio Mine (site 1, figure 2) and most satellite deposits are located on the east side of the HSP. There the plagioclase in the anorthosite is andesine and most deposits are closely associated with jotunite or oxide-rich norite (Rose, 1969; Bergeron, 1986; Force, 1991). These deposits occur as dykes, sills, or stratoid lenses. Most associated norite or jotunite intrusions show an ilmenite enrichment at the base. Jotunite intrusions are composed of plagioclase (An41-44), orthopyroxene, apatite, ilmenite, and magnetite. Locally, modal proportions of apatite and oxides reach 10 % and 20 %, respectively. Recent models suggest that these massive ilmenite deposits originated from the separation of an immiscible iron- and titanium-rich liquid from a jotunitic parent liquid (Force, 1991; Gross, 1998). This immiscible oxide-rich magma then moved into fractures and shear zones in the crystallizing anorthosite to form dykes, sills, and tabular intrusions of massive ilmenite, such as observed at the Tio Mine (Bergeron , 1986, and Force, 1991).

The Tio Mine is composed of a subhorizontal, massive ilmenite intrusion forming three deposits separated by normal faults. The main deposit measures 1097 m in the N-S direction and 1036 m E-W. Its thickness is estimated at 110 m and the deposit is inclined 10° to the east. The deposit is divided into 3 zones. The upper zone is composed of massive hemo-ilmenite, the intermediate zone of alternating layers of massive to semi-massive hemo-ilmenite and anorthosite, and the lower zone of massive hemo-ilmenite. The Northwest deposit forms a band 7 to 60 m in thickness of massive ilmenite alternating with anorthosite. The deposit is gently inclined to the east.The Cliff deposit forms a hill that overlooks the Tio Mine, and has an ellipsoidal shape. Both the Main and the Northwest deposits are mined. The ore is composed of a dense, coarse-grained aggregate of hemo-ilmenite. Accessory minerals are plagioclase, spinel, pyrite, and chalcopyrite. Locally, the modal proportion of sulphides reaches 2 %. The mean composition of the ore is 34,2 % TiO_2, 27,5 % FeO, 25,2 % Fe_2O_3, 4,3 % SiO_2, 3,5 % Al_2O_3, 3,1 % MgO, 0,9 % CaO, 0,1 % Cr_2O_3, and 0,41 % V_2O_5. The Main deposit is estimated at 125

millions tons. The Northwest deposit contains 5 Mt at 37,4 % Fe and 32,32 % TiO_2, and the Cliff deposit contains 8,4 Mt at 39,2 %Fe and 33,9 % TiO_2. Since 1950, QIT has extracted an estimated 60 Mt of ore grading 38,8 % Fe and 33,6 % TiO_2.

Other similar deposits occur around Lakes Allard and Puyjalon. The most promising deposits include Grader (which was mined in 1950 for a short period), Springer, and Lac-au-Vent. All these deposits and smaller showings are composed of massive ilmenite dykes emplaced in the andesine-bearing anorthosite. One exception worthy of mention is the Big Island deposit (site 2; figure 2). This deposit is composed of a rutile and sapphirine-bearing, massive hemo-ilmenite dyke with fragments of oxide-rich norite and anorthosite. Rutile can be as high as 15 modal %. Typical grab samples collected for assays gave values of 26 % FeO, 21,1 % Fe_2O_3, 40,3 % TiO_2, 3,12 % MgO, 0,36 % V_2O_5, 4,35 Al_2O_3, and 6,26 % SiO_2 for a sapphirine and rutile-bearing ilmenitite, and 29,1 % FeO, 29,8 % Fe_2O_3, 38,9 % TiO_2, 2,99 % MgO, 0,39 % V_2O_5, 1,54 % Al_2O_3, and 0,91 % SiO_2 for massive ilmenitite. The dyke is 15 m wide and outcrops over 500 m..

Magnetite-ilmenite-apatite mineralizations

Most ilmenite-magnetite-apatite mineralizations are associated with jotunite on the east side of the HSP (figure 2). These rocks are present at the contact between the anorthosite and mangeritic rocks The jotunite is usually coarse-grained, dense, and highly magnetic. Close to the contact with the anorthosite, a primary layering is well developed (Rose, 1969; Hocq, 1982; Bergeron, 1986). Several deposits were discovered along with the hemo-ilmenite deposits. Two typical deposits are described here. The Everett deposit (site 3; figure 2) outcrops along the northwest shore of Lake Puyjalon. The ilmenite-magnetite-apatite mineralization is associated with a band of jotunite 3 km long and up to 300 m thick. The mineralization is composed of 20 to 30 % ilmenite, hematite, magnetite, and apatite, along with plagioclase and orthopyroxene. Locally, oxides and apatite make up to 50 % of the rock. Gulf Titanium Limited has estimated geological reserves in the deposit at 293 Mt grading 16,2 % Fe, 9,75 % TiO_2, and 4 % P_2O_5.

Other showings are located northeast of the Everett deposit and about 60 km NE of Tio Mine (site 4; figure 2). The mineralizations are similar to the Everett deposit and are associated with jotunite emplaced at the contact of the anorthosite with the mangerite. The main showing outcrops over 1 km and is 100 m wide. The mineralization occurs as magnetite- and ilmenite-rich layers from a few centimetres to half a meter in thickness in the jotunite. The rock shows a well-developed banded structure. The jotunite is composed of 50 to 60 % magnetite and ilmenite, 10 to 30 % plagioclase, 10 to 30 % orthopyroxene, and accessory apatite and green spinel.

Massive ilmenite veins with ilmenite-rich leuconorite

This type of mineralization is observed on the southwest side of the HSP (site 6; figure 2). It is closely associated with leuconoritic rocks intruding the labradorite-bearing anorthosite. The leuconorite forms thick dykes that invaded a partially crystallized anorthosite. The dykes are emplaced parallel to the foliation observed in the anorthosite and contain large enclaves of the host rocks. Contacts between the two rock types are usually sharp but are locally diffuse. Ilmenite (up to 10 %) and orthopyroxene are disseminated in the leuconorite and large corroded and broken xenocrysts of labradorite are common. The labradorite xenocrysts are fragments of the host anorthosite. Massive ilmenite lenses and irregular veins are common within accumulations of orthopyroxene phenocrysts in the norite. The thickness of these lenses and veins varies from 10 cm to 60 cm. The ilmenite veins are intrusive in the leuconorite and locally they cross the contact between the anorthosite and the norite and form thin veins of massive ilmenite in the anorthosite. The ilmenite-rich veins are composed of lamellar ilmenite (60 to 80 %), plagioclase, orthopyroxene, green spinel and locally apatite, clinopyroxene and magnetite. Late biotite after ilmenite is commonly observed. Values of 46.3 to 59.3 % Fe_2O_3, 30.6 to 38.7 % TiO_2, 2.06 to 2.42 % MgO, 0.33 to 0.43 % V_2O_5, 1.64 to 13.0 % SiO_2, 1.35 to

5.90 % Al_2O_3, 0.2 to 1.35 % CaO, and 0.01 to 1.1 % S were obtained on 3 samples of ilmenitite veins.

Titaniferous magnetite mineralizations

Non-economic, titaniferous magnetite mineralizations are common in labradorite-bearing anorthosite and are mostly observed in the southwest part of the HSP (figure 2). The mineralizations occurs in several forms:

as layers of magnetitite in anorthosite;

as layers, discordant veins, or dykes of magnetite-rich melanorite or melagabbronorite;

as discordant veins and lenses of remobilized magnetitite;

as magnetite-rich monzonitic pegmatite; and

as magnetite-rich lenses or veinlets in late ductile and brittle shear zones cutting anorthosite.

Two localities are worth mentioning. At the mouth of Rivière Chaloupe (site 7; figure 2) and at Cap Rond (site 6; figure 2), the magnetite mineralization forms centimetre-thick layers of semi-massive and massive magnetite in the anorthosite. Most of the layers are interpreted as primary; however, some of the magnetite-rich layers are associated with the development of a tectonic foliation in ductile shear zones cutting anorthosite. This is particularly well-developed at the western margin of the HSP in the Rivière-au-Tonnerre lobe. Locally, in well-exposed outcrops along the shoreline, the layers are folded and locally reoriented in the ductile shear zones. Near the contact with the magnetitite layers, the anorthosite shows an increase in magnetite content. In the same outcrop, remobilized magnetite veins originating from the layers cross-cut the tectonic foliation at a low angle. Fragments of undeformed labradorite xenocrysts are common in these veins. Plagioclase in the host anorthosite is highly deformed and recrystallized.

Veins of magnetitite or magnetite-rich melanorite from a few centimetres to 15 metres thick are quite common in this part of the HSP. These veins cut at a low angle the tectonic and primary foliation and are oriented more or less parallel to the regional tectonic fabric. Large xenocrysts of labradorite and enclaves of the host anorthosite are common. Layered anorthosite enclaves also occur in these magnetite-rich veins. The magnetite content varies from over 70 % in the oxide-rich veins to 30 to 50 % in the melanorite. Other minerals included plagioclase, orthopyroxene, hornblende, green spinel, ilmenite, pyrite, chalcopyrite, clinopyroxene, and apatite. Values of 49.5 % Fe and 16.34 % TiO_2 were obtained on one magnetite-rich vein with a thickness of 15 m. Analyses of thinner veins show that the Fe_2O_3 content varies from 50 % to 66 %, TiO_2 from 10 % to 19.2 %, and V_2O_5 from 0.24 to 0.36 %. However, due to the small scale of these veins and also to the nature of the titaniferous magnetite, they are non-economic.

Conclusion

In the Havre-Saint-Pierre anorthositic suite, two contrasting styles of Fe-Ti mineralization are present. In the eastern part of the HSP, massive hemo-ilmenite and Fe-Ti-P_2O_5 mineralizations are commonly found. Massive hemo-ilmenite deposits are interpreted as immiscible Fe-Ti rich liquid derived from a parental jotunitic or oxide-rich noritic magma, which intruded a partially crystallized andesine-bearing anorthosite. On the opposite side of the HSP, on the southwest border, Fe-Ti mineralizations are mostly composed of titaniferous magnetite and a lesser amount of ilmenite. The style of emplacement of the mineralization ranges from primary massive magnetite layers in a labradorite-bearing anorthosite to weakly discordant magnetitite and oxide-rich leuconorite veins emplaced roughly parallel to the regional tectonic fabric in the anorthosite. Finally, remobilized magnetite veins, magnetite-rich monzonitic pegmatites and magnetite veins emplaced in late ductile to brittle shear zones cut the HSP anorthosite.

References

Bergeron, R., 1986. Minéralogie et géochimie de la suite anorthositique de la région du Lac Allard, Québec : evolution des membres mafiques et origine des gites massifs d'ilménite. Unpublished PhD. Thesis, Université de Montréal, 480 pages.

Clark, T., 2000. Le potentiel en Cu-Ni ±Co ±ÉGP du Grenville québécois : exemples de minéralisations magmatiques et remobilisées. Chronique de la Recherche minière, 539, 85 – 100.

Emslie, R.F. and Hunt, P.A., 1990. Ages and petrogenetic significance of igneous mangerite-charnockite suites associated with massif anorthosites, Grenville Province. Journal of Geology, 98, 213 – 231.

Force, E., 1991. Geology of titanium-mineral deposits. Geological Society of America, Special Paper 259, 112 pages.

Hocq, M., 1982. Région du lac Allard. Ministère de l'Énergie et des Ressources, Québec. DPV-894, 99 pages.

Rose, E.R., 1969. Geology of titanium and titaniferous deposits of Canada. Geological Survey of Canada, Economic Geology Report 25, 177 pages.

Van Breemen, O. and Higgins, M.D., 1993. U-Pb zircon age of the southwest lobe of the Havre-Saint-Pierre Anorthosite Complex, Grenville Province, Canada. Canadian Journal of Earth Sciences, 30, 1453 – 1457.

Verpaelst, P., Gobeil, A., Brisebois, D., Clark, T. and Chevé, S., 2001. La géologie de la Moyenne Côte-Nord. In preparation.

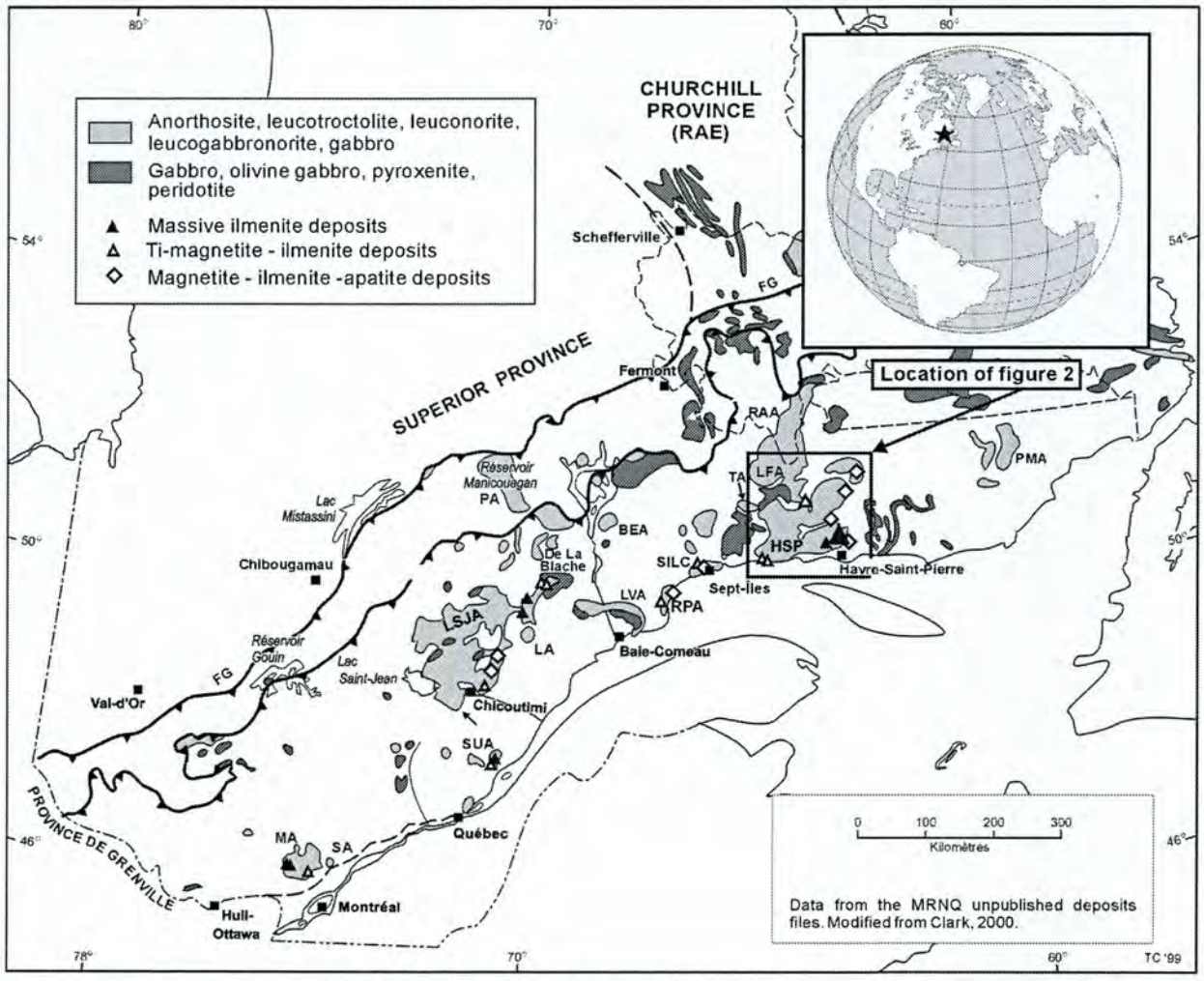

Figure 1. Location of the studied area in the Grenville Province. HSP, Havre-Saint-Pierre anorthosite; LFA, lac Fournier anorthosite; LSJA, Lac Saint-Jean Anorthosite; RPA, Rivière Pentecôte Anorthosite; TA, Tortue Anorthosite; PMA, Petit-Mécatina Anorthosite; RAA, Atikonak River Anorthosite; BEA, Berté Anorthosite; LA, Labrie Anorthosite; LVA, Lac Vaillant Anorthosite; PA, Pambrun Anorthosite; MA, Morin Anorthosite; SUA, Saint-Urbain Anorthosite; SILC, Sept-Iles Layered Complex; FG, Grenville Front.

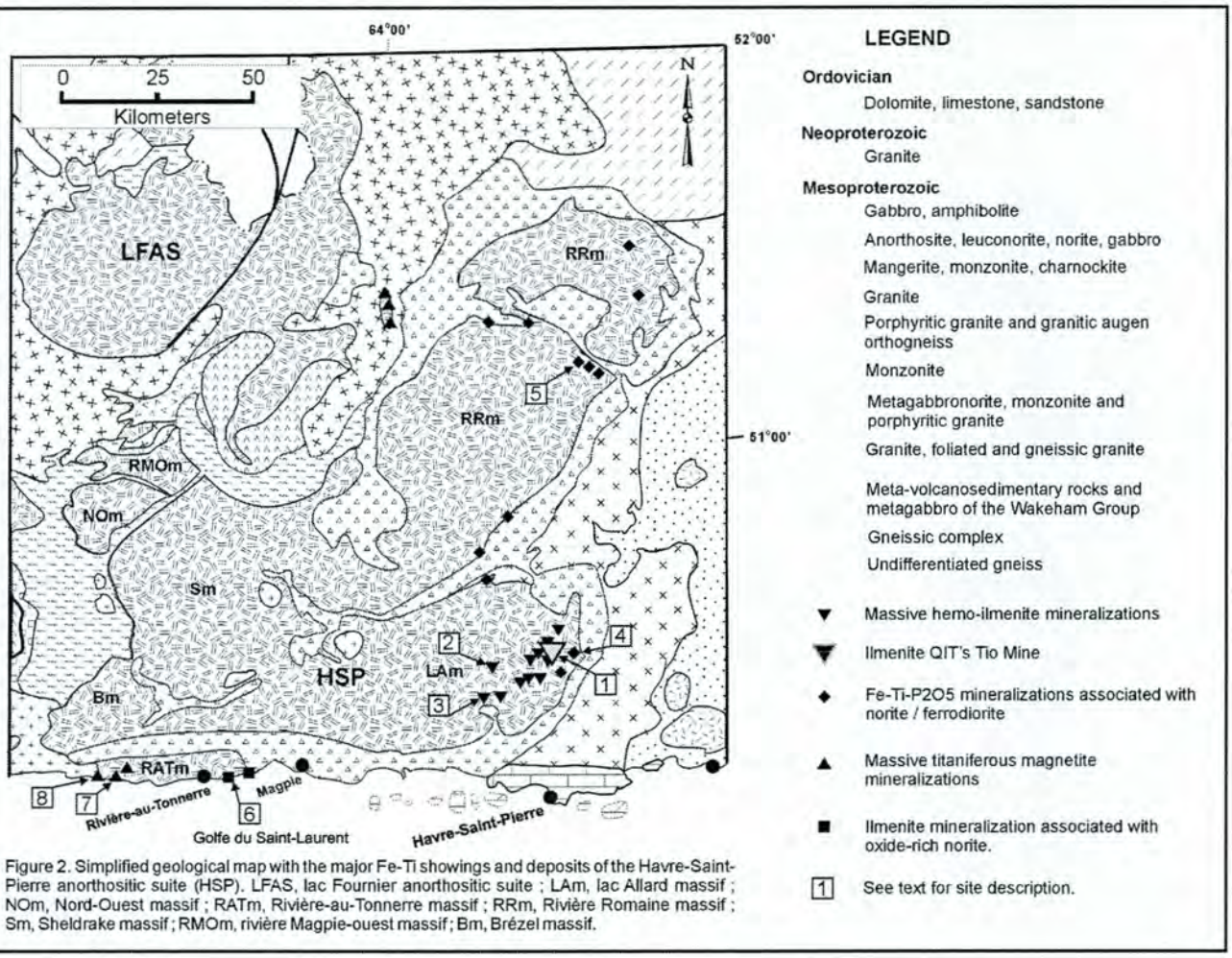

Figure 2. Simplified geological map with the major Fe-Ti showings and deposits of the Havre-Saint-Pierre anorthositic suite (HSP). LFAS, lac Fournier anorthositic suite ; LAm, lac Allard massif ; NOm, Nord-Ouest massif ; RATm, Rivière-au-Tonnerre massif ; RRm, Rivière Romaine massif ; Sm, Sheldrake massif ; RMOm, rivière Magpie-ouest massif ; Bm, Brézel massif.

Robinson P, Kullerud K, Tegner C, Robins B & McEnroe SA:

Could the Tellnes ilmenite deposit have been produced by in-situ magma mixing?

Peter Robinson [1,4], Kåre Kullerud [2], Christian Tegner [1], Brian Robins [3] & Suzanne A. McEnroe [1]

[1] Geological Survey of Norway, N7491 Trondheim, Norway. (peter.robinson@ngu.no, christian.tegner@ngu.no, suzanne.mcenroe@ngu.no)
[2] Inst. for Biology and Geology, University of Tromsø, N9037 Tromsø, Norway (kaarek@ibg.uit.no),
[3] Dept. of Geology, University of Bergen, N5007 Bergen, Norway (brian.robins@geol.uib.no)
[4] Dept. of Geosciences, University of Massachusetts, Amherst, MA 01003, USA.

Wilson *et al.* (1996) presented convincing arguments that ilmenite-rich cumulates in the Layered Series of the 930 Ma Bjerkreim-Sokndal Intrusion formed by mixing residual magma with recharging more primitive jotunitic magma of related composition. During mixing, exemplified by rocks at the contact between Megacyclic Units III and IV, the hybrid magma temporarily found itself within the "volume" of single-phase ilmenite crystallization, resulting in a burst of ilmenite precipitation. After crystallisation of ilmenite, the magma returned to co-

saturation with plagioclase and orthopyroxene. These mixing events were sufficiently common to produce dark layers 10-20 cm thick with modal ilmenite amounts of 50% or more, that extended across the floor of a chamber having a horizontal area of ~625 km^2. One such 10 cm layer could contain ~31,250,000 m^3 of ilmenite.

Modal and cryptic layering in the Tellnes Ilmenite Norite "dike" (an elongate body with steep-sided lopolith-like cross section) is extremely hard to detect. Nevertheless bulk chemical studies of thousands of mine samples and cores plus mineral analyses from selected specimens indicate a range of silicate compositions (An37 to An51, En65 to En81, Fo71-76) similar to but exceeding the range encountered in the regression at the base of MCU IV of the Bjerkreim-Sokndal (An44 to An54, En68 to En76, Fo75). In Tellnes, the most evolved rocks occur near margins of the intrusion and the most primitive rocks in the interior. In the Bjerkreim-Sokndal intrusion, the regression takes place over 100 meters of layered rocks across the MCU III-IV boundary.

The similar compositional ranges in the two intrusions, both associated with concentrations of ilmenite, suggest a parallel origin from similar magmas and possibly similar mixing events but within chambers of different shape. A common magma source cannot be ruled out by recent geochronology (Schärer *et al.*, 1996), but contact relationships suggest it is unlikely. Geochronology shows ages near 930 for several of the surrounding anorthosites and a mangerite dike in the Tellnes fracture system cutting the Åna-Sira anorthosite, and 920±3 Ma for Tellnes. Bjerkreim-Sokndal intrudes and has inclusions of surrounding anorthosites, and shares a later ductile fabric as well as a thermal contact aureole with them. The thermal model of Schumacher and Westphal (2001) suggests a hiatus of 3-4.5 m. y. between the anorthosites and the younger Bjerkreim-Sokndal intrusion. For Tellnes we suggest that magma mixing and precipitation took place within a narrow, steep-sided chamber. Earlier (Robinson *et al.*, 2001), we suggested that the ilmenite-rich cumulates formed either as a consequence of density sorting or by in-situ crystallization along the walls. We also suggested that magma recharge took place through a conduit at the end or side of the chamber so that precipitate ilmenite, with lesser pyroxene and plagioclase, all of gradually changing composition, accumulated on the bottom and walls of the chamber, whereas the residual liquid moved laterally upward. This hypothesis for concentration of ilmenite in Tellnes called a) upon a process well documented in the same district, b) upon jotunitic (monzodioritic) magma which has produced chemically similar precipitates, and c) not upon an unusually oxide-rich magma, occurrence of which is not supported by experimental studies (Skjerlie *et al.* 2001, Lindsley, 2001).

Since our initial proposal we have considered genetic models in more detail and done more evaluation of available mineralogical and whole-rock data. A first model was to pump a large volume of primitive magma into a chamber already containing a large volume of evolved magma, along lines similar to the recharge event in the Bjerkreim-Sokndal magma chamber. This major mixing would then place a mixed liquid well into the ilmenite field of primary crystallization, allowing massive showers of ilmenite precipitate to fall to the floor of the chamber. This model of a single, though possibly progressive mixing, would have two consequences: 1) The great volume of ilmenite would have a limited range of composition consistent with precipitation from a single mixing event, and 2) The showers of ilmenite would presumably have fallen into more evolved magma, trapping interstitial liquids that would be expected to react with the cumulate grains. We began to explore the composition relations of the ilmenite itself, and to seek evidence of a trapped liquid component either in mineral composition data or in bulk rock analyses. We also remained cautious with mineral chemical data because of the possibilities for re-equilibration depending on grain locations within individual samples.

The perceptive reader will understand that the mineral chemical data already given is hardly compatible with a simple mixing model, and our further explorations only made matters worse. $Mg/ (Mg + Fe^{2+})$ ratios of ilmenite, despite a certain scatter due to local re-equilibration, give a range from ~ 0.01 (1% geikielite component) up to 0.20 (i.e. 20% geikielite) and this range

correlates well with the most magnesian orthopyroxene in each rock from En 67 to En 81.5. Ca / (Ca + Na) ratios in plagioclase, like ilmenite, also show some scatter, but the most sodic plagioclases (An 36-43) occur with ferrous pyroxenes (En 67-68), and the most calcic plagioclases (An 44-50) occur with the most magnesian pyroxenes (En 77-81).

The bulk-rock analyses are all averages of intervals several meters thick and cause doubt that such rock analyses can be compared to mineral analyses from a single thin section within that interval. However, Kullerud (1994) made a careful study of smaller sampling intervals and showed that there are very few places in the ore body where there are abrupt changes in composition, so we feel strongly justified in comparing bulk chemistry of ore intervals with mineral compositions in single thin sections. Because the amount of ilmenite controls all other elemental abundances, we found no meaningful plots of wt.% TiO_2 versus any other oxides, but learned much from plots of TiO_2 versus mineral compositions or some mineral normative components in the bulk rock samples. In TiO_2 versus measured En in orthopyroxene, there is a distinct positive correlation from 7% TiO_2, En 65-68 up to 25% TiO_2, En 77-81. Two sample intervals with 28 and 33% TiO_2 both contain En 80-81. In TiO_2 versus measured Mg/ (Mg + Fe^{2+}) ratios of ilmenite, there is a good correlation from 7-14% TiO_2, geikielite 0.01-0.04 up to 25% TiO_2, geikielite 0.10-0.19. The two samples with 28 and 33% TiO_2 contain both the most uniform and most magnesian ilmenite at 0.18-0.20. In TiO_2 versus measured An in plagioclase, there is a good correlation from 7% TiO_2, An 37-41 up to 25% TiO_2, An 44-50. The two samples with 28 and 33% TiO_2 contain plagioclase An 46 and 47.5 respectively, well below the most calcic extreme, possibly due to a trapped liquid component.

Because there were no bulk analyses for FeO/Fe_2O_3, we restricted norm calculations to the ratio An/ (An+ Ab). In intervals with analyzed minerals, normative plagioclase correlates nearly linearly with En %, from 0.41, En 67, to 0.54, En 81, except that the most calcic plagioclase at 0.59 is also in a rock with En 81. In the same sample intervals with analyzed minerals, there is a nearly perfect linear positive correlation in bulk analyses between wt. % TiO_2 and normative plagioclase. In the larger data set of all ore analyses, there is a similar linear relation, with a handful of analyses above An 55, forming two diverse trends.

These new results militate strongly against crystallisation of ilmenite produced from a single hybrid magma, and also show no evidence of an important component of evolved liquid trapped between rapidly accumulating ilmenite primary precipitate grains. Is there then any remaining way to apply a magma mixing model to the Tellnes Intrusion? We think that there is, but it requires a special set of circumstances, perhaps not so difficult to achieve in nature, and plumbing that will allow it to happen.

Our proposal involves an adjacent or underlying magma chamber of fairly wide aspect ratio which is stratified with relatively evolved, cool and light magma at the top and with more primitive, hotter, and denser jotunitic magma at the bottom (Campbell, 1996). There is strong evidence for the existence of such chambers in layered intrusions such as Fongen-Hyllingen (Wilson and Sorensen, 1996). In the case of the Tellnes district, the Bjerkreim-Sokndal Intrusion was probably stratified (Wilson *et al.*, 1996). The key to our solution is that such a discontinuously stratified magma chamber existed in the area that was able to maintain a strong chemical and thermal gradient.

Eventually the top of the zoned chamber began to be evacuated and injected turbulently into the present Tellnes chamber. As each pair of adjacent magma layers were evacuated and mixed with each other, the resulting hybrid magma was temporarily in the ilmenite field of primary crystallization, although perhaps not staying there for long. When not singly saturated with ilmenite, the magmas would be multiply saturated with pyroxene and plagioclase with close to equilibrium compositions. As the mixing magmas moved along the Tellnes chamber, probably from the southeast (Bolle *et al.*, 2001) and across its floor, primary precipitate ilmenite, commonly in much more than cotectic proportions would have a tremendous density advantage over the sinking of primary precipitate plagioclase and pyroxene, but they would also be trapped locally. The great density effect of ilmenite would also provide for very efficient

expulsion of trapped liquid. As more and more primitive magmas from the subjacent zoned chamber were tapped and mixed into the Tellnes chamber, phase relations dictate that the cotectic proportion of ilmenite would increase even in areas of multiphase saturation, while at the same time ilmenite and all other precipitate phases would become chemically more primitive, so that the most ilmenite-rich layers would have precipitated from the last and most primitive part of the subjacent stratified intrusion. Meanwhile most of the residual liquids and many of the lighter precipitate crystals would have risen or migrated laterally away from the deepest part of the Tellnes trough, to locations today eroded away. We speculate that the evolved rocks at the top of the intrusion represent material that crystallised in situ on the roof during the injection process, but we still find it conceptually difficult that such rocks would still retain a moderately high ilmenite content.

The model presented here is an attempt to account for all of the known attributes of the Tellnes Intrusion, and uses processes and jotunite magmas that are documented either in the district or elsewhere, including evidence for precipitation from a relatively low-Ti magma (Skjerlie *et al.*, 2001). It needs extensive further documentation in terms of more detailed mineralogical and petrological studies of other core samples, including detailed modal and textural studies to identify primary precipitate and trapped liquid components. Such studies should provide further predictive tools of benefit for future of mining operations and ore beneficiation at Tellnes. The model also requires application of more quantitative magma dynamics.

References

Bolle, O.; Diot, H.; Lambert, J-M.; Launeau, P.; and Duchesne, J-C., 2001, Emplacement mechanism of the Tellnes ilmenite deposit (Rogaland, Norway) revealed by a combined magnetic and petrofabric study (abstract). This Volume.

Campbell, I. H., 1996, Fluid dynamic processes in basaltic magma chambers. In Cawthorn, R. G., Editor, Layered Intrusions. Elsevier Science, 45-76.

Kullerud, K., 1994, MgO-innhold i ilmenitt fra Tellnesforekomsten. Avsluttende Rapport, Institut for Biologi og Geologi, Universitet i Tromso, 14 p., 18 figures, 41 p. of tables.

Lindsley, D.H., 2001, Do Fe-Ti oxide magmas exist? Geology: Yes; Experiments: No! (abstract). This Volume.

Robinson, P.; Robins, B.; Kullerud, K.; Tegner, C.; and McEnroe, S. A., 2001, Formation of ilmenite-rich cumulates by magma mixing: Comparisons of mineral chemistry in the layered series of the Bjerkreim-Sokndal Intrusion and the Tellnes Ilmenite Norite, Norway. Journal of Conference Abstracts, v. 6, no. 1, p. 770.

Schumacher, J. C. and Westphal, M., 2001, Thermal modelling, reaction textures and mineral zoning in granulites surrounding the Rogaland anorthosite province (abstract). This Volume.

Schärer, U., Wilmart, E., and Duchesne, J. C. (1996) The short duration and anorogenic character of anorthosite magmatism: U-Pb dating of the Rogaland complex, Norway. Earth and Planetary Science Letters, 139, 335-350.

Skjerlie, K. P., Kullerud, K., and Robins, B., 2001, Preliminary melting experiments on the Tellnes ilmenite norite from 0.5 to 1.2 GPa, implications for the composition of cumulus melt (abstract). This Volume

Wilson, J. R., and Sorensen, H. S., 1996, The Fongen-Hyllingen Layered Intrusive Complex, Norway. In Cawthorn, R. G., Editor, Layered Intrusions, Elsevier, Science, 303-329.

Wilson, J. R., Robins, B., Nielsen, F. M., Duchesne, J. C. and Vander Auwera, J. (1996) The Bjerkreim-Sokndal Layered Intrusion, Southwest Norway. In Cawthorn, R. G., Editor, Layered Intrusions. Elsevier Science, 231-255.

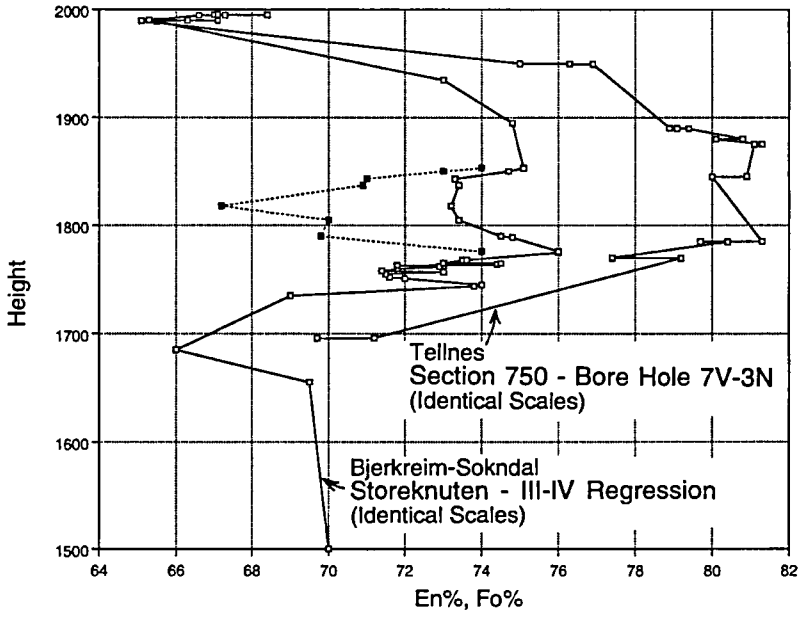

Figure 1. Compositions measured by electron probe of orthopyroxenes (open symbols) and of olivines (closed symbols) from the MCU III-IV boundary region at Storeknuten, on the west limb of the Bjerkreim lobe of the Bjerkreim-Sokndal Intrusion. Vertical scale gives elevations in meters in a measured section. All data is from J. R. Wilson and Frank Nielsen illustrated in the Guidebook Article for Day 2 of the Geode Meeting. Superimposed on this are the electron probe analyses of orthopyroxene from deep bore hole 7V-3N from Kullerud (1994). These are plotted using **the same** height and composition scales as the Storeknuten section, but vertically positioned to show the parallel nature of the two magma regressions.

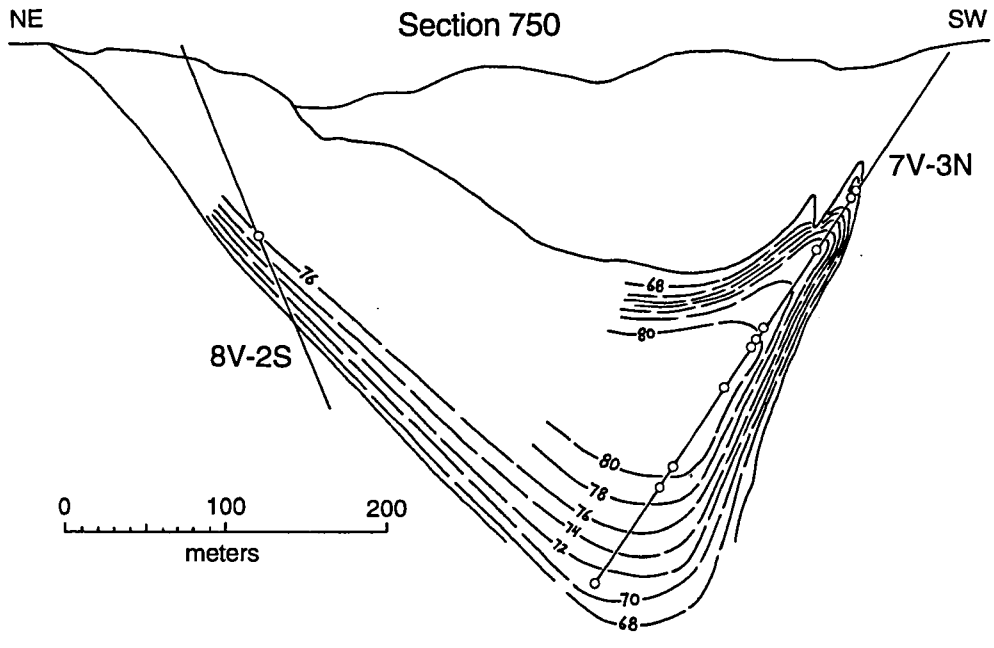

Figure 2. Vertical section 750 from northeast to southwest across the Tellnes ore body showing compositions of analyzed orthopyroxenes in bore holes 7V-3N and 8V-2S. Compositions were contoured by hand according to authors' prejudice.

Figure 3. Simple phase diagram illustrating hypothetical ilmenite -plagioclase cotectic boundary. The boundary is curved. As a result of this curvature, when chemically evolved cotectic magma A is mixed with primitive cotectic magma B, the resulting mix lies entirely within the ilmenite field of primary crystallization. This mixed magma, in this case produced in a single mixing, will precipitate only ilmenite, moving directly away from the ilmenite composition until reaching the cotectic boundary where plagioclase rejoins ilmenite as a primary precipitate. This sense of cotectic curvature is essential to produce one-phase ilmenite precipitation by magma mixing. A corollary is that the more primitive magmas (such as B) must precipitate a higher cotectic proportion of ilmenite than the more evolved magmas (such as A).

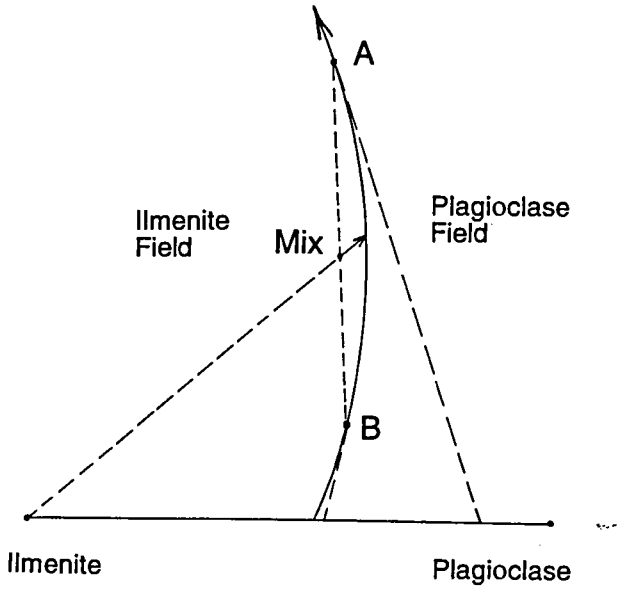

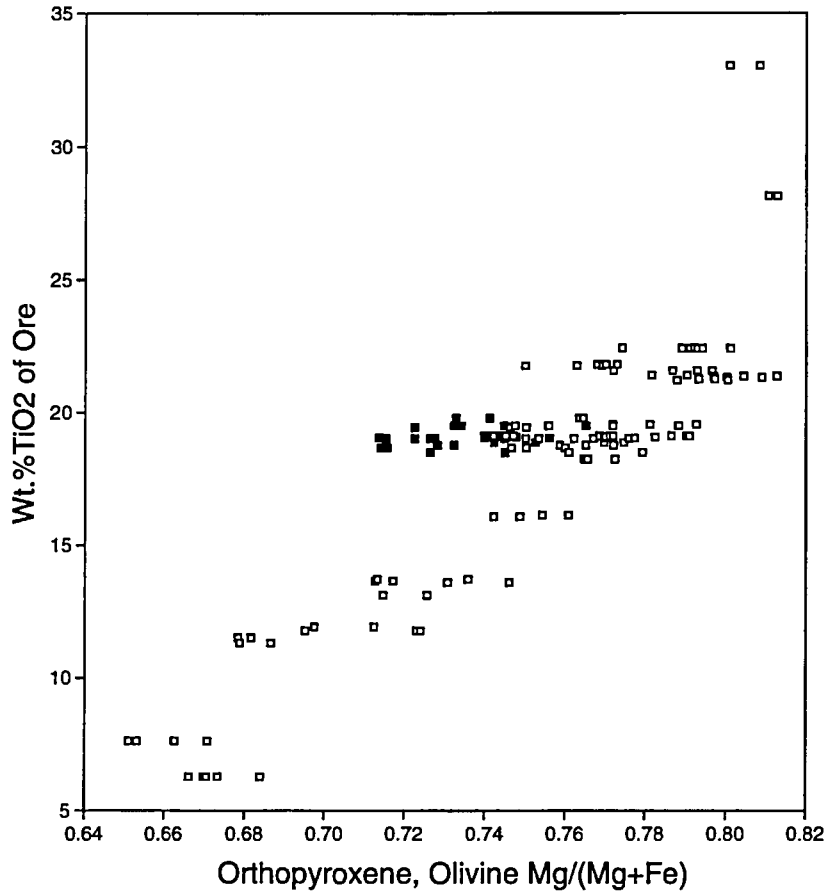

Figure 4. Graph showing all composition data for orthopyroxene (open symbols) and for olivine (closed symbols) in the Tellnes Intrusion plotted against wt. % TiO_2 of the ore interval containing the probe section. There is a strong positive correlation between pyroxene composition in Mg / (Mg + Fe) and wt. % TiO_2 of the ore, except for the two most TiO_2-rich samples where the pyroxene composition remains at the maximum value of 0.80-81.

Figure 5. Phase diagram like Figure 3 illustrating a curved ilmenite - plagioclase cotectic boundary necessary to produce one-phase ilmenite precipitation. Instead of a single mixing event, as in Figure 3, this diagram illustrates the principle of multiple mixing events caused by turbulent mixing in a dike-like chamber of successive pairs of magma batches that had been progressively evacuated from a chemically, thermally and density stratified subjacent magma chamber. While the net distance of shift into the ilmenite field of primary crystallization is less than in Figure 3, there is a still an opportunity for excess ilmenite precipitation, and in addition, during returns to cotectic precipitation of silicates, the silicate compositions will reflect magma compositions very close to those that precipitated the ilmenite.

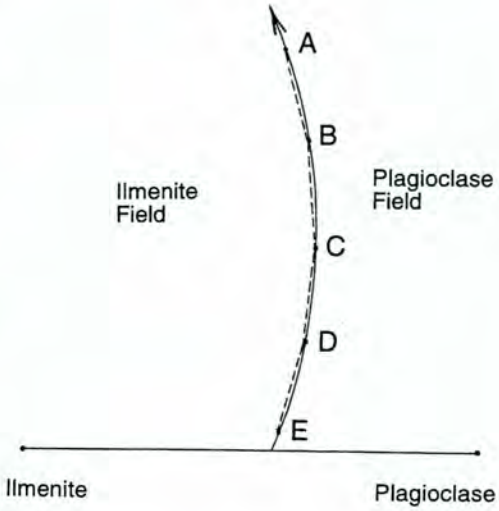

Schiellerup H, Lambert DD & Robins B:

Sulfides in the Rogaland Anorthosite Province

Henrik Schiellerup [1], David D. Lambert [2] & Brian Robins [3]
[1]Department of Geology and Mineral Resources Engineering, Norwegian University of Science and Technology, 7491 Trondheim, Norway.
[2]Division of Earth Sciences, National Science Foundation, Arlington, VA 22230, USA.
[3]Department of Geology, The University of Bergen, N5007 Bergen, Norway.

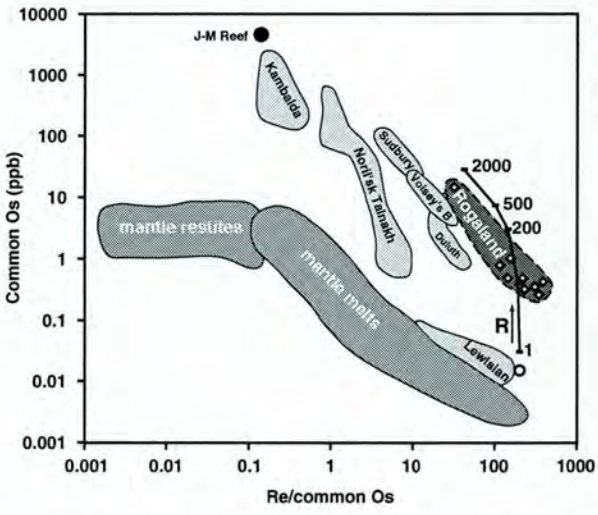

Fig. 1. Common Os (Os concentration at the time of formation) vs. Re/Os ratio in Rogaland sulfides compared to major magmatic sulfide deposits and mantle melt compositions. Diagram and global data fields adopted from Lambert et al. (1999). All sulfide data have been normalized to 100% sulfide. Inferred parental magma composition shown with open circle.

The Rogaland Anorthosite Province in Southwest Norway is a composite massif-type anorthosite province consisting of a number of anorthositic plutons, mafic, dominantly jotunitic or noritic intrusions, as well as a collection of granitoid bodies. Many mafic intrusions form significant deposits of Fe-Ti oxides.

Sulfide occurrences in Rogaland may be divided into two types. 1: minor disseminated, lumpy or semi-massive occurrences within anorthosite bodies, and 2: disseminated sulfides hosted by noritic or orthopyroxenitic cumulates believed to derive from jotunitic magmas. Type 2 occurrences include a number of noritic intrusions that contain dispersed sulfide droplets, but only in one instance did a concentration process accompany the sulfide saturation, to form a significantly sulfide-enriched cumulate.

Type 1 deposits are hosted by anorthosite plutons, but usually occur in spatial association with slightly more-evolved noritic or even pyroxenitic cumulate pockets, pegmatite dykes or intrusions. The sulfide occurrences are not confined to marginal sites, but may be found scattered throughout the anorthosite bodies. Re-Os and other chalcophile element modeling (Fig. 1) suggest that all anorthosite-hosted deposits, except one, are characterized by very low R-factors (ratio between amounts of silicate melt in effective equilibrium with the sulfide melt). The low R-factors (~50) imply that little interaction between silicate and exsolved sulfide melt took place. The scattered occurrence, low R-factors and association with lower-temperature cumulates, imply that the sulfide melt exsolved from the interstitial silicate melt, at a late stage in the anorthosite formation. Elevated R-factors (~500) in anorthosite-hosted occurrences are only observed in the Fossfjellet deposit located in the deformed margin of the Egersund-Ogna anorthosite.

Sulfide droplets are ubiquitous in all major mafic intrusions in Rogaland, which must have been near-saturated in sulfur prior to emplacement. Fractional segregation generally dispersed sulfide melt droplets evenly in the mafic cumulates, and only in the Bjerkreim-Sokndal Layered Intrusion did sulfides segregate to form a significant stratiform type 2 deposit in a noritic intrusion. An elevated R-factor (3-500) is required to explain the composition of this occurrence.

Isochronous relationships among Fe-Ti rich norites, anorthosites and contained sulfides have been recorded by Re-Os and Sm-Nd isotopes, that yield isochron ages of 917±22 and 914±35 Ma respectively (Fig. 2). These ages strongly corroborate existing U-Pb dating in the province (Schärer et al., 1996), and the existence of isochrons is good evidence that the source characteristics for the mafic intrusions, anorthosites and sulfides are similar. Rare marginal chills, correlated mineral chemistry, restricted initial Sr isotope ratios and phase equilibrium considerations imply that all mafic rocks are cumulates formed at various stages during the differentiation of jotunitic magmas. In addition, experimental studies have recently shown that the Rogaland anorthosite bodies may also be derived from jotunitic magmas (Longhi et al., 1999). R-factor processes and modal variations are indeed able to account for all compositional variability among the sulfides, whether hosted by anorthosite or mafic intrusions.

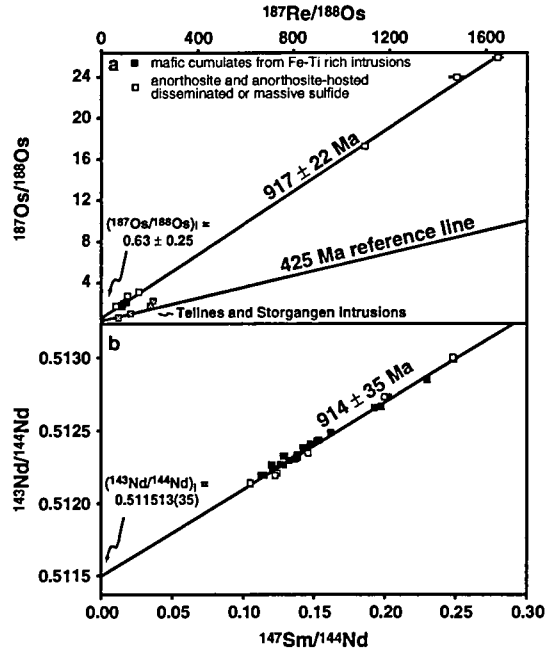

Fig. 2. Regional Re-Os and Sm-Nd isochron diagrams. 10 Re-Os samples form a model 3 isochron with an elevated MSWD of 519. Data from the Storgangen and Tellnes intrusions form a poorly defined trend close to the Caledonian 425 Ma reference line. 30 Sm-Nd samples yield a model 3 isochron with an MSWD of 27. Initial ratios correspond to $\gamma_{Os} = +419$ and $\varepsilon_{Nd} = +1.47$.

The late sulfide saturation in the anorthosites, the appearance of sulfides in lower-temperature mafic intrusions, and the compositional similarities, suggest that sulfide saturation in the anorthosites and mafic intrusions resulted from the differentiation of silicate magmas of comparable compositions. No external source for sulfur seems to be required.

References

Lambert, D.D., Foster, J.G., Frick, L.R. and Ripley, E.M. (1999). Re-Os isotope geochemistry of magmatic sulfide ore systems. In: D.D. Lambert and J. Ruiz (eds.) "Application of Radiogenic

Isotopes to Ore Deposit Research and Exploration". *Rev. Econ. Geol.* (Soc. of Econ. Geol.) **12**, 29-57.
Longhi, J., Vander Auwera, J., Fram, M.S. and Duchesne, J.C. (1999). Some phase equilibrium constraints on the origin of Proterozoic (massif) anorthosites and related rocks. *J. Petrol.* **40**, 339-362
Schärer, U., Wilmart, E. and Duchesne, J.C. (1996). The short duration and anorogenic character of anorthosite magmatism: U-Pb dating of the Rogaland Complex, Norway. *Earth Planet. Sci. Lett.* **139**, 335-350

Schumacher JC & Westphal M:

Thermal modelling of the metamorphism of the Rogaland granulites

John C. Schumacher [1] and Mathias Westphal
1 University of Bristol, Dept. of Earth Sciences, Wills Memorial Building, Queen's Road, Bristol BS8 1RJ, UK, j.c.schumacher@bristol.ac.uk

The Proterozoic Egersund Anorthosite Complex is composed of anorthosite and related rock types, which intrude intercalated charnockitic and garnetiferous migmatites. The highest metamorphic temperatures are spatially associated with the intrusion, and previous workers recognized high-temperature mineral isograds for pigeonite-in, osumilite (OSM)-in and orthopyroxene (OPX)-in. The P-T conditions at a distance of 16 km from the contact are about 700 °C and 5 kbar and increase to more than 1000 °C and 5 kbar at 2.5 km.

The high-temperature metamorphism in the country rocks found near the contacts of the northeastern part Rogaland intrusive complex (surface area of about 1000 square km) cannot be explained by assuming the heat source was a simple, single-phase of intrusion. In order to obtain the observed metamorphic temperatures and isograd distribution, thermal modelling indicates that the heat source must have had at least two main phases that were separated by a hiatus of about 3 - 4.5 m.y. In this model, emplacement and crystallization of the anorthosite (areal extent: 30 x 40 km) produces a thermal gradient (750-600 °C) in the country rocks. While this thermal gradient is developing, a second, smaller intrusion (Bjerkreim-Sokndal lopolith, areal extent: 9 x 12 km) is emplaced at the anorthosite-country rock contact. Because the country rocks nearest the anorthosite have undergone appreciable heating, the second intrusive can provide enough thermal input to obtain the observed high-temperatures. Recent work indicates that the entire magmatic emplacement occurred over a time interval of about 10 m.y. (930-920 Ma) which is consistent with the thermal model of the metamorphism.

The P-T estimates from 5 and 10 km from the intrusive contact and data from thermal model were used to estimate cooling rates and time intervals. Maximum temperatures are 860°C and 800°C and temperatures greater than 750°C (apparent end of new garnet growth) were maintained for 4.5 to 8.5 m.y. About 5 km from the intrusion calculated post-peak cooling rates indicate a decrease from 30° to 10°/m.y. over about 7 m.y., while at about 10 km calculated post-peak cooling rates decrease from 12° to 7°/m.y. over about 7 m.y.

During this time interval, retrograde and fine-grained Gar-Qz rims formed around orthopyroxene and primary garnet (outermost 150-200μ) present in assemblages of garnet-quartz-plagioclase-orthopyroxene +/- spinel. Based on the widths of preserved zoning profiles in garnet and orthopyroxene and diffusion data, estimates of cooling rates that can be made and these agree well with the calculated temperatures and cooling rates from the model. Where garnet and orthopyroxene are in direct contact, the retrograde exchange may have continued as

long as 15-25 m.y., which resulted in more highly developed Fe/Mg-zoning at the rims (outermost 40-240μ) of both orthopyroxene and garnet.

Shumlyanskyy L:

First approach to the petrology of the Kamenka peridotite-gabbro-anorthosite intrusion

Leonid Shumlyanskyy
Institute of Fundamental Studies, P.O.Box 291 Kyiv 01001, Ukraine, E-mail: lshum@mail.univ.kiev.ua

The Kamenka layered intrusion was discovered in 1965 by A. Rolick during geological surveying. Initially on a basis of a few shallow wells it was attributed to the Korosten anorthosite-rapakivi complex, which occurs about 50 km on the southeast from Kamenka. However, strong differences in chemical composition between the leucocratic Kamenka basites and anorthosites of the Korosten complex were recognised later [0]. Some characteristics in the whole-rock chemistry of the Kamenka intrusion were used recently [0] to argue for an affiliation with paleoproterozoic continental flood basalt (CFB) province. Meanwhile, some aspects of the Kamenka composition, and its genesis remain to be explained.

Geological setting

The Kamenka peridotite-gabbro-anorthosite layered intrusion is situated on the northern edge of the Ukrainian shield, where the crystalline basement, including most of the Kamenka intrusion, is fault-bounded and down-thrown about 500 m and overlain by Phanerozoic sediments.

It is assumed from the geophysical data that Kamenka is a typical batholith with total area of about 500 km^2 and thickness of up to 1300-1500 m. The main part of the intrusion is overlain by a thick sequence of phanerozoic sediments and only a small 2-3-km-wide southern strip occurs near the surface beneath a 10-m-thick Quaternary sedimentary cover (Figure 2).

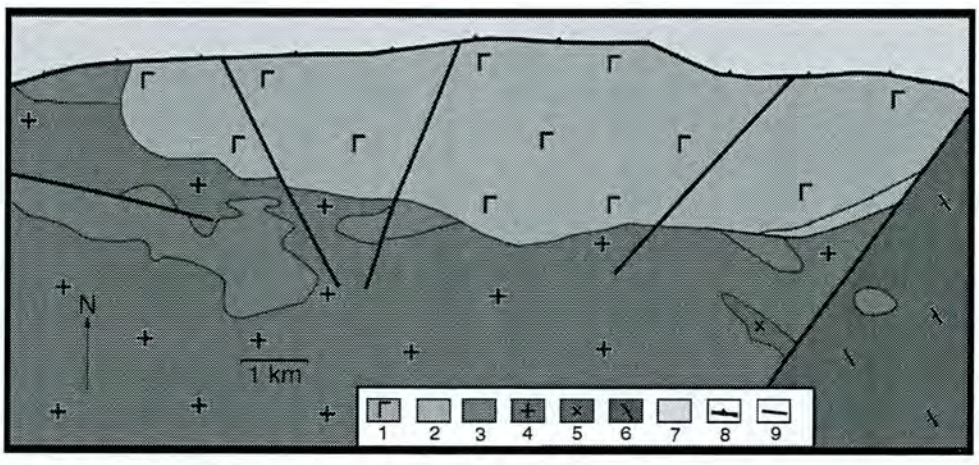

Figure 2. Sketch map of the Kamenka intrusion (after P.A. Kondratenko, 1992, unpublished report). 1 and 2 - rocks of the Kamenka intrusion: 1 - meso-leucocratic rocks, mainly leucocratic gabbro and anorthosites, 2 - peridotites and plagioclase-bearing peridotites; 3 - amphibolized country-rock gabbro; 4 - granite; 5 - diorite; 6 - metamorphic rocks (gneisses and migmatites); 7 - phanerozoic sediments of the Pripyat' depression; 8 - main latitude fault; 9 - local faults.

The Kamenka massif intrudes into 1.975 Ga granites, and their comagmatic altered basites, and into metamorphosed volcanic and sedimentary rocks. The age of the Kamenka intrusion, as

concluded from thermo-ionic emission method on zircon is 1.98 Ga. The rocks of the Kamenka intrusion are fresh, with only olivine-rich cumulates being moderately serpentinized.

Petrography of the Kamenka intrusion

Bottom (BZ) and Main Layered (MLZ) zones were distinguished within the Kamenka intrusion.

The *Bottom zone* is composed of material contaminated with acid country-rock, melano- and mesocratic mafic rocks (orthoclase-bearing gabbro and peridotite, monzonitic gabbro, monzonite, syenite etc.), which have heterogeneous, quite often inequigranular (ataxite) fabrics. Thin granite veins were noted in places within these rocks. The usual thickness of BZ is about 10 m.

Main Layered zone is composed of peridotites, plagioclase-bearing peridotites, olivine-bearing melanocratic gabbros and melanocratic troctolites, meso- and leucocratic olivine-bearing gabbroids and anorthosites. These rocks grade consecutively into each other and appear to constitute a natural line of differentiation. At least three layered units (lower, middle and upper) are recognized within the MLZ.

Peridotites and plagioclase-bearing peridotites are concentrated mainly in the lower unit. Upward they grade into more leucocratic rocks. The thickness of this unit is 200-300 m. It is noteworthy that small-scale bands of leucocratic troctolite are present even in this lowest level of the intrusion.

Alternation of melano-, meso- and leucocratic basites commonly occurs within the middle unit, which appears to be rather thick (400-600 m). Although gradual enrichment of these rocks with plagioclase is typical, sharp fluctuations in the abundance of the main minerals is quite usual.

The upper unit of the MLZ is composed of leucocratic varieties of troctolites, gabbro, gabbro-norites, and anorthosites. Small-scale bands of mesocratic troctolite and gabbro were noted in places. The observed (i.e. incomplete) thickness of this unit is 950 m.

Peridotites and plagioclase-bearing peridotites occur mainly in the lower unit of the MLZ; but, plagioclase-bearing peridotites were also noted in the middle unit of the MLZ. These rocks are composed of mainly euhedral crystals of olivine (chrysolite Fa_{22-26}) – 50-80%, which are usually serpentinized. Pyroxenes (15-50%, mainly diopside $Fs_6En_{47}Wo_{47}$–$Fs_9En_{43}Wo_{48}$ with abundant orthopyroxene less than 5%) are represented by large interstitial oikocrysts. Plagioclase-bearing peridotites contain 5-10% of interstitial plagioclase of variable composition – An_{57}-An_{77}. Interstitial biotite is a minor mineral. Usually fine grains of chrome-spinel, magnetite, titanomagnetite, and sulphides are present as opaque minerals.

Troctolites, gabbro and related rocks (olivine gabbro, gabbro-norite, norite, leucogabbro) are typical for all the units of the MLZ, especially the middle one. Plagioclase in these rocks is represented by two crystal generations. The first one forms tabular rather euhedral grains of labradorite (An_{55-64}), while the second one makes up isometric anhedral grains of andesine (An_{40-52}). Olivine (chrysolite Fa_{27-30}) forms isometric, usually euhedral grains, which are hardly serpentinized in places. For olivine-plagioclase contacts complex orthopyroxene-clinopyroxene-amphibole-biotite rims are common. Pyroxenes (augite $Fs_{14}En_{45}Wo_{41}$-$Fs_{21}En_{40}Wo_{39}$, pigeonite-augite $Fs_{32}En_{47}Wo_{21}$, and hypersthene $Fs_{37}En_{62}Wo_1$-$Fs_{47}En_{52}Wo_1$) occupy interstitial spaces between the olivine and plagioclase or form symplectitic intergrowths with opaque minerals. Late-magmatic mineral assemblages include opaque minerals, biotite, and apatite, and loclly also pyroxenes and amphibole.

Anorthosites and gabbro-anorthosites are widely distributed rocks, especially within upper unit of the MLZ, where their abundance exceeds 80%. Taking into account the fact that the upper unit of the MLZ composes more then 60% of the Kamenka's thickness, it follows that the Kamenka intrusion is predominantly anorthositic, although more melanocratic rocks, up to peridotites, also occur in significant amounts.

Anorthosites and gabbro-anorthosites are composed mainly of plagioclase (80-98%), while olivine and clinopyroxene contents do not exceed 10%, orthopyroxene and opaque minerals - up to 2-5% of each, biotite - to 1%, potassic feldspar - occasional grains. These rocks have medium- to coarse-grained, equigranular, subophitic to ophitic fabric, which are very similar to those of the more melanocratic rocks. Plagioclase is represented by labradorite An_{58-60} (up to An_{62-63} on deeper horizons), olivine - Fa_{31}, clinopyroxene - $Fs_{15}En_{50}Wo_{35}$.

Chemical composition of minerals of the Kamenka intrusion

Plagioclase is the main mineral within the rocks of Kamenka intrusion. Its composition ranges from An_{77} to An_{39}, but labradorites with An_{54-64} are predominant. The tendency to reduce plagioclases basicity from An_{66-77} in peridotites to An_{58-65}, in places - down to An_{37-52}, in leucocratic gabbro and anorthosite, is observed. Plagioclases contain 0.16-0.60% FeO, 0.05-0.27% MgO and 0.12-0.65% K_2O. Sporadic impurities of MnO (to 0.04%), Cr_2O_3 (0.01-0.21%), NiO (to 0.04%), and TiO_2 (to 0.09%) are also typical.

Olivine's composition varies from Fa22 in melano-mesocratic rocks to Fa_{31} in anorthosites. Impurities are represented by MnO (to 0.44%, increases along with iron content in olivine), CaO (0.01-0.05%), Na_2O (0.05, rare), Cr_2O_3 (0.01-0.06%), and NiO (to 0.14%).

Clinopyroxene composition varies regularly from diopside $Fs_{4-9}En_{43-47}Wo_{47-48}$ in BLZ's rocks and peridotites to low-Ca augite $Fs_{17-21}En_{37-44}Wo_{39-45}$ in gabbro and anorthosites. Usual impurities are TiO_2 (0.5-1.5%, absent in diopside), Al_2O_3 (0.7-2.5%), MnO (0.2-0.7%), and Na_2O (0.28-0.84%). The abundance of MnO and Na_2O increases along with iron content. Small amounts of K_2O (0.03-0.08%), P_2O_5 (0.01-0.03%), Cr_2O_3 (to 0.87%), and NiO (0.02-0.04%) were also found in some pyroxenes.

Rhombic pyroxene (mainly hypersthene) shows significant variations in chemical composition - from $Fs_{33}En_{63}Wo_4$ to $Fs_{47}En_{51}Wo_1$, which seem to be irregular. A wide range of impurities was found in orthopyroxenes: TiO_2 (0.03-0.18%), Al_2O_3 (to 2.34%), MnO (0.23-0.62%), CaO (to 1.33%), Na_2O (0.20-0.33%), Cr_2O_3 (to 0.87%), and NiO (0.02-0.13%). Some of these (TiO_2, Al_2O_3, MnO) increase their abundance along with increase in plagioclase abundance in the rocks, while other impurities have exactly the opposite behaviour.

Composition of the only analysed *biotite* may be expressed as $K_{1.2}(Mg_{4.82}Mn_{0.01}Fe_{1.61}Ni_{0.01})_{6.45}[Si_{5.16}Ti_{0.46}Al_{2.46}O_{20}](OH)_4$, i.e. it has high content of Ti and Mg, but is deficient in K.

Oxides (magnetite, titanomagnetite, ilmenite and chromite) and sulphides (troilite, pyrrhotite, pyrite, chalcopyrite and others) occur as accessory ore minerals [0].

The composition of *magnetite*, which is a widely distributed mineral, is close to ideal: $Fe^{3+}_{1.98}Cr_{0.02}Fe^{2+}_{1.0}O_4$; impurities of Ti (0.03%) and V (0.05%) were noted.

Troilite also has an almost stoichiometrical composition: FeS - $FeS_{1.01}$ with only small (0.1-0.2%) amount of Ni, Co, and Cu.

Monoclinic pyrrhotites have some lack of iron: Fe_7S_8, but contain marked amounts (3.2-3.7%) of nickel.

Pentlandite composition ranges from $(Fe, Ni)_8S_7$ to $(Fe, Ni)_{10}S_9$, while the Fe:Ni ratio varies from 1.07 to 0.98. Only Co (0.4-1.1%) was noted as an impurity.

Pyrite and *chalcopyrite* contain small (0.2%) amount of Ni and Co.

Chemical composition of rocks of the Kamenka intrusion

Rocks of the Kamenka intrusion are tholeiitic and were attributed recently to the paleoproterozoic continental flood basalt province [0]. Nevertheless, some features in their composition are somewhat unusual (Table 1).

Among these, are very high Mg-number, calculated as $\#Mg=Mg^{2+}/(Mg^{2+}+Fe^{2+}+Fe^{3+}\times 0.9)$, high Al_2O_3 abundance and high content of Ni and Sr. By contrast abundances of TiO_2, CaO, Cu, Zn, V, Sc, Rb, Zr, Nb, Yb, and Y are relatively low compared with typical CFB.

As mentioned above, at least three units can be recognized within the MLZ of the Kamenka intrusion. In drill holes the unit's boundaries can be seen by the appearance of peridotites and in the chemical section - by a sharp increase of Mg-number of rocks and decrease in abundance of many components (Al_2O_3, CaO and so on, Figure 3).

Variations in chemical composition are simple and may be easily predicted using the mineral composition data of the rocks. Correlation between major elements (with the exception of TiO_2 and P_2O_5) is very good. Similar good correlation can be seen between #Mg and Cr, and some other pairs, but most of the minor elements (P, Rb, Li, Ba, Zr, Cu, Sc, V, Zn) evidently connected with TiO_2, and thus accumulated in the residual melt.

First approach to the genesis of the Kamenka intrusion

The Kamenka massif formed as a result of crystallization of high-Al tholeiitic melt which belonged, probably, to a huge paleoproterozoic CFB province. Calculated average composition of the Kamenka intrusion (Table 1) shows that the melt underwent extended crystallization prior to emplacement into the ultimate chamber. Although Mg# of the average melt was rather high (0.62), at least 10% of high-Mg olivine (Fo_{91}) must be added to it in order to bring it into equilibrium with mantle residua. Meanwhile, the high Al_2O_3/CaO ratio (2.15 in average) provides evidence of extended crystallization of clinopyroxene or clinopyroxene plus plagioclase (in addition to olivine) *en route* to the ultimate chamber.

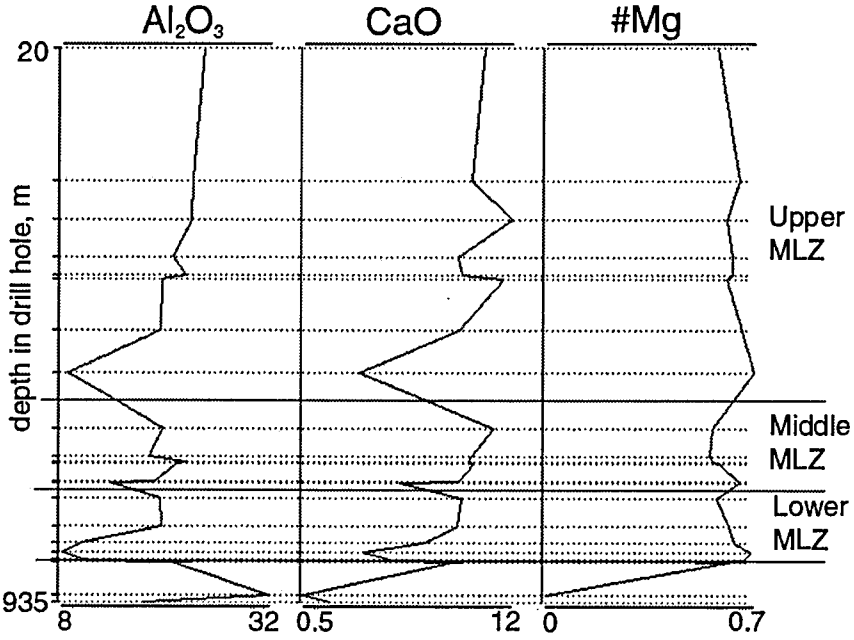

Figure 3. Variations in Al_2O_3 and CaO abundances and Mg-number within the drill hole, which crossed the Kamenka intrusion at its maximal thickness. Three units can be distinquished within the main layered zone. Approximate boun-daries between units are shown with solid horizontal lines. The bottom zone is not shown. Country rocks (below MLZ) are granites.

Table 1. Mean composition of different rock types within the Kamenka intrusion and its average composition

	Peridotites	Melanogabbro, olivine gabbro, troctolite	Al-rich troctolite, gabbro and norite	Leucogabbro, anorthosite	Average composition
SiO_2	38.96	43.54	47.70	47.97	46.85
TiO_2	0.51	0.77	0.86	0.38	0.50
Al_2O_3	7.02	12.80	19.34	21.47	19.27
Fe_2O_3	4.70	3.67	2.19	2.20	2.52
FeO	9.85	9.29	6.95	4.83	5.94
MnO	0.19	0.16	0.11	0.086	0.10
MgO	25.32	16.84	8.99	7.91	10.19
CaO	3.65	6.09	9.02	9.95	8.98
Na_2O	0.92	2.02	2.57	2.94	2.65
K_2O	0.25	0.60	0.56	0.48	0.49
P_2O_5	0.15	0.18	0.19	0.09	0.12
SO_3	0.25	0.32	0.29	0.12	0.17
CO_2	0.24	0.30	0.27	0.23	0.28
H_2O	0.18	0.15	0.08	0.09	0.11
LOI	8.10	3.78	1.23	1.33	2.04
N	15	22	26	55	-
Ni	840	610	290	250	333
Cu	70	52	25	22	29
Co	113	98	85	52	66
Zn	126	95	80	55	68
Cr	570	543	177	200	256
V	60	168	140	70	89
Sc	7	15	15	10.5	11
Li	15.5	32	23	14	17
Rb	1.7	9	12	6	7
Sr	200	433	613	653	593
Ba	152	345	425	255	282
Ga	7	24	16.5	14	15
Zr	40	76	73	53	57
Nb	9	9	7.7	9.3	9
La	12	30	42	23	26
Yb	0.9	1.5	1.7	1.2	1.3
Y	12	12	18	14	14
#Mg	0.71	0.64	0.57	0.61	0.62
Al_2O_3/CaO	1.92	2.10	2.14	2.16	2.15

It is noteworthy that Kamenka's average composition lies on an extension of the differentiation trend, defined by paleoproterozoic CFB dykes (Figure 4). This trend appears to be due to precipitation of an assemblage of An_{92}+Fo_{79} in the proportion 1.5:1.0, which suggests shallow (up to 10km) crystallization [0]. This trend can be extended to the high-#Mg composition (if an assumption of precipitation of 60% of An_{92} and 40% of Fo_{79} *en route* from the mantle source is made), however this calculation results in a "primary" composition that is impossible: for example, TiO_2 abundance would lie below 0.

Thus, at least a two-stage evolution must be invoked for the Kamenka intrusion. The first stage involved crystallization of high-Mg olivine along with clinopyroxene at depth, while the second stage involved precipitation of Pl+Ol in a shallow intermediate chamber, and terminated with at least three injections into Kamenka's ultimate magma chamber.

Although a genetic link between the Kamenka intrusion and other intrusions of the Paleoproterozoic CFB province seems to be clear, the *origin* of the melt with the observed chemical features is still unexplained.

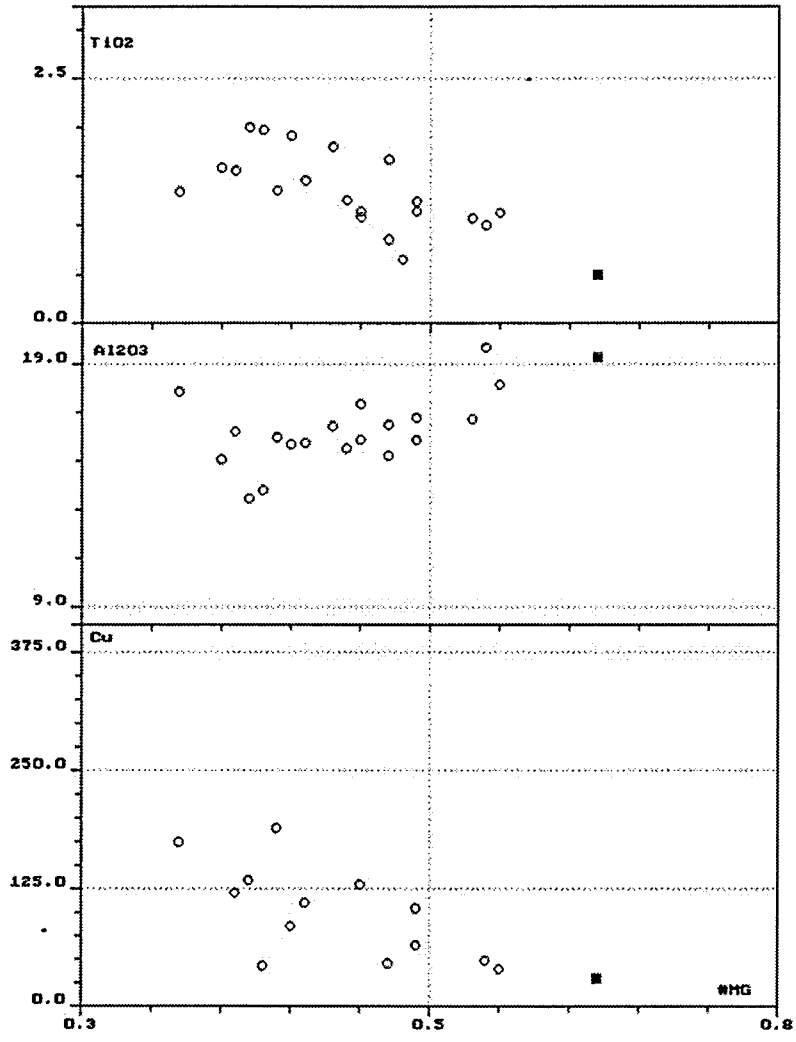

Figure 4. Diagrams, which show variations of TiO_2, Al_2O_3 and Cu abundances *vs.* #Mg in intrusions of the Paleoproterozoic CFB province. Open circles – dolerite dikes, solid square – Kamenka massif.

Extended (up to 30-40%) partial melting of a dry pyrolite source at a depth of 70-100 km is usually accepted [0] for tholeiite-picrite liquid that is believed to be primary for continental tholeiites. Known partition coefficients and assumed mantle composition [0] predict that the abundances of most of trace elements should be much higher than observed. Supposed precipitation of an olivine plus clinopyroxene assemblage and possible contamination with crustal material *en route* can only increase abundances of most incompatible minor elements. Three melt composition models, which include 1) simple equilibrium 5% partial melting of undepleted mantle; 2) simple equilibrium 30% partial melting of depleted in model 1 mantle, and 3) model 2, complicated by precipitation of 10% of olivine and contamination with product of 3% partial melting of lower crust, were calculated. Compared with the Kamenka's average melt composition all models reveal similar features: 1) the abundances of Ba, Sr, Co, and Ni in the Kamenka's melt are much higher then predicted in models; 2) abundances of Rb, Zr, Y, Sc, V, Zn, Cu, and Cr are much lower than predicted. Among them only the high content of Ba and Sr can be explained by contamination with crustal material, whereas low Cr content may be attributed to extraction of clinopyroxene or spinel. It should be noted here that the Sr content of the Kamenka rocks is at least a factor of two higher than typical for other CFB rocks and require a special explanation. Neither incompatible elements, such as Rb, Zr, Y, Sc, V, Zn, nor compatible (Ni) or partly-compatible (Co) fit the models. It is especially difficult to explain the high Ni content, which may appear due to sulphur presence in the melt, coupled with extremely low Cu abundance.

It seems to the author that any reasonable explanation could not be found presently, to fit the observed abundances of minor and major (especially high content of Al and low contents of Ti and P) elements. Extended geochemical investigations are required.

References

Kogut K.V., Galiy S.A., Skobelev V.M. et. al. Petrology and nickel mineralization of the Kamenka massif, north-western part of the Volynian block of the Ukrainian shield. Geol. Zhurnal, 1992., N 6, pp. 109-118 (In Russian).

Zinchenko O.V., Shumlyanskyy L.V., Molyavko V.G. Continental flood basalt province at the south of the East-European craton, its composition, volume and stratigraphic position. In: Geology and stratigraphy of the precambrian deposits of the Ukrainian shield, 1998., pp. 102-104.

Skobelev V.M., Yakovlev B.G. et al. Petrogenesis of the nickel-bearing gabbroic intrusions of the Volynian megablock of the Ukrainian shield. Nauk. Dumka publisher, 1991. – 140 p.

Green D.H. A review of experimental evidence on the origin of basaltic and nephelinitic magmas// Phys. Earth. Planet. Interiors, 1970, **3**, p. 221-235.

Frey F.A., Green D.H. and Roy S.D. Integrated models of basalt petrogenesis: a study of quartz tholeiites to olivine melilitites from south-eastern Australia utilizing geochemical and experimental petrological data// J.Petrology, 1978, **19**, p. 463-513.

Skjerlie KP, Kullerud K & Robins B:

Preliminary melting experiments on the Tellnes ilmenite norite from 0.5 to 1.2 GPa, implications for the composition of intercumulus melt

Kjell P Skjerlie[1], Kåre Kullerud[1] and Brian Robins[2]
[1]Department of Geology, University of Tromsø, 9037 Tromsø
[2]Department of Geology, University of Bergen, Allegaten 41, 5017 Bergen

There is general agreement that the Tellnes ilmenite norite is a magmatic intrusion that was emplaced at ca 0.5GPa as a cumulate with minor amounts of intercumulus melt. The composition of the interstitial melt is unknown, but it has been assumed that it was Ti-rich. If the cumulate hypothesis is correct, partial-melting experiments should yield important information on the composition of the melt and equilibrium solid phases. In accordance with this line of reasoning we have performed melting experiments in a piston-cylinder apparatus on a sample of the Tellnes ilmenite norite from 0.5 to 1.2Gpa and at various temperatures.

The experiments show that the intercumulus melt at 0.5 GPa and T=1050°C (solidus <950°C) is jotunite-like with SiO_2 58.9 wt.%, TiO_2 2.2, Al_2O_3 17.9, FeO 7.2, MnO 0.1, MgO 3.2, CaO 5.3, P_2O_5 1.3, Na_2O 2.3, K_2O 1.6 and in equilibrium with abundant euhedral plagioclase (An_{50}) and ilmenite (He_{15}) together with some olivine ($Fo_{72.5}$). The interstitial glasses in near-solidus experiments are not particularly rich in TiO_2. This is not surprising and is observed in other melting experiments with residual ilmenite or rutile. The amount of a component like TiO_2 will be buffered by ilmenite or rutile, but the amount of dissolved TiO_2 in a liquid is independant of the amount of the saturated phase. The melt fraction increases with increasing pressure and temperature due to progressive dissolution of plagioclase and of ilmenite, and the melt compositions become FeTi-dioritic/FeTi-basaltic. High-temperature melting yields homogeneous glasses with very high abundances of dissolved ilmenite, showing that Ti-rich liquids can exist without the intervention of liquid immiscibility.

Our experiments support the hypothesis that the Tellnes intrusion is an ilmenite-rich, plagioclase-ilmenite cumulate, but the intercumulus melt was jotunite-like and not particularly

rich in TiO_2. Increasing dissolution of Fe and Ti at higher P and T suggest that at least some cumulation of ilmenite may have occurred during decompression. Our experiments do not support an origin of the Tellnes ore by liquid immiscibility.

Stein HJ, Hannah JL, Morgan JW, Scherstén A & Wiszniewska J:

Parallel Re-Os isochrons and high $^{187}Os/^{188}Os$ initial ratios: constraints on the origin of the Suwalki Anorthosite Massif, Northeast Poland

[1] Stein HJ, [1] Hannah JL, [1] Morgan JW, [1] Scherstén, A, & [2] Wiszniewska J.
[1] AIRIE Program, Department of Earth Resources, Colorado State University, Fort Collins, CO 80523-1482 USA [hstein@cnr.colostate.edu]. [2] Polish Geological Institute, Rakowiecka 4, 00-975 Warsaw, Poland

In the past decade the Re-Os chronometer and the associated initial $^{187}Os/^{188}Os$ ratio have provided powerful isotopic tracers leading to much improved understanding of source for magmas and mineralization. Notably, the Re-Os system applied to sulfide- and oxide-bearing anorthosite systems documents unique processes involved in the formation and emplacement of mineralized Proterozoic anorthosite massifs.

Recognition of parallel isochrons and high $^{187}Os/^{188}Os$ ratios reflecting synchronous emplacement with variable crustal contamination was first intimated at the Proterozoic Suwalki anorthosite complex in Poland (Stein *et al.* 1998; Morgan *et al.* 2000). Petrologically, these parallel isochrons reflect complex mingling and addition of crustally-derived Os with anorthosite and related melts. Stoping of crustal rocks by ascending magmas, armoring of crustal conduits, and influx of new batches of melt making their way through new conduits results in highly variable mixtures of crustally-derived and primitive Os. This results in highly variable initial $^{187}Os/^{188}Os$ ratios in the intruding melts. Because of variable initial $^{187}Os/^{188}Os$ with different melt batches, it is essential that the resulting Re-Os data be treated on a batch-by-batch basis, and not lumped together on a single isochron. Improper lumping of data combined with a large data set may result in an isochron with an approximately correct age and a moderate to low uncertainty. However, assessment of the MSWD value is essential. A high MSWD, assuming assignment of appropriate analytical errors, is a clear indication of geologic variation in the $^{187}Os/^{188}Os$ initial ratio and that different magma batches with different Os isotopic histories are represented in the data population. Excess geologic scatter resulting from variable $^{187}Os/^{188}Os$ initial ratios characterizes these data sets (e.g., Schiellerup *et al.* 2000; Lambert *et al.* 2000). The correct plotting and interpretation of Re-Os data for these mineralized anorthosite systems requires a careful look at the geologic relationships associated with the sample population, and an analysis of the possible balance between crustally-derived Os obtained during the emplacement process and original Os inherent in the anorthosite melt.

In this presentation, we make use of a Re-Os data set derived from three different deposits at the Suwalki anorthosite complex in Poland (Stein *et al.* 1998; Morgan *et al.* 2000). The data from these three deposits lie on two parallel isochrons with ages of ~1555-1560 Ma. Samples from a single deposit define one isochron, while combined samples from two different deposits define the other. These isochrons are defined by magmatic magnetite (Re = 0.4-1.5 ppb and Os = 0.036-0.144 ppb) and co-existing sulfide (pyrrhotite, chalcopyrite, pyrite, with Re = 30-55 ppb and Os = 1-6 ppb) hosted in anorthosite and related rocks. The $^{187}Os/^{188}Os$ initial ratios for the two isochrons are 1.16 ± 0.06 and 0.87 ± 0.20, a clear indication of crustal Os and variable initial ratios. It is suggested that the apparent paucity of sulfide in Proterozoic anorthosite

systems reflects the happenstance intersection of ascending anorthosite melt with a distinctly older, crustal, sulfide-bearing rock package. In this way, high $^{187}Os/^{188}Os$ may be added to an anorthosite system of primitive derivation through the volatilization of older crustal sulfide.

References

Lambert, DD, Frick, LR, Foster, JG, Li, C, and Naldrett, AJ (2000) Re-Os isotope systematics of the Voisey's Bay Ni-Cu-Co magmatic sulfide system, Labrador, Canada: II. Implications for parental magma chemistry, ore genesis, and metal redistribution: *Economic Geology*, v. 95, p. 867-888.

Morgan, JW, Stein, HJ, Hannah, JL, Markey, RJ, Wiszniewska, J (2000) Re-Os study of ores from the Suwalki anorthosite massif, northeast Poland: *Mineralium Deposita*, v. 35, p. 391-401.

Schiellerup, H, Lambert, DD, Prestvik, T, Robins, B, McBride, JS, and Larsen, RB (2000) Re-Os isotopic evidence for a lower crustal origin of massif-type anorthosites: *Nature*, v. 405, p. 781-784.

Stein, HJ, Morgan, JW, Markey, RJ, and Wiszniewska, J (1998) A Re-Os study of the Suwalki anorthosite massif, northeast Poland: *Geophysical Journal*, no. 4, p. 111-114.

Stepanov VS:

Ti, V, Pt, Pd and Au in Travyanaya Guba ore peridotites and their possible genetic relation with Belomorian Mobile Belt anorthosites

V. S. Stepanov, Institute of Geology Karelian Research Center RAS, Russia

Ore peridotites are exposed near Travyanaya Bay of Lake Keret, North Karelia (Russia) in the Belomorian Mobile Belt (BMB) eastern Fennoscandian Sield as a part of the differentiated Palojarvi massive. Mineralization, represented by ilmenite, magnetite and, locally, by very small percentages (<< 1%) of pyrite and chalcosine, occurs in ore rocks, such as harzburgite, lherzolite, websterite and amphibolite. The harzburgite shows a sideronite texture and consists of 25 % olivine (Fa_{41}), 21% orthopyroxene (Fs_{34}), 41% magnetite, 10% ilmenite and secondary minerals, such as hornblende (f – 0.25%), chlorite, serpentine, garnet, carbonate and spinel. Augite is commonly present in lherzolite and websterite. These rocks are associated by gradual transitions and, obviously, form a continuous differentiated sequence. During amphibolization they pass into ore amphibolites which are most similar in chemical composition to websterite.

The valuable components of the ore rocks are represented by TiO_2 (3.0-7.40 wt.%), V_2O_5 (0.21-0.36 wt.%), Pt (up to 0.52 ppm), Pd (up to 2.8 ppm) and Au (up to 2.5 ppm). Ilmenite is a major concentrator mineral for Ti. Magnetite, clinopyroxene and amphibole are major concentrator minerals for V (in decreasing order). Separate mineral phases of Pt and Pd are unknown, but their maximum concentrations are observed in olivine and ilmenite. Au concentrations are maximum in ilmenite and much smaller in magnetite and olivine. The average amount of Pt + Pd is 1.23 ppm in ore peridotites and olivine websterites, 1.48 ppm in amphibolized websterites and 1.022 ppm in ore amphibolites.

Ore rocks form small bodies in a Fe-rich (f > 0.5) garnet-feldspathic amphibolite zone. About 10 bodies composed of ore rocks have been found. The largest and most thoroughly studied body has a visible thickness of 30 m, dips steeply east and has been traced for 100 m along the strike. The boundary between the body and plagioamphibolite extends across a 30-40 cm thick thin-laminated zone formed by compositionally variable amphibolite. The ore rock body wedges out northwards and southwards. Other ore rock bodies are much smaller.

The association of the ore rocks and garnet plagioamphibolites is interpreted as a metamorphosed differentiated series in the fairly big (about 8 km^2) Palojärvi massif which falls

tectonically into three big fragments differing markedly in chemical composition. The biggest, western fragment is built up by garnet-feldspathic amphibolite, which has zones exhibiting well-preserved gabbro structures. The eastern fragment is structurally similar, but its relict zones contain both gabbronorite and plagioperidotite. The southern fragment is richer in Fe ($f > 0.5$) than the western and eastern fragments, and is presumably composed of late differentiates. Ore peridotites have only been found in this fragment, and are interpreted as melanocratic cumulates. Leucocratic plagioamphibolite, similar to apoanorthositic rocks, are encountered in the eastern portion of the fragment.

The Palojärvi massif is thus differentiated from Mg-rich plagioperidotite (eastern fragment) to rocks similar to ferrogabbro and ore peridotite. An intermediate position is occupied by mesocratic and leucocratic amphibolites ($f < 0.5$) that correspond in chemical composition to gabbro and leucogabbro.

Comparison of Palojärvi rocks with the BMB intrusive rocks shows that the ore rocks have no counterparts among the rocks known in the province. The Mg-rich portion of the massif is most similar to mesocratic units in the gabbro-anorthosite complex (Nizhnepopovsky, Boyarsky, Severopezhostrovsky and other massifs). Both the gabbro-anorthosites and Palojärvi rocks are intensely metamorphosed and foliated; therefore, gabbroids pass into plagioamphibolites throughout the study area. Ilmenite, which is essential in Travyanaya Guba rocks, is a major ore mineral in gabbro-anorthosites.

To sum up, ore rocks, similar to those in Travyanaya Guba, are likely to be found in connection with the gabbro-anorthosite massifs in the BMB.

Stepanov VS & Stepanova AV:

Precambrian anorthosites in the Belomorian Mobile Belt, Eastern Fennoscandian Shield

V. S. Stepanov and A.V. Stepanova

In the Belomorian Mobile Belt (western White Sea region), anorthosites are known in at least three geological settings:

1. The most strongly differentiated leucocratic portion of an Early Proterozoic (2.4 Ga) drusitic lherzolite-gabbronorite complex (Stepanov, 1981) is represented by anorthosites. They are subordinate and form small lenses up to tens of metres in thickness and schlieren in olivine gabbronorites and plagioclase lherzolites. Massives of this complex have primary intrusive contacts with chill zones (1.5-2 m), apophyses and enclosing rock xenoliths. In addition to these intrusive forms, dykes are also characteristic of the complex. The parent magma of these intrusives corresponded to high-MgO, high-Cr tholeiite rich in SiO_2 (in chilled rocks 15-20% MgO and 8-11% Al_2O_3). This type of anorthosites is described as stratiform. The geological position and age of their host complex raise no doubt.

2. Anorthosites are an essential component of gabbro-anorthosite massifs (gabbro-anorthosite complex; Stepanov, 1981). In these bodies, anorthosites as well as leucocratic and mesocratic gabbro strongly dominate over melanocratic rocks that display a cumulate nature and commonly occur in the lower part of intrusives. Judging by the composition of chilled rock autoliths in the Boyarsky complex, the parent magma of this complex seemed to correspond in composition to high-alumina gabbro with 9% MgO and 16.1% Al_2O_3.

The isotopic age of the gabbro-anorthosites is 2450 Ma in the Kolvitsa massif (Mitrofanov et al., 1993) and 2452 Ma in the Severopezhostrovsky massif (Alexejev et al., 2000). These ages show that their formation was as close as possible in time to the formation of the

lherzolite-gabbronorite complex. Based on this evidence, some authors combine these units in one drusitic complex. However, the above groups of intrusives (complexes) differ substantially in the composition of parent melts and relative geologic ages. The dykes of the lherzolite-gabbronorite complex cut the gabbronorite massifs. The latter are typically strongly reworked. Their primary contacts are unknown. Intrusive rocks usually pass gradually into banded garnet amphibolites. Lherzolite-gabbronorite bodies have crosscutting contacts with similar amphibolites. Therefore, differentiated gabbro-anorthosite massifs should be more closely studied isotopically.

3. Anorthosites also occur in thin (several metres to tens of metres) lenticular beds in banded amphibolites that are widespread in BMB and form thick horizons. Anorthosites are typically coarse-grain-structured and gneissose. Their boundaries with hosting amphibolites have no magmatic indications, suggesting that anorthosites are the easiest recognizable fragment of a differentiated series in which the gabbroid portion is fully transformed to amphibolites. Small anorthosite bodies, rimmed by alumina-rich feldspathic amphibolites, occur near Lakes Skalnye, Lake Nigrozero, Kivguba, Point Kartesh in the White Sea and in other parts of BMB. The largest massif of this type is the crescentiform Kotozero massif which has a visible thickness of 1.5-2 km. Its axial part is composed of gneissic meta-anorthosites and less common massive anorthosites that retain relics of magmatic structure. The most strongly altered anorthosite in the Kotozero massif has the following composition (mass.%, ppm): 50.90 SiO_2; 0.25 TiO_2; 29.04 Al_2O_3; 0.75 Fe_2O_3; 1.32 FeO; 0.032 MnO; 0.61 MgO; 12.76 CaO; 3.53 Na_2O; 0.21 K_2O; 0.06 H_2O; 0.42 LOI; 0.05 P_2O_5; 15 Cr; 28 V; 32 Ni; 16 Co; and 40 Cu. On the periphery, the gneissose anorthosites are rimmed by a feldspathic amphibolite band – presumably a mesocratic constituent of the massif. Occurring in metaanorthosites are dykes of fine-grained norites (50.86 SiO_2; 0.56 TiO_2; 10.93 Al_2O_3; 1.37 Fe_2O_3; 9.08 FeO; 0.179 MnO; 15.22 MgO; 0.834 CaO; 0.154 Na_2O; 0.42 K_2O; $H_2O < 0.07$; 0.91 LOI; 0.09 P_2O_5; 1183 Cr; 190 V; 150 Ni; 63 Co and 80 Cu) and garnet-diopside-plagioclase rocks (51.40 SiO_2; 1.90 TiO_2; 12.75 Al_2O_3; 2.88 Fe_2O_3; 12.93 FeO; 0.221 MnO; 4.35 MgO; 8.70 CaO; 1.46 Na_2O; 1.04 K_2O; 0.10 H_2O; 1.54 LOI; 0.28 P_2O_5; 102 Cr; 302 V; 79 Ni and 120 Cu), possibly the dykes of a complex composed of lherzolites, gabbronorites and garnet gabbro. They are deformed together with anorthosites, but the extent of deformation is lower in dykes than in the rocks of the massif. The structural line traced by the Kotozero massif and by the smaller gabbro-anorthosite bodies that lie on its extension, seems to correspond to a dislocation zone which evolved in an extension regime in Late Achaean and early Lower Proterozoic time and in a compression regime in Svecofennian time. The close relationship between these gabbro-anorthosites and amphibolites appears to reflect their Archean age. At the same time, the extent of amphibolisation is not a principal criterion which can be used to distinguish them from the gabbro-anorthosite massifs described above (point 2). Based on this evidence (Stepanov, 1981; Stepanov & Slabunov, 1989), they were described earlier as part of one complex. The isotopic age of this variety of gabbro-anorthosites has not yet been estimated. They are morphologically similar to autonomous anorthosites (massive type).

4. The formation of a lherzolite-gabbronorite complex is commonly attributed to Early Proterozoic rifting. The position of gabbro-anorthosite magmatism in BMB is more obscure. We (Stepanov & Slabunov, 1989) assumed its formation as a manifestation of Late Archean activation (post-collisional stage of evolution). The available isotopic dates indicating the Early Proterozoic age of several massifs typical of the complex have led us to conclude that some generally accepted views should be revised and that the situation should be investigated more thoroughly.

5. Associated with the gabbro-anorthosite massifs of BMB are the occurrences of Au-Pt mineralization in two parageneses: 1) in association with sulphide mineralization (Ileiki Islands, White Sea) and 2) in association with ilmenite-magnetite mineralization (Travyanaya Guba ore peridotites).

The study was supported by RFRF, Project 00-05-64295.

Sukhanov MK & Sugnatulin RH:

Titanium ore deposits in the massif-type anorthosites of the Aldan Shield (Siberia)

Sukhanov M.K.[1], Sugnatulin R.H.[2]
[1] Institute of geology of ore deposits, petrography, mineralogy and geochemistry, Russian Academy of Sciences. [2] Tatarstangeologia, Russian ministry of Geology.

The Aldan Shield is a vast denuded part of the basement of the Siberian platform. This fragment of Precambrian Earth's crust resulted from long evolution of several mobile belts, namely Achaean Aldan (aging apparently up to 3.5 b.y.); A Late Achaean-Proterozoic Olekma-Stanovoy (3.1- 2.6 b.y.); Proterozoic Baikal-Patom (2 - 1.8 b.y) and Late Proterozoic the Akitkan volcano-plutonic belt (1.7-1.6 b.y.)

Anorthosite massifs are widespread along the southern margin of the Aldan massif which was formed in the course of evolution of the most ancient mobile belt of the Aldan Shield. This is the largest province of the massif-type anorthosites not only in the Russia but also in the world in general. Anorthosite massifs varying in size and composition are concentrated in the junction of the Aldan massif and Stanovoy folded area. They constitute a latitudinal belt more than 1000 km long. This chain of anorthosite massif is sometimes called the East Asia anorthosite belt. There are andesine-type, labradorite-type anorthosites massifs associated with charnocites andrapakivi-like granites and alkaline anorthosites enriched in potassium due to potassium feldspar exclusions in plagioclase. The spatial association with deeply metamorphosed rocks of granulite facies is the basis for the opinion of the Achaean age for both anorthosite and associated rocks. This is reflected in many recent publications, and many published geologic and tectonic maps. However, based on the studies of tectonic setting, geochemistry and isotopic dating of a number of anorthosite massifs authors have come to the conclusion of Protherozoic age for the East Asia Anorthosite Belt. This conclusion is very important, not only for the understanding of the origin of the massif-type anorthosites, but also the origin of the large titanium ore deposits connected with these massifs in Siberia. The most important among them are the deposits connected with Kalar (western part of the anorthosire belt), Geran (eastern part of the anorthosite belt) massifs. Besides these massifs are situated near the Baikal-Amur railroad and were dated by Sm-Nd method.

The name Kalar massif refers to two closely located anorthosite massifs. Kuronakh in the north and Imangakite in the South. Unlike other massifs in the Aldan Shield, it is obviously connected with the Stanovoy deep-seated fault separating the Aldan massif from the Stanovoy folded area.

Commonly in the fault zone are green schist diaphtorites, after various rocks and ultramafic and mafic intrusions. Both anorthosite manifestations are latitudinal and bordered by fault zones in the south, where anorthosites are metamorphosed in green schist facies. In the north both of the massifs have contacts with charnockites. The rocks of Kalar massif are metamorphosed in granulite facies and proper unrecrystallized anorthosites are found only as relics in the central parts of the massifs. Gravimetric data showed that anorthosites can be traced as far as 10 km north of the Kuronakh massif and underlie metamorphic complexes at a depth of 1-5 km. Sm-Nd investigations gave the evidence of the Proterozoic age of this massif. Anorthosite and gabbro-anorthosite points are considerably dispersed on the isochrone diagram and indicate within error limits the same age of about 1.9 b.y. Unlike basic rocks, the dispersion of points on the mineral charnockites isochrone diagram is relatively insignificant, so they form a regression line corresponding to the age of 1.7 b.y.

There are two types of titanium ore deposits in the Kalar massif: early- and late-magmatic origin. The Sayim ore field is situated in the boarder south part of the Kuronah massif, it is a good example of the ores of the first type. The area of this ore field is about 10 sq. km. Titanium ores form two zones which are conform with the layered anorthosite-gabbro-norites-pyroxenite sequence. These zones are 150-400 m thick and abut 1000 m along. Ores forms layers in the lower

parts of the rhythms of magmatic rocks which start from melano-gabbro and pyroxenites and finish leuco-gabbro-norites and anorthosites, but in the sections of the ore zones the most rich ores are in the upper parts. As usually, there are pepper titanomagnetite-ilmenite and apatite-magnetite-ilmenite ores. Percentage of ore minerals is about 10-60% (TiO_2 5-15%). Massif ores containing more 60% ore minerals (more than 15% TiO_2) are rare.

The Kuronah ore field is situated in the central part of the Kuronah massif among anorthosites and represents the late-magmatic ore type. Titanium ores form dyke-like bodies that cut the surrounding anorthosites. Width of such bodies is about 1-100 m, they are traced up to 2 km on the surface and 150-200 m in depth. Ore bodies composed of ore norites or massif ores. Magnetite is the main mineral of such ores. In massif ores, the ratio magnetite/ilmenite is about 2-3, in pepper ores is about 1. Ilmenite of this ore field contents up to 60% TiO_2; 1,3%MgO. Titanomagnetite contains ilmenite lamella and up to 18% TiO_2 and up to 2%V_2O_5 and Cr_2O_3. All rocks of Kalar massif titanium ores are metamorphosed. During metamorphism in some parts of ore fields metasomatic ores were formed. It is apatite-magnetite-gemoilmente ores which form irregular zones and veins up to some hundred meters in width, but it is the more titanium-rich ore type. During metamorphism and recrystallization of titanomagnetite, Ti is concentrated in large homogeneous ilmenite grains.

The Geran massif is well exposed and is not metamorphosed. Two rocks groups are clearly distinguished in this complex: the main central one, composed mostly of proper anorthosites and the marginal one, located along the peripheral part of the anorthosite core and constituted by gabbro, gabbro-anorthosite, anorthosite and mangerite. The complex forms a plate-like body gently pitching north-eastwards. Its thickness is about 3-5 km. The central anorthosite group is coarsely stratified. The sequence is composed of alternating anorthosite and gabbro-anorthosite layers up to several hundred meters thick with gradual replacement of one by the other. The marginal group of Geran massif is about 2 km thick. It is clearly stratified with alternating layers varying from ultramafics to anorthosites from several centimeter to several hundred meters thick. In some cases stratification obviously displays rhythmic aspects. Besides, there are layers of syenites and gabbro-syenites in this group. For anorthosites of the Geran massif central and marginal group, two mineral isochrones were obtained indicating the same age about 1.7 b.y. We decided that this time refers to the moment of "closing" the isotopic system in the minerals and indicates the minimum age of the whole multiphase Geran massif. Whole rock points on the isohrone diagram do not fall onto the same straight line, displaying a considerable dispersion. The modal ages of the whole rocks are about 2.3 b.y. and only one sample gave the modal age 2.9 b.y. This sample is from the contact marginal group with enclosing granulites and it is possible influence of the ancient crust material.

In this region, there are some types of large deposits of apatite-ilmenite-titanomagnetite ores. These ore deposits are unusual for the massif-type anorthosites as these deposits are complex and composed of apatite and ilmenite-titanomagnetite ores. Apatite is a common mineral for all ore types. There are the following ore types: (1) ilmenite ores, apatite-titanomagnetite-ilmenite ores (ore anorthosites, gabbro, and syenites), (2) apatite-ilmenite ores (ore pyroxenites), (3) apatite-ilmenite-titanomagnetite massif ores (nelsonites and ore pegmatites). The first and second types are early-magmatic. Deposits of such ores are situated in the border parts of the Geran massif (Bogide and Maimakan ore fields). Ores form layers in the clearly stratified anorthosite-gabbro-norite syenite sequense, from bottom, thickness in meters: 1-gabbro-norites (150), ore anorthosites with apatite and titanomagnetite (60), massif ores (50-150), gabbro-anorthosites with pepper ores (100). Contents of fluorine-apatite (2,2-2,4% F) are 10-15% in pepper ores and up to 40% in massif ores.

Late-magmatic ore deposit (Gaium ore field) is situated in the central part of the Geran massif.

Ore bodies (consist of ores type 3) form cross cutting dyke-like bodies (width is 10-100 m , they are traced up to 1 km). These bodies are accompanied by mafic rocks (norites and gabbro-norites) close in composition to the same rocks of the marginal group. Sometimes they contain gigantic (10-20 cm) crystals of plagioclase (An 38-48) and hyperstene (not high aluminium)

which form pegmatite-like bodies. Typical ore type is nelsonites, which are composed of apatite (10-20%), ilmenite (up to 10%), titanomagnetite (50-70%), also there are small amount of iron olivine, spinel, rutile, leucoxene, sulfides and graphite. The most part of the ore is titanomagnetite without exsolution structures, and ilmenite forms single large grains. Apatite belongs to the podolite group. Graphite is the typical accessory mineral, its grains (0,1-0,5 mm) dispersed in the whole ore and in the surrounding anorthosites. Value of $\square C^{13}/_{oo}$ for graphite is -17,08 and corresponds with deep origin, high temperatures, and reduced conditions ($f O_2 = -11.5$, T= 970-800°C).

Petrological and geochemical data, such as distribution of rare elements in anorthosites, contents of Sr and anorthite content in their plagioclase and isotopic data show that the Aldan Shield anorthosites are very similar to Proterozoic anorthosites widespread through all continents and having no analogy in Achaean and in Phanerozoic. The data obtained for the Aldan Shield indicate that the first to be formed in the course of tectono-thermal reworking of the ancient craton's margin. The nature of such zones is still obscures. This is obvious an exclusively Precambrian phenomena. Still indispensable for their formation are the presence of sufficiently thick continental crust and a powerful up welling mantle flow.

The origin of anorthosite parental magmas is connected with the differentiation in large magma reservoirs. Associated acid rocks were crystallized from magmas of crustal origin. Depending on the tectonic setting different types of anorthosites massif were formed. Therefore, in stable blocks anorthosites crystallized in still conditions and were not metamorphosed, like Geran massif. However, if the intrusion of anorthosites were connected with a fault zone, as in the case of Kalar massif, they were strongly deformed and metamorphosed. These are the two different ways of the evolution of Proterozoic anorthosites. Origin of the ilmenite and apatite-ilmenite ores connected with two process – differentiation of mafic magmas of mantle origin and liquation of the residuum melts in the late stage of evolution of the massif-type anorthosites. The source of the apatite could be crustal origin as indicate isotopic data and origin of the ore deposits like in Geran massif probably connected with contamination processes. This research supported by Russian Foundation of Basic Researches, grant 00-65-65000.

Table 1. Typical chemical compositions of the titanium ores connected with massif-type anorthosites of the Aldan Shield (Siberia)

Components	1	2	3	4	5	6	7	8
SiO_2	41,40	16,61	29,70	2,88	14,50	2,88	31,70	10,35
TiO_2	6,06	18,16	10,68	17,64	6,80	19,10	9,40	10,20
Al_2O_3	12,90	7,79	9,90	5,53	1,55	2,60	14,70	3,20
Fe_2O_3	8,09	20,72	16,87	39,49	17,06	14,60	15,77	8,51
FeO	10,78	22,76	21,08	30,42	26,25	34,56	16,94	13,45
MnO	0,18	0,24	0,28	0,23	0,37	0,29	0,22	0,13
MgO	5,21	6,66	3,53	1,43	7,02	1,21	1,12	1,05
CaO	8,31	3,35	3,48	0,46	13,88	12,80	23,84	11,08
Na_2O	2,41	0,67	1,49	0,24	0,29	0,21	0,37	2,96
K_2O	0,64	0,23	0,24	0,15	0,07	0,06	0,16	0,26
P_2O_5	1,10	0,39	0,08	0,02	10,32	9,31	15,59	4,16
V_2O_5	0,08	0,21	0,34	0,77	0,03	0,04	0,16	0,19
Cr_2O_3	-	-	0,27	0,48	0,06	0,98	0,02	0,13

1-4 - Kalar massif, 5-8-Geran massif. 1,7,8-early-magmatic ores, 2,3,6,7 –late magmatic ores, 5- metasomatic ores.

Vander Auwera J, Longhi J & Duchesne JC:

Some results on the role of P, T and fO_2 on ilmenite composition

Vander Auwera J.[1], Longhi J.[2] & Duchesne J.C.[1]
[1] Université de Liège, B-4000 Sart Tilman, Belgium. [2] Lamont-Doherty Earth Observatory, Palisades, NY 10964, USA

Experimental data performed in anhydrous conditions from 1 atm (fO_2 at NNO, FMQ-1 and MW-2.5) up to 13 kb (FMQ-2, FMQ-4) on the so-called Tjörn (TJ) primitive jotunite (Vander Auwera and Longhi, 1994) are used here to assess the possible role of pressure, temperature and fO_2 on ilmenite composition (Al, Mg, Cr). In Rogaland, it has been shown that the parent magmas of the Åna-Sira massif-type anorthosite and the layered mafic intrusion of Bjerkreim-Sokndal, which both contain ilmenite deposits (Duchesne, 1999), are generally similar to this primitive jotunite (Duchesne and Hertogen, 1988; Vander Auwera and Longhi, 1994; Vander Auwera *et al.*, 1998; Longhi *et al.*, 1999). These experimental data can thus bring information concerning the behaviour of poisonous elements like Mg and Cr during polybaric crystallization of ilmenite in anorthosite complexes.

In the TJ primitive jotunite, ilmenite is a near liquidus phase and experiments corresponding to the first appearance of this phase at a given pressure have been selected in order to limit the extent of liquid compositional variability. These experimental data indicate that the most important effects are an increase of D_{Al2O3} (Ilm/liq) with increasing fO_2, a slight increase of $D_{Fe/Mg}$ (Ilm/liq) and a decrease of ilmenite Cr_2O_3 content with increasing pressure. Nevertheless, this latter effect could result from the earlier appearance of opx with increasing pressure which decreases liquid Cr content. Besides that, there is no significant variation of D_{MgO} with increasing pressure and D_{Al2O3} only slightly increases.

These experimental data thus suggest that the compositional variability observed in ilmenites from different orebodies (Duchesne, 1999) probably result from variable parent magmas composition and/or subsolidus readjustments (Duchesne, 1972).

References

Duchesne, J.C. 1972. *J. Petrol.* **13**, 57-81.
Duchesne, J.C. and Hertogen, J. 1988. *C.R.Acad.Sci.Paris* **306**, 45-48.
Duchesne, J.C. 1999. *Miner. Deposita* **34**, 182-198.
Longhi, J., Vander Auwera, J., Fram, M. and Duchesne, J.C. 1999. *J. Petrol.*, **40**, 339-362.
Vander Auwera, J. and Longhi, J., 1994. *Contrib. Miner. Petrol.* **118**, 60-78.
Vander Auwera, J., Longhi, J. and Duchesne, J.C., 1998. *J. Petrol.* **39**, 439-468.

Wilson JR & Overgaard G:

Relationship between the layered series and the overlying evolved rocks in the Bjerkreim-Sokndal intrusion, Southern Norway

J. Richard Wilson and Gitte Overgaard
Department of Earth Sciences, Aarhus Universitet, 8000 Århus C, Denmark

The Bjerkreim-Sokndal layered intrusion consists of a >7000 m thick Layered Series comprising anorthosites, leuconorites, troctolites, norites, gabbronorites and jotunites (hypersthene monzodiorites), overlain by an unknown thickness of massive, evolved rocks (mangerites (MG), quartz mangerites (QMG) and charnockites (CH)). The Layered Series is subdivided into 6 megacycic units (MCUs) that represent the crystallisation products of successive major influxes of magma. The relationship between the Layered Series and the overlying, evolved rocks has long been debated. Are the two parts of the intrusion comagmatic or do the evolved rocks represent a separate magma influx?

We have studied a ca. 1200 m thick profile that straddles the sequence from gabbronorites belonging to the top of the uppermost MCU to the quartz mangerites in the northern part of the intrusion (the Bjerkreim lobe). Mineral compositions in 37 samples become continuously more evolved in the lower part of the sequence up to the middle of the MG unit (plagioclase An36-18; olivine Fo39-7; Ca-poor pyroxene Mg# 57-16; Ca-rich pyroxene Mg# 65-22). Above this compositions are essentially constant in the upper part of the MG unit and in the QMG (An20-13; Fo6-4; Mg#opx17-13; Mg#cpx25-18). There is no evidence of a compositional break that could reflect a magma influx event in this profile.

Whole rock chemical compositions also show a continuous evolutionary trend. The MG unit defines a cumulate trend essentially controlled by the amount of alkali-feldspar (which is mostly mesoperthite). All of the QMG samples lie in a small field with e.g. 0.8-0.3% MgO and 59-65%SiO2. Duchesne & Wilmart (1997; J. Petrology 38, 337-370) identified two compositionally distinct types of QMG-CH in the upper part of the intrusion. One type (olivine-bearing QMG and CH) defines an olivine trend (OT) which they interpret essentially as reflecting fractional crystallisation of the mangerite liquid resident in the chamber. The other (two-pyroxene QMG and CH) defines the "main liquid line of descent" derived from a jotunitic melt that was emplaced into the evolved magma already residing in the uppermost part of the chamber. All of our QMG samples fall on the OT-trend, despite the fact that they comprise both two-pyroxene and olivine-bearing lithologies. We therefore agree with Duchesne & Wilmart that the OT-trend comprises samples that are comagmatic with the underlying Layered Series, but that the mineralogical distinction between rocks that define the two chemical compositional trends is not always clear.

Zagnitko VM:

The isotope composition of oxygen and carbon in minerals from titanium and rare metal deposits of Ukraine

Zagnitko, V.M.
Institute of Geochemistry, Mineralogy and Ore Formation, NAS Ukraine, Kyiv

Ukraine is rather rich with deposits of Ti and rare metals. The investigation of distribution of O and C isotopes in minerals from these deposits gives a possibility to judge more confidently about physico-chemical parameters of formation of the deposits. The Azov deposit of Zr and TR in the Trans-Azov area is a typical magmatic deposit, in which, by our point of view [1], the ore-forming differentiation has been a main process of crystallization. A concentration of zircon in the ore bodies reaches up to 50%, while the total of rare earths reaches up to 10 %. Ore zones are sometimes enriched with ilmenite up to 10%.

We investigated isotope composition of oxygen in zircon, feldspars, biotite and ilmenite. The temperature isotope equilibrium of these minerals (600-800C) is somewhat lower than the temperatures, which were determined on solid inclusions, 1100C [2].

The isotope composition of oxygen in coexisting silicates and oxides from other high-temperature associations of the Ukrainian Shield does not always specify the equilibrium conditions of their formation. This is especially obvious in case of metamorphic paragenesis. In particular, in some lithium deposits (Polohiv), which is considered as a metamorphic pegmatitic one, a low-temperature distribution of oxygen isotopes between quartz and feldspars is observed. It is not excluded, that a part of these minerals was formed at a postmagmatic low-temperature stage.

In anorthosite of Korosten pluton, ilmenite corresponds to deep-seated conditions of formation and is mostly in equilibrium with other oxygen-based minerals. The isotope composition of carbon from rocks of this and some other complexes of alkaline and subalkaline rocks ($\delta^{13}C$ = -10 - 12) indicates a deep-seated origin of carbon. The isotope composition of O and C in carbonates from both veins of these plutons and carbonatitic massifs (the latters are very important sources TR), also suggests mantle origin of the carbonate substance. This conclusion is confirmed by ratios of Sr and Nd isotope contents.

Thus, the isotope data indicate the deep-seated sources of Ti and TR in the deposits studied, in spite of the presence of low-temperature secondary and metamorphic formations in them. These latter formations are well determined under the study of equilibrium of isotope distribution in coexisting pairs of minerals.

References

Krivdik S.G., Zagnitko V.N., Strekozov S.N. et al. Rare-Metal Syenites of the Ukrainian Shield: Survey Prospects of Rich Ores in Zirconium and Lanthanoides// Mineralogical Journal, 22, N1, 2000. – P. 62-72.

Melnikov V.S., Voznyak D.K., Grechanovskaya E.E. et al.The Asov zirconium-Rare-Earth deposit:Mineralogical and Genetic Properties// Mineralogical Journal, 22, N1, 2000. – P. 42-61.

Årebäck H:

Concentration of ilmenite in the late Sveconorwegian norite-anorthosite Hakefjorden Complex, SW Sweden

Hans Årebäck
Department of Geology, Earth Science Centre, Göteborg University, Box 460, SE-405 30 Göteborg, Sweden. Present address: Boliden Mineral AB, SE-936 81 Boliden, Sweden;
hans.areback@boliden.se

The c. 916 Ma Hakefjorden Complex (HFC) comprises a composite norite-monzonorite-anorthosite intrusion (Årebäck, 1995; Scherstén et al., 2000). It is situated c. 25 km NNW of Göteborg, SW Sweden, in the Sveconorwegian Province and forms two east-west elongated bodies, both about 500 m wide and 3.6 and 1.2 km long respectively, intruding Mesoproterozoic supracrustal gneisses (Fig. 1). The intrusion is dominated by a medium-grained norite-monzonorite (An_{54}) containing massive anorthosite blocks, 2 cm to 50 m in diameter, and 2-20 cm large andesine megacrysts (disaggregated anorthosite blocks). The coarse-grained anorthosite blocks (An_{45}) occur in all mafic rock types with a preferred occurrence along the contacts. Subordinate ilmenite-rich leuconorite, hybrid rock and granitic pods are recorded. Gradual transitions (mineralogy and geochemistry) between the norite and the marginal monzonorite and the granitic pods as well as between the norite and the ilmenite-rich leuconorite, indicate their close relationship and that they are products from the same magma.

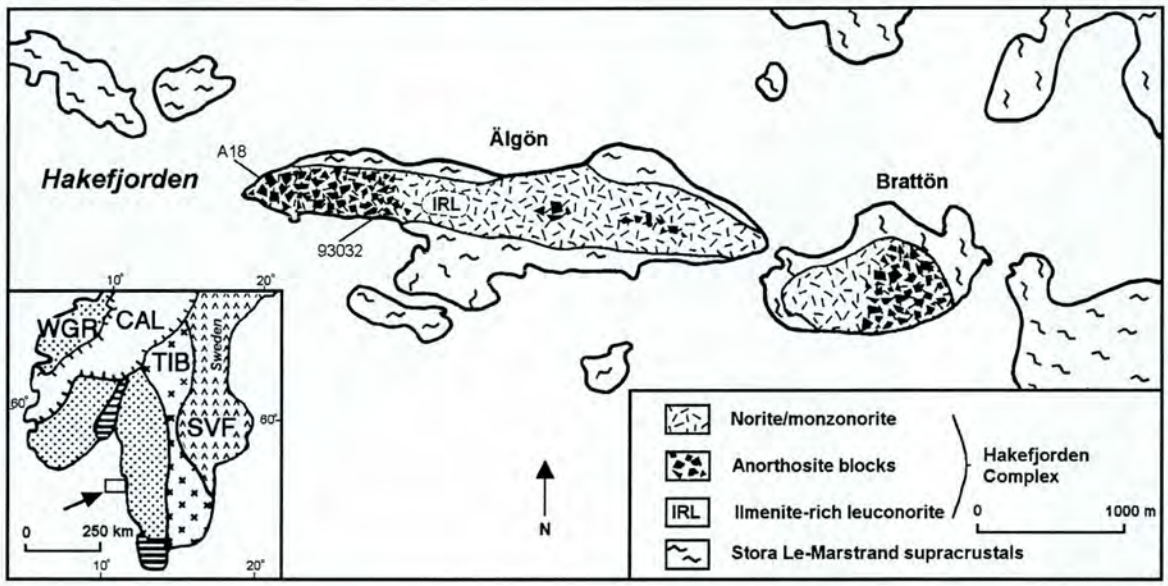

Fig. 1. Generalised bedrock map of Hakefjorden Complex region, SW Sweden. The inset map shows the major lithotectonic units of southwestern Fennoscandia. CAL = Caledonian; SVF = Svecofennian; TIB = Transscandinavian Igneous Belt; WGR = Western Gneiss Region; dotted areas = rocks affected by the Sveconorwegian Orogeny; ruled areas = Phanerozoic rocks.

The emplacement mechanism has been inferred to involve deep-crustal (high pressure) anorthosite and ultramafic crystallisation followed by mid-crustal norite-monzonorite crystallisation involving crustal contamination and Fe-Ti enrichment during fractional crystallisation (Årebäck & Stigh, 1997; 2000).

The liquid composition from which the HFC-norite/monzonorite crystallised is not straightforward to determine since most rocks are affected by accumulation of cumulus plagioclase ± orthopyroxene ± Fe-Ti oxides ± apatite, crustal contamination or both. However, a

slightly more fine-grained margin (chilled margin) where the marginal monzonorite is not developed is suggested to represent the best estimate of the liquid composition of the exposed HFC-norite/monzonorite. In a QAP-diagram this rock plots in the lower left part of the quartzjotunite (quartzmonzonorite) field. Mineral mode and whole-rock geochemistry of two samples from the chilled margin is presented in Table 1. Rocks that are chemically more primitive than this composition are, indicated from thin-section observation, affected by accumulation of ± plagioclase ± orthopyroxene ± Fe-Ti oxides ± apatite, while rocks more evolved are affected by fractionation ± crustal contamination.

In the central part of the intrusion there is a limited area consisting of an extremely ilmenite-rich leuconorite (IRL; Ereвдck & Stigh, 2000). The IRL occurs as a "disc-like", c. 10-15 m thick, 100×300 m wide subhorizontal unit within the norite. The lateral and lower contacts with the surrounding norite are gradual. The IRL-matrix is fine- to medium-grained and characterised by a subhorizontal magmatic foliation defined by the preferred orientation of tabular plagioclase crystals (An_{55}). This foliation is restricted to the IRL-unit. Various types of enclaves occur in the IRL-matrix. They can be divided into two main groups. The first consists of decimetre- to meter-sized anorthosite and norite blocks from the host HFC. The second group consists of massive to semi-massive, millimetre- to decimetre-sized Fe-Ti oxides, fine-grained anorthosite and fine-grained, fine-scale igneous layered plagioclase-orthopyroxene. The second group is restricted to the IRL and is considered to represent disrupted layering within IRL. The foliation of the IRL-matrix is wrapped around all inclusions and interpreted to result from deformation in the magmatic state.

The IRL-matrix contains subequal amounts of ilmenite (32-66 vol. %) and silicates (34-68 vol. %; Table 1). For obvious reasons, the IRL-matrix is anomalously high in major and trace elements entering Fe-Ti oxides, i.e. Ti, Fe, Cr, Sc, Ni and V (Table 1). Ilmenite grains are typically rounded, equidimensional, and either homogeneous or contain thin hematite lenses arranged in the {0001} planes (hemo-ilmenite). Ilmenite in the massive Fe-Ti oxide enclaves is high in MgO, ranging from 2.17 up to 5.00% (average 3.21%), compared to the IRL-matrix ilmenite (1.35 to 2.79%; average 1.97%), which in turn is more Mg-rich than ilmenite in the surrounding norite (0.03-0.3%; average 0.13%). Magnetite rarely exceeds 1 vol. % in the matrix whereas the Fe-Ti oxide enclaves contain 20-60 vol%. Ilmenite intergrowths occur as microlamellae along the {111} planes (trellis type) of magnetite or as thicker lamellae restricted to one set of the {111} planes (sandwich type). The trellis type is most frequent and occurs in at least two generations; a rather coarse set and a network of very fine-grained lamellae represented by submicroscopic exsolutions occurring as domains in the magnetite. Exsolution of pleonaste is frequent in the {100} planes of magnetite. The lamellae occur in several generations and tend to be most frequent in the centre of the host grain. Textural evidence indicates that a certain amount of pleonaste was exsolved simultaneously with ilmenite, as indicated by the presence of pleonaste microcrystals within exsolved ilmenite. All magnetite has a very low X_{usp} component and is therefore high in X_{mag}. However, this does not necessarily mean that the magnetite phase was low in TiO_2 during crystallisation, as their compositions are affected by subsolidus reequilibration.

Crystal accumulation in a late stage noritic magma residual after anorthosite crystallisation is put forward to be the main mechanism forming the IRL, where the liquid from which it was produced must have been strongly enriched in Fe and Ti. The origin of such liquids is characteristic for residual liquids after anorthosite crystallisation (e.g. McLelland et al., 1994; Emslie et al., 1994). Deformation in the magmatic state arranged the solid phases according to the stress regime.

Table 1. Whole-rock geochemistry and mineral mode of sample A18 and 93032 proposed to represent the best estimate of the liquid composition of the exposed Hakefjorden Complex norite/monzonorite and two samples from the ilmenite-rich leuconorite, sample B7 and 98003

Rock type	Norite/monzon.		IRL		Norite/monzon.		IRL	
Sample no.	A18	93032	B7	98003	A18	93032	B7	98003
SiO_2 (wt%)	50.9	51.3	20.0	31.3	Be (ppm)	-	2.7	-	3.3
TiO_2	3.00	2.91	27.3	17.8	Br	3	4	3	4
Al_2O_3	15.6	14.8	8.51	14.3	Cr	710	120	3300	1300
$Fe_2O_{3,tot}$	12.6	12.1	35.6	25.3	Ni	<200	66	<200	172
MnO	0.15	0.15	0.15	0.15	Co	60	28	120	45
MgO	4.75	4.70	3.59	3.64	Sc	16.6	20.5	40.8	30
CaO	6.92	6.98	3.09	5.35	V	-	190	-	739
Na_2O	2.91	2.93	1.14	2.21	Cu	-	29.3	-	114
K_2O	1.62	1.67	0.24	0.59	Zn	100	130	180	122
P_2O_5	0.70	0.74	0.15	0.33	W	140	-	71	<3
LOI	0.25	0.70	-1.38	<0	Sb	3.4	<5	<0.2	<0.2
					Rb	43	46	19	<2
Tot	99.7	99.2	98.9	100.4	Cs	2	3	2	<1
Fe#	57.3	56.5	83.4	77.8	Ba	525	685	144	289
					Sr	451	415	184	525
Plagioclase (vol%)	52.4	49.7	35.8	46.2	Ta	<1	<1	2	1
K-feldspar	3.5	7.1		0.5	Nb	25	39	38	34
Quartz	5.4	3.7			Hf	9.1	6.9	9.4	7
Orthopyroxene	13.7	9.1	6.3	11.9	Zr	330	313	179	216
Clinopyroxene	5.7	5.3	0.2	0.8	Y	18	37	<10	12
Biotite	3.7	11.5	2.2	3.2	Th	2.3	2.9	<0.5	1.0
Hornblende	0.8	4.3			U	0.6	0.8	0.5	<0.5
Ilmenite[a]	3.6	3.5	53.6	35.3	La	36.6	47.4	10.3	15.1
Magnetite[b]	6.1	1.7	1.6		Ce	78	84	22	32
Apatite	1.8	2.4		0.1	Nd	40	43	10	15
Chlorite	1.0	1.7	0.1	0.9	Sm	9.1	10.4	2.1	3.2
Fe-sulphides[c]	1.6	+	0.2	0.9	Eu	2.7	2.9	1.0	0.9
Other[d]	0.7	+	+	0.2	Tb	1.3	1.6	<0.5	<0.5
					Yb	3	3.7	1.0	1.1
Total counts	2100	1500	1500	1500	Lu	0.45	0.49	0.15	0.18

Data from Årebäck (1995) and Årebäck & Stigh (2000), whole-rock analyses done by XRAL, Canada.
[a] Include minor amounts of hematite.
[b] Include minor amounts of ilmenite and pleonaste.
[c] Include pyrite, pyrrhotite and marcasite.
[d] Other include calcite, zircon, epidote, chalocopyrite and rutile.
+ = Trace amounts.

Textures and compositions of ilmenite and magnetite in the Fe-Ti oxide enclaves indicate post-crystallisation modification. These enclaves were probably formed, at least in part by annealing, i.e. consolidation of loose grains into polycrystalline materials at subsolidus temperatures.

Despite the sizes of the Hakefjorden IRL and the Tellnes ilmenite deposit, similarities in age, petrography and geochemistry occur. The Tellnes ilmenite-rich norite (920±2 Ma; Schärer et al., 1996), which dates the end of the magmatic activity in the Rogaland Anorthosite Complex, is interpreted as a noritic cumulate emplaced as a crystal mush with Fe-Ti rich intercumulus liquid (e.g. Duchesne, 1999).

References

Årebäck, H., 1995: The Hakefjorden Complex - geology and petrogenesis of a late Sveconorwegian norite-anorthosite intrusion, south-west Sweden. *Fil. Lic. Thesis. Geovetarcentrum, Göteborgs universitet, A9*, Göteborg, 84 pp.